Role of the microtubule-associated protein ATIP3 in cell migration and breast cancer metastasis

Angie Molina Delgado

Université Paris Descartes
Ecole doctorale BioSPC

Thesis submitted towards fulfillment of the requirement for the degree of

DOCTOR of Health & Life Sciences
Specialized in Cellular and Molecular Biology

Role of the microtubule-associated protein ATIP3 in cell migration and breast cancer metastasis

By

Angie Molina Delgado
Under supervision of Dr. Clara Nahmias

Thesis defense 3 September, 2014

Members of jury:

Dr. Ali BADACHE	Reviewer
Dr. Laurence LAFANECHERE	Reviewer
Dr. Franck PEREZ	Examiner
Dr. Stéphane HONORE	Examiner
Dr. Clara NAHMIAS	Thesis Director

Table of Contents

Table of Figures

Table of Tables

List of abbreviations

+TIP	Plus-end Tracking Protein
Akt	Protein Kinase B (PKB)
AMER2	APC Membrane Recruitment 2
APC	Adenomatous Polyposis Coli
AR	Androgen Receptor
Arl13B	ADP-Ribosylation factor-Like protein 13B
AT2R	Angiotensin II AT2 receptor
ATIP	Angiotensin II AT2 receptor-Interacting Protein
ATP	Adenosine Triphosphate
BM	Basement Membrane
BPAG1	Bullous Pemphigoid Antigen-1
BRCA	Breast Cancer gene
BrdU	BromodeoxyUridine
CAF	Cancer-Associated Fibroblast
CAP-Gly	Cytoskeleton-Associated Proteins Gly-rich protein
CENP-E	CENtromere-associated Protein E
CH	Calponin Homology
CLAMP	CaLponin-homology And Microtubule-associated Protein
CLASP	CLIP-associating protein
CLIP	Cytoplasmic Linker Protein
CTC	Circulating tumor cells
DCIS	Ductal Carcinoma *in situ*
DIC	Differential Interference Contrast
DNA	DeoxyriboNucleic Acid
EB	End Binding protein
EBH	End Binding Homology
ECM	Extracellular Matrix
ER	Estrogen Receptor
Fhit	Fragile Histidine Triad
GAS2L1	Growth Arrest-Specific 2 Like 1
GDP	Guanosine-5'-Diphosphate
GEF	Guanine nucleotide Exchange Factor
GFP	Green Fluorescent Protein
GST	Gluthatione S-Transferase
GTP	Guanosine-5'-Triphosphate
HCC	HepatoCellular Carcinoma
HER2	Human Epidermal factor Receptor 2
HURP	Hepatoma UpRegulated Protein
ICIS	Inner Centromere kin-I Stimulator

IF	Intermediate Filaments
LCIS	Lobular Carcinoma *in situ*
LZTS1	Leucine Zipper putative Tumor Suppressor 1
MACF	Microtubule-Actin Crosslinking Factor (ACF7)
MAP	Microtubule-Associated Protein
MAPK	Mitogen-activated protein kinases
MARK1	MAP/Microtubule Affinity-Regulating Kinase 1
MaSC	Mammary Stem Cells
MATSP	Microtubule-Associated Tumor Suppressor Proteins
MCAK	Mitotic Centromere-Associated Kinesin
MT	Microtubule
MTA	Microtubule Targeting Agent
MtLS	Microtubule Tip Localization Signal
MTOC	Microtubule Organizing Center
MTUS1	Microtubule TUmor Suppressor gene 1
MURF	MUscle-specific RING-Finger protein
NF2	NeuroFibromatosis 2 protein Merlin
NuMA	Nuclear protein that associates with the Mitotic Apparatus
NuSAP	Nucleolar Spindle-Associated Protein
Op18	Oncoprotein 18
PI3K	Phosphatidylinositol 3-kinase
PLA	Proximity Ligation Assay
PR	Progesterone Receptor
RasL11B	Ras-Like, family 11, member B
RASSF1A	RAS Association domain Family 1A
RCC	Renal Cell Carcinoma
RCP	Rolling Circle Product
RHAMM	Receptor for Hyaluronan-Mediated Motilty
ROCK	Rho-associated protein Kinase
RTK	Receptor Tyrosine Kinase
RT-PCR	Reverse transcription polymerase chain reaction
STIM1	Stromal Interaction Molecule 1
TACC	Transforming Acidic Coiled-Coil
TCGA	The Cancer Genome Atlas
TIAM	T-lymphoma Invasion And Metastasis-inducing protein
TNBC	Triple Negative Breast Cancer
TPX2	Targeting Protein for Xklp2
UTR	UnTranslated Region
VAP	Vesicle-Associated membrane Protein
VHL	von Hippel–Lindau

"Rôle de la protéine associée aux microtubules ATIP3 dans la migration cellulaire et la formation de métastases du cancer du sein"

Le cancer du sein touche une femme sur huit dans le monde et représente un problème majeur de santé publique. Alors que la majorité des tumeurs du sein sont aujourd'hui la cible de traitement efficaces, il reste une sous-population de tumeurs (dites triple-négatives) à fort potentiel métastatique qui ne sont pas accessibles aux thérapies ciblées et demeurent de mauvais pronostic. L'élucidation des processus impliqués dans la progression tumorale et la formation de métastases reste un challenge majeur dans la recherche de nouvelles thérapies contre le cancer du sein de mauvais pronostic.

ATIP3 (*AT2-interacting protein 2*), produit du gène candidat suppresseur des tumeurs *MTUS1* (*Microtubule-Associated Tumor Suppressor*), a été identifiée par le laboratoire comme étant un biomarqueur des tumeurs du sein les plus agressives. En effet, les résultats précédents de notre équipe ont montré que l'expression d'ATIP3 est diminuée dans 85% des tumeurs de haut grade, 83% des tumeurs triples négatives et dans 62% des tumeurs métastatiques. Il a également été montré qu'ATIP3 inhibe la prolifération cellulaire *in vitro*, ainsi que la croissance tumorale *in vivo*. Au niveau moléculaire, ATIP3 a été identifiée comme étant une nouvelle protéine associée aux microtubules (MAP) localisée au centrosome, le long de microtubules dans les cellules en interphase, au fuseau mitotique pendant la division cellulaire et au pont intercellulaire lors de la cytokinèse. La localisation cellulaire d'ATIP3, étroitement associée aux microtubules, prend toute son importance du fait du rôle de ce cytosquelette dans la division et migration cellulaire, deux étapes essentielles du processus tumoral.

Mon projet de thèse a pour objectif principal d'évaluer le rôle potentiel d'ATIP3 dans la migration cellulaire et la formation de métastases tumorales.

Dans un premier temps, les niveaux d'expression d'ATIP3 ont été analysés dans des séries de puces à ADN issues de trois cohortes indépendantes de patientes atteintes d'un cancer du sein invasif, et les données ont été comparées avec les caractéristiques cliniques des patientes. Ces analyses transcriptomiques ont permis de montrer que l'expression d'ATIP3 est un marqueur pronostic de la survie des patientes et de façon intéressante, qu'ATIP3 est un nouvel indicateur de la progression métastatique.

L'effet d'ATIP3 sur la progression des métastases a alors été évalué dans un modèle de bioluminescence *in vivo*, ce qui a permis de montrer que cette protéine est une molécule

anti-métastatique qui réduit la progression, le nombre et la taille des foyers métastatiques. La colonisation métastatique inclut la migration des cellules cancéreuses à travers la matrice extracellulaire (invasion) et l'endothélium vasculaire (extravasation), puis leur prolifération au site secondaire. L'évaluation détaillée de ces étapes a montré qu'ATIP3 diminue tous ces processus. En ce qui concerne la migration, une réduction de vitesse, de la direction de migration et possiblement de la polarité cellulaire, pourraient expliquer les effets inhibiteurs d'ATIP3 sur la migration des cellules.

Comme de nombreuses études ont démontré que la migration et la polarité cellulaires dépendent du cytosquelette de microtubules, je me suis intéressée aux effets d'ATIP3 sur la dynamique microtubulaire. Des expériences de vidéomicroscopie ont permis de montrer que l'extinction d'ATIP3 augmente la dynamique des microtubules en incrémentant les épisodes et la vitesse de croissance et en diminuant le temps passé en pause et la fréquence des catastrophes. Ces résultats, couplés à des expériences de dépolymérisation et de re-croissance ont permis de conclure qu'ATIP3 est une MAP qui stabilise les microtubules et diminue leur dynamique pour contrôler la polarité et la migration cellulaires. L'ensemble de ces travaux font l'objet d'une publication parue en 2013 (Molina *et al*., Cancer Res 73, 2905).

Dans une seconde partie de mon travail, je me suis intéressée à la protéine EB1 (*End-Binding 1*), protéine majeure des bouts croissants des microtubules qui sert de plate-forme au recrutement de protéines régulatrices appelées +TIP (*plus end tracking protein*) et qui induit la croissance persistante des microtubules en diminuant la fréquence des catastrophes. L'analyse de la séquence d'acides aminés d'ATIP3 a révélé que cette protéine possède trois motifs consensus potentiels d'interaction à EB1. En utilisant la technique de GST pull-down, l'interaction entre ATIP3 et EB1 a été mise en évidence via un domaine appelé CN, qui se trouve dans la partie centrale d'ATIP3. Cette interaction est directe et fait intervenir un motif protéique un peu atypique (RPLP) sur la séquence d'ATIP3. De façon intéressante, nous avons pu montrer que des mutants de délétion dépourvus du domaine (ou du motif) d'interaction à EB1 ne sont plus capables de délocaliser EB1 de l'extrémité dynamique des microtubules, indiquant que l'interaction entre ATIP3 et EB1 est essentielle aux effets d'ATIP3 sur l'accumulation d'EB1 aux bouts plus.

Dans le but de mieux comprendre la fonctionnalité de l'interaction entre ATIP3 et EB1, nous avons recherché la présence de complexes moléculaires à l'intérieur de la cellule. De façon étonnante, contrairement à la plupart des protéines interagissant avec EB1, ATIP3 ne s'accumule pas au bout dynamique et reste plutôt localisée au réseau de microtubules. Des expériences de PLA (*Proximity Ligation Assay*) réalisées à l'aide d'anticorps anti-ATIP

et anti-EB1 ont montré que l'interaction se produit majoritairement dans le cytoplasme et que les complexes ATIP3/EB1 se retrouvent également associés tout le long du microtubule.

Sur la base de ces résultats, un modèle a été proposé. Dans ce modèle, l'interaction entre ATIP3 et EB1 dans le cytosol pourrait réduire la concentration d'EB1 disponible à proximité du microtubule, avec pour conséquence de limiter sa diffusion dans le cytosol et de réduire sa dynamique d'interaction avec les bouts des microtubules. Selon ce modèle, en absence d'ATIP3 les protéines EB1 pourraient diffuser librement dans le cytosol et s'accumuler en plus grand nombre à l'extrémité du microtubule, avec pour conséquence d'augmenter la dynamique microtubulaire. In fine, l'interaction d'ATIP3 avec EB1 pourrait ainsi rendre compte des effets anti-prolifératifs, anti-migratoires et anti-métastatiques d'ATIP3.

L'importance clinique de ce modèle en pathologie humaine a été testée en évaluant les niveaux d'expression d'ATIP3 et EB1 dans des tumeurs de patientes atteintes d'un cancer du sein invasif. Les résultats extraits de l'analyse par puces à ADN ont montré que les niveaux relatifs d'expression des protéines ATIP3 et EB1 ont valeur pronostic de la survie des patientes. Ainsi, les patientes atteintes de tumeurs ayant des niveaux élevés d'EB1 et bas d'ATIP3 présentent un mauvais pronostic clinique par comparaison avec les tumeurs ayant des niveaux faibles d'EB1 et ATIP3. D'après notre modèle, une tumeur avec une expression élevée d'EB1 et une faible expression d'ATIP3 présenterait un défaut de stabilisation d'EB1 dans le cytosol, avec comme conséquence un nombre élevé de molécules d'EB1 libres capables de s'accumuler aux bouts plus des microtubules pour favoriser la dynamique des microtubules et la progression tumorale. Cette seconde partie de mon étude fait l'objet d'un article actuellement en cours de révision (Velot*, Molina* et al., first co-authors)

Dans une troisième partie de cette thèse, je présente les données préliminaires que j'ai obtenues, montrant qu'ATIP3 interagit avec d'autres +TIPs telles MCAK (*Mitotic Centromere-Associated Kinesin*) et APC (*Adenomatous Polyposis Coli*). MCAK est une kinésine qui s'associe aux bouts des MTs via EB1 et est impliquée dans la dépolymérisation des microtubules, et le contrôle de la dynamique microtubulaire. La protéine APC, quant-à elle, est un partenaire majeur d'EB1 qui s'accumule également aux bouts plus des microtubules et est impliquée dans la formation de microtubules stables lors de la migration cellulaire. La fonction des complexes d'interaction ATIP3/MCAK et ATIP3/APC reste encore à déterminer.

En conclusion, ces travaux de thèse ont permis d'identifier ATIP3 comme étant une nouvelle molécule anti-migratoire et anti-métastatique, qui interagit avec EB1 et régule la

dynamique des microtubules. A l'avenir il sera nécessaire de clarifier le mécanisme d'action par lequel ATIP3 régule la dynamique des MTs en interphase et pendant la mitose, et de déterminer si cette régulation est dépendante de l'interaction d'ATIP3 avec EB1, MCAK et APC. De plus, le rôle d'ATIP3 sur la polarité devra être approfondi, en analysant l'effet de cette protéine sur la dynamique de l'actine ou l'activation des petites protéines G (Rho, Rac et Cdc42). Ces travaux devraient permettre de mieux comprendre les mécanismes d'action intracellulaires d'ATIP3 et de déterminer comment la perte d'ATIP3 est associée à un processus cancéreux, dans le but à terme d'envisager un nouveau traitement personnalisé contre les tumeurs de sein métastatiques ayant perdu l'expression d'ATIP3.

I. INTRODUCTION

1. Breast Cancer

1.1.Anatomy of the breast

Mature female breast is mainly composed by glandular tissue, adipose tissue, blood vessels, lymphatic vessels, and nerves, all surrounded by a supportive structure of connective tissue (Figure 1) (Hassiotou F & Geddes D, 2013).

Lobules or mammary glands are structures involved in milk production during pregnancy and lactation. Several lobules can group together to form lobes, which organize around the nipple in a "wheel spoke" shape. Lobes deposit milk into the collecting ducts that go through the breast until it opens at the nipple surface (Cooper AP, 1840; Hassiotou F & Geddes D, 2013).

Surrounding the lobes are the fat pad and the connective tissue which bring support to the ducts and lobules. Cooper's ligaments connect the chest wall muscle and the skin overlaying the breast to hold the breast and maintain the structural integrity (Cooper AP, 1840; Hassiotou F & Geddes D, 2013).

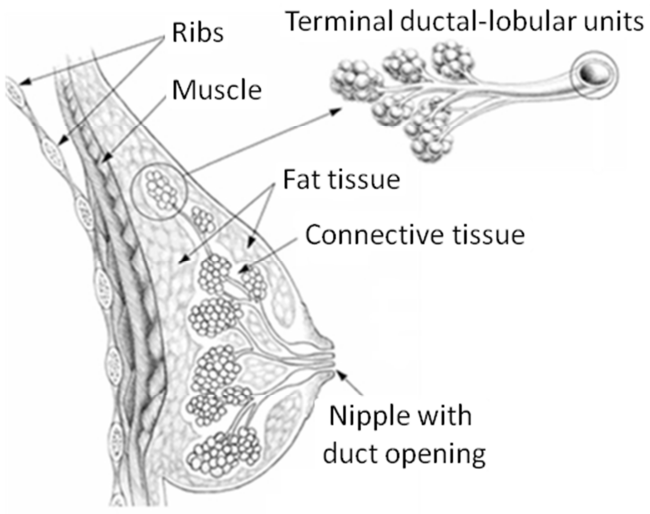

Figure 1.

Schematic representation of the mammary gland (Modified from Mannello F *et al.* 2008).

1.2.Histology of the mammary gland

The mammary gland is a complex structure constituted by different cell types which generate a network of branching ducts inside the fibrous collagen- and adipose-rich

stromal matrix (Figure 2). This structure includes epithelial and endothelial cells as well as fibroblasts and adipocytes (Neville MC & Daniel CW, 1987; Schmeichel KL *et al*. 1998).

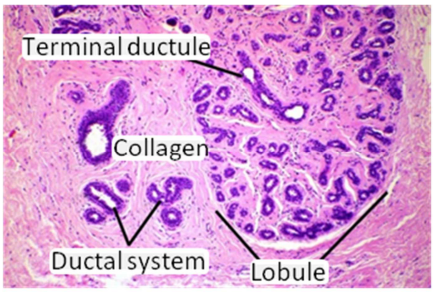

Figure 2

Low magnification of a normal breast tissue. Shown are the ducts, a lobule and the stroma (Modified from Wilson R, 2006).

1.2.1. Epithelial cells

Luminal and myoepithelial cells are the two major epithelial cell types present in the mammary gland. Luminal cells isolate and line the ductal lumen and alveoli, forming an inner continuous layer. These cells are characterized by their cuboidal shape, basoapical polarization and by the presence of apical microvilli (Figure 3) (Schmeichel KL *et al*. 1998; Visvader JE, 2009; Vidi PA *et al.* 2013; Hassiotou F & Geddes D, 2013). On the other hand, myoepithelial cells compose the outer or basal layer. They form a discontinuous line behind the luminal cells (Figure 3) and have properties of smooth muscle cells (Hassiotou F & Geddes D, 2013).

The mammary gland is involved in milk production and delivery, and these functions are accomplished by epithelial cells. Differentiation of luminal cell into lactocytes allows milk production during lactation, and contraction of myoepithelial cells allows the milk flow into the ducts (Visvader JE, 2009; Vidi PA *et al.* 2013; Hassiotou F & Geddes D, 2013).

Epithelial cells (luminal and myoepithelial) express estrogen (ER), progesterone (PR) and androgen (AR) receptors at their surface. It has been reported that these three steroid hormones play a key role in the development and function of the mammary gland (Li S *et al*. 2010).

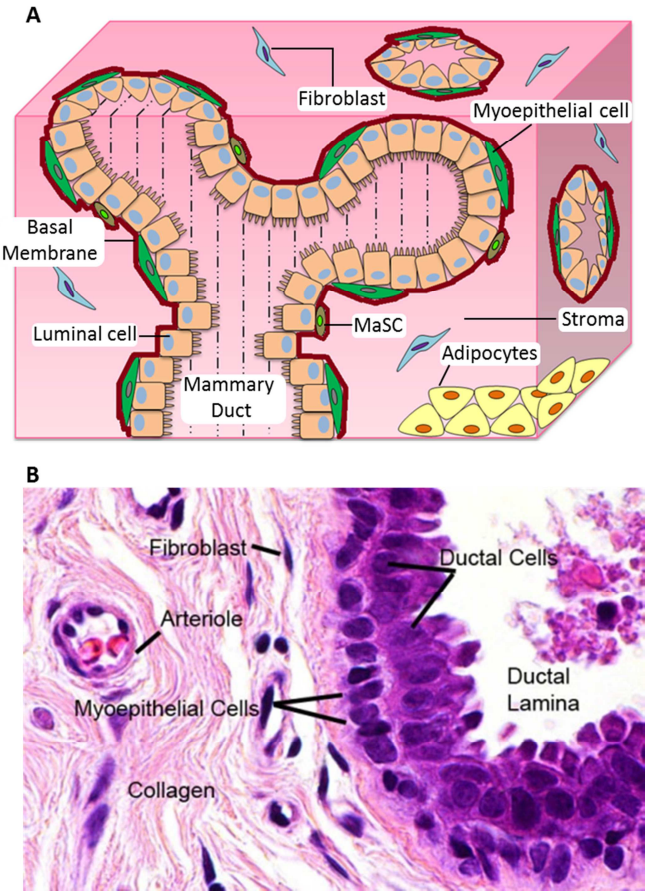

Figure 3

The mammary epithelium. **(A)** Schematic representation of the epithelium (luminal epithelial cells, myoepithelial cells and basal membrane) surrounded by the fibrous and fatty stromal compartment. **(B)** High magnification of a normal breast tissue. Shown are the epithelium and stroma. Panel B is from Wilson R, 2006.

Within the basal layer, bi-potent mammary stem cells (MaSC) can be found. MaSC are undifferentiated cells which give rise to progenitors that in turn can differentiate into luminal and myoepithelial cells (Figure 4) (Prat A & Perou CM, 2009; Visvader JE, 2009; Hassiotou F & Geddes D, 2013). It has been suggested that transformation of MaSC at the different stages of differentiation can be the origin of each breast cancer molecular subtype (Prat A &Perou CM, 2009; Visvader JE, 2009). This will be discussed in chapter 1.3.4.1.

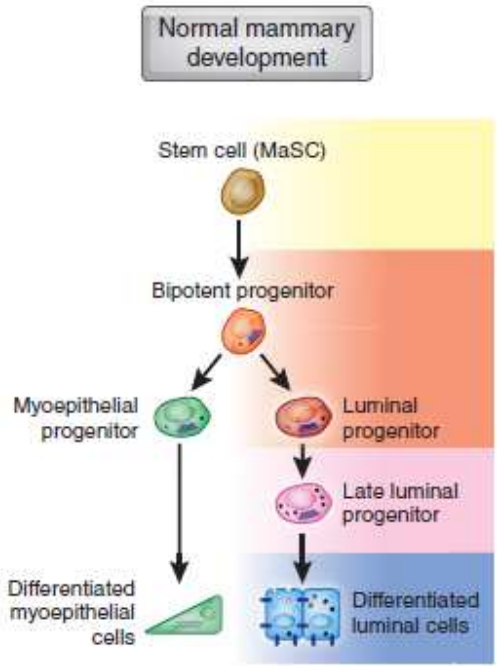

Figure 4

Human mammary epithelial hierarchy from the mammary stem cell (MaSC) until the latest differentiation stage into myoepithelial and luminal cells (From Prat A & Perou CM, 2009).

1.2.2. The mammary stroma

The mammary stroma is a highly fibrous and complex structure that is separated from the epithelial tissue by the basement membrane (BM). The BM is a special form of extracellular matrix (ECM) which is mainly composed of collagen IV and laminins, which are synthetized by myoepithelial and stromal cells, and connected by nidogen and perlecan (Schmeichel KL *et al*. 1998; Nelson CM & Bissell MJ, 2006; Rowe RG & Weiss SJ, 2008; Vidi PA *et al.* 2013).

The stroma includes (i) an adipose-rich fat pad which mainly gives support to all the other stromal components; (ii) blood and lymphatic vessels that provide immune surveillance, lymphatic drainage and accomplish an important function during lactation, delivering nutrients and removing of the waste metabolites; and (iii) an extracellular matrix-rich environment where epithelial cells grow, differentiate and regress (Schedin P & Hovey RC, 2010).

The cellular content of the stroma is mainly composed by endothelial cells, pericytes, fibroblasts and leukocytes, which will play an important role during cancer progression due to cross-talk and close interactions with tumor cells (for review Pietras K & Ostman A,

2010). Nevertheless, the interaction of tumor cells with the stroma will not be described here.

1.3.Breast Cancer

1.3.1. Cancer generalities

Cancer is the leading cause of death worldwide, accounting for 8,2 million of deaths in 2012 mainly by lung, liver, stomach, colorectal, breast and esophageal cancer (GLOBOCAN 2012, IARC).

Cancer is a complex process which can be divided in three phases: tumor initiation, cancer progression and metastasis formation. Hanahan D and Weinberg RA (2011) described the hallmarks of cancer as eight biological properties that are acquired during the development of human tumors. These include sustaining proliferative signaling, evading growth suppressors, evading immune destruction, enabling replicative immortality, activating invasion and metastasis, inducing angiogenesis, resisting cell death and reprogramming of energy metabolism. Underlying these hallmarks are genomic instability and inflammation which favor cancer progression (Figure 5).

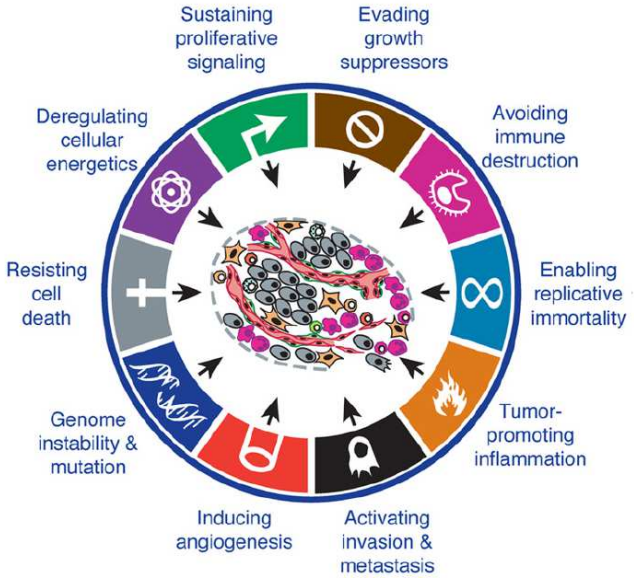

Figure 5

Hallmarks of cancer (From Hanahan D and Weinberg RA, 2011).

Tumors can initiate at any part of the body. According to this initial location, cancer can be classified in five broad categories: Carcinoma (affects epithelial cells and accounts for 85% of all cancers), sarcoma (bone, cartilage, fat, muscle, blood vessels, connective or supportive tissue), leukemia (blood-forming tissue as the bone marrow), lymphoma and myeloma (cells of the immune system) and central nervous system cancer (brain and spinal cord) (National Cancer Institute, NIH).

Metastasis is a fatal complication of cancer and the leading cause of death by this disease. It is a multistep process that includes the spreading from the primary site to another organ in the body to form a secondary tumor in a tissue-specific manner. The metastatic process will be reviewed in chapter 2.

1.3.2. Breast Cancer Epidemiology

Breast cancer is the most common diagnosed cancer in woman worldwide, being detected in 140 of 184 countries during 2012. In this same year, more than 1,5 million (11,9%) of new cases were reported and around 520.000 patients died from this disease (Ferlay J *et al*. 2013). According to the IARC last reports in 2008, breast cancer incidence and mortality have increased by 20% and 14%, respectively (Figure 6A, 6B) (GLOBOCAN, 2012).

Increased incidence was higher in developed countries as compared with less developed ones. Nevertheless, mortality rates were higher in less developed countries mostly due to the late detection and difficulties to access to treatment (Figure 6A, 6B) (GLOBOCAN, 2012).

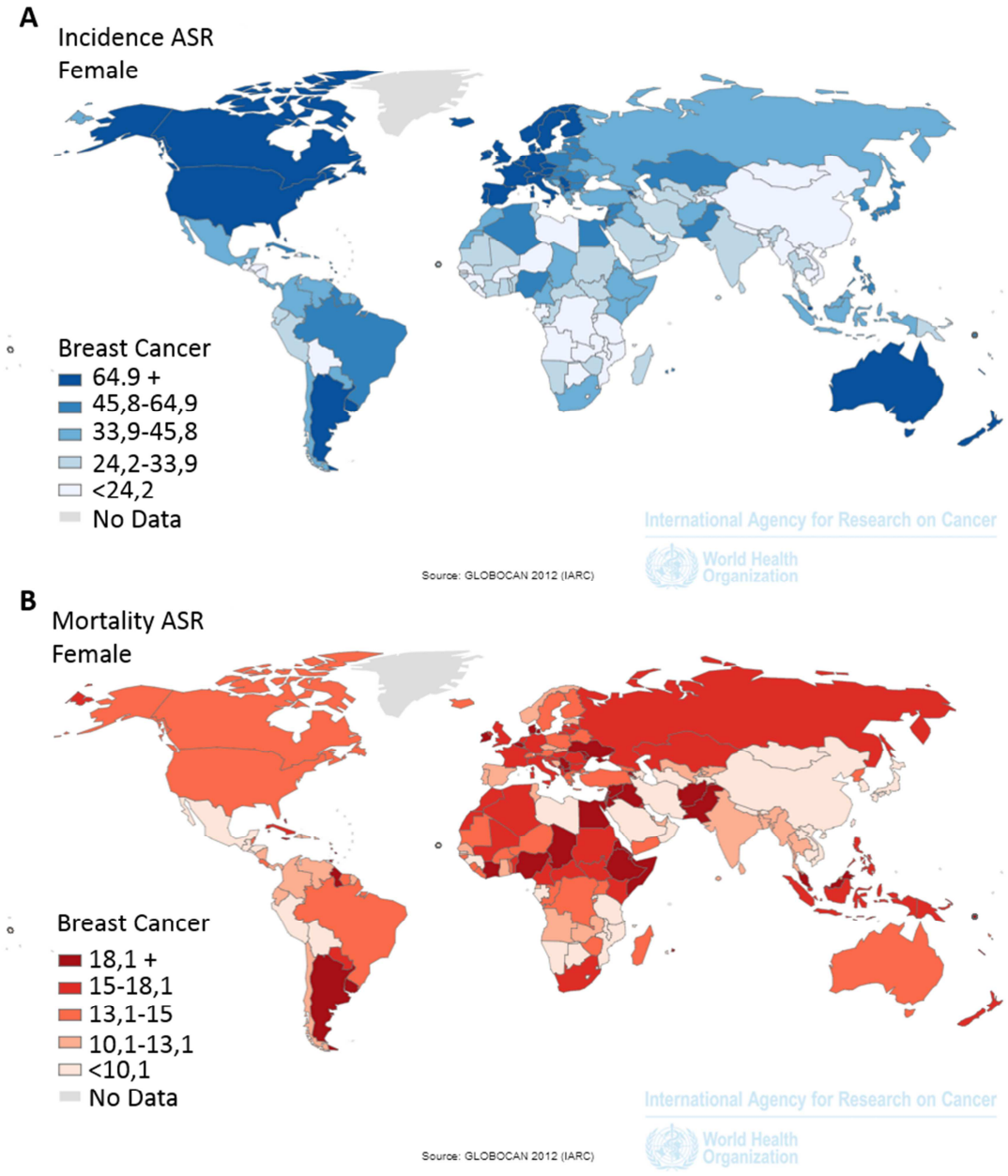

Figure 6

Age-standardized incidence **(A)** and mortality **(B)** rates for breast cancer in women worldwide in 2012. Color intensities indicate incidence (blue) and mortality (red) rates per 100.000 (From GLOBOCAN 2012).

1.3.3. Breast Cancer Classification

Until 2003, breast cancer classification relied on histological appearance of breast tumors and allowed to distinguish between two major groups: *in situ* carcinomas and invasive breast cancer.

In situ carcinoma refers to tumors that do not spread to the surrounding tissue and whose proliferation does not rip the basal membrane. This type of carcinoma can be, as well, subdivided in two: ductal carcinoma *in situ* (DCIS) and lobular carcinoma *in situ* (LCIS).

DCIS is the most frequent type of *in situ* carcinomas and makes reference to the presence of tumoral cells inside the milk duct (Figure 7A). High grade DCIS could turn into invasive breast cancer if left untreated. On the other hand, LCIS (also known as lobular neoplasia) refers to the presence of abnormal cells inside the breast lobules or milk glands (Figure 7B). LCIS is considered as a marker of increased risk of developing invasive breast cancer; in fact, women with LCIS have an eightfold to tenfold increased risk of invasive breast cancer (Portschy PR *et al*. 2013).

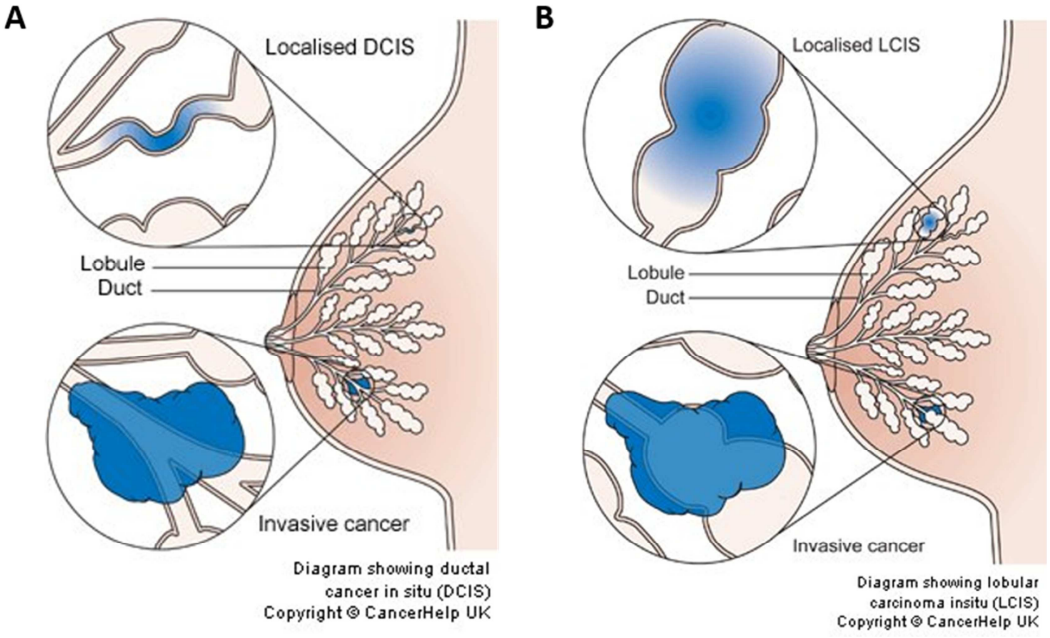

Figure 7

Schematic representation of **(A)** Ductal Carcinoma *in situ* and **(B)** Lobular Carcinoma *in situ*. Invasive ductal and lobular breast cancers are also represented (From CancerHelp UK, 2012).

Invasive breast carcinoma refers to the group of malignant epithelial tumors able to invade adjacent tissues and with the tendency to metastasize to distant sites. Invasive breast carcinoma exhibits a heterogeneous range of morphological phenotypes with particular prognosis or clinical characteristics. The 2003 World Health Organization (WHO) classification recognized 18 histological types of invasive breast cancer. Within these,

invasive ductal and lobular carcinomas are the most prevalent (Weigelt B & Reis-Filho JS 2009).

Invasive ductal cancer refers to the uncontrolled proliferation and spread of epithelial cells lining the ducts (Figure 7A), and is the most common type of breast cancer (70-80%). In contrast, invasive lobular carcinoma (Figure 7B) originates from the epithelial cells inside the lobules. It is much less frequent than the ductal (around 10-15%) and is often diagnosed in both breasts at the same time.

Some other types of breast cancer which are less frequent and sometimes classified as special breast cancer types (given the particular features of tumor cells) are:

- Inflammatory breast cancer (frequency of 1-4%) in which cancer cells block the lymph ducts of the breast, causing tissue inflammation.
- Medullary breast cancer (frequency of 5%) which is characterized by cancer cell shape. Tumor cells tend to be bigger and tumoral tissue is clearly isolated from the normal tissue when analyzed under the microscope. Women with mutation in the *BRCA1* gene are more prone to develop this type of cancer.
- Mucinous breast cancer (frequency of 2%) is characterized by the presence of malignant cells that "float" in pools of mucus.
- Other, very rare types of cancer include: tubular, adenoid cystic, metaplastic, angiosarcoma of the breast, lymphoma of the breast, phyllodes and papillary breast cancer.

At the clinical level breast cancer is not only defined by its morphology. The use of predictive biomarkers (known as surrogate markers), such as the expression of estrogen receptor (ER), progesterone receptor (PR) and the assessment of HER2 status by immunohistochemical methods are currently used.

1.3.4. Breast Cancer Molecular Classification

Over the last decade, microarray-based gene expression studies demonstrated that breast cancer is a heterogeneous disease with different molecular characteristics. One of the advantages of molecular classification over the morphological-histological classification is that the diagnostic criteria to define the different types are less subjective and can be shared across different cancer centers in the world (Rakha EA *et al*. 2010).

A key study for detailed molecular classification of breast tumors was performed by Perou CM *et al*. (2000). In this report, Perou CM and collaborators redefined breast cancer as a complex disease with specific gene expression profiles. Thus, using tumors with different

histopathological characteristics, they were able to describe an “intrinsic gene” list that allowed the hierarchical clustering of four breast cancer tumor subtypes: luminal, normal breast-like, HER2 and basal-like breast cancer (Figure 8).

Interestingly, the major molecular subgroups identified by large-scale transcriptomic approach (luminal, HER2, basal-like) were very close to those previously classified as luminal, HER2 and triple-negative, by means of immunohistochemistry.

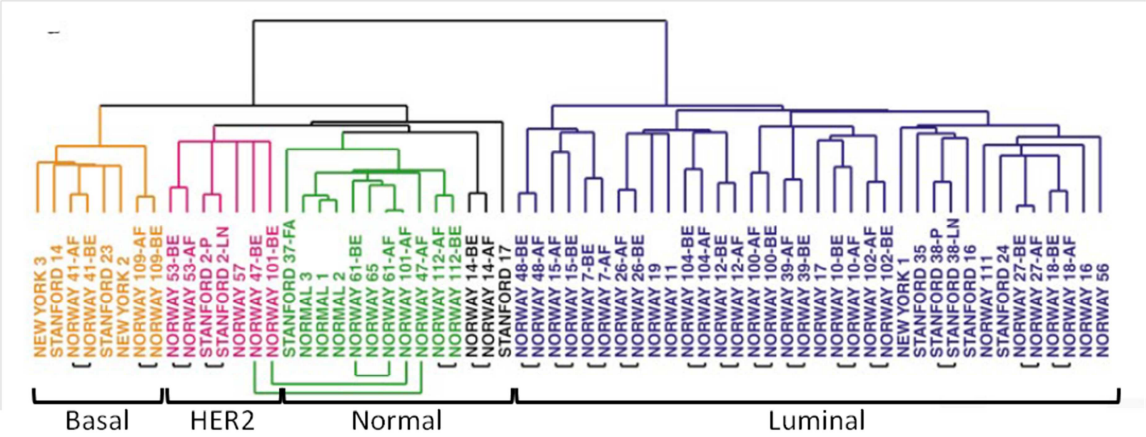

Figure 8

Cluster analysis of different breast cancer molecular subtypes. Branches are coloured as: Basal-like, orange; HER2, pink; normal breast, green; luminal, blue (Modified from Perou *et al*. 2000).

One year later, the same group showed that the estrogen (ER)-positive group (luminal cluster) could be classified into three distinct subgroups: Luminal A, Luminal B and Luminal C (Figure 9) (Sorlie T *et al*. 2001). Nevertheless a few years later, Sorlie T *et al*. (2003) continued the molecular classification studies of breast cancer using an expanded data set, and realized that luminal C was not a true subgroup of this disease but belonged to the luminal B subtype.

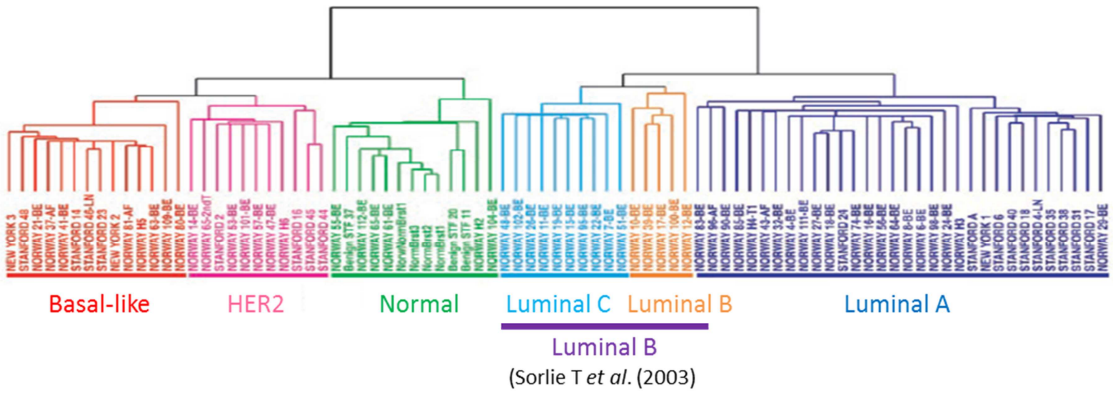

Figure 9

Hierarchical clustering analysis from gene expression patterns of normal breast and cancerous samples. Branches correspond to: Basal-like, red; HER2, pink; Normal breast-like, green; Luminal subtype C, light blue; Luminal subtype B, orange; Luminal subtype A, dark blue (Modified from Sorlie T *et al*. 2001). In 2003, Sorlie T and coworkers indicated that Luminal C subtype belonged to Luminal B subtype (purple).

In 2011, the four subtypes defined by gene expression profile studies (Luminal A and B, HER2 and basal-like) were included in the St Gallen International Expert Consensus. In addition, a concordance between these molecular subtypes and immunohistochemical surrogate markers was proposed (Goldhirsch A *et al*. 2011).

Thus, knowledge acquired using microarray analysis resulted in better understanding of the cellular and molecular heterogeneity of breast cancer. Of importance, the classification of breast tumors into distinct subtypes, based on the expression of molecular biomarkers, allowed more accurate orientation of patient treatment decisions and clinical trial design (Reis-Filho JS *et al*. 2006) (Table 1).

Table 1.

Breast Cancer molecular classification characteristics (Modified from Lam SW *et al.* 2014).

Molecular Subtype	Prevalence	IHC definition				Prognosis	Treatment
		ER	PR	HER2	Ki-67		
Luminal A	50-60 %	+	+	-	Low	Good	Endocrine
Luminal B (HER2 negative)	15-20 %	+	+	-	High	Intermediate	Endocrine ± chemotherapy
Luminal B (HER2 positive)	6 %	+	+	+	Any	Intermediate	Endocrine + cytotoxic + anti-HER2 therapy
HER2-amplified	10-15 %	-	-	+	Any	Poor	Chemotherapy + anti-HER2 therapy
Basal-like	10-20 %	-	-	-	High	Poor	Chemotherapy

1.3.4.1. *Breast cancer molecular subtypes origins*

Prat A & Perou CM (2009) suggested that cancer cells may either be generated by transformation of normal mammary stem cells (MaSC) or progenitor cells (Figure 10), or result from the acquisition of stem cells-like characteristics by cancer cells.

Lim E *et al*. (2009) were the first to propose the human mammary epithelial hierarchy (Figure 4) as a framework to understand the cellular origins of the various molecular subtypes of breast cancer (Figure 10). Epithelial gene expression signatures established for the different mammary epithelial populations have revealed that MaSC signature is most concordant with the one of the "normal-like" subtype (Lim E *et al*. 2009; Visvader EJ 2009). Surprisingly, the expression profile of basal-like cancers shares a striking similarity with the luminal progenitor gene signature and not with the MaSC as expected. While the luminal cancer subtypes (Luminal A and Luminal B) where closest to mature ductal cells, to date correlation of the HER2 subtype with a specific subpopulation has not been clearly defined, but it is presumed that they may derive from a cell with luminal origin (Figure 10) (Lim E *et al*. 2009; Visvader JE, 2009; Visvader JE, 2011; Fu N *et al*. 2014).

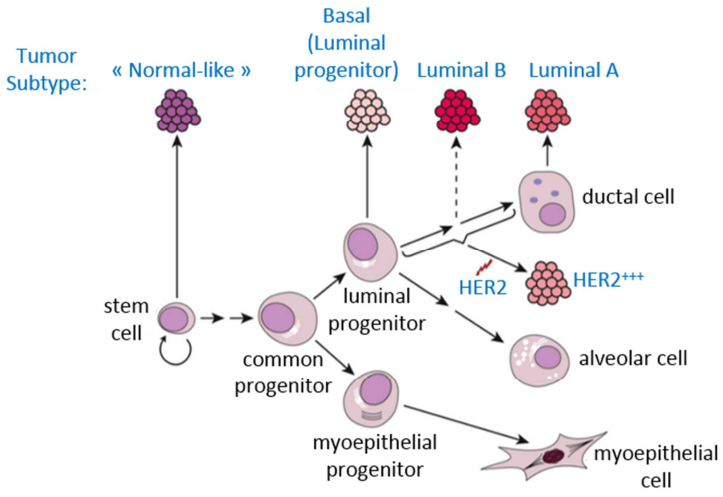

Figure 10

Human breast epithelial hierarchy at the origin of the different cancer subtypes (From Visvader JE, 2009).

1.3.4.2. *Luminal subtype*

Luminal subtype is characterized by the presence of luminal epithelial markers and can be divided in three groups: luminal A, luminal B/HER2-negative and luminal B/HER2-positive. All three subtypes present a characteristic gene expression profile, prognosis and response to appropriate treatment (Sorlie T *et al*. 2001; Langlands FE *et al*. 2013;

Ignatiadis M & Sotiriou C, 2013; Lam SW *et al.* 2014). According to the histological classification, luminal tumors can be invasive or *in situ* and be classified as ductal, lobular, mixed ductal-lobular, mucinous or tubular carcinomas (Schnitt SJ, 2010; Ignatiadis M & Sotiriou C, 2013).

Luminal A is the most common breast cancer subtype, it represents two-thirds of all breast cancer cases and it is characterized by the overexpression of genes related with the luminal mammary cells, estrogen receptor (ER) and ER transcription factors (Perou *et al*. 2000; Sorlie T *et al*. 2001; Weigelt B *et al*. 2010; Lam SW *et al.* 2014). Luminal A breast cancer patients have a 5-year survival of 90% and few lymph node dissemination (O'Brien KM *et al*. 2010).

The luminal B subtype represents 10-30% of breast carcinomas. Unlike luminal A, luminal B is associated with the overexpression of proliferation and cell cycle-related genes. Patients with Luminal B tumors present a 5-year survival rate of 50% (Sorlie T *et al*. 2001; Reis-Filho JS *et al*. 2006; Weigelt B *et al*. 2010; Lam SW *et al.* 2014). Two subtypes of luminal B tumors have been described according to their HER2 status (HER2 positive and HER2 negative). Among them, luminal B/HER2 negative is the most frequent (Lam SW *et al.* 2014).

Clinically, luminal tumor subtypes are treated using endocrine therapy (Table 1). Tamoxifen and aromatase inhibitors (such as letrozole, anastrozole and exemestane) are the most commonly used therapies (Ignatiadis M & Sotiriou C, 2013). Hormone treatment can be used together with chemotherapy or anti-HER2 therapy according to the luminal subtype and high risk patients (Table 1) (Lam SW *et al.* 2014).

1.3.4.3. HER2 subtype

This subtype comprises tumors expressing low levels of hormone receptors but overexpressing the *Erb-B2* oncogene that encodes for the Human Epidermal factor Receptor 2 (HER2) (Perou *et al*. 2000). HER2 is a member of the ErbB receptor tyrosine kinases (RTKs) family, with no known ligand but with a high kinase catalytic activity (Rexer BN & Arteaga CL, 2012; Langlands FE *et al*. 2013).

Amplification of HER2 represents approximately 15% of human breast tumors and is associated with an increased risk of metastasis (to the brain, lungs and liver) (Kennecke H *et al*. 2010), high relapse rate, short overall survival and poor patient outcome if not treated (Sorlie T *et al*. 2001; Reis-Filho JS *et al*. 2006; Rexer BN & Arteaga CL, 2012; Lam SW *et al.* 2014).

Several therapeutic strategies have been used to treat HER2 breast tumors. Within those, the most commonly used are trastuzumab and lapatinib. Trastuzumab (Herceptin) is a humanized monoclonal antibody which targets the extracellular domain of the receptor, thereby suppressing HER2 activity by disrupting downstream signaling. In contrast, lapatinib is a tyrosine kinase inhibitor that blocks HER2 phosphorylation, thereby inhibiting PI3K-Akt and MAPK pathways (Rexer BN & Arteaga CL, 2012; Langlands FE *et al*. 2013).

1.3.4.4. Basal-like subtype and Triple negative breast cancer (TNBC)

The basal-like subtype is characterized by the very low or negligible expression of ER, PR and no amplification of HER2. Due to the absence of these three receptors, basal-like tumors are sometimes referred as triple negative breast cancer (TNBC) (Langlands FE *et al*. 2013; Lam SW *et al.* 2014). Nevertheless, while basal-like denomination is based on microarray gene expression analysis, TNBC is according to predictive biomarkers classification (ER, PR and HER2 negative).

Basal-like and TNBC subtypes share a number of characteristics. They are high grade, invasive ductal carcinomas, with preference to metastasize to viscera (lungs and brain) more than to bones (Foulkes WD *et al*. 2010). Additionally, both breast cancers are associated with an adverse prognosis and by the presence of germline BRCA1 mutations (Foulkes WD *et al*. 2010; Lam SW *et al.* 2014).

However, clinical, microarray and immunohistochemical analysis have shown that basal-like and triple negative subtypes are overlapping but not identical, most of the basal-like breast cancer being TNBC (around 60%), and most of the TNBC (approximately 80%) being of the basal-like subtype (Weigelt B *et al*. 2010).

Triple Negative subtype accounts for 15% of breast cancer cases but is responsible for 25% of deaths by breast cancer. Due to its clinical heterogeneity, its highly proliferative and metastatic capacities, and the absence of targeted therapies, it remains the subtype with the worst prognosis.

Chemotherapy is the main treatment option for these patients. Chemotherapy targets cells that proliferate rapidly, and therefore is more effective on TNBC tumors (29% of pathological complete response to anthracycline in TNBC patients versus 10% in HER2, 8% luminal B and 6% luminal A) (Carey LA *et al*. 2007). However, just a small subgroup of TNBC patients will benefit from this treatment due to development of tumor drug resistance and tumor relapse.

1.3.5. Chemotherapy as a treatment for breast cancer

In addition to TNBC, patients diagnosed for hormone-refractory disease, hormone receptor-negative disease and metastatic breast cancer are treated using chemotherapies. Chemotherapy can be divided in two groups (DNA-targeting compounds and microtubule-targeting agents) with different mechanism of action (Fumoleau P & Guiu S, 2012). Chemotherapeutic drugs can be applied sequentially or in combination with other active cytotoxic agents depending on the patient status, its previous treatments and tumor characteristics (Morris PG *et al*. 2009).

DNA targeting agents include anthracyclines, gemcitabines and capecitabines. These agents induce cancer cell apoptosis through the inhibition of DNA synthesis. Doxorubicin is an anthracycline commonly used for several types of cancers due to its high efficacy against tumors. This chemotherapy drug intercalates between DNA base pairs causing deformation of the double helix, stabilization of the topoisomerase II-DNA complex and the induction of double strand breaks (Hortobagyi GN, 1997; Morris PG *et al*. 2009).

MTAs (Microtubule Targeting Agents) include vinca alkaloids, colchicinoids, eribulin, taxanes and epothilones. These cytotoxic drugs inhibit cell proliferation through the modulation of mitotic spindle formation and chromosome attachment, which causes mitotic arrest and cell death. Recent observations have shown that MTAs can also have anti-migratory and anti-angiogenic properties when used at low concentrations (Yang H *et al*. 2010; Fumoleau P & Guiu S, 2012; Pagano A *et al*. 2012). MTAs mainly target the microtubule cytoskeleton and mitotic spindle that will be reviewed in details in chapter 3.3.

2. Breast Cancer Metastasis

Cancer metastasis, the ability of tumor cells to disseminate and grow at secondary sites, is a fatal complication of breast cancer. Approximately 10-15% of women diagnosed with breast cancer develop distant metastasis within 3 years after detection of the primary tumor (Weigelt B *et al*. 2005, Scully OJ *et al*. 2012).

Several studies have reported that breast cancer cells can metastasize to different distant organs, with preference for the lungs, liver and bones (Figure 11) (Weigelt B *et al*. 2005).

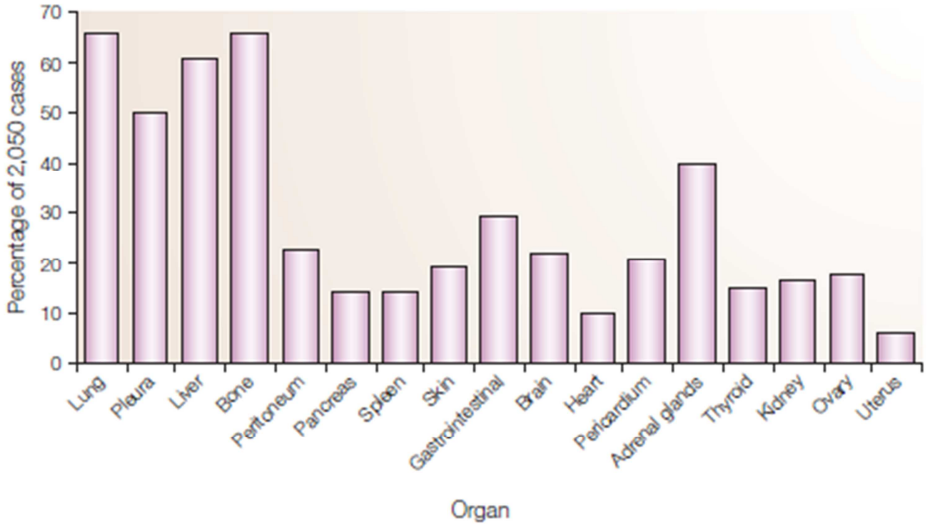

Figure 11

Most common metastatic sites of breast cancer cells. Lungs, liver and bones are the organs of preference to metastasize (From Weigelt B *et al*. 2005).

2.1.The metastatic process

Metastasis is a complex multistep process which mainly depends on cancer cell properties and tumor microenvironment (Guise T, 2010). Failure to achieve one of the steps of the process will stop it (Poste G & Fidler IJ, 1980).

The metastatic process (Figure 12) starts with the local invasion of the surrounding tissue by cancer cells. As the tumor grows, a higher requirement of oxygen and nutrients will activate neoangiogenesis, which in turn will contribute to tumor progression. In highly aggressive tumors, metastatic cells will detach from the primary tumor, invade the surrounding stroma, migrate until they reach the blood or lymphatic vessels in which they enter by intravasation (Hunter KW *et al*. 2008; Guise T, 2010; Scully OJ *et al*. 2012).

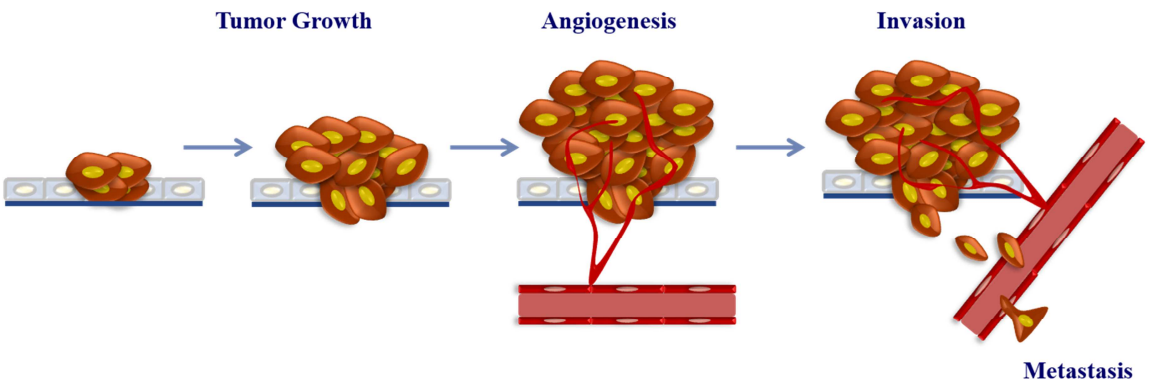

Figure 12

The metastatic process. Metastasis to a secondary organ is the result of several steps that include tumor growth, angiogenesis, invasion of the surrounding tissue, intra and extravasation and final colonization of the new tissue (From Nahmias C & Rodrigues-Ferreira S. *Accepted, Waiting for Copy Editing*).

Even if a large number of cells reach the blood flow, most of them stay quiescent or do not survive host defense mechanisms and stressful microenvironments, leading to the notion that metastasis is an inefficient process (Chambers AF *et al*. 2002; Hunter KW *et al*. 2008; Scully OJ *et al*. 2012). However, those few circulating tumor cells (CTC) capable to arrest and cross the vasculature endothelium, a process termed extravasation, are suitable to grow as a metastasis in a distant organ (colonization) (Hunter KW *et al*. 2008). Interestingly, the organ distribution of full-blown metastasis is not random. In 1889 Stephen Paget proposed that metastatic cancer cells (or seeds) would only colonize organ microenvironments (or soils) that were compatible with their growth (Paget S, 1889). In this line of thought, metastatic tropism will depend on the viable premetastatic niche within the target organ and on the display of the appropriate functions of the metastatic cell to effectively colonize the new organ (Reviewed in Gupta GP & Massagué J, 2006). The generation of a viable niche has been extensively studied, however this will not be detailed here.

2.2.Tumor cell invasion and migration

Tumor cell invasion, the first step of the metastatic process, refers to the penetration of tissue barriers, such as basement membrane and interstitial stroma, by cancer cells. Cell invasion is a heterogeneous, adaptive and cyclic process in which the cell adheres, degrades the extracellular matrix (ECM) components and changes its shape to produce a

morphological asymmetry resulting in a gain of migratory skills (Friedl P & Alexander S, 2011).

Cell migration is an essential process of normal cells during embryogenesis, development, tissue regeneration and immune-cell trafficking. Even if the migration process is increased and deregulated in cancer, tumor cells use mechanisms that are similar to those that occur in normal cells during physiological processes to spread within the tissues (Friedl P & Wolf K, 2003).

Two types of cell migration (single and collective) have been described for cancer cells (Figure 13). The way cancer cells migrate depends on the tumor type, its differentiation stage and the surrounding microenvironment. Thus, epithelial tumor cells (as breast cancer cells) are more prone to migrate in a collective manner, while lymphomas, leukaemias and most of the solid stromal tumors (such as sarcomas) spread by single cell migration (Friedl P & Wolf K, 2003; Yilmaz M. *et al*. 2007; Vicente-Manzanares M & Horwitz AR, 2011; Friedl P & Alexander S, 2011).

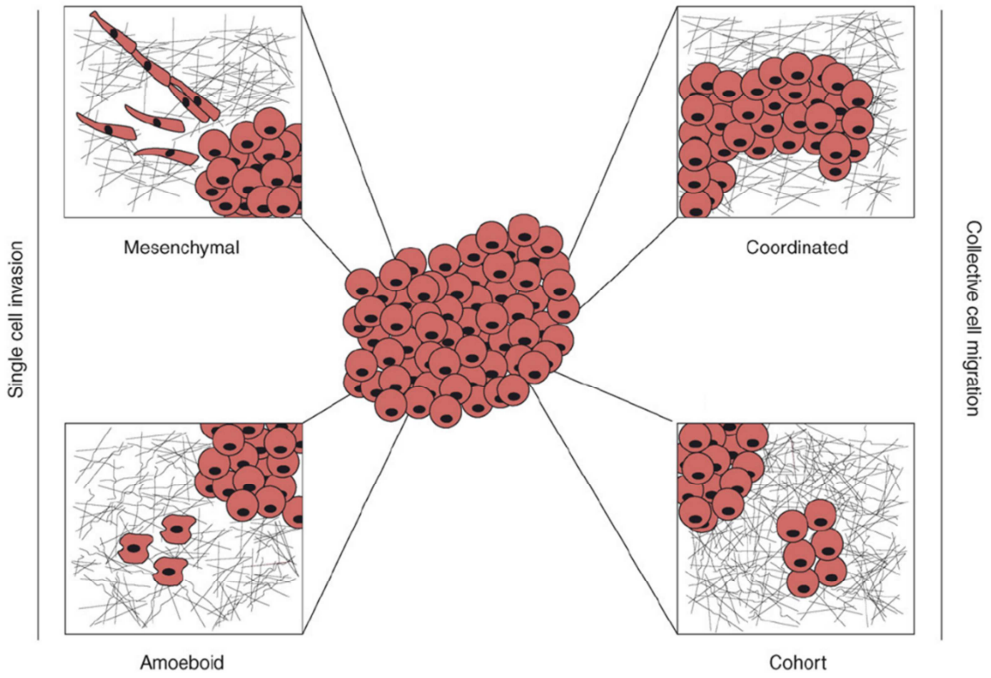

Figure 13

Different types of cell migration. Tumor cells can migrate alone (single mesenchymal or amoeboid cell migration, left side) or grouped (collective coordinated or cohort cell migration, right side) (From Yilmaz M. *et al*. 2007).

2.2.1. Collective Cell Migration

Collective cell migration refers to the movement of a coherent cell group of up to several hundred cells. This migration type contributes to numerous normal processes including embryological development, development of glands and ducts of mammary tissue, formation of blood vessels by endothelial cells, lung formation and wound healing. Additionally, it has been described that multicellular structures of cancer epithelial cells (such as acini, cords, glands or cell strands) can penetrate the surrounding stroma as elongated strands of connected tumor cells (Hegerfeldt Y *et al*. 2002; Friedl P & Wolf K, 2003; Friedl P & Gilmour D, 2009; Friedl P *et al*. 2012).

Collective migration models stand for a structure where there is a leader cell (or several cells) at the migration front and follower cells behind. Considering that leader cells must pull the inner and trailing cells behind, collective migration depends on the strongly cell-cell adhesions provided by cell junctions (Hegerfeldt Y *et al*. 2002; Friedl P & Wolf K, 2003; Friedl P & Gilmour D, 2009; Friedl P *et al*. 2012). Thus, the leading cell will have one or several actin-rich protrusions, that will generate adhesive traction for forward movement, and matrix degradation activity to create a zone that guides the group (Wolf K *et al*. 2007). On the other hand, follower cells do not associate with the ECM directly, but will contact neighboring cells and intercellular matrix present along cell-cell junctions (Figure 14) (Friedl P *et al*. 2012).

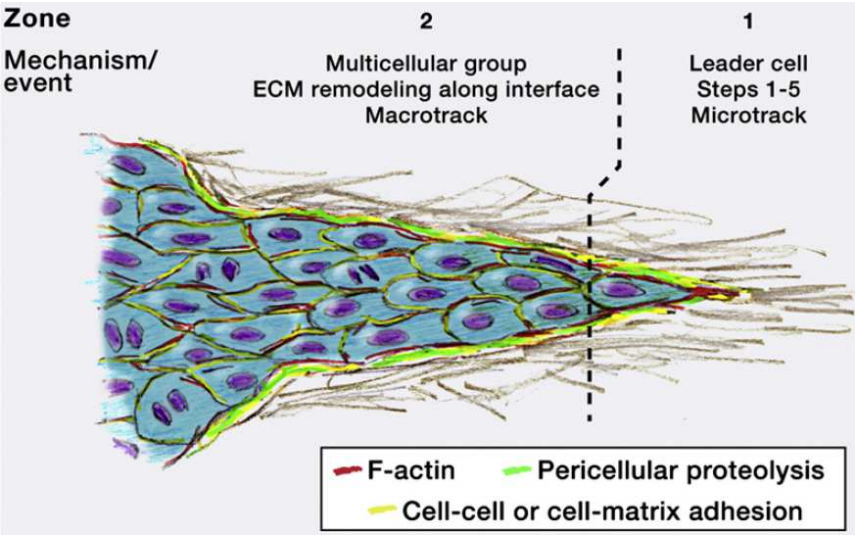

Figure 14

Collectively migrating cells form two major zones: zone 1, in which a leader cell generates a proteolytic track at the front of the migrating group, and zone 2, in which the subsequent cells then widen this track (From Friedl P & Alexander S, 2011).

Various subtypes of collective migration have been stratified according to the degree of cell-cell adhesion and the multicellular morphology. In fact, depending on cell-cell adhesion, cell-matrix adhesion, proteolysis and the type of tissue encountered, the size and shape of a collective invasion structure (and mostly its front) can vary. According to this, invading cell groups include strands of one or two cells in diameter, broad compact masses and masses that can form luminal structures (Figure 15).

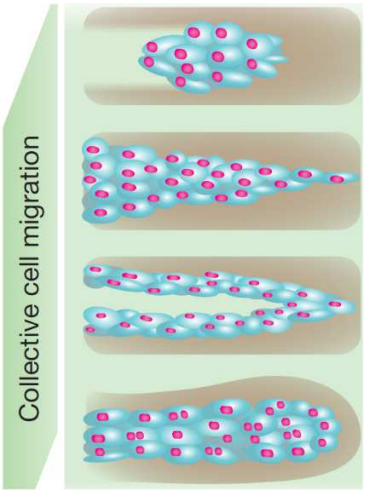

Figure 15

Schematic diagram of collective cancer cell migration (Modified from Friedl P *et al*. 2012).

Collective cancer cell migration can be classified in coordinated and cohort migration (Figure 13 and Figure 15). Coordinated migration consists in the sheet-like movement of tumor cells without detaching from the primary tumor. Contrariwise, cells that migrate in cohort detach from the primary site generating nests of migrating cells that can be detected at any stage of the metastatic process (Friedl P & Wolf K, 2003). Both subtypes of collective migration have been observed in invasive breast epithelial cancers (Friedl P *et al*. 1995; Nabeshima K *et al*. 1999; Nabeshima K *et al*. 2000).

Breast cancer cells can also migrate in a "chain manner" or multicellular streaming. In this type of migration, a leader cell directs the migration of a stream of followers through the matrix (Friedl P & Wolf K, 2003; Vicente-Manzanares M & Horwitz AR, 2011; Friedl P & Alexander S, 2011). It has been reported that chains of tumor cells can align between stromal fibers, a characteristic that improves the penetration mechanisms and thus, is associated with high metastatic capacity and poor prognosis (Friedl P & Wolf K, 2003; Bacac M & Stamenkovic, 2008; Roussos ET *et al*. 2011). Tumor cells sometimes follow nerve trajectories (perineural migration) and cancer-associated fibroblasts (CAFs) (Friedl P & Wolf K, 2003; Choi YP *et al*. 2014).

2.2.2. Single Cell Migration

The single cell migration process includes several steps that imply changes in cell morphology and stiffness (Figure 16). First, the cell has to polarize and elongate. A pseudopod is then formed, via the extension and ruffling of the leading edge which is mainly composed by an actin-rich lamellipodia. After protrusion formation, cell leading edge binds to the ECM substrate. Subsequently, cell contracts in order to allow the forward movement of the entire body and the trailing edge. Finally, disassembly of adhesion contacts at the trailing edge allows cell displacement (Friedl P & Wolf K, 2003).

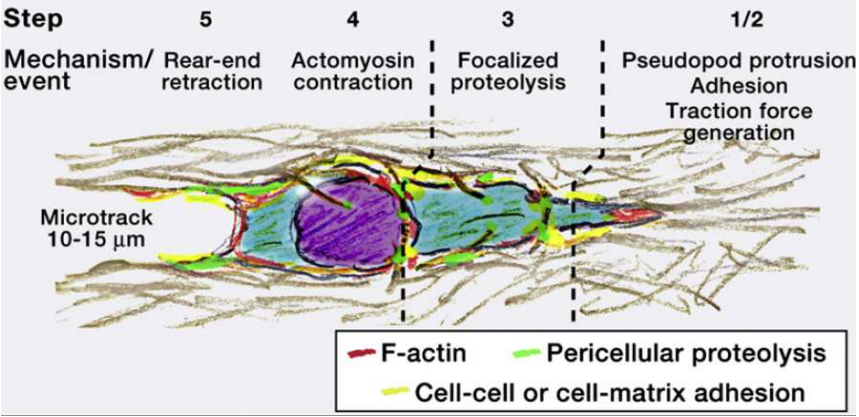

Figure 16

Single cell migration involves five molecular steps that change the cell shape, its position, and the tissue structure through which it migrates (From Friedl P & Alexander S, 2011).

Two types of single cell migration (mesenchymal and ameboid) have been described (Figure 13). Mesenchymal migration is characterized by the presence of fibroblast-like shape, increased cell invasiveness, increased cell-stroma interaction and decreased cell proliferation. This migration mechanism is dependent on ECM adhesion proteins, as well as on the activation of proteins involved in the matrix degradation (reviewed in Yilmaz M. *et al*. 2007, Friedl P & Alexander S, 2011).

In contrast, in the amoeboid phenotype, cells are more deformable due to weak interactions between the cell membrane and the matrix. The absence of mature adhesion contacts make these cells faster than mesenchymal migrating cells (10 to 30-fold higher velocities). Therefore, more than grip, the amoeboid cells have to adapt their morphology to preformed matrix structures in order to glide through (Friedl P & Wolf K, 2003; Yilmaz M. *et al*. 2007).

3. Microtubule (MT) Network

The eukaryotic cell cytoskeleton is a network composed of proteinaceous fibers and is required for the majority of essential cellular functions such as cell motion, cell division, intracellular transport and maintenance of cellular shape. It is a complex and often highly dynamic structure built of three major components: microtubules (MT), actin and intermediate filaments (IF) (Figure 17).

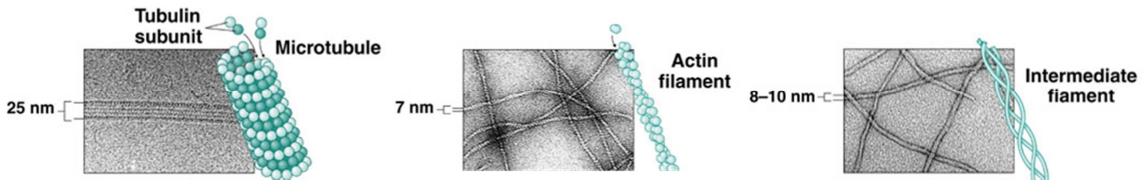

Figure 17

Microtubules, actin and intermediate filaments are the principal components of eukaryotic cell cytoskeleton (From Tobin & Dusheck, 2001).

Actin cytoskeleton is composed of semi-flexible filaments able to arrange in a variety of architectures, generating cellular organizations including branched or cross-linked networks in the lamelipodium, parallel bundles in filopodia and anti-parallel structures in contractile fibers (Blanchoin L *et al*. 2014). Intermediate filaments (IF) are assembled from a diverse group of fibrous proteins (such as vimentin and keratin) with intermediate size between actin and microtubules. IFs are elastic non-polarized fibers, expressed in a cell type-specific manner (Yi H & No Ku, 2013). Microtubules (MTs) are the subject of this third chapter: its organization, functions and the proteins capable to interact with them in order to regulate their dynamics will be described below.

3.1.Microtubule organization

Microtubules are cylindrical hollow tubes of 25 nm of diameter and variable length. They are composed of αβ tubulin heterodimers that are organized head-to-tail to form a polarized protofilament. Thirteen of these filaments will interact laterally to subsequently form the MT lattice (Figure 18) (Amos L & Klug A, 1974; Brinkley WBR, 1997; Desai A & Mitchison TJ, 1997; Valiron O *et al*. 2001).

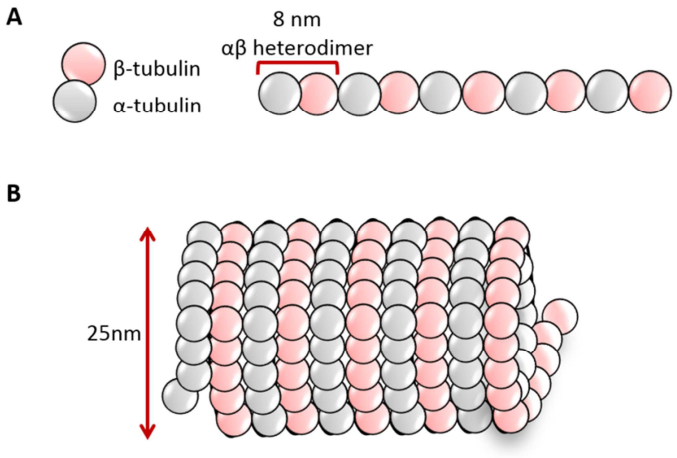

Figure 18

Microtubule structure. **(A)** Representation of the head-to-tail interactions of αβ dimers to form a linear protofilament. **(B)** Thirteen linear protofilaments associate laterally to form a MT polymer.

Each tubulin monomer can be divided into three functional domains: the N-terminal domain containing the GTP-binding site, an intermediate domain containing the taxane-binding site in β-tubulin, and the C-terminal domain which contains the binding surface for motor proteins (Figure 19) (Nogales E *et al*. 1998).

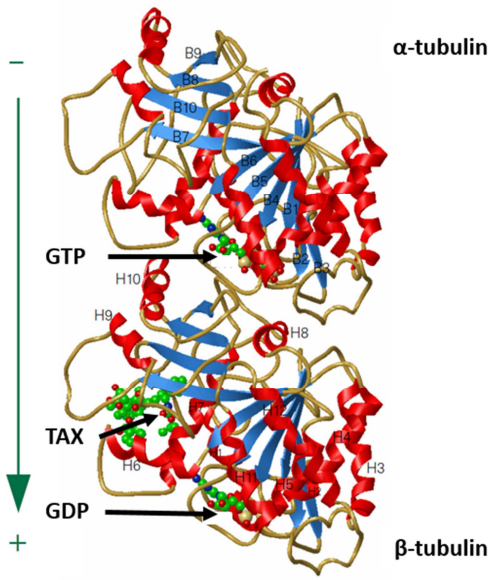

Figure 19

Ribbon diagram of the tubulin dimer showing α-tubulin with bound GTP (top), and β-tubulin containing GDP and taxane (TAX) (bottom). Green arrow indicates the direction of the protofilament and MT axis (Modified from Nogales E *et al*. 1998).

Even if α- and β-tubulin are similar, there are two unambiguous ways to distinguish them: (i) β-tubulin binds to taxanes, and (ii) β-tubulin monomer contains an exchangeable (E) GTP site, while the α-tubulin monomer has the non-exchangeable (N) site, always filled with GTP (Spiegelman BM *et al*. 1977; Hyman AA *et al*. 1992; Valiron O *et al*. 2001).

The denomination of E site on β-tubulin monomer owes to the possibility of binding GTP or GDP. During or after αβ tubulin dimers addition to the protofilament, GTP hydrolyzes to GDP and the latter gets locked in the protofilament during MT growing. After depolymerization, the GDP-β tubulin exchanges to GTP in solution (Hyman AA *et al*. 1992).

MTs display an intrinsic polarity, generated by the head-to-tail assembly of tubulin dimers, with one end growing at three times the rate of the other (Summers K & Kirschner MW, 1979). The faster growing and more dynamic extremity is termed the plus-end and the slower growing extremity, the minus-end (Allen C & Borisy GG, 1974). Experiments using GTP-coated fluorescent beads showed that GTP specifically binds to the plus-ends, indicating that β-tubulin monomer is exposed toward the plus end, while the α-tubulin monomer is directed to the minus end (Mitchison TJ, 1993). This observation was further confirmed when beads coated with anti-α-tubulin antibodies were shown to bind the minus end of MTs (Fan J *et al*. 1996).

MT minus-ends are usually capped by centrosomal proteins. From the centrosome or MTOC (for MicroTubule Organizing Center), MTs grow out and their plus-ends explore the cytoplasmic space, often interact with the cell cortex and work as a search-and-capture tool (Mimori-Kiyosue Y & Tsukita S, 2003; Honoré S *et al*. 2005; Bornens M, 2008). The polarity of MTs is important to the function of motor proteins, kinesins and dyneins, which use ATP hydrolysis to transport various cargos along MTs (Desai A & Mitchison TJ, 1997).

MTs within cells can be found in two states: (i) transiently unstable, as the radial array in interphase cells, the bipolar spindle during mitosis and meiosis, the parallel array in polarized cells and the linear array in neuronal extensions, or (ii) highly stable, like in the centrioles, basal bodies and axonemes of cilia and flagella (Brinkley WBR, 1997).

3.2.Microtubule dynamics

Microtubules are dynamic polymers that cannot be understood in terms of the classical polymerization theory of Oosawa F (1970), where subunit exchange at polymerization state was limited to the slow association-dissociation of tubulin dimers at MT ends. Rather they present a non-equilibrium dynamic behavior which allows the organization and rapid

remodeling of the cytoskeleton, allowing MTs to search in the three-dimensional space (Kirschner M & Mitchison T, 1986; Holy TE & Leibler S, 1994).

In order to explain what MT dynamics means, several studies were performed *in vitro* and *in vivo*. Some of these studies and the important concepts are listed below.

3.2.1. MT dynamics *in vitro*

The characterization of the dynamic properties of MTs began when, in 1972, Weisenberg RC discovered that pure tubulin self assembles and disassembles in the presence of GTP. Later on, observation of continuous incorporation of tubulin into MT, when polymer length is constant, led to the concept of treadmilling (Margolis RL & Wilson L, 1978; Margolis RL & Wilson L, 1998). Treadmilling is defined as the unidirectional flux of tubulin subunits from one polymer end to another. This concept indicates that a treadmilling MT might have a constant assembly rate of tubulin subunits at one end, with a balanced loss at the opposite end (Margolis RL & Wilson L, 1998).

A few years later, in 1984, the observation of a population of fixed MTs by Mitchison and Kirschner led to the discovery of a new MT dynamic mechanism termed dynamic instability (Mitchison T & Kirschner M, 1984). In this process MTs switch between continuous phases of polymerization and depolymerization. Soon after, a large number of studies using differential interference contrast (DIC) microscopy confirmed this concept and dynamic instability became the predominant mechanism to explain MT dynamics (Horio T & Hotani H, 1986; Cassimeris LU *et al*. 1987; Hotani H & Horio T, 1988; Walker RA *et al*. 1988; Gelfand VI & Bershadsky AD, 1991; Erickson HP & O'Brien ET, 1992).

To date, MT dynamic instability is described as a three-state model that includes MT growing, MT pause and MT shrinking (Figure 20). MT growing or polymerization stands for the elongation of the lattice in a GTP-tubulin concentration dependent manner. This elongation was described by Chrétien D *et al*. (1995) as the extension of protofilaments rather than the helical subunit addition (Figure 20, upper panel).

During or soon after polymerization, GTP hydrolyzes to GDP, a process not required for further polymerization but essential for dynamic instability (Hyman AA *et al*. 1992; Caplow M *et al*. 1994). In fact, Caplow M and coworkers (1994) showed that the free energy released after GTP hydrolysis is store in the MT lattice as a mechanical strain and might destabilize the MT network. Unstable GDP-microtubules undergo catastrophe, releasing the energy that in turn promotes and maintains rapid depolymerization. Additionally, Melki R *et al*. (1989) provided a model where GTP hydrolysis causes a change in tubulin conformation, having GTP-tubulin with a "straight" conformation and GDP-tubulin with a

"curved" conformation. Curved protofilaments peel outwards and promote MT depolymerization.

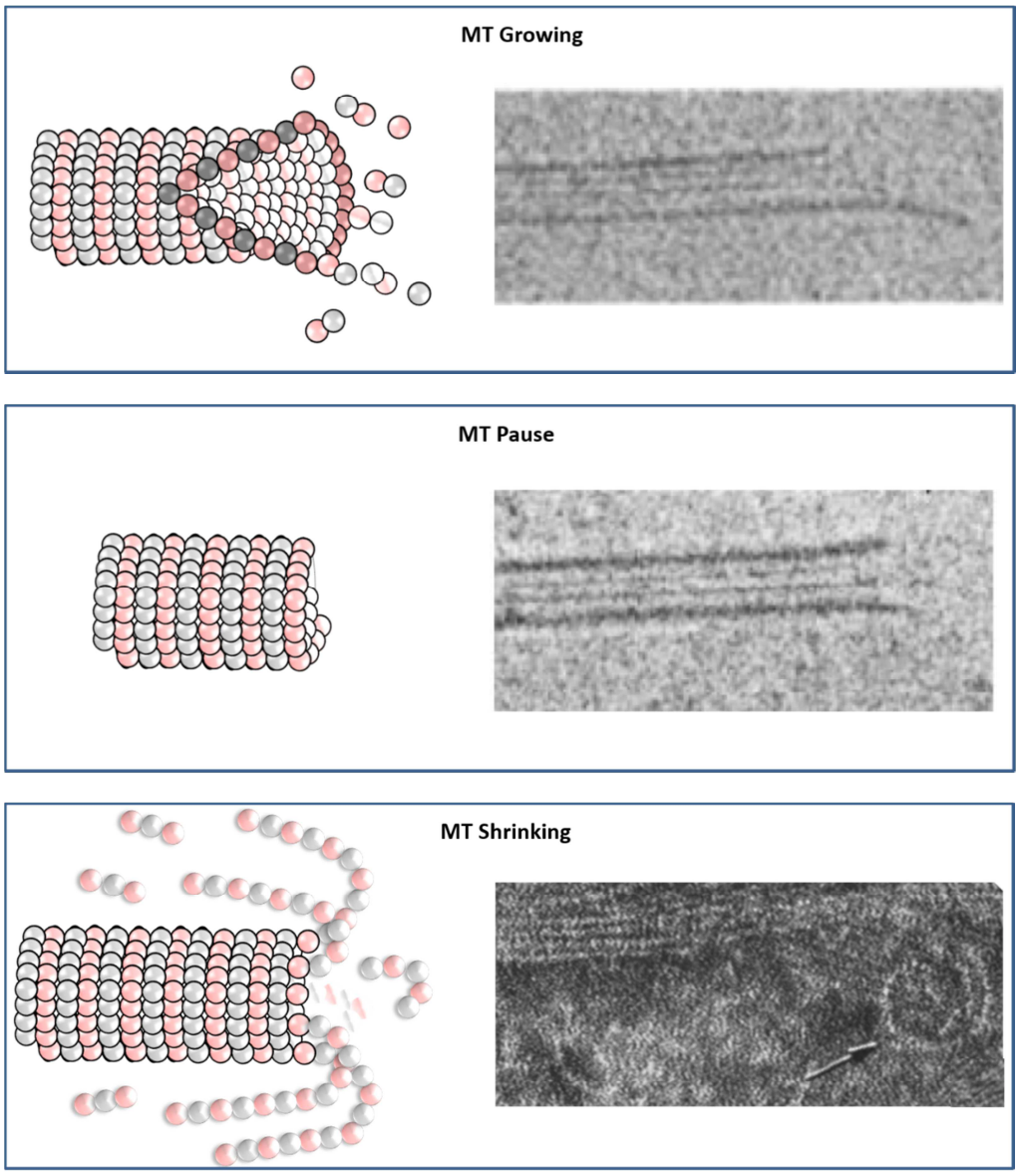

Figure 20

MT dynamics *in vitro* and *in vivo*. Microtubules can polymerize (upper panel), stay in pause (middle panel) or depolymerize (lower panel). Cryoelectron microscopy pictures are from Chrétien D *et al*. 1995 (growing), Janosi IM *et al*. 2002 (pause) and Warner FD & Satir P, 1973 (shrinking).

This unstable “curved” lattice promotes the disassembly of the polymer. During MT shrinking, GDP-tubulin is released from the MT end. Cryoelectron microscopy studies revealed that depolymerizing ends contain highly curved protofilaments (Figure 20, lower panel) (Mandelkow EM & Mandelkow E, 1985; Mandelkow EM *et al*. 1991; Tran PT *et al*. 1997) suggesting that the driving force for MT depolymerization is the curling up of protofilament ends.

Finally, MTs can undergo pause moments, where MTs do not grow nor shrink (Figure 20, middle panel). Pauses were described by Keller PJ *et al*. (2007) as stochastic events that were not so commonly seen *in vitro* (Walker RA *et al*. 1988; Shelden E & Wadsworth P, 1993). Chrétien D *et al*. (1995) described MT pause as the moment when protofilament sheets close to form the cylindrical shape of MTs. This process could occur at a variable rate and as MTs cannot stay in this close shape for long time, it would finish by the induction of depolymerization.

Four parameters have been proposed to describe MT dynamic instability: growth rate, shrinking rate and frequencies of catastrophes (transition from polymerization to depolymerization) and rescues (transition from depolymerization to polymerization) (Figure 21).

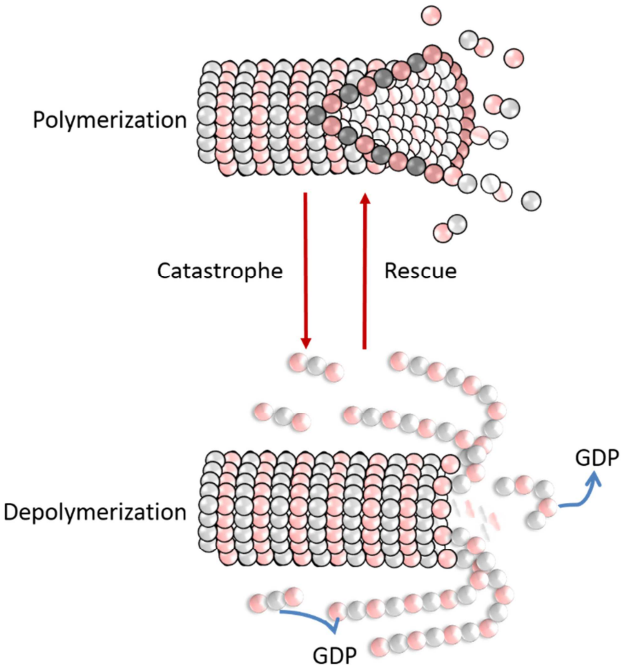

Figure 21

MT dynamic instability is characterized by continuous cycles of polymerization, where GTP-tubulin is added to the plus end of the MT, and depolymerization, where GDP-tubulin is rapidly released from the lattice. Catastrophe and rescue transitions are indicated as red arrows.

The growth velocity depends on the soluble tubulin concentration, on the rate constant for GTP-tubulin association, the temperature and the presence of MAPs. In contrast, the shortening rate does not depend on tubulin concentration but it depends on temperature and presence of MAPs. The catastrophe (or rescue) frequency is calculated as the number of catastrophes (or rescues) observed during the total time the MT spends in growing state. Erickson HP and O'Brien ET (1992) showed that *in vitro* catastrophe frequencies were lower than rescue frequencies in both the plus and minus ends. Nevertheless, these MT dynamic instability parameters can vary according to tubulin concentration and polymerization buffer composition.

All MT dynamic instability parameters can be visualized and determined on kymographs (Smal I *et al*. 2009). Kymographs are graphical representations of spatial position over time (Figure 22).

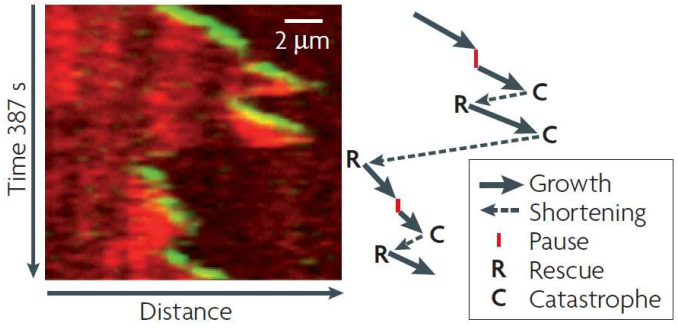

Figure 22

Kymograph representation showing different phases of MT dynamic instability. The spatial axis shows a MT visualized with mCherry-α-tubulin in red and its growing end stain with EB3-GFP in green (From Akhmanova A & Steinmetz MO, 2008).

In vitro minus-ends are able to assemble and disassemble pure tubulin and thus exhibit dynamic instability as the plus-ends but with slower rate constants (Walker RA *et al*. 1988).

3.2.2. MT dynamics *in vivo*

Current models of MT dynamics accept both treadmilling and dynamic instability as intrinsic properties of MTs that coexist in cells. Treadmilling have been reported in the mitotic spindles even if the MT ends are anchored at the spindle poles and kinetochores (Rodionov VI & Borisy GG, 1997; Waterman-Storer CM & Salmon ED, 1997; Margolis RL & Wilson L, 1998).

MT dynamic instability *in vivo* shares most characteristics with the *in vitro* model, except that cellular MTs have higher assembly rates (up to 10 times faster), more transition frequencies (Cassimeris L, 1993) and more frequent pause events (Keller PJ *et al*. 2007). Moreover, MT dynamics *in vivo* can vary according to regulatory signals (interphase versus mitosis) (reviewed in McNally FJ, 1996), cell type (Bré MH *et al*. 1990; Bass PW *et al*. 1991), measured zone inside the same cell (Komarova YA *et al*. 2002b), and differentiation stage (Bulinsky JC & Gundersen GG, 1991).

The most important function of MTs is their participation in mitosis, as segregation of chromosomes towards cell poles during anaphase requires regulated and coordinated MTs dynamics. However, MT dynamic instability in living cells also allows MT spatial organization, rapid remodeling of the cytoskeleton and cell shape (Figure 23A). Additionally, this permits MTs to search and find specific targets (search-capture model) and guides MTOC movement (Figure 23B).

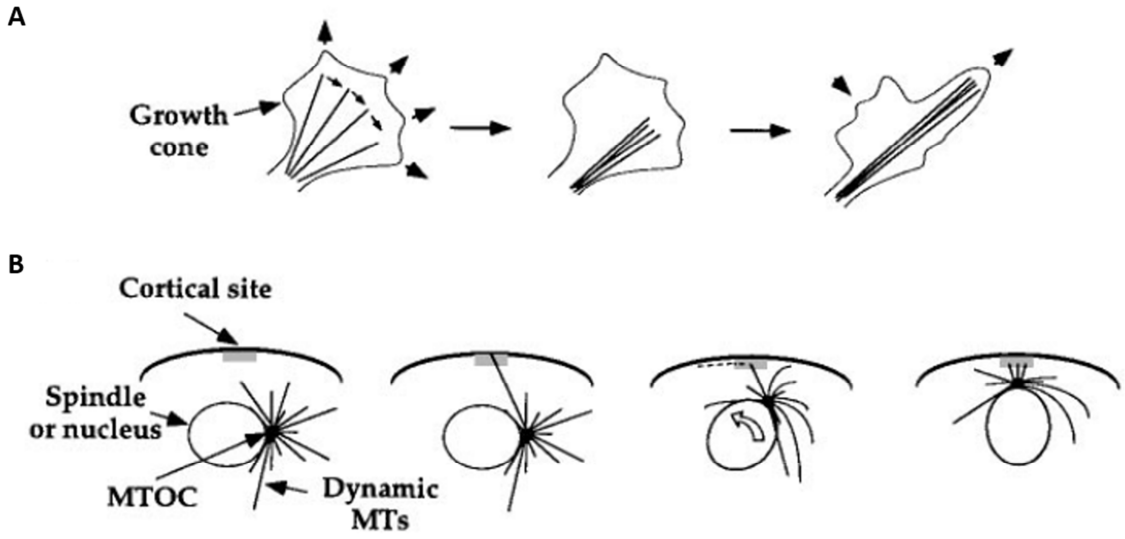

Figure 23

MT dynamic instability allows cytoplasm and cell shape remodeling **(A)** and interphase centrosome positioning to a specific cortical site **(B)** (From Desai A & Mitchison TJ, 1997).

But MT dynamics not only depends on tubulin polymerization/depolymerization. Dynamic instability is also regulated by tubulin post-translational modifications and by microtubule-associated proteins (MAPs). Of importance, microtubule-targeting agents (MTAs) also act by modulating MT dynamic instability parameters.

3.3. Microtubule-targeting agents (MTAs)

Microtubule-targeting agents constitute a class of chemotherapeutic drugs that target microtubules and disrupt the normal function of the mitotic spindle to cause cancer cell death by mitotic arrest. Microtubule targeting agents (MTA) can be classified in microtubule (MT)-stabilizing and destabilizing drugs according to their effects on MT dynamics (Figure 24).

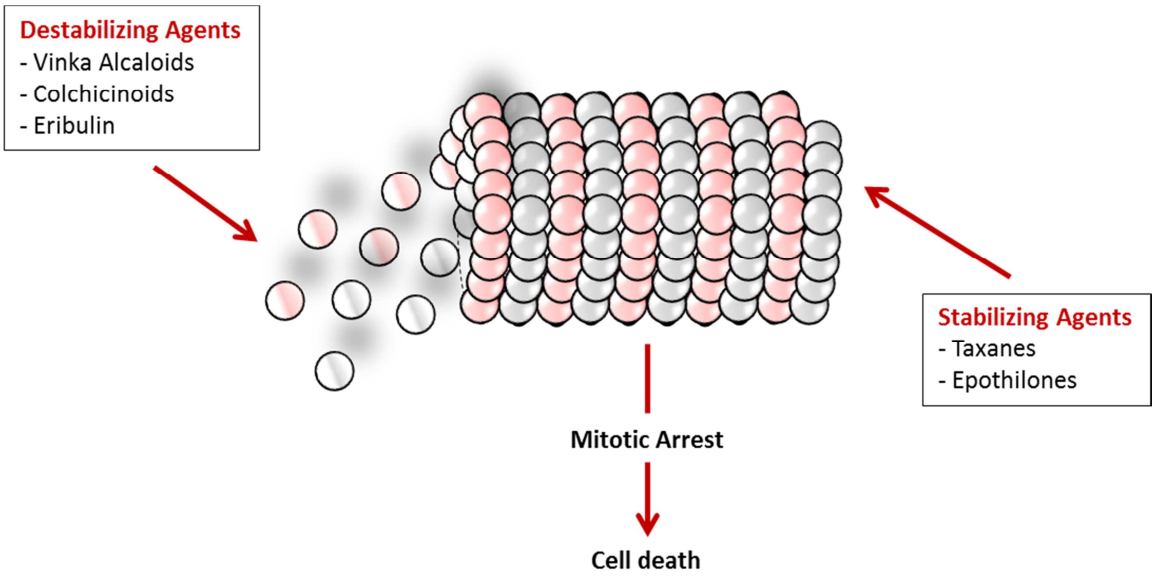

Figure 24

Effect of Microtubule Targeting Agents (MTAs) on microtubule dynamics. MTAs can destabilize (left side) or stabilize (right side) the MTs in order to induce cancer cell apoptosis.

Some representatives of MT-destabilizing agents are the vinca alkaloids, the colchicinoids, and eribulin (Figure 24). The vinca alkaloids (vincristine, vinblastine, vinorelbine) prevent MT polymerization by binding to β-tubulin subunits, which causes a metaphase arrest. These agents also decrease polymerization and depolymerization velocities and increase the percentage of time MTs spend in an attenuated or paused phase (Himes RH, 1991; Jordan MA *et al*. 1992; Morris PG *et al*. 2009; Fojo AT & Adelberg DE, 2010). Vinka alcaloids are currently used in clinics, however, an inconvenient reported for these cytotoxic agents is the sensitivity to cancer cells resistance pumps (Fumoleau P & Guiu S, 2012).

Binding of colchicine to tubulin induces a conformational change in the tubulin that locks the colchicine in a complex where it can poorly dissociate. Colchicine depolymerizes MTs,

inhibits MT polymerization and increases the time MTs spend in pause state (Reviewed in Fojo AT & Adelberg DE, 2010).

Eribulin is a destabilizer molecule which acts through the suppression of microtubule growth (with no effect in the shortening) and sequestration of tubulin into nonproductive aggregates. Thus, tubulin retention impedes mitotic spindle formation inducing a mitotic blockage (Cortes J *et al*. 2012; Scarpace SL, 2012).

The second group of MTAs is the MT-stabilizing agents. MT-stabilizing agents are mainly composed by Taxanes and epothilones (Figure 24). Taxanes bind tubulin to inhibit MT depolymerization, enhance MT assembly, and thereby bundling and stabilizing MTs (Morris PG *et al*. 2009; Fojo AT & Adelberg DE, 2010; Pagano A *et al*. 2012). Paclitaxel and Docetaxel are widely used for the treatment of metastatic breast cancer. Nevertheless, two complications are associated with taxane use: toxicity (neurotoxicity and hematopoietic toxicity) and acquired tumor resistance (Morris PG *et al*. 2009).

Epothilones treatment is frequently used in taxane-resistant and taxane-insensitive tumors. Epothilones and ixabepilones are natural antibiotics that bind to microtubules in the taxane-binding site and are involved in tubulin polymerization, MT bundling and the inhibition of depolymerization (Morris PG *et al*. 2009; Fojo AT & Adelberg DE, 2010; Pagano A *et al*. 2012).

Even if these agents are used to impede tumor progression, the risk of treatment resistance and patient relapse along with the acute and long-term side effects of the chemotherapy, have created an urgent need to understand how endogenous factors modulate MT dynamics in order to target them as tools against cancer.

3.4.Microtubule post-translational modifications

The MT network is composed by sets of dynamic and stable MTs. Stable MTs can incorporate several post-translational modifications mostly in the C-terminal tail of both, α- and β-tubulin. As these tails are located on the outside of the microtubule, they are therefore well positioned to influence interactions with other proteins (Westermann S & Weber K, 2003; Verhey KJ & Gaertig J, 2007).

MT post-translational modifications are conserved throughout evolution and are thought to act (individually or in combination) to regulate specific MT based functions (Hammond JW *et al*. 2008). Some of these modifications are described in Table 2 and in Figure 25 and

include acetylation, detyrosination, polyglutamylation, polyglycylation and phosphorylation.

Acetylation occurs in lysine 40 of α-tubulin; it is a very common modification that can be found on stable MTs in most cell types (Hammond JW *et al*. 2008). It has been reported that acetylated MTs are more resistant to depolymerization by nocodazole but are not protected against cold depolymerization (Piperno G *et al*. 1987).

Detyrosination involves the removal of the C-terminal tyrosine of α-tubulin in MTs, generating a detyrosinated tubulin (also known as Glu-tubulin) which has been observed in long-lived MTs (Westermann S & Weber K, 2003; Verhey KJ & Gaertig J, 2007). Removal of the preceding glutamate residue in Glu-microtubules results in Δ2-tubulin. This type of tubulin is found in neurons and axonemes, where MTs are also highly polyglutamylated (Lafanechère L & Job D, 2000)

Polyglutamylation and polyglycylation are post-translational modifications in which glutamate and glycine side chains of variable length are added to glutamate residues in the C-terminal tails of both α and β-tubulin. Glycylation is mostly found in axonemes of motile cilia and flagella, whereas, glutamylation is present on MTs in neurons, centrioles, mitotic spindle and cilia (Westermann S & Weber K, 2003; Verhey KJ & Gaertig J, 2007).

Tubulin modifications can have different biological roles. For example, decreased MT acetylation increases cell motility (Hubbert C *et al*. 2002); polyglycylation and polyglutamylation are important for axonemal structure, ciliary motility and cytokinesis (reviewed in Verhey KJ & Gaertig J, 2007); and deregulation in the tyrosination/detyrosination cycle result in spindle orientation defects (Peris L *et al*. 2006).

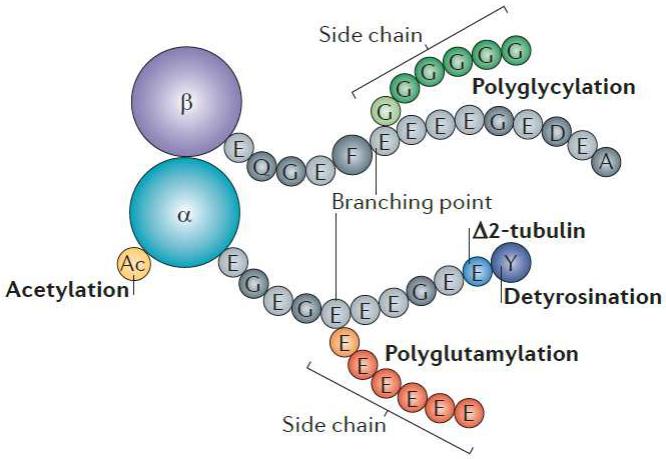

Figure 25

Tubulin post-translational modifications. The C-terminal tails of α and β tubulin can be modified by different enzymes in order to polyglycylate, detyrosinate, polyglutamylate or acetylate (From Janke C & Bulinski JC, 2011).

Finally, MT modifications are linked to MT dynamics regulation: they work as a readable code for the recruitment of MAPs and motor proteins (reviewed in Janke C & Kneussel M, 2010; Wloga D & Gaertig J, 2010).

Table 2

Tubulin post-translational modifications (Modified from Westermann S & Weber K, 2003; Verhey KJ & Gaertig J, 2007).

Modification	Description	Site	Proposed Function	Comments
Acetylation 	Addition of acetyl group	Lys40 of α-tubulin	Regulation of cell motility, binding of MAPs to microtubules	Marker for stable MTs
Detyrosination 	Removal of tyrosine	C-terminal tail of α-tubulin	Crosstalk to intermediate filaments; differentiation	Reversible
Δ2 Tubulin 	Removal of penultimate glutamate from detyrosinated tubulin	C-terminal tail of α-tubulin	Removing tubulin from tyrosination cycle; marking MTs for polyglycilation	Marker for stable MTs
Polyglutamylation 	Addition of one or more glutamates as a side chain	C-terminal tail of α- and β-tubulin	Centriole maturation and stability; flagellar and cilliary motility; regulation of interaction with MAPs	Up to 20 side-chain residues
Polyglycylation 	Addition of one or more glycines as a side chain	C-terminal tail of α- and β-tubulin	Essential in *Tetrehymena* for: axonemal organization, cilliary motility, cytokinesis (severing of MTs)	Up to 30-40 side-chain residues
Phosphorylation 	Addition of phosphate	Ser172/441/444 of β-tubulin, unknown sites of α-tubulin	Neuronal differentiation?	

3.5.Microtubule-regulating proteins

MTs are controlled by factors that regulate different parameters of their dynamics. These factors can act directly or indirectly through the action of other proteins (Lyle K *et al*. 2009a; Lyle K *et al*. 2009b).

All MTs regulators are Microtubule-Associated Proteins (MAPs) able to interact with tubulin or MTs *in vitro* or *in vivo*. A particular group of MAPs that act predominately at the MT growing end are the plus-end tracking proteins (+TIPs) that will be reviewed below in chapter 3.6. MT-regulating proteins can be classified in two main groups: proteins that stabilize MTs and proteins that destabilize them.

3.5.1. Microtubule-stabilizing proteins

MTs can be stabilized by different ways: by promoting polymerization, by preventing catastrophes, by rescuing depolymerizing MTs, by decreasing shrinking velocity, by bundling or by capping MTs. According to these characteristics, a large number of proteins are able to stabilized MTs and can be grouped in five categories: (i) classical MAPs, (ii) MT assembly promoters, (iii) MT stabilizers with mitosis-specific functions, (iv) MT stabilizers through cell cortex interaction, and (v) other MT-stabilizing proteins (Lyle K *et al*. 2009a; Lyle K *et al*. 2009b).

The first proteins reported as MT stabilizing factors were the classical MAP proteins. The MAP family of proteins has been extensively studied and is mainly composed by MAP1 (MAP1A and MAP1B), MAP2 and Tau (which are highly abundant in neurons) and MAP4 (non-neuronal cells) (Desai A & Mitchison TJ, 1997). It has been reported that MAP1A, MAP1B, MAP2 and Tau are able to (i) reduce catastrophe frequencies, (ii) increase rescue frequencies and therefore they are able to (iii) reduce tubulin turnover rates and (iv) increase steady state tubulin. Additionally, these proteins can inhibit protofilament peeling and thus depolymerization induction (Drechsel DN *et al*. 1992; Pryer NK *et al*. 1992; Dehmelt L & Halpain S, 2005). Contrariwise, MAP4 is able to increase rescue frequencies without changing catastrophe frequency (Ookata K *et al*. 1995).

The group of MT assembly promoters is mainly composed by MAPs that accumulate at the MT growing end, i.e. +TIPs. End-binding proteins (EBs), chTOG, CLIPs proteins and CRMP-2 are some examples of assembly promoters and are implicated in the promotion of rescue frequencies and in accelerating MT polymerization (Lyle K *et al*. 2009a). This group of proteins will be reviewed in detail in chapters 3.6 and 3.7.

MT stabilization also includes its capping at both ends, the plus-ends and the minus-ends. During mitosis, MTs can be captured at spindle poles by NuMA (Nuclear protein that

associates with the Mitotic Apparatus), RHAMM (Receptor for Hyaluronan-Mediated Motilty), TACC (Transforming Acidic Coiled-Coil) proteins and TPX2 (Targeting Protein for Xklp2). All these proteins play a role organizing the MTs at the polar region of the mitotic spindle (Gaglio T *et al*. 1995; Maxwell CA *et al*. 2003; Fant X *et al*. 2004; Barros TP *et al*. 2005). In addition, proteins that capture MTs at kinetochores near the chromosomes includes the kinesin-7 CENP-E (CENtromere-associated Protein E) and NuSAP (Nucleolar Spindle-Associated Protein) (Yao X *et al*. 2000; Putkey FR *et al*. 2002; Raemaekers T *et al*. 2003; Manning AL & Compton DA, 2008), which have a relevant function in chromosome alignment at metaphase. Finally, some other MT-stabilizing proteins with mitosis-specific functions are Astrin, which localizes at spindle poles and kinetochores of bioriented chromosomes and functions to crosslink and stabilize MTs, and HURP (Hepatoma UpRegulated Protein), that is located at kinetochores fibers and contributes to chromosome alignment (Manning AL & Compton DA, 2008).

Representatives of the MT stabilizers through cell cortex interaction are APC (adenomatous polyposis coli), CLASPs (CLIP-associating protein) and the spectraplakins MACF/ACF7 (Microtubule-Actin Crosslinking Factor) which mediate interactions with cortical sites, Golgi and actin, respectively. These proteins and some stabilizers involved in MT capture will be described in chapter 3.6.

The last group of MT stabilizers includes some miscellaneous proteins such as CLAMP (CaLponin-homology And Microtubule-associated Protein) (Dougherty GW *et al*. 2005), VHL (von Hippel–Lindau) (Hergovich A *et al*. 2002; Thoma CR *et al*. 2010), YB-1 (Chernov KG *et al*. 2008), BPAG1 (Bullous Pemphigoid Antigen-1) (Yang Y *et al*. 1999), the formins Dia1 and Dia2 (Palazzo AF *et al*. 2001b; Gundersen GG *et al*. 2004; Wen Y *et al*. 2004; Bartolini F & Gundersen GG, 2010), MAP6/STOP (Guillaud L *et al*. 1998; Bosc C *et al*. 2003), tektins which crosslink and stabilize axoneme MTs in cilia and flagella (Steffen W & Linck RW, 1988; Tanaka H *et al*. 2004; Amos LA, 2008), MURFs (MUscle-specific RING-Finger proteins) that stabilize MTs in striated muscle (Spencer JA *et al*. 2000), Lis1 and Doublecortin that stabilize MTs during neuronal migration (Sapir T *et al*. 1997; Gleeson JG *et al*. 1999; Coquelle FM *et al*. 2002; Fourniol F *et al*. 2013), VAPs (Vesicle-Associated membrane Protein) that stabilize presynaptic MTs, the kinesin-5 Eg5, the MAP65 and DDA3 that are involved in MT bundling by crosslinking antiparallel MTs (Manning AL & Compton DA, 2008; Lyle K *et al*. 2009b).

3.5.2. Microtubule-destabilizing proteins

The difference in the catastrophe frequencies between free tubulin and tubulin in living cells suggests the presence of factors involved in the depolymerization of MTs. These

cellular factors would modulate MT dynamics *in vivo*, by promoting MT disassembly and increasing tubulin turnover. MT-destabilizing proteins include microtubule-associated proteins, microtubule-severing proteins and microtubules plus-ends tracking proteins (+TIPs).

It is now clear that the oncoprotein 18 (Op18)/stathmin is a catastrophe inducer, but its mechanism of action is still controversial. Some experimental observations stand for a hijacker effect of Op18/stathmin over tubulin dimers: as the oncoprotein is able to interact with free tubulin dimers it could reduce the available free tubulin concentration and thus induce MT depolymerization (Belmont L *et al*. 1996; Howell B *et al*. 1999a). Other studies suggest that Op18/stathmin may be a catastrophe promoting factor at the plus ends by promoting GTP hydrolysis without having an effect on MT growth rate (Howell B *et al*. 1999a; Howell B *et al*. 1999b). An interesting study showed that it was possible to dissociate the tubulin-sequestering and MT catastrophe-promoting activities *in vitro* by controlling the pH at which experiments were performed. At pH 6.8, Op18/stathmin acts through tubulin sequestration, and at pH 7.5 it acts as a catastrophe promoter (Howell B *et al*. 1999b).

Other MT disassembly promoters are the kinesin-8 KIF18A and the kinesins-13 KIF2A, KIF2B and KIF2C (MCAK). These kinesins are able to induce conformational changes in both the plus-ends and minus-ends that will trigger catastrophe (reviewed in Mayr MI *et al*. 2007 and Ems-McClung SC & Walczak CE, 2010). MCAK is the most studied MT depolymerase and will be described in more detail in chapter 3.6.

The last proteins that induce MT disassembly are the MT-severing proteins katanin, spastin and fidgetin. These three proteins are able to cleave the MT lattice, releasing free ends that will depolymerize. MT-severing proteins function to control the number and length of MTs, which is necessary for the assembly and dynamics of the mitotic spindle (McNally FJ *et al*. 1996; Zhang D *et al*. 2007). Indeed, katanin severs MTs near the plus-ends and helps depolymerization of MTs near the chromosome attachment site for continued movement of chromosomes towards spindle pole in late anaphase. In contrast, spastin and fidgetin sever MTs near the minus-ends to cause active depolymerization and to fasten chromosome movement towards the spindle pole (Ghosh DK *et al*. 2012).

3.6.Microtubule plus-ends tracking proteins (+TIPs)

Microtubule plus-end tracking proteins (+TIPs) belong to a class of MAPs that accumulate at the growing end of the MTs (Schuyler SC & Pellman D, 2001). When fused with a fluorescent tag, +TIPs appear as comets at the plus-ends which move throughout the cell

as the MTs grow to then disappear when MTs undergo catastrophe (Howard J & Hyman AA, 2003).

Since 1990 when CLIP170, the first MT plus-end tracking protein, was reported (Rickard JE & Kreis TE, 1990) a large number of proteins have been identified as +TIPs including motor, non-motor, MT polymerases, depolymerases, regulatory and adaptor proteins. Although these proteins are functionally diverse and structurally unrelated, they are often highly conserved in eukaryotes and associate preferentially with the growing and not the shrinking MT end (Mimori-Kiyosue Y *et al*. 2000; Schuyler SC & Pellman D, 2001; Akhmanova A & Steinmetz MO, 2008).

+TIPs are able to participate in MT dynamics regulation and in the coordination of cell architecture through their interaction with different proteins and/or cell structures.

3.6.1. Structural +TIPs classification

+TIPs are a very heterogeneous group of proteins that differ in structure, function, size and plus-end tracking mechanism. Structural classification will be the subject of this part of the chapter and includes: End-Binding family of proteins, Cytoskeleton-associated proteins Gly-rich (CAP-Gly) proteins, proteins that contain basic and Ser-rich sequence (SxIP) and MT motor proteins (Figure 26) (Akhmanova A & Steinmetz MO, 2008).

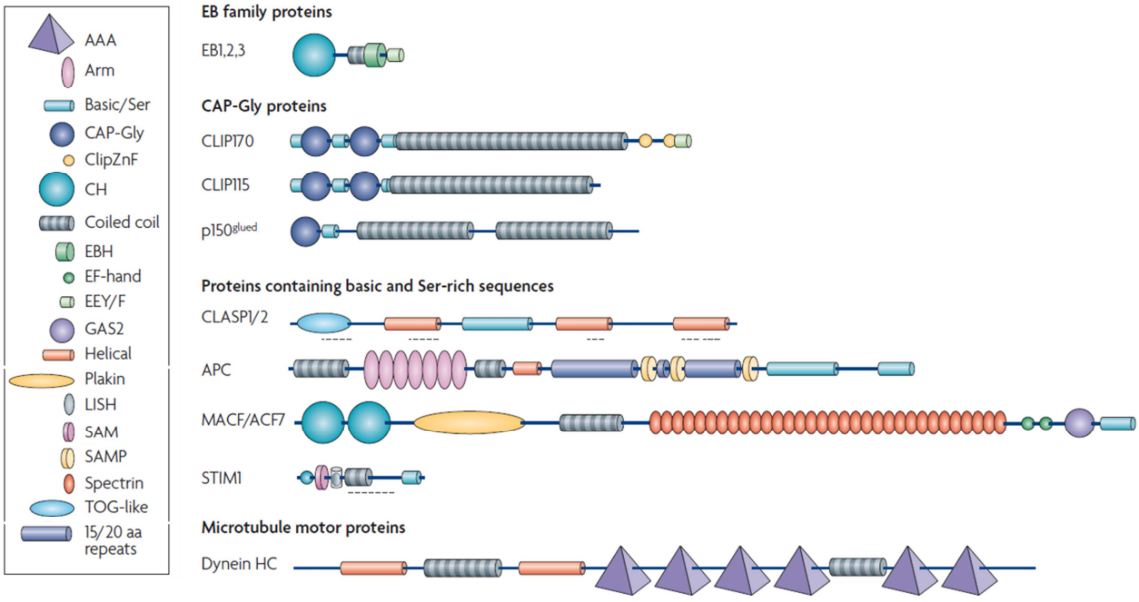

Figure 26

Structural classification of plus-end tracking proteins. Four groups of +TIPs have been described according to the structural elements that are involved in tracking the MT plus-end (Modified from Akhmanova A & Steinmetz MO, 2008).

End-binding (EB) family proteins are small globular dimers that contain highly conserved N- and C-terminal domains. The N-terminal domain is responsible for the binding to MTs (Hayashi I & Ikura M, 2003) while in the C-terminal region a coiled-coil domain allows the dimerization of EB monomers (Honnappa S *et al*. 2005). EBs are considered as the core of +TIP network, as they are able to interact with almost all CAP-Gly and serine-rich proteins. The specific details of EB proteins and their interactions will be discussed below (chapter 3.7).

The cytoskeleton-associated proteins Gly-rich (CAP-Gly) domain is a specialized module of approximately 80 residues that is highly conserved in eukaryotes (Riehemann K & Sorg C, 1993). This domain can be found in single or multiple copies and is involved in protein-protein interactions, in particular with α-tubulin monomers, dimers, MTs and EB proteins by the recognition of a C-terminal EEY sequence motif (Steinmetz MO & Akhmanova A, 2008).

CAP-Gly proteins include some +TIPs such as the cytoplasmic linker proteins (CLIPs) and the large subunit of the dynactin complex $p150^{glued}$. In these proteins the CAP-Gly domains are located in the N-terminal part and will interact with the C-terminal EEY motif on MTs and EB proteins (Honnappa S *et al*. 2006; Ligon LA *et al*. 2006; Mishima M *et al*. 2007).

CLIP170 was the first protein where the interaction between a CAP-Gly domain and MTs was shown (Pierre P *et al*. 1992) and also the first protein for which MT plus-end tracking behavior was described (Perez F *et al*. 1999). CLIP proteins contain two similar CAP-Gly domains surrounded by serine and basic residues rich regions in the N-terminal part, which contribute to MT interaction (Hoogenraad CC *et al*. 2000). CLIP170 is involved in MT dynamics in interphase and during mitosis (Arnal I *et al*. 2004; Tanenbaum ME *et al*. 2006) and in the recruitment of the MT minus-end-directed motor dynein to the MT growing end (Lomakin AJ *et al*. 2009).

The largest group of +TIPs are enriched in basic and serine residues. These regions, which are predicted to be flexible, often mediate interactions with MTs and EB proteins (Steinmetz MO & Akhmanova A, 2008; Kumar P & Wittmann T, 2012). Inside this region there is a small 4-residue motif SxIP (Ser-x-Ile-Pro) which is implicated in the targeting of a large number of +TIPs to the growing MT end in an EB1-dependent manner. This

conserved motif is now considered as a microtubule tip localization signal (MtLS) (Honnappa S *et al*. 2009).

Representative examples of this group of +TIPs are the adenomatous polyposis coli (APC), the mitotic centromere-associated kinesin (MCAK), TIP150, the MT-actin crosslinking factor (MACF or ACF7), the stromal interaction molecule 1 (STIM1), the CLIP-associating proteins (CLASPs), p140Cap, DDA3, RhoGEF2, Navigators, melanophilin and CDK5RAP2. I will review here a few SxIP-containing +TIPs that will be of relevance for this work.

APC is a highly conserved multidomain tumor suppressor implicated in the regulation of the Wnt signaling pathway (Mimori-Kiyosue Y & Tsukita S, 2001). Considering the different subcellular localizations of APC (Bienz M, 2002), it has been linked to multiple processes as cell migration, cell adhesion, chromosome segregation, spindle assembly, neuronal differentiation and apoptosis (Hanson CA & Miller JR, 2005; Aoki K & Taketo MM, 2007). Biochemical studies have mapped the EB1-APC interaction to a basic, serine-rich sequence of 39 residues in the APC C-terminal domain, termed APCp1 (Honnappa S *et al*. 2005) which contains one SxIP motif that allows tip tracking in living cells through interaction with EB1 (Berrueta L *et al*. 1998; Morrison EE *et al*. 1998; Mimori-Kiyosue Y *et al*. 2000).

MCAK was initially identified as a member of the KinI subfamily of kinesins and was classified as a MT depolymerase that induces conformational changes at the MT plus-end (Desai A *et al*. 1999). Later on, the kinesin nomenclature was standardized and MCAK (KIF2C) was grouped as a member of the kinesin 13 family along with mammalian KIF2A and KIF2B (Lawrence CJ *et al*. 2004; Moores CA *et al*. 2006). This family has a particular characteristic because rather than walk along MTs (as other kinesins), they use ATP hydrolysis to depolymerize MTs from both ends (Desai A *et al*. 1999; Hunter AW *et al*. 2003; Helenius J *et al*. 2006). MCAK is a homodimeric molecule with a motor domain located in the central part of the protein, which is involved in MT depolymerization *in vitro* and *in vivo* (Maney T *et al*. 2001; Newton CN *et al*. 2004; Ogawa T *et al*. 2004; Moores CA *et al*. 2006). In spite of being a MT depolymerase, MCAK is able to track MT plus-ends in living cells (Moore AT *et al*. 2005) by one-dimensional diffusion (Helenius J *et al*. 2006) or by its association with EB proteins via its basic/serine rich region and the SxIP motif located in the N-terminus of the protein (Lee T *et al*. 2008).

TIP150 was identified *in silico* as a +TIP candidate with an EB1-binding domain rich in serines, prolines and basic residues. Further experiments showed that it binds EB1 and tracks growing MT plus-end via an SxIP motif located in the C-terminal part of the protein. TIP150 also binds to MCAK and knockdown experiments suggested that TIP150 could play a role in targeting MCAK to the plus-end (Jiang K *et al*. 2009). Recently, a role has been

attributed to TIP150-EB1 interaction in the dynamic regulation of kinetochore MTs and chromosome alignment during metaphase (Ward T *et al*. 2013).

The last group of +TIPs comprises the motor proteins kinesins and dyneins. In eukaryotes, these motor proteins are essential partners of MTs during interphase and mitosis, and can accumulate at the MT plus-end through the association with other +TIPs (Akhmanova A & Steinmetz MO, 2008).

Kinesins were first described in neurons as plus-end directed motors needed for axonal transport (Vale RD *et al*. 1985). Later studies involved kinesins in the organization of the MT cytoskeleton in interphase, directional organelle movement and cell division (Wade RH, 2009).

Cytoplasmic dynein is a large multisubunit complex whose activity *in vivo* requires the dynactin complex (Wade RH, 2009). Dynein has relevant roles in minus-end transport of cargoes along the MTs, formation and orientation of the mitotic spindle and MT array, and in nuclear positioning (reviewed in Wu X *et al*. 2006). In mammalian cells, dynein has been observed at the MT plus-ends showing comet-like structures that co-localize with EB1 (Vaughan KT *et al*. 1999; Kobayashi T & Murayama T, 2009). It has also been proposed that dynein is targeted to MT growing ends by dynactin or by LIS1, which both require CLIP170 for efficient plus-end accumulation (Akhmanova A & Steinmetz MO, 2008).

3.6.2. Plus-end tracking mechanisms

+TIPs can target MT growing ends in two ways, either directly by association with tubulin or MTs, or indirectly, through other factors (Figure 27). It has been described that some +TIPs (e.g. CLIP170, APC) tip track the MT plus-end using different mechanisms (Folker ES *et al*. 2005; Kita K *et al*. 2006).

Different plus-end tracking mechanisms can be classified in four groups: end recognition, copolymerization, directed transport and hitchhiking (Figure 27). Within these groups a sub-classification can be done. Indeed, the end recognition mechanism can be divided according to the binding kinetics in slow (treadmilling) and fast exchange, and the directed transport can be motor-based or by one-dimensional diffusion.

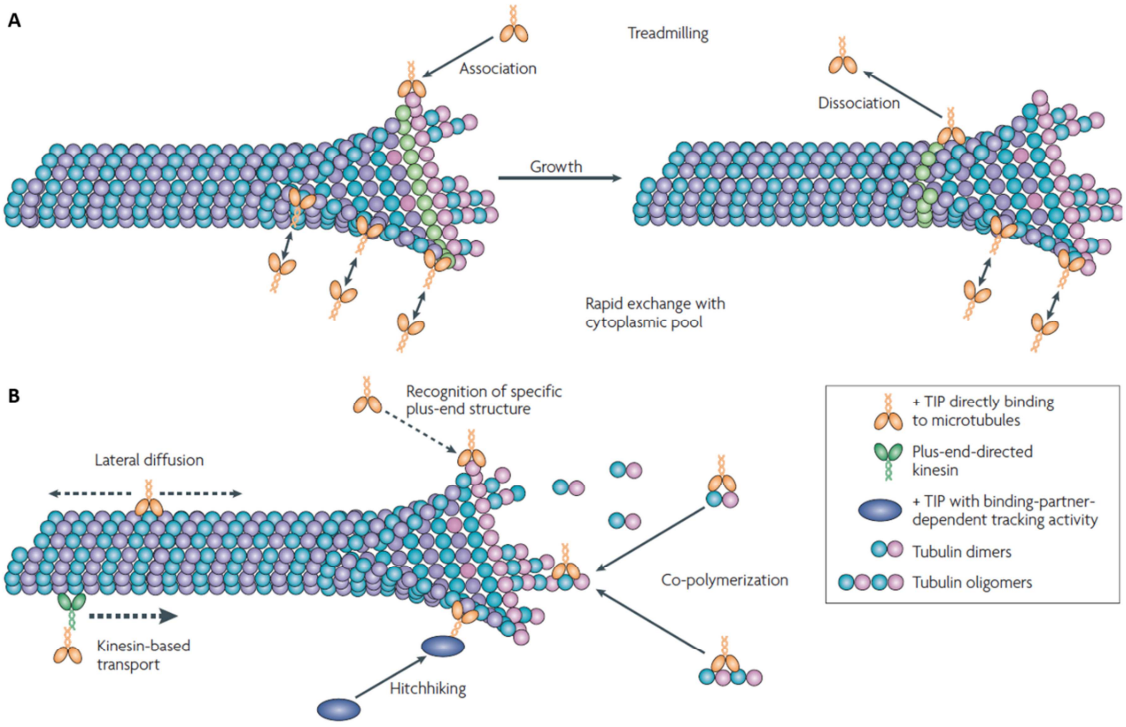

Figure 27

Mechanisms of MT plus-end tracking. +TIPs can **(A)** recognize a specific structure at the growing end of the MT (right diagram) and get released after tubule closure (left diagram) or **(B)** can bind the plus-ends by co-polymerization with tubulin dimers, by hitchhiking, by lateral diffusion or by kinesin-based transport (Modified from Akhmanova A & Steinmetz MO, 2008).

The end recognition model stands for the identification of a specific characteristic in the structure of the growing end that is different from the lattice. In accordance, +TIPs could recognize the GTP cap, the tubulin sheets, the individual protofilaments or some hidden sites at the inner side of MTs (Figure 27A) (Akhmanova A & Steinmetz MO, 2008). Once the +TIPs bind the MT plus-ends, its turnover can be slow (treadmilling), meaning that the +TIP binds the MT plus-end and only dissociates when the MT lattice becomes mature (Carvalho P *et al*. 2003). Alternatively, +TIPs can be highly dynamic and bind/unbind repeatedly the same MT close to its tip, which allows several binding events on a single binding site. Some examples are EB1, EB3 and CLIP170 (Bieling P *et al*. 2008; Dragestein KA *et al*. 2008).

Besides interacting with MT growing ends, some +TIPs can bind tubulin dimers and oligomers and thus, be copolymerized with tubulin. This is the case for mammalian CLIPs, which can co-polymerize with tubulin and are then released from the mature lattice (Figure 27B) (Diamantopoulos GS *et al*. 1999; Folker ES *et al*. 2005).

+TIPs can also move along the MT lattice until they reach the growing end in two ways, either by associating with motor proteins or by one-dimensional diffusion (Figure 27B). In the motor-based transport, growing end movement is driven by a plus-end directed kinesin, in an ATP-dependent manner; nevertheless, it should be noted that reaching the growing end does not imply an accumulation mechanism per se. That is why +TIP accumulation requires that kinesin moves faster that MT polymerization. An example of motor-based transport is APC that can be transported to the MT growing end by kinesin 2 (Jimbo T *et al*. 2002).

The MT lattice diffusion, unlike motor transport, implies +TIP targeting to the plus-end without energy consumption (Cooper JR & Wordeman L, 2009). This type of movement has been reported for some kinesins including Eg5 (Kwok BH *et al*. 2006) and CENP-E (Kim Y *et al*. 2008) and some MAPs as MCAK (Helenius J *et al*. 2006) and Tau (Konzack S *et al*. 2007).

Most of the +TIPs accumulate at the plus-end by hitchhiking on EB proteins through CAP-Gly domains or SxIP motifs (Figure 27B). This indicates that hitchhikers do not interact (or less efficiently) with tubulin or MTs and are mostly transported to the growing end. Some examples of these hitchhikers +TIPs are MCAK, APC, MACF/ACF7, CLASPs, STIM1 and CLIP170 proteins (Carvalho P *et al*. 2003). Of note, CLIP170 and MCAK can also track MT plus-ends autonomously as mentioned before.

3.6.3. +TIPs functions

Being located at the growing end of the MTs allows +TIPs to control microtubule dynamics, the anchoring of MTs to other cellular structures and the transport of molecules (Akhmanova A & Steinmetz MO, 2008).

Even if they can interact and co-localize at the plus-end, +TIPs effects on MT dynamics can be different and sometimes opposed. +TIPs can induce MT growth, MT shrinkage or MT stabilization.

Binding of +TIPs to MT plus-ends can cause MT stabilization by the reduction of catastrophe frequencies and the promotion of rescues and pauses states. CLIP170 is involved in MT stability as it has been described as a rescue factor in mammalian cells (Komarova YA *et al*. 2002a). Similarly, proteins with basic and serine rich regions, such as CLASPs, MACF/ACF7 and APC are MT stabilizing factors which act by preventing MT catastrophes and promoting rescues and pauses (Mimori-Kiyosue Y *et al*. 2005; Kita K *et al*. 2006; Akhmanova A & Steinmetz MO, 2008; Al-Bassam J *et al*. 2010)

The kinesin 13 MCAK is considered a potent MT depolymerizer able to induce conformational changes in order to bend and peel off tubulin individual protofilaments (reviewed in Hunter AW *et* al. 2003; Moores CA & Milligan RA, 2006 and Ems-McClung SC & Walczak CE, 2010).

EB proteins are able to make MTs more dynamic and promote MT polymerization by increasing MT rescue frequencies and decreasing depolymerization and pausing *in vivo* (Nakamura M *et al*. 2001; Komarova YA *et al*. 2009). EB1 implication in MT dynamics will be reviewed in the next chapter. SLAIN2 can also promote MT polymerization during interphase through the interaction with other +TIPs (van der Vaart B *et al*. 2011).

Besides regulating MT dynamics, +TIPs have been reported to be involved in the attachment of MTs to other cellular structures like the kinetochores or the plasma membrane (Gundersen GG *et al*. 2004; Lansbergen G & Akhmanova A, 2006). This often requires the combined effect of several +TIPs. For example, APC together with IQGAP1 and mDia1 attach MT growing ends to the cell cortex (Watanabe T *et al*. 2004; Wen Y *et al*. 2004) and CLIP170 also seems to target cortical cell sites in a complex with IQGAP1 (Fukata M *et al*. 2002).

+TIPs can also facilitate MT-intracellular membranes binding. For example STIM1 participates in the MT growth-dependent extension and remodeling of endoplasmic reticulum tubes through the interaction with EB1 (Grigoriev I *et al*. 2008). Dynamic MT plus-ends are also implicated in remodeling of focal adhesions and in the formation of cell contacts and gap junctions (Akhmanova A & Steinmetz MO, 2008).

During mitosis, one of the most important functions of the MT growing ends is to capture chromosomes and ensure their correct segregation. Indeed, most of the +TIPs are able to localize to mitotic kinetochores where they can mediate the interface between MTs and chromosomes. From this position, +TIPs can participate in mitotic spindle assembly, spindle orientation and positioning, and MT-kinetochore attachment (Maiato H *et al*. 2004a; Maiato H *et al*. 2004b). For example, CLASPs are essential for the assembly and maintenance of the mitotic spindle (Maiato H *et al*. 2002), whereas MCAK, which localizes at the centromeres, is necessary for correct chromosome position at the metaphase plate (Walczak CE *et al*. 2002) and serves as a correction mechanism through the depolymerization of MTs when they are incorrectly attached (Ohi R *et al*. 2003).

Many +TIPs are present at the spindle pole and the centrosomes (EBs, MCAK, APC, CLASPs, dynein) where they can have a role in MT anchoring and nucleation or in the stabilization of MT minus-ends (Yan X *et al*. 2006; Fong KW *et al*. 2008). +TIPs can also crosslink MT and actin cytoskeletons, interact with actin motors and modulate actin

dynamics (Kodama A *et al*. 2003; Wu XS *et al*. 2005; Moseley JB *et al*. 2007; Tsvetkov AS *et al*. 2007).

Finally, +TIPs are involved in cargo transport from the periphery to the minus-end through dyneins (Vaughan PS *et* al. 2002; Lomakin AJ *et al*. 2009) and in the plus-end transport along the MT lattice to organize the array as for the mitotic spindle formation (Goshima G *et al*. 2005).

3.7.End-binding protein 1

EB1 is the leading member of the family of End Binding proteins. This family also comprises EB2 (RP1) and EB3 (EBF3). EB proteins are evolutionary conserved and in mammals are encoded by the *MAPRE* gene family (Su LK & Qi Y, 2001). EB1 and EB3 are ubiquitously expressed, but EB3 is especially abundant in the central nervous system (Nakagawa H *et al*. 2000), whereas expression levels of EB2 differ in various cell lines (Su LK & Qi Y, 2001).

EB proteins contain two highly conserved domains connected by a linker sequence (Figure 28). The N-terminus of the EBs consist of a calponin homology (CH) domain, which is necessary and sufficient for binding to MTs and recognizing their growing ends (Hayashi I & Ikura M, 2003). The C-terminal domain (EB1c), contains a coiled-coil motif responsible for protein dimerization (Su LK & Qi Y, 2001). This motif partially overlaps with the end binding homology (EBH) domain, which is involved in the interaction with EB binding partners (Akhmanova A & Steinmetz MO, 2008). An acidic tail at the C-terminus contains a highly conserved EEY sequence motif, similar to those found in α-tubulin and CLIP170 (Komarova Y *et al*. 2005; Honnappa S *et al*. 2006), that is implicated in the interaction with other proteins (Honnappa S *et al*. 2005; Hayashi I *et al*. 2005).

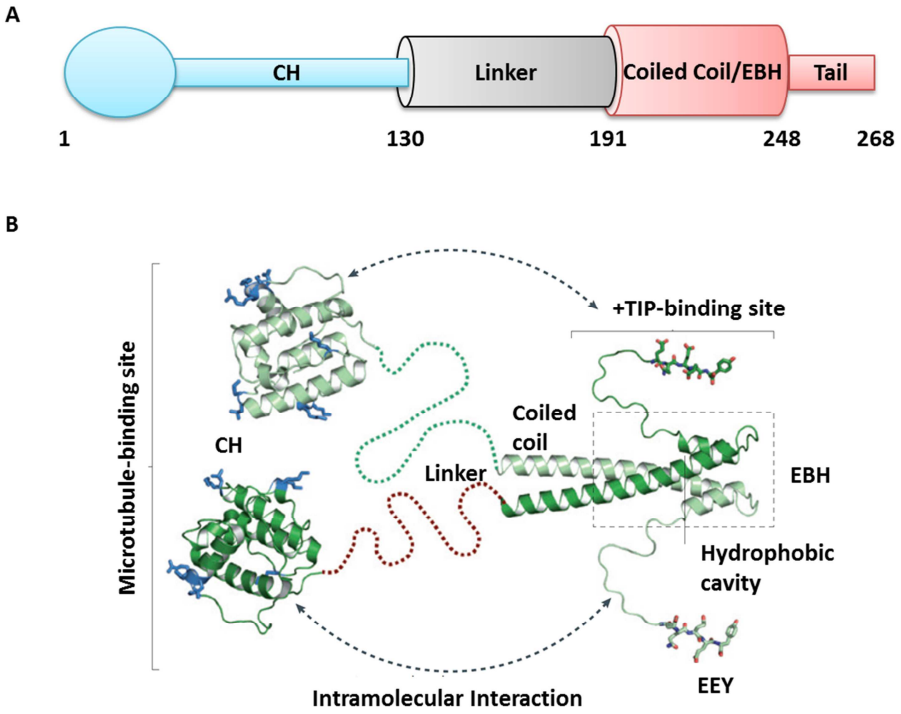

Figure 28

EB1 protein structure. **(A)** Schematic representation of EB1. Calponin homology (CH), coiled coil and EB homology (EBH) domains are represented. Amino acids are shown on the bottom (Adapted from Buey RM *et al*. 2011). **(B)** Structural organization of homodimeric end-binding proteins. The structures of the CH and EBH domains are shown. The EEY sequence motifs are also shown. Dashed, curved lines show the linker segments (From Akhmanova A & Steinmetz MO, 2008).

EB1 and EB3 are able to interact with a large number of proteins (Bu W & Su LK, 2003). EB2 is also able to interact with some EB1/EB3 partners (Bu W & Su LK, 2003) although with lower affinity, mainly due to the presence of fewer acidic residues contained in its C-terminal tail. The N-terminal region of EB2 is also different from EB1/EB3 proteins and contains an extension of approximately 40 amino acids. The residue difference is critical for MT binding and reduces EB2 accumulation at the MT plus-ends (Komarova YA *et al*. 2009).

EB1 was initially discovered as an APC-interacting partner by yeast two-hybrid screen (Su LK *et al*. 1995). Later studies published in 1998 showed that EB1 was associated with the MTs and often concentrated at their tips (Morrison EE *et al*. 1998). But it was in 2000 that Mimori-Kiyosue Y and collaborators demonstrated, using time-lapse videomicroscopy of EB1-GFP construct, that EB1 was localized at the end of growing MTs independently of APC.

Later after, the "EB1 boom" started and several studies about its structure, its relation with MTs and other +TIPs filled the journals pages. After Mimori-Kiyosue Y *et al*. work in 2000, the pursuit of how EB1 was able to bind the growing ends of MTs began. Bieling P and coworkers (2007) showed, using an *in vitro* model, that EB1 could track autonomously the tip of the MT by fast exchange, meaning that EB1 associates and disassociates from the plus-end in a dynamic way.

Besides binding APC via its C-terminal portion, EB1 also binds to multiple partners (through the same domain) and works as a scaffold protein that brings different proteins to the MT growing end (Jiang K *et al*. 2012). EB1 is thus considered as the "key stone" or core component of +TIP network. Two major binding regions have been described: the EBH domain that is recognized by the SxIP-containing proteins (Honnappa S *et al*. 2009) and the EEY motif which in turn is recognized by the CAP-Gly proteins (Bieling P *et al*. 2008).

In 2012, the analysis of a large number of SxIP binding partners of EB1 by Jiang K and coworkers led to the outstanding discovery that not all the proteins that interact with EB1 are tip trackers. Using GST pull-down and mass spectrometry they found that some proteins were membrane-associated as AMER2 (plasma membrane) and Syntabulin (mitochondria membrane); some were actin-binding proteins (GAS2L1); small GTPases (RasL11B); or kinases as MARK1, TTBK1 and TTBK2. Surprisingly, they also found two proteins (namely, tastin and DDA3) that in addition to tracking the growing end, were able to track shrinking MTs.

EB1 localizes at the growing ends of MTs in interphase and during mitosis (Figure 29) and from this strategic position it has a role in controlling MT dynamics *in vitro* and *in vivo*, by promoting MT polymerization (Tirnauer JS & Bierer BE, 2000; Vitre B *et al*. 2008; Komarova Y *et al*. 2009). However, its precise influence on dynamic instability parameters (*in vitro* and *in vivo*) is still controversial. The first evidence for a role of EB1 in controlling MT dynamics, in particular by promoting MT growth, was done studying EB1 yeast homologues (Mal3 and Bim1) (Tirnauer JS & Bierer BE, 2000). These results were confirmed in *Drosophila* cells. EB1 was shown to stimulate catastrophes and rescues, making MTs more dynamic, while it decreased the time spent pausing (Rogers SL *et al*. 2002). Conversely, in *Xenopus* extracts, it was demonstrated that EB1 stimulated MT polymerization, MT rescues and inhibited catastrophes, suggesting a stabilizer role for EB1 (Tirnauer JS *et al*. 2002b). Later in 2006, using mouse fibroblasts Kita K and coworkers showed that depletion of EB1 promoted MT pausing and decreased the time MT spend in growth (Kita K *et al*. 2006). Finally, using CHO-K1 cells it was shown that EB1 and EB3

promote persistent MT growth by suppressing catastrophes, with little effect on MT growth rate or rescues (Komarova Y *et al*. 2009).

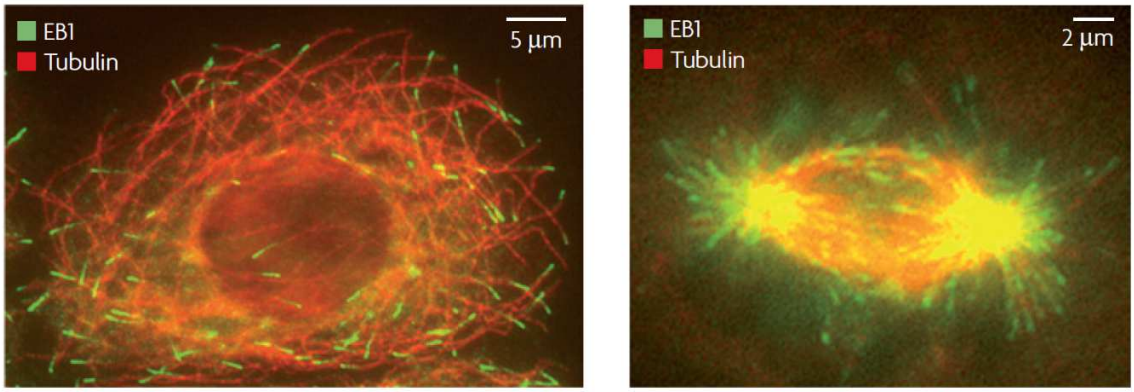

Figure 29

Localization of EB1 (green) in an interphase cell (left panel) and in a mitotic cell (right panel). Red stain corresponds to β-tubulin (From Akhmanova A & Steinmetz MO, 2008).

EB1 also accumulates at MT plus-ends at the interface between kinetochores and growing MTs, suggesting that it could have a role in the dynamic behavior during mitosis (Tirnauer JS *et al*. 2002a; Mimori-Kiyosue Y & Tsukita S, 2003). In addition, it was shown that EB1 may partially depends on APC interaction to regulate spindle dynamics and chromosome alignment (Green RA *et al*. 2005), and may also be implicated in spindle positioning by the stabilization of astral MTs (Toyoshima F & Nishida E, 2007).

The accumulation and tip tracking characteristics of EB1 at the MT growing end can be considered as a useful tool for the measurement of dynamic instability parameters, as have been described in different studies (Piehl M & Cassimeris L, 2003; Salaycik KJ *et al*. 2005; Long JB *et al*. 2013; Lowery LA *et al*. 2013).

EB1 can also be found localized at other cellular structures such as the centrosomes and the cilia, where it may play a role in MT anchorage (Berrueta L *et al*. 1998; Louie RK *et al*. 2004) and primary cilia assembly (Schroder JM *et al*. 2007). In addition, EB1 together with its partners can link MT plus-ends with other structures such as actin (through MACF/ACF7 (Kodama A *et al*. 2003)), the cell cortex (through CLASPs (Mimori-Kiyosue Y *et al*. 2005)), melanosomes (through melanophilin and myosin Va (Wu XS *et al*. 2005)) and the endoplasmic reticulum (through STIM1 (Grigoriev I *et al*. 2008)).

Overexpression of EB1 has been associated with hepatocellular (Fujii K *et al*. 2005; Orimo T *et al*. 2008), gastric (Nishigaki R *et al*. 2005), oesophageal (Wang Y *et al*. 2005), breast

(Dong X *et al*. 2010) and in early colorectal (Stypula-Cyrus Y *et al*. 2014) carcinomas. It would be interesting to investigate if the oncogenic functions of EB1 are related with its effects on MT dynamics and/or with the interaction with other +TIPs. Overexpression of EB1 could be implicated in the deregulation of MT-mediated cell activities such as cell division and cell migration, which lead to cancer progression.

3.8.Microtubules in cell migration

The cell cytoskeleton plays an essential role in cell migration. The participation of the actin network has been studied extensively (reviewed in Carlier MF & Pantaloni D, 2007), but is not the goal of this chapter. This last chapter will rather summarize current knowledge on the role of MTs in cell migration.

According to the cell type, MTs can be dispensable or not for cell migration. For example, in small cells as fish keratocytes, hematopoietic cells, T lymphocytes and neutrophils, migration is possible even in the absence of MTs. In contrast, in fibroblasts, epithelial cells and neurons a disrupted MT network implicates problems in cell adhesion turnover, actin dynamics, membrane trafficking and thus directed cell migration (Kaverina I & Straube A, 2011 and Etienne-Manneville S, 2013).

MTs act as spatiotemporal coordinators of cell migration due to their involvement in the turnover and distribution of adhesion complexes and the localization and activation of Rho GTPases. And the most important function of MTs during migration is related to the establishment and maintenance of cell polarity to promote a persistent and directed cell migration (Gundersen GG & Bulinski JC, 1988; Etienne-Manneville S, 2013).

Cell polarity accounts for the asymmetrical distribution of signals, molecules and arrangement of actin and MT cytoskeletons, in order to distinguish a front (named leading edge) that is characterized by the local activation of Cdc42 and Rac GTPases (Ridley AJ *et al*. 2003), and by the presence of a lamellipodial protrusion which indicates the migration direction. There is also a rear (known as trailing edge) that is located in the opposite direction of the lamellipodium and is characterized by the local activation of RhoA GTPase (Figure 30) (reviewed in Watanabe T *et al.* 2005; Kaverina I & Straube A, 2011 and Etienne-Manneville S, 2013).

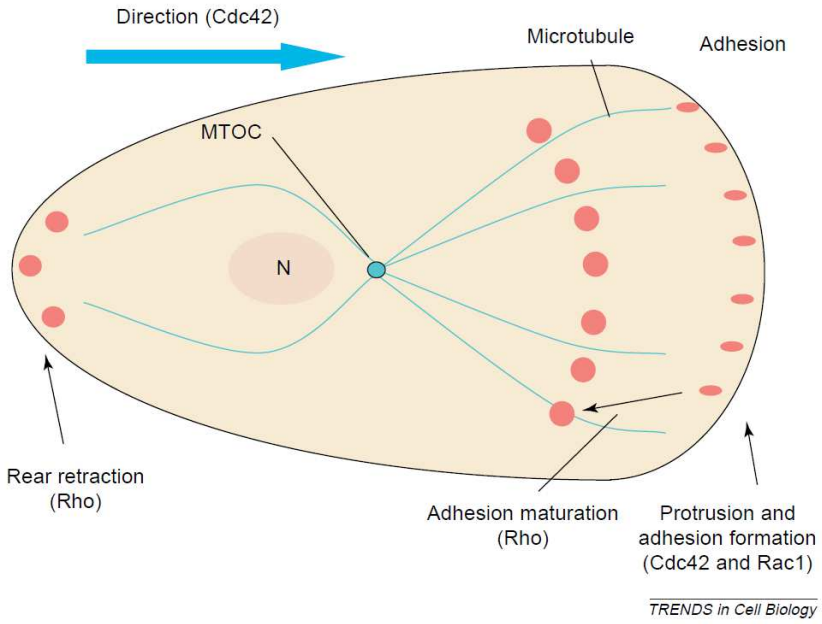

Figure 30

Cell polarity is intrinsic to a migrating cell. Asymmetric distribution of cellular organelles allows the distinction of a leading edge (right side) and a trailing edge (left side). N: nucleus, MTOC: centrosome (From Watanabe T et al. 2005).

A key feature of cell polarity is the differential distribution of MT network and MT dynamics between the leading and the trailing edge. Even if the lamellipodium is mainly composed by actin filaments, some MTs (around a dozen), known as pioneer MTs, can enter into the protrusion to contribute to pushing forces, cellular trafficking and signaling (Figure 31) (Watanabe T *et al.* 2005; Etienne-Manneville S, 2013).

Several studies have reported that different activities occur at the front and at the rear of a migrating cell. At the leading edge, MTs are captured and stabilized at cortical and adhesion sites (Fukata M *et al*. 2002; Krylyshkina O *et al*. 2003; Watanabe T *et al*. 2004; Mimori-Kiyosue Y *et al*. 2005; Manneville JB *et al*. 2010). They are post-translationally modified (acetylation) enabling the binding of motors that will crosslink the different cytoskeleton filaments (Figure 31A) and will transport factors associated with cell protrusion (membrane vesicles, membrane-associated signaling molecules such as Rac and Cdc42) (Figure 31B) (Etienne-Manneville S, 2013). Of note, +TIP complex formation at the cell cortex, such as EB1-APC, EB1-CLASP, EB1-MACF/ACF7, CLIP170-IQGAP, APC-IQGAP (Fukata M *et al*. 2002; Kodama A *et al*. 2003; Watanabe T *et al*. 2004; Wen Y *et al*. 2004; Drabek K *et al*. 2006) and inactivation of Op18/Stathmin at the leading edge (Niethammer P *et al*. 2004; Wittmann T *et al*. 2004) will lead to MT stabilization.

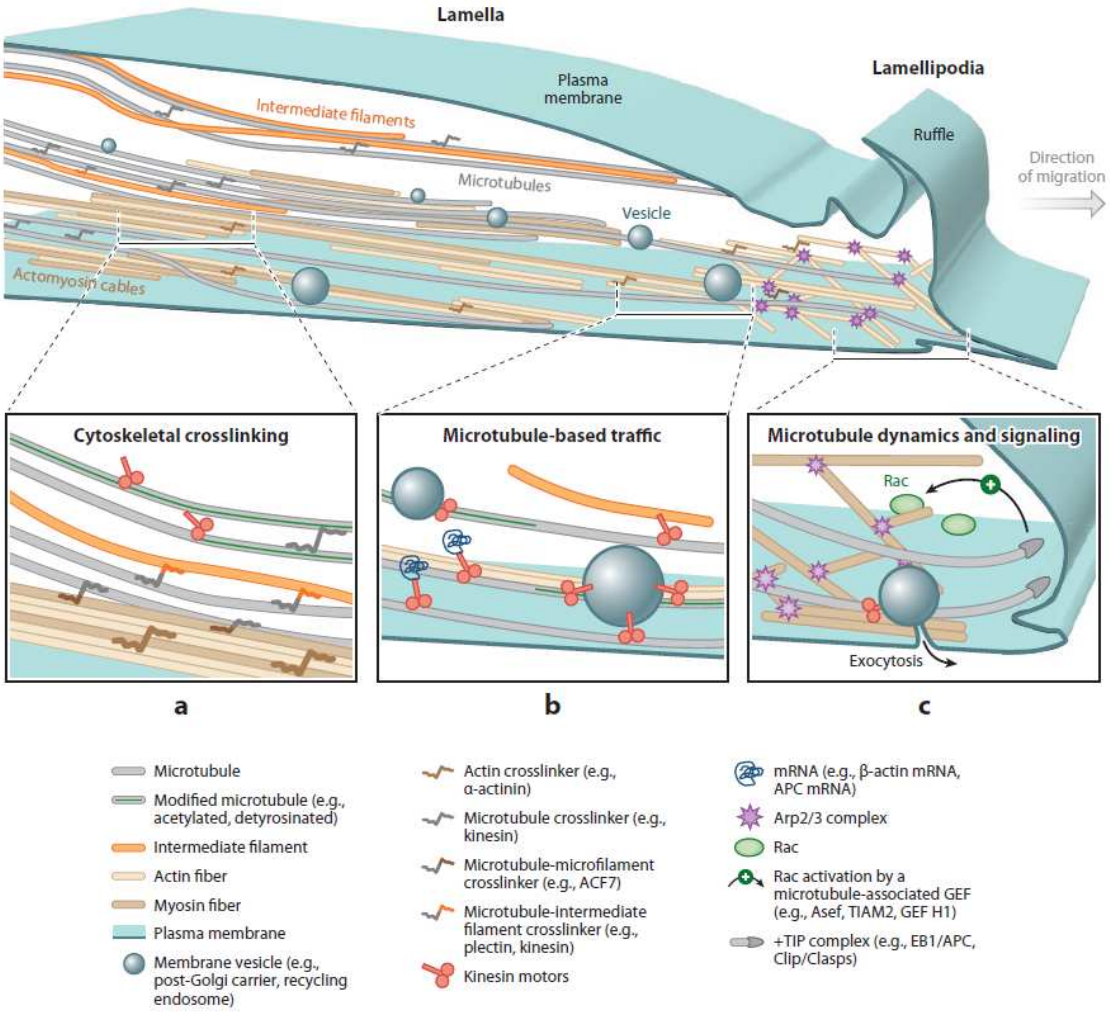

Figure 31

MT in cell protrusions. MT can bind actin and intermediate filaments through different crosslinkers **(A)**. MTs functions in cellular trafficking **(B)** and signaling **(C)** are shown (From Etienne-Manneville S, 2013).

MTs also possess signaling properties that will promote cell migration through the activation/deactivation of Rho GTPases (Figure 31C) that in turn will impact on actin polymerization (reviewed in Watanabe T *et al.* 2005; Kaverina I & Straube A, 2011 and Etienne-Manneville S, 2013). One of the first studies to demonstrate the effect of MTs on actin polymerization at the leading edge was performed by Waterman-Storer CM *et al*. (1999). In their study, they showed that MT polymerization activates Rac1 to promote protrusion formation in nocodazole washout experiments. Later studies showed that MT growth towards the leading edge also activates Asef, a Rac GEF, which interacts with APC at the tips of the protrusions to induce membrane ruffles (Kawasaki Y *et al*. 2000;

Kawasaki Y *et al*. 2003). Some other Rac/Cdc42 effectors (TIAM1, TIAM2/STEF, IQGAP1, Trio and GEF H1) can be found at the leading edge and interact with either MTs, MAPs or +TIPs to induce actin polymerization (reviewed in Watanabe T *et al.* 2005; Kaverina I & Straube A, 2011 and Etienne-Manneville S, 2013).

On the other hand, at the trailing edge MT are more dynamics, Op18/Stathmin is still activated (Niethammer P *et al*. 2004) which means more catastrophe events (Salaycik KJ *et al*. 2005). Additionally, MT depolymerization induces RhoA activation (Ren XD *et al*. 1999) which is implicated in the maturation and dissociation of adhesion complexes at the trailing edge together with the assembly of contractile actin and myosin in the rear part of the cell (Watanabe T *et al.* 2005).

Various MAPs have been involved in the regulation of cell polarity through their effects on MT dynamics, mostly at the leading edge. For example, down-regulation of EB1 results in decreased lamellipodium formation, cell velocity and cell directionality in melanoma cells (Schober JM *et al*. 2009). EB1 is also implicated in MT stabilization at the front edge together with APC and downstream RhoA and mDia (Wen Y *et al*. 2004). Additionally, CLASPs, CLIP170 and MACF (ACF7) are also able to stabilize MTs and therefore increase directional cell migration (Akhmanova A *et al*. 2001; Kodama A *et al*. 2003; Drabek K *et al*. 2006; Nakano A *et al*. 2010).

Besides MT organization, some other characteristics of cell polarity during migration include nucleus, centrosome (MTOC) and Golgi repositioning (Figure 32). The position of the centrosome is controlled by signaling pathways downstream Cdc42 and by the action of dynein and dynactin that will act in MT pulling forces from the plus-end to the minus-end (Palazzo AF *et al*. 2001a; Etienne-Manneville S & Hall A, 2001; Tzima E *et al*. 2003).

Nuclear positioning depends on cell type and physiological context (Dupin I & Etienne-Manneville S, 2011) but is mostly driven by actin retrograde flow (Gomes ER *et al*. 2005). Nucleus is pushed toward the rear of the cell, behind the centrosome, and in that way the nucleus-centrosome axis is defined parallel to the migration direction.

Finally, the MTOC positioning affects the localization of the Golgi complex. These two cellular organelles are maintained in close proximity by dynein (Sütterlin C & Colanzi A, 2010) and are involved in MT nucleation.

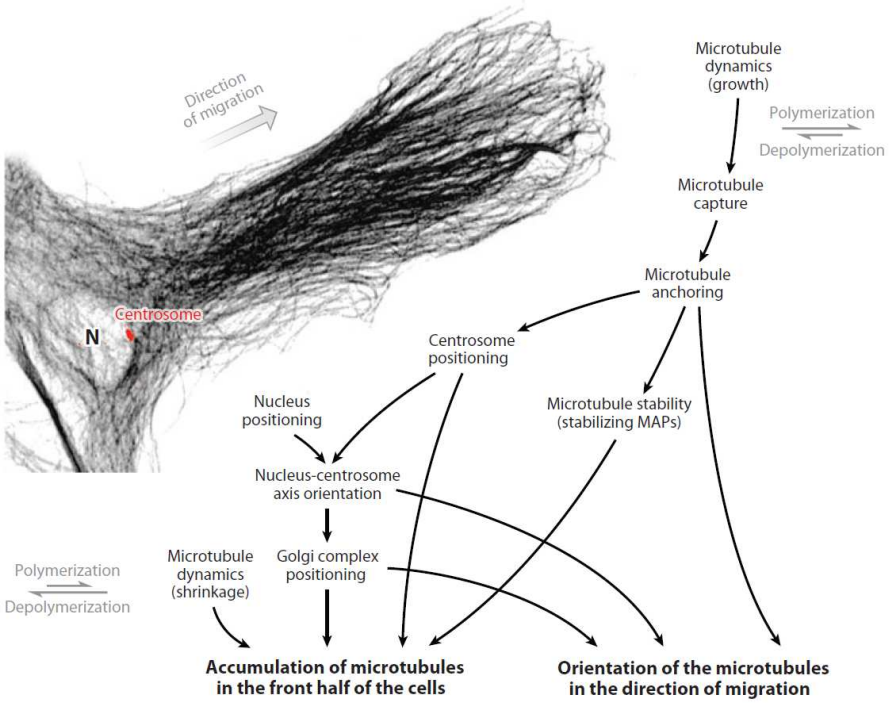

Figure 32

Cell polarization during migration (From Etienne-Manneville S, 2013).

4. ATIP3 a novel therapeutic target against breast cancer

In this last chapter of the manuscript I will present *MTUS1*, a candidate tumor suppressor gene located at chromosome position 8p22, a region frequently lost in a large number of human cancers. I will describe *MTUS1* gene's major product ATIP3, its main characteristics and functions.

4.1.MTUS1, a candidate tumor suppressor gene

Before being designated as a Microtubule Tumor Suppressor gene 1 (*MTUS1*), this gene was named *GK1* (Kinjo T *et al*. 2000), *MTSG1* (Seibold S *et al.* 2003), *ATIP* (Nouet S *et al*. 2004) and finally *MTUS1* (for mitochondrial tumor suppressor 1) (Di Benedetto M *et al*. 2006a).

GK1 was described for the first time by Kinjo T *et al*. (2000). Through large-scale sequencing of genomic DNA from human chromosome 8p22-p21.3, this group isolated a new gene that encoded a 1270 amino-acid protein. *In silico* analysis revealed that the gene product contained putative leucine-zipper domains and a mitochondrial targeting motif. Immunofluorescence stain confirmed the co-localization of GK1 with the mitochondria.

Then in 2003, with the aim to identify new molecular regulators of carcinogenesis Seibold S *et al.* reported a new potential tumor suppressor gene located in a position frequently lost in several types of human cancers: 8p21.3-22. In their study, immunofluorescence and western blot analysis demonstrated a mitochondrial localization of the mature protein, and BrdU proliferation assays showed a reduction in the compound incorporation when the gene product was expressed. According to the functional data and intracellular localization, they named this gene *MTSG1*: mitochondrial tumor suppressor gene 1.

One year later, Nouet S *et al*. (2004) while investigating for new interacting partners of the angiotensin II AT2 receptor, using yeast two-hybrid assay, found a new protein that they called ATIP (for Angiotensin II AT2 receptor-Interacting Protein). They also found that this ATIP protein was a gene product out of four (ATIP1, ATIP2, ATIP3 and ATIP4), generated by alternative splicing of the *ATIP* gene. Interestingly, they showed that all these ATIP proteins shared the C-terminal sequence where the AT2 binding domain was present.

Later studies from the same group (and then confirmed by Yu J *et al*. 2009) reported the exon/intron organization of human *MTUS1* (mitochondrial tumor suppressor gene 1) (Figure 33) (Di Benedetto M *et al*. 2006a): *MTUS1* comprises 17 coding exons distributed

over 112 kb, with three different gene promoters (Yu J *et al*. 2009), three 5' UTR (untranslated regions) and ATG initiating codons located at exons 8, 1 and 5, that generate the three major ATIP transcripts: ATIP1, ATIP3 and ATIP4, respectively. They also described that exons 9 to 17 are common to all ATIP members and encode a large and highly conserved coiled-coil domain involved in the dimerization of ATIP proteins that is now considered as the "ATIP-signature".

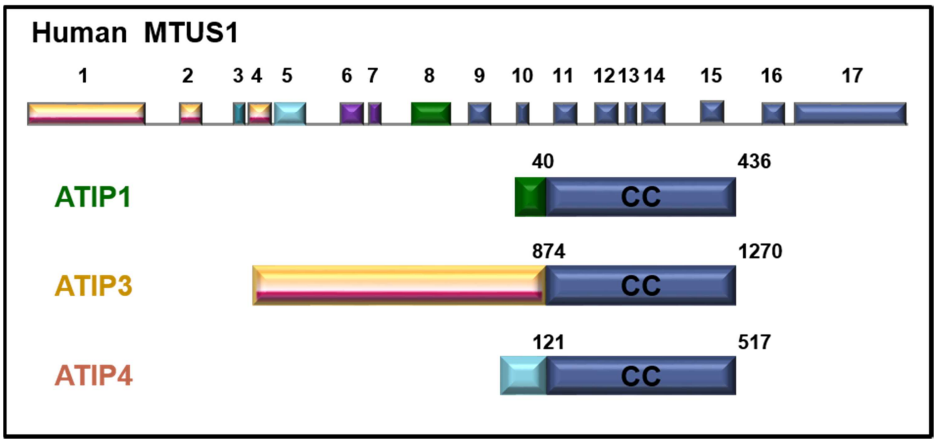

Figure 33

Structural organization of *MTUS1* and *MTUS1* gene products (ATIPs) (From Rodrigues-Ferreira S & Nahmias C, 2010).

A number of studies have shown that *MTUS1* expression levels are reduced in breast (Rodrigues-Ferreira S *et al*. 2009), pancreas (Seibold S *et al*. 2003), ovary (Pils D *et al*. 2005), colon (Lee S *et al*. 2006; Zuern C *et al*. 2010), head-and-neck (Ye H *et al*. 2007; Ding X *et al*. 2012), bladder (Xiao J *et al*. 2012; Rogler A *et al*. 2014) and gastric carcinomas (Li X *et al*. 2014). At the genomic level, a mutational analysis of *MTUS1* gene in a series of 51 primary hepatocellular carcinomas (HCC) and 51 HCC cell lines led to the identification of five nucleotide sequence variations (in the exonic sequence) that were absent in non-tumoral control DNA (Di Benedetto M *et al*. 2006b). Some of these variations (four) were also found (along with nine single-nucleotide sequence variants) in an analysis performed in 41 head and neck squamous cell carcinoma cell lines (Ye H *et al*. 2007). Additionally, in a case-control study Frank B *et al* (2007) showed that deletion of the entire exon 4 of the *MTUS1* gene was associated with a decreased risk for familial breast cancer. All these data together support the notion of *MTUS1* as a tumor suppressor gene.

Genomic sequence comparison reveals the presence of a human paralog *MTUS2* (chromosome position 13q12) which presents similar genomic organization as *MTUS1*. This gene can generate two proteins by alternative splicing (CAZIPa or TIP150 (Jiang K *et*

al. 2009) and CAZIPb) which are structurally similar to ATIP3 and ATIP1, respectively. Additionally, CAZIP proteins share their C-terminal portion (coiled-coil domains) and differ in the N-terminal part, similar to ATIP proteins (Du Puy L *et al*. 2009). Amino acid sequence comparison of the C-terminal region revealed a 35% identity between coiled-coil domains of CAZIPs and ATIPs (Rodrigues-Ferreira S & Nahmias C, 2010). Indeed, this region is highly conserved among mammals (86 to 96% amino acid sequence identity between human, canine, bovine, murine and rat sequences) (Di Benedetto M *et al*. 2006a).

The *Xenopus* ortholog of *MTUS1* encodes for a protein structurally similar to ATIPs proteins. ICIS (Inner Centromere kin-I Stimulator) contains two coiled-coil domains, one of them located at the C-terminal portion of the protein, which presents 60% identity with ATIPs C-terminus (Di Benedetto M *et al*. 2006a). ICIS has been identified as an inner centromere protein which acts as a scaffold protein to bring two depolymerizing kinesins (MCAK and KIF2A) at the kinetochore during mitosis in order to ensure proper chromosome segregation (Ohi R *et al*. 2003; Knowlton AL *et al*. 2009).

4.2.A family of ATIP proteins

The family of angiotensin II AT2 receptor-interacting proteins is composed by three major proteins (ATIP1, ATIP3 and ATIP4) which share the same C-terminus but differ in their N-terminus and therefore in their length (Figure 33). In 2006, a study performed by Di Benedetto M and co-workers analyzed the tissue distribution of each ATIP transcript in a large number of human normal tissues by means of real-time quantitative RT-PCR. Consistent with the different promoter use, ATIP1, ATIP3 and ATIP4 show different tissue distribution in normal human tissues (Figure 34). Of note, two ATIP3 variants (ATIP3a and ATIP3b) showing similar tissue distribution have been described and will be presented below in more details.

ATIP3 is the major transcript expressed in almost all tissues, except for the brain. In contrast, ATIP1 is mainly expressed in central nervous system tissues, in female reproductive tissues (placenta, breast, ovary and uterus), thyroid and heart. Finally, ATIP4 mRNA is exclusively detected in the brain and most specifically in the cerebellum and the fetal brain.

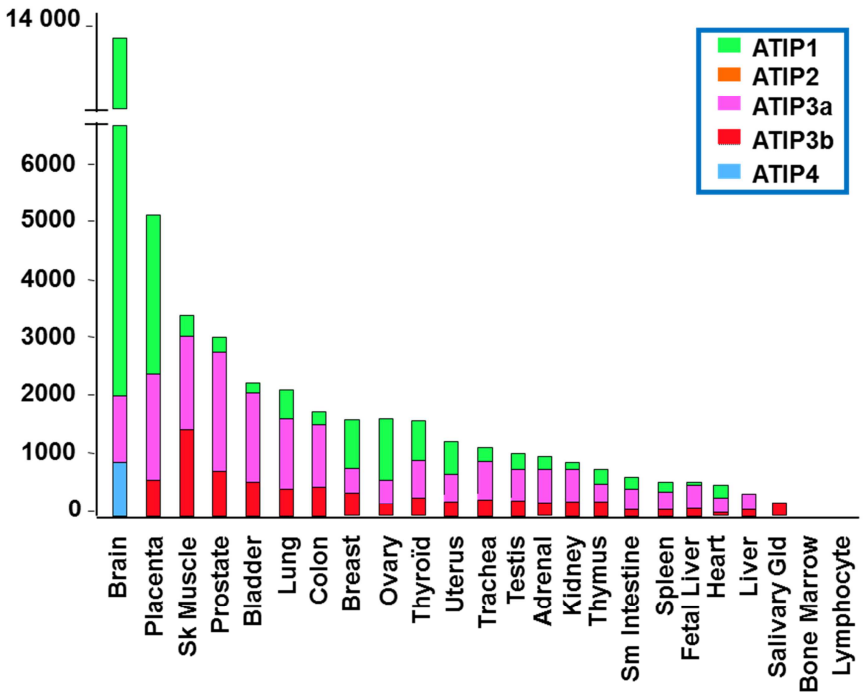

Figure 34

Quantitative RT-PCR of total ATIP transcripts in human normal tissues (From Di Benedetto M *et al*. 2006).

ATIP1 was the first characterized member of ATIP proteins. The 5' UTR and initiating codon of ATIP1 are contained in exon 8 (the only N-terminal exon of ATIP1 protein). The first 40 amino acids of exon 8 also contain a mitochondrial targeting signal (Seibold S *et al.* 2003). To date, ATIP1 is the only ATIP member in which it has been shown an interaction with AT2 receptor in eukaryotic cells (Nouet S *et al*. 2004; Wruck CJ *et al*. 2005; Li JM *et al*. 2007). ATIP1 interacts with AT2 in the absence of ligand angiotensin II and is involved in AT2R activation and in the transport of the receptor to the cell membrane (Wruck CJ *et al*. 2005). Additionally, ATIP1-AT2 interaction contributes to AT2 effects on neuron differentiation (Li JM *et al*. 2007), vascular remodeling (Fujita T *et al*. 2009), vascular senescence (Min LJ *et al*. 2012) and adipose function (Jing F *et al*. 2013) (Figure 35).

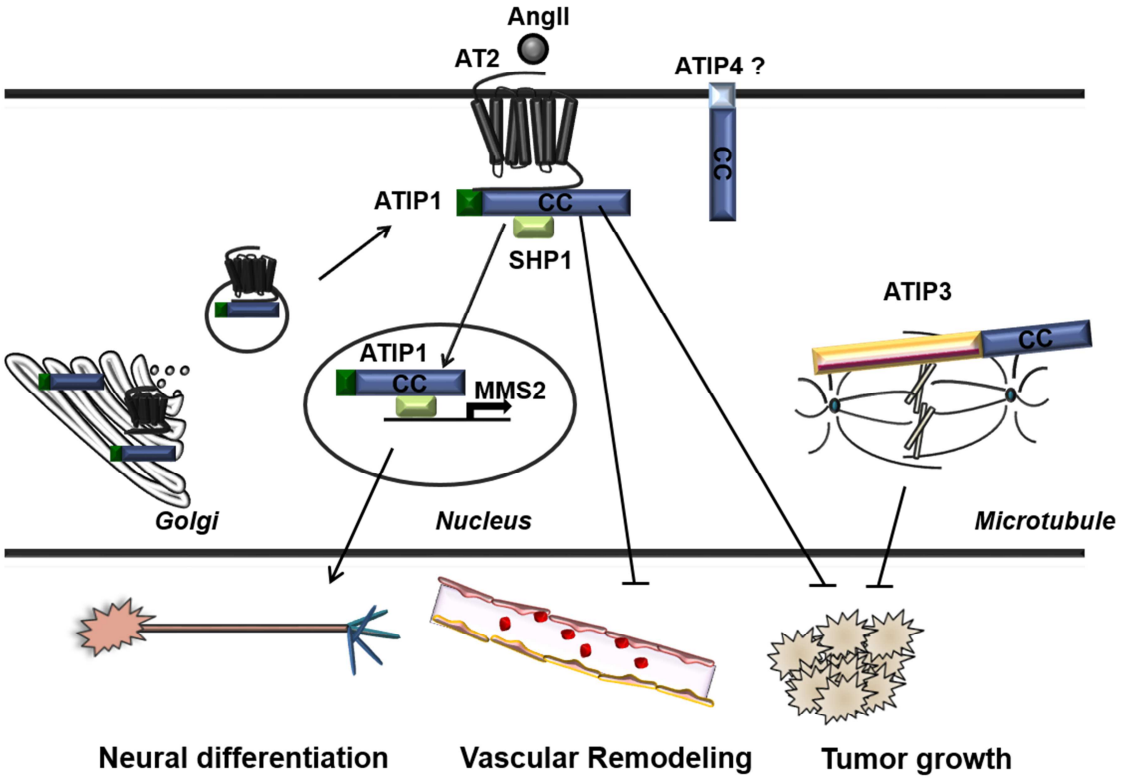

Figure 35

A family of multifunctional ATIP proteins with diverse subcellular locations (From Rodrigues-Ferreira S & Nahmias C, 2010).

ATIP3 is the major and the longest *MTUS1* gene product. It includes three alternative splice variants: ATIP2, ATIP3a and ATIP3b. ATIP3a is characterized by the presence of exons 1, 2, 4, 6 and 7. Of these, exon 1 contains the initiating codon, exon 4 contains a polyproline-rich motif (PRPLP) that usually participate in interaction with both SH3 and WW domains (but to date it has not been demonstrated for ATIP3), exon 6 contains a second polyproline-rich motif (PPKP) and is always joined to exon 7 that harbors a nuclear localization signal (Di Benedetto M *et al*. 2006a).

On the other hand, ATIP3b differs from ATIP3a by the absence of exon 4 indicating that these two proteins may interact with distinct intracellular partners and exhibit different cellular functions. Finally, and although ATIP2 contains the same exons that ATIP3a, it also uses exon 3 that contains an in-frame stop codon that potentially translates a truncated protein that does not contain the coiled-coil region (Di Benedetto M *et al*. 2006a). ATIP2 is hardly expressed in normal tissues (Figure 34), suggesting that its expression may be regulated by a mechanism of nonsense-mediated decay.

Up to now, cDNA cloning and functional characterization of ATIP4 have not been undertaken. Nevertheless, due to its restricted expression in the brain and the presence of a membrane spanning domain located in exon 5, it may be possible that ATIP4 mediates AT2R functions in the brain (Di Benedetto M *et al*. 2006a; Rodrigues-Ferreira S *et al*. 2013).

4.3.ATIP3, A TIP top protein down-regulated in Breast Carcinoma

While several studies have demonstrated down-regulation of *MTUS1* gene in various types of cancers, Rodrigues-Ferreira S *et al* (2009) were the first to provide evidence that ATIP3, and not ATIP1 or ATIP4, was the major *MTUS1* gene product whose expression is decreased in human breast cancer as compared to normal tissue.

Indeed, Affymetrix DNA array conducted in a series of 151 invasive ductal breast carcinomas, further validated by real-time RT-PCR analysis using specific primers for different ATIP variants, revealed that *MTUS1*, and more specifically ATIP3, is down-regulated in 85% of high grade tumors (grade III); in 83% of triple negative breast cancer, as well as in 62% of metastatic tumors (Figure 36) (Rodrigues-Ferreira S *et al*. 2009).

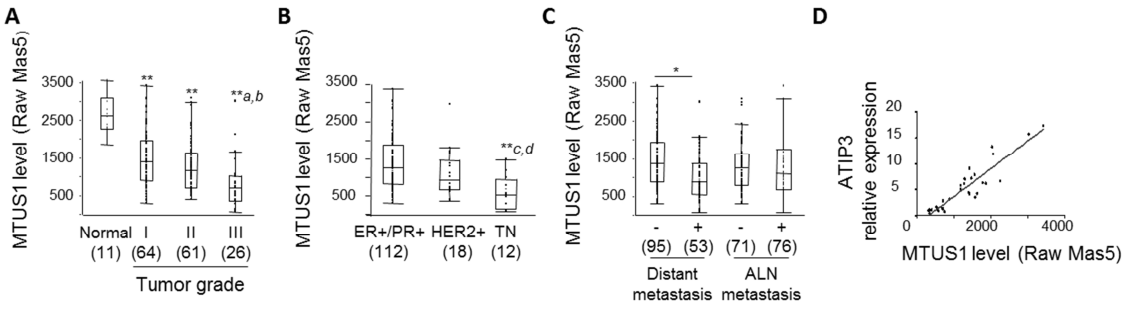

Figure 36

ATIP3 down-regulation in invasive breast carcinoma. *MTUS1* levels are decreased in high histological grade **(A)**, triple negative (TN) **(B)** and metastatic tumors **(C)**. Real-time RT-PCR using ATIP3 specific primers indicate that this is the *MTUS1* transcript down-regulated in breast cancer **(D)** (From Rodrigues-Ferreira S *et al*. 2009).

At the functional level, different *in vitro* experiments (clonogenicity, MTT and BrdU assays) showed that re-expression of ATIP3 into ATIP3-deficient breast cancer cells lines (MCF7 and MDA-MB-231) reduces cell proliferation whereas ATIP3-silencing in ATIP3-positive MDA-MB-468 cells leads to increased cell proliferation. Interestingly, time-lapse videomicroscopy of HeLa-H2B stable clones expressing ATIP3 revealed that decreased cell proliferation was due to an extension of the time spent in mitosis. Indeed, time

measurements of all mitosis phases indicated that ATIP3 expressing cells spent more time in metaphase than cells lacking the protein (Figure 37) (Rodrigues-Ferreira S *et al*. 2009).

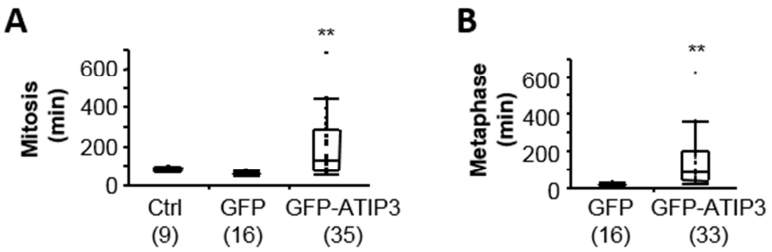

Figure 37

ATIP3 delays mitosis **(A)** and more specifically delays the time to achieve metaphase **(B)** (From Rodrigues-Ferreira S *et al*. 2009).

On the other hand, *in vivo* experiments showed that ATIP3 also reduces tumor growth (incidence and size) after subcutaneous injection of MCF7 breast cancer cells expressing or not ATIP3 into immunodeficient mice (Rodrigues-Ferreira S *et al*. 2009). All these results indicate that ATIP3 is a novel biomarker for breast tumor of poor prognosis and an interesting therapeutic target for aggressive breast cancer.

4.4.ATIP3 is a novel Microtubule-associated protein

At the molecular level, ATIP3 decorates the microtubule (MT) cytoskeleton and the microtubule organizing center (MTOC) in interphase, the mitotic spindle during cell division and the intercellular bridge during cytokinesis (Figure 38). Co-sedimentation assays on cells expressing GFP or GFP-ATIP3 confirmed that ATIP3, and not GFP, associated with microtubules (Rodrigues-Ferreira S *et al*. 2009).

Due to its association to MTs, in 2010 the nomenclature committee of the National Center for Biotechnology Information (NCBI) changed the name of *MTUS1* gene to Microtubule-associated TUmor Suppressor 1.

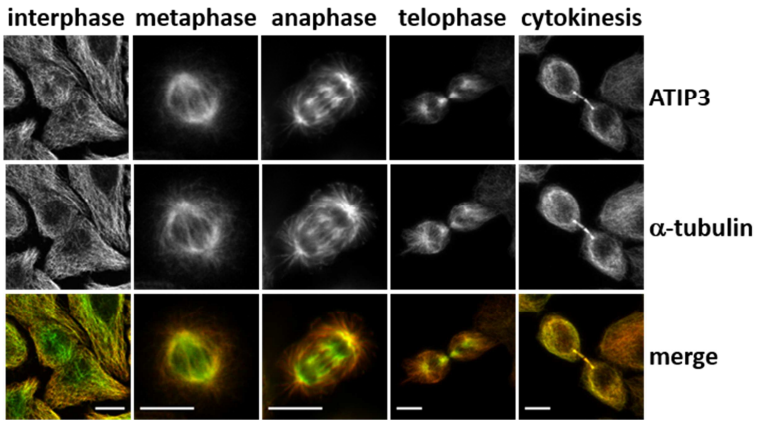

Figure 38

ATIP3 associates with microtubules during interphase and mitosis (From Rodrigues-Ferreira S *et al*. 2009). Scale Bar, 10 µm

Overexpression of GFP-ATIP3 in a large number of cell lines (SKMES, HeLa, RPE1, MDA-MB-231 and MCF7) led to the formation of bundles, suggesting that ATIP3 may induce MT stabilization.

4.5.A functional family of Microtubule-Associated Proteins in cancer

As state by Kaverina I and Straube A (2011) "the loss of microtubule-associated proteins and subsequent alteration of interphase microtubule dynamics stimulate uncontrolled motility in cancer cells that is associated with invasiveness and poor prognosis in cancer patients."

Additionally, a large number of studies have shown that loss of microtubule-associated proteins cause the stabilization of microtubule-kinetochore attachment errors during mitosis which will result in chromosome mis-segregation, aneuploidy and chromosomal instability (CIN) (Reviewed in Thompson SL *et al*. 2010).

Besides ATIP3, a number of MAPs have been reported to display tumor suppressor functions, suggesting the existence of a functional superfamily of "Microtubule-Associated Tumor Suppressor Proteins (MATSP)" (Table 3). At the molecular level, these MATSPs can either stabilize or promote MT assembly. Representatives of this group of proteins are the RAS Association domain Family 1A (RASSF1A), the von Hippel–Lindau (VHL), the neurofibromatosis 2 (NF2) protein Merlin, the cylindromatosis tumor suppressor CYLD, the Adenomatous Polyposis Coli (APC), the Breast Cancer 1 (BRCA1), the leucine zipper putative tumor suppressor 1 (LZTS1) and the Fragile Histidine Triad (Fhit).

Table 3

"Microtubule-Associated Tumor Suppressor proteins" (MATSP) characteristics.

Protein Name	Related-Cancer	Inactivated by	Subcellular localization	Effect on MT	References
CYLD	Skin appendages tumors or cylindromas, familial trichoepithelioma and Brooke-Spiegler syndrome	Gene mutations	MT network Midbody	- Stabilization: - Promotes MT assembly and decreases depolymerization velocity - Promotes stability of astral MTs	Bignell GR *et al*. 2000; Stegmeier F *et al*. 2007; Gao J *et al*. 2008; Steinmetz MO & Akhmanova A, 2008; Massoumi R, 2011 ; Li D *et al*. 2014; Yang Y *et al*. 2014
Merlin	Tumors in central and peripheral nervous system, colorectal cancer, melanoma and renal carcinoma	Gene mutations and protein inactivation by phosphorylation	MT network Mitotic Spindle	- Stabilization: - Decreases tubulin turnover, growth and shrinkage rates, catastrophe frequencies - Inhibits GTP hydrolysis	Xu HM & Gutmann DH, 1998; Muranen T *et al*. 2007; Cooper J & Giancotti FG, 2014; Smole Z *et al*. 2014
RASSF1A	Several carcinomas and solid tumors	Promoter hypermethylation	MT network Mitotic Spindle MTOC	- Stabilization: - Decreases catastrophes, MT polymerization and depolymerization rates - Increases rescue frequency, pause events and MT lifetime - Bundles MTs - Decreases MT outgrowth towards cell cortex - Protect from depolymerization	Liu L *et al*. 2003; Rong R *et al*. 2004; Dallol A *et al*. 2004; Dallol A *et al*. 2005; Richter AM *et al*. 2009 ; Arnette C *et al*. 2014
VHL	Haemangliоblastomas and clear-cell RCC	Gene mutations and promoter hypermethylation	MT network Mitotic Spindle Primary cilia	- Stabilization: - Blocks tubulin turnover, inhibits GTP activity, inhibits catastrophes, increases rescue frequency - Protect from depolymerization	Hergovich A *et al*. 2002; Lolkema MP *et al*. 2004; Nyhan MJ *et al*. 2008; Thoma CR *et al*. 2009; Thoma CR *et al*. 2010; Haddad NM *et al*. 2013
APC	Sporadic Colorectal and familial adenomatous polyposis	Gene mutations	MT network/ MT growing end	- Stabilization: - Protects from depolymerization - Interacts with other +TIPs (EB1, Amer2, KIF17, IQGAP and mDia)	Nagase H & Nakamura Y, 1993; Munemitsu S *et al*. 1994; Smith KJ *et al*. 1994; Su LK *et al*. 1995; Polakis P, 1997; Mimori-Kiyosue Y *et al*. 2000; Goss KH & Groden J, 2000; Zumbrunn J *et al*. 2001; Nakamura M *et al*. 2001; Watanabe T *et al*. 2004; Wen Y *et al*. 2004; Jaulin F & Kreitzer G, 2010; Pfister AS *et al*. 2012
BRCA1	Breast, ovarian, gastric, non-small cell lung cancer	Gene mutations	MTOC Mitotic Spindle* Spindle Poles* Midbody*	- Stabilization: - Decreases MT outgrowth towards cell cortex - Decreases growth and shrinkage rates, and MT dynamicity	Hsu LC & White RL, 1998; Russell PA *et al*. 2000; Lotti LV *et al*. 2002; Lynch HT *et al*. 2008; Rosell R *et al*. 2009; Wei J *et al*. 2011; Foulkes WD & Shuen AY, 2013; Sung M & Giannakakou P, 2014
LZTS1	Gastric, ovarian, breast, lung, oral squamous cell carcinomas, bladder, prostate, esophageal cancers, uveal melanoma and kidney	Gene mutations and promoter hypermethylation	MT network	- MT assembly dependent on MAP (mitogen-activated protein) 2	Ishii H *et al*. 1999; Ishii H *et al*. 2001; Vecchione A *et al*. 2001; Vecchione A *et al*. 2002; Ono K *et al*. 2003; Nonaka D *et al*. 2005; Onken MD *et al*. 2008 ; Chen L *et al*. 2009; Califano D *et al*. 2010
Fhit	Ovarian, prostate, non-small cell lung cancer and primary breast cancer	Promoter hypermethylation	MT network	- MT assembly	Chaudhuri AR *et al*. 1999; Yang Q *et al*. 2002 ; Wali A, 2006; Wali A, 2010

* Reported only in one paper Lotti LV *et al*. 2002

A large number of studies have reported the inactivation, down-regulation or mutation of the genes encoding for these MAPs in several solid tumors (Table 3 for references). Of note, two of these proteins (APC and BRCA1) have been extensively studied and to date are considered masterpieces in the colorectal and breast/ovary cancer field, respectively.

Six tumor suppressors have been shown to stabilize MTs either *in vitro* or in cell-based assays. For most of these proteins, few studies are available to explain the mechanism of MT stabilization.

CYLD decorates the MT network to stabilize MTs by promoting their assembly and decreasing MT depolymerization velocity. This protein also decorates the midbody (known to be composed of stable MTs) and the astral MTs highlighting its role during mitosis (Stegmeier F *et al*. 2007; Gao J *et al*. 2008; Steinmetz MO & Akhmanova A, 2008; Li D *et al*. 2014; Yang Y *et al*. 2014).

Merlin has been described as a protein that binds MTs, anchors the actin cytoskeleton, controls cell proliferation, cell adhesion and epithelial polarization (Xu HM & Gutmann DH, 1998; Muranen T *et al*. 2007). Its effects on MT dynamic instability parameters include decrease on tubulin turnover, as well as reduction of growth and shrinkage rates and catastrophe frequencies. These effects together with the inhibition of GTP hydrolysis make of this protein as a potent MT stabilizer (Muranen T *et al*. 2007; Smole Z *et al*. 2014).

RASSF1A associates with interphase MTs, mitotic spindle and the MTOC. It bundles and stabilizes MTs through the reduction of catastrophes and MT polymerization and depolymerization rates. RASSF1A also increases the rescue frequencies, the percentage of time spent in pause and MT lifetime. Additionally, reduces MT regrowth and protects MTs from induced depolymerization (Liu L *et al*. 2003; Rong R *et al*. 2004; Dallol A *et al*. 2004; Arnette C *et al*. 2014). At the functional level, RASSF1A reduces cell migration, cell polarity and prevents CIN (Rong R *et al*. 2004; Dallol A *et al*. 2005; Arnette C *et al*. 2014).

VHL accomplishes important roles in the renal epithelium. It has been described as a MAP that binds MTs in interphase and mitosis and associates with the primary cilia. It stabilization effects include inhibition of tubulin turnover and GTP activity, decrease of catastrophes, increase of the rescue frequency, as well as protection from depolymerization (Hergovich A *et al*. 2002; Lolkema MP *et al*. 2004; Thoma CR *et al*. 2010). Similar as RASSF1A, VHL prevents cell migration, CIN and spindle misorientation (Thoma CR *et al*. 2009).

APC has been involved in a large number of functions as cell proliferation and survival preventing CIN and spindle misorientation, and in the promotion of cell migration (Polakis P, 1997; Watanabe T *et al*. 2004; Wen Y *et al*. 2004; Pfister AS *et al*. 2012). APC binds

directly the MTs or indirectly via EB1 (Munemitsu S *et al*. 1994; Smith KJ *et al*. 1994; Su LK *et al*. 1995; Mimori-Kiyosue Y *et al*. 2000; Zumbrunn J *et al*. 2001; Nakamura M *et al*. 2001). APC is able to stabilize MTs mostly through the interaction with other +TIPs such as IQGAP (Watanabe T *et al*. 2004), mDia and EB1 (Wen Y *et al*. 2004), KIF17 (Jaulin F & Kreitzer G, 2010) and Amer2 (Pfister AS *et al*. 2012).

BRCA1 has been shown to stabilize MTs but its mechanism remains controversial. Unlike the other MATSPs, BRCA1 does not localize at the MT lattice and rather regulates MT stability from the MTOC (Lotti LV *et al*. 2002; Sung M & Giannakakou P, 2014). BRCA1 decreases MT outgrowth towards the cell cortex, as well as growth and shrinkage rates (Lotti LV *et al*. 2002; Sung M & Giannakakou P, 2014).

Other members of the MATSPs family have been shown to promote MT assembly. LZTS1 and Fhit are reported as MAPs that bind assembled MTs and tubulin, and function to promote MT assembly (Chaudhuri AR *et al*. 1999; Ishii H *et al*. 2001). Nevertheless, the mechanism of action has not been elucidated for any of the two proteins.

It may be interesting to investigate if members of the MATSP superfamily can interact with each other and function in a concerted and cooperative way to regulate tumorigenesis. Interestingly, van der Weyden L and coworkers (2008) showed that cooperation between inactivation of RASSF1A and APC results in accelerated intestinal tumorigenesis, through the interfering of β-catenin pathway. It would now be of interest to evaluate whether these tumor suppressors may also coordinately regulate cancer progression by a mechanism involving their effects on MT dynamics.

Finally, ATIP3 being part of the functional superfamily of MATSP, the question can be raised of whether ATIP3 may regulate some parameters of MT dynamic instability and/or cooperate with other members of the superfamily to exert its tumor suppressor effects.

Based on these observations, my PhD project aims at elucidating the effects of ATIP3 on the regulation of MT dynamic instability, with possible consequences on cancer cell migration, and metastasis (Article 1). Additionally, the search for ATIP3 interacting partners that may contribute to the effects of ATIP3 on dynamic instability and/or cell migration shall constitute the second objective of this work (Article 2 and Unpublished results).

II. RESULTS

ARTICLE 1:

ATIP3, a Novel Prognostic Marker of Breast Cancer Patient Survival, Limits Cancer Cell Migration and Slows Metastatic Progression by Regulating Microtubule Dynamics

Previous data from the laboratory identified a new microtubule-associate protein named ATIP3, encode by the candidate tumor suppressor gene *MTUS1*, whose expression is down-regulated in 48% of invasive breast carcinoma and 62% of metastatic tumors. Additionally, that ATIP3 re-expression at normal levels in breast cancer cell lines significantly reduced cancer cell proliferation *in vitro* and tumor growth *in vivo*.

Based on these results, the aim of the first part of my PhD work, which was published in the Cancer Research Journal, was to elucidate whether ATIP3 was involved on breast cancer metastasis, and if ATIP3 may represent a new biomarker for breast cancer metastasis. As mentioned in the introduction cancer metastasis is a multistep process that involves cancer cell migration and invasion, followed by extravasation and colonization. Thus, we wonder how does ATIP3 could alter the metastatic process and through which mechanism.

Using the DNA microarray data from three independent cohorts (Institut Curie, Institut Gustave Roussy and the Kaplan-Meier plotter database) of breast cancer patients with known clinical data, the prognostic value of ATIP3 as a marker for metastatic progression and overall survival was evaluated. Comparison of *MTUS1* probeset intensities with clinicopathologic data of the patients showed that low expression levels of ATIP3 significantly decrease the overall probability of survival and the relapse-free survival of breast cancer patients when compared with patients expressing normal levels of ATIP3. Additionally, when compared the percentage of patients with metastatic disease surviving after 5 years, those expressing low levels of ATIP3 had a reduced survival percentage than the ATIP3-normal expression group. Of note, this difference (and overall survival difference) was no longer found in non-metastatic patients. These results suggest that ATIP3 is an important prognostic marker of clinical outcome for patients with metastatic disease.

Given the association of low ATIP3 and metastatic patients' outcome, the effects of ATIP3 on metastatic progression were then evaluated. Using an *in vivo* experimental mouse model of metastasis, D3H2LN highly invasive breast cancer GFP and GFP-ATIP3 stable clones (expressing luciferase) were injected intracardiacally into nude mice to elucidate the late steps of the metastatic process. The metastatic dissemination was followed by intravital bioluminescence imaging every 2 days during 24 days. Quantification of photon number/s showed that mice injected with GFP-ATIP3-expressing cells presented a delay in metastasis time course, a decrease in the number of metastasis per mouse and a reduction in the number of large metastatic foci (at the end of the experiment) when compared with GFP-expressing mice. Altogether these data indicate a strong effect of

ATIP3 in the metastatic progression and suggest a role for this protein in metastatic growth and colonization *in vivo*.

To investigate the effect of ATIP3 on the colonization step, extravasation, invasion and migration experiments were performed using Boyden chambers. Different conditions were tested, where the upper chambers were either plated with HCMEC/D3 cells or coated with collagen I or no coated, before D3H2LN GFP and GFP-ATIP3 stable clones were seeded above. Re-expression of ATIP3 revealed a markedly reduction in migration (included the transendothelial migration or extravasation). These results were confirmed using MDA-MB-468 cells that express endogenous levels of ATIP3. Migratory behavior was increased followed ATIP3 down-regulation, suggesting that loss of ATIP3 allows the acquisition of a promigratory phenotype that may be more prone to develop distant metastasis.

Directional migration was then evaluated through a wound-healing experiment in ATIP3-expressing cells in which ATIP3-specific siRNAs were transfected. In accordance with Boyden chamber results, silencing of ATIP3 increased directional cell migration. These results were confirmed using breast cancer (D3H2LN and MCF7) stable clones expressing GFP or GFP-ATIP3. Indeed, expression of ATIP3 significantly reduced wound closure. Wound-healing time-lapse videomicroscopy using D3H2LN GFP and GFP-ATIP3 stable clones was performed to follow the migration process. Cell tracking analysis revealed that ATIP3 expression impairs cancer cell velocity and directionality, effects that explain the reduction of cell migration induced by ATIP3.

It has been shown that ATIP3 is a microtubule-associated protein (MAP) that reduces cell proliferation and migration, suggesting that the effect of ATIP3 on essential cell process is due to the possible regulation of microtubule (MT) dynamic instability parameters. Nocodazole incubation at 37°C during 1h and nocodazole washout experiments were performed to analyze the effect of ATIP3 on MT depolymerization and MT regrowth, respectively. Results shown that in ATIP3-expressing cells, nocodazole (1µmol/L) incubation did not depolymerize all the MTs. Of note, anti-acetylated tubulin staining revealed that the remaining MTs were stable MTs which were post-translationally modified. On the other hand, ATIP3-silencing induces a high decrease on MT density and few stable acetylated MTs remained, indicating that ATIP3 stabilizes MTs and protects them from depolymerization. The same experiment was performed in MCF7 breast cancer cell line stably expressing GFP and GFP-ATIP3 and incubated with nocodazole (10 µmol/L). ATIP3 re-expression in MCF7 breast cancer cell line increases stable MTs, while GFP-expressing cells did not.

RPE1 cells were used to evaluate the effect of ATIP3 in MT regrowth. GFP and GFP-ATIP3 were transiently transfected for 24h and MTs were depolymerized with nocodazole (10µmol/L) at 4°C. Nocodazole washout showed that ATIP3 expression significantly delayed MT regrowth, strongly suggesting an effect of ATIP3 in MT dynamics.

EB1 accumulation at the MT plus-ends was then used as an indicator of MT dynamics. RPE1 cells were transiently transfected for 24h with mCherry-ATIP3 construct and stained with an anti-EB1 antibody. Immunofluorescence images indicated that ATIP3 expression lead to a significant reduction of EB1 comet size that was not associated with a reduction of EB1 expression. Similar results were obtained in ATIP3-expressing HeLa cells transfected with ATIP3-specific siRNA. Silencing of the protein resulted in a significant increment of EB1 comet size and fluorescence intensity at the MT growing ends that was not the case for control siRNA transfected cells. These results indicate that loss of ATIP3 may increase MT dynamics.

Soon after, the role of ATIP3 on MT dynamic instability parameters was elucidated by TIRF time-lapse videomicroscopy using EB1-GFP as plus-end marker. HeLa cells were co-transfected with siRNAs (control or ATIP3-specific) and EB1-GFP during 48h. Tracking results revealed that loss of ATIP3 leads to an increase of MT growth episodes and growth rate, and a decrease of the time spent in pause and catastrophe frequency. These results confirm the role of ATIP3 in MT dynamic instability.

We then hypothesize that MT stabilization and decreased growth could impair MT correct anchoring at the cell cortex during migration. To test this hypothesis, D3H2LN cells transiently transfected with GFP or GFP-ATIP3 were grown until confluence before being scratched and kept at 37°C for 90 minutes. In GFP-expressing cells, MT were radially organized toward the cell periphery with the MT plus-ends close to the cell margin; instead, in ATIP3-expressing cells MTs bend before reaching the cell edge and consequently MT plus-end did not anchor the cell cortex. This difference in MT polarization was traduced in a defect of cell polarity in ATIP3-positive cells in respect with GFP cells. This indicates that ATIP3 impairs MT dynamics, MT polarization and therefore cell polarity and cell migration.

Cleavage of ATIP3 into three domains (D1, D2 and D3) allows the characterization of the full length protein. Transfection of GFP-D1, GFP-D2 and GFP-D3 into RPE1 cells followed by immunostaining using anti-GFP, anti-tubulin and anti-EB1 antibodies was performed. Immunofluorescence images shown that the central D2 was the only able to associate to MTs and to impair EB1 comet accumulation at the plus-ends. Interestingly, D2 also retain the functional properties of the full-length protein, reducing cell proliferation and cell migration and directionality. Thus, D2 recapitulates the functional characteristics of ATIP3.

To conclude, in this study ATIP3 was identified as an important indicator of metastatic progression that regulates early (tumor growth) and late (colonization) stages of cancer development through its ability to regulate MT dynamics. Additionally, the functional domain of the protein was characterized, and termed D2, which is of highly importance for the future targeted therapeutic approaches against breast tumors that have lost ATIP3 expression.

ATIP3, a Novel Prognostic Marker of Breast Cancer Patient Survival, Limits Cancer Cell Migration and Slows Metastatic Progression by Regulating Microtubule Dynamics

Angie Molina, Lauriane Velot, Lydia Ghouinem, et al.

Cancer Res 2013;73:2905-2915. Published OnlineFirst February 8, 2013.

ATIP3, a Novel Prognostic Marker of Breast Cancer Patient Survival, Limits Cancer Cell Migration and Slows Metastatic Progression by Regulating Microtubule Dynamics

Angie Molina[1,2,3], Lauriane Velot[1,2,3], Lydia Ghouinem[1,2,3], Mohamed Abdelkarim[4,7], Benjamin Pierre Bouchet[10], Anny-Claude Luissint[1,2,3], Imène Bouhlel[1,2,3], Marina Morel[1,2,3], Elène Sapharikas[1,2,3], Anne Di Tommaso[1,2,3], Stéphane Honoré[8], Diane Braguer[8], Nadège Gruel[5], Anne Vincent-Salomon[5], Olivier Delattre[5], Brigitte Sigal-Zafrani[5], Fabrice André[9], Benoit Terris[1,2,3,6], Anna Akhmanova[10], Mélanie Di Benedetto[4,7], Clara Nahmias[1,2,3], and Sylvie Rodrigues-Ferreira[1,2,3]

Abstract

Metastasis, a fatal complication of breast cancer, does not fully benefit from available therapies. In this study, we investigated whether ATIP3, the major product of 8p22 *MTUS1* gene, may be a novel biomarker and therapeutic target for metastatic breast tumors. We show that ATIP3 is a prognostic marker for overall survival among patients with breast cancer. Notably, among metastatic tumors, low ATIP3 levels associate with decreased survival of the patients. By using a well-defined experimental mouse model of cancer metastasis, we show that ATIP3 expression delays the time-course of metastatic progression and limits the number and size of metastases *in vivo*. In functional studies, ATIP3 silencing increases breast cancer cell migration, whereas ATIP3 expression significantly reduces cell motility and directionality. We report here that ATIP3 is a potent microtubule-stabilizing protein whose depletion increases microtubule dynamics. Our data support the notion that by decreasing microtubule dynamics, ATIP3 controls the ability of microtubule tips to reach the cell cortex during migration, a mechanism that may account for reduced cancer cell motility and metastasis. Of interest, we identify a functional ATIP3 domain that associates with microtubules and recapitulates the effects of ATIP3 on microtubule dynamics, cell proliferation, and migration. Our study is a major step toward the development of new personalized treatments against metastatic breast tumors that have lost ATIP3 expression. *Cancer Res; 73(9); 2905–15. ©2013 AACR.*

Introduction

The occurrence of distant metastasis is a dreadful complication of breast cancer and a leading cause of death by malignancy in women worldwide. Metastasis is a multistep process that involves cancer cell migration and invasion across the extracellular matrix to reach the blood flow, followed by extravasation and colonization of secondary organs (1). Among millions of invasive cancer cells that reach the blood circulation, only few will establish at distant sites and grow as metastases (2–5). Breast cancer metastases can remain latent for several years following primary tumor removal, and the identification of molecular markers that may predict the risk of metastasis occurrence, and/or progression is of invaluable help for the follow-up of the patients and choice of therapeutic options (5, 6). Over the past decade, extensive studies have led to the classification of breast tumors into distinct molecular subtypes, allowing subsequent development of efficient targeted treatments for a majority of primary tumors (7–9). However, available therapies have limited effect on cancer metastasis and new genetic determinants contributing to essential steps of the metastatic process need to be characterized.

Microtubule-targeting drugs such as taxanes are used for standard first-line treatment of breast cancer metastasis, and new microtubule-targeting agents, such as epothilones and eribulin, are under clinical evaluation (10). Microtubules are polarized and highly dynamic structures that rapidly switch between periods of polymerization (growth) and depolymerization (shrinkage) at the plus ends, a process termed dynamic

Authors' Affiliations: [1]Institut National de la Santé et de la Recherche Medicale (Inserm), U1016, Institut Cochin; [2]CNRS, UMR8104; [3]Université Paris Descartes, Sorbonne Paris Cité; [4]CNRS7033, UMRS940, IGM; [5]Institut National de la Santé et de la Recherche Medicale (Inserm), U830, Translational Research Department, Institut Curie; [6]Pathology Department, Hopital Cochin, Paris; [7]Université Paris 13, Bobigny; [8]Aix-Marseille University, CRO2, Institut National de la Santé et de la Recherche Medicale (Inserm) UMR911, Marseille; [9]Department of Medicine, Institut Gustave Roussy, Institut National de la Santé et de la Recherche Medicale (Inserm), U981, Villejuif, France, and [10]Cell Biology, Faculty of Science, Utrecht University, Utrecht, the Netherlands

Note: Supplementary data for this article are available at Cancer Research Online (http://cancerres.aacrjournals.org/).

C. Nahmias and S. Rodrigues-Ferreira contributed equally to this work.

Corresponding Author: Clara Nahmias, Institut Cochin, Dept EMC, 22 rue Méchain 75014 Paris, France. Phone: 33-1405-16410; Fax: 33-1405-16430; E-mail: clara.nahmias@inserm.fr

doi: 10.1158/0008-5472.CAN-12-3565

instability (11–13). The extent and rate of microtubule growth, as well as transitions between growth and shrinkage, are parameters of dynamic instability that can be measured by tracking end-binding proteins at the microtubule plus ends (13–15). Dynamic instability is essential for the microtubule plus ends to explore the cytosol and ensure cytoskeleton reorganization during cell division and migration. Targeting the expression or activity of metastasis genes that regulate microtubule dynamics represents a promising option for cancer therapy.

ATIP3 is a microtubule-associated protein encoded by 8p22 candidate tumor suppressor gene *MTUS1* (16–18). We have previously shown that ATIP3/*MTUS1* levels are significantly downregulated in 47.7% of invasive breast carcinomas and 62.4% of metastatic tumors (19). Restoring ATIP3 expression at normal levels in breast cancer cells significantly reduces cancer cell proliferation *in vitro* and tumor growth *in vivo* (19). However, effects of ATIP3 on breast cancer metastasis have not yet been evaluated.

In this study, we investigated whether ATIP3 may represent a new biomarker and therapeutic target for breast cancer metastasis. We present evidence that low ATIP3 levels correlate with the decreased probability of survival among patients with breast cancer metastasis, and that ATIP3 expression into ATIP3-deficient cancer cells markedly impairs the establishment of metastatic foci *in vivo*. Loss of ATIP3 increases breast cancer cell migration and alters microtubule dynamics. We show that ATIP3 associates with microtubules through a central basic domain that retains the functional properties of the full-length protein. Our study thus identifies ATIP3 as a new promising therapeutic target against metastatic breast tumors of poor prognosis.

Materials and Methods

Breast tumor samples and gene arrays

Microarray data for a series of 150 infiltrating ductal primary breast carcinomas and 11 normal breast tissues from the Institut Curie (Paris, France) and clinical data for the patients were described elsewhere (19, 20). Gene expression profiles from an independent cohort of 162 invasive breast carcinomas were obtained from patients included in the prospective database of the Institut Gustave Roussy (IGR; Villejuif, France) between 1984 and 1994. This study was approved by the Institutional Review Boards of the IGR. Data have been submitted to the Array Express data repository at the European Bioinformatics Institute (Saffron Walden, United Kingdon; http://www.ebi.ac.uk/arrayexpress/) under accession number E-MTAB-1389. *MTUS1* gene expression in a meta-analysis of 2,898 patients with breast cancer with known clinical outcome was retrieved from Kaplan–Meier plotter database (21, 22).

Cell lines, plasmid constructs, and transfections

Human breast cancer cell lines MDA-MB-468 and MCF7 and stable clones were described previously (19). MDA-MB-231-Luc-D3H2LN breast cancer cells (designated D3H2LN) obtained from Caliper Life Science (Xenogen) were derived from an *in vivo*-selected metastatic subclone of MDA-MB-231 cells expressing luciferase and grown as described (23). HeLa cells were provided by Dr. Mounira Amor-Gueret (Institut Curie, Orsay, France). RPE-1 [human telomerase reverse transcriptase (h-TERT)-immortalized, retinal pigment epithelial] cells were from Dr. Franck Perez (Institut Curie, Paris). MRC5-SV lung fibroblasts were grown in Dr. A. Akhmanova's laboratory as described (24). All cells were used at passages 2 to 20 after thawing and grown as described by the provider. Cells were routinely authenticated by morphologic observation and tested for absence of mycoplasma contamination using MycoAlert Assay detection kit (Lonza).

Plasmid constructs are described in the Supplementary Methods. Transfections using ATIP3-specific siRNAs (si#1 and si#2) were conducted as described (19) and verified by immunoblotting using anti-MTUS1 polyclonal antibodies (ARP-44419, Aviva Systems).

Intracardiac experimental mouse model of metastasis

Experimental metastasis was conducted as described (23, 25, 26) following intracardiac injection of stable ATIP3-negative [WT (wild-type), GFP] or positive (Cl3, Cl6) D3H2LN cell clones. All injected cells showed similar viability as measured by Annexin V apoptosis kit (Beckman Coulter). The experiment was carried out with the approval of the Département d'Expérimentation Animale, Institut d'Hématologie, Hopital St-Louis ethical committee, and was conducted twice (9 mice per group).

Clonogenicity, cell migration, and adhesion assays

Analyses of colony formation, Boyden chambers chemotaxis, transendothelial migration, wound healing, and cell adhesion were conducted as described (23). Time-lapse videomicroscopy analyses of cell motility are described in the Supplementary Methods. For cell polarity measurements, transiently transfected D3H2LN were allowed to migrate for 90 minutes and analyzed using bright field microscopy. Polarized cells were identified on the basis of nucleus position and cytoplasm extension at the leading edge.

Immunostaining, fluorescence microscopy, analysis of microtubule dynamics

Cells were plated on glass coverslips and transfected for 24 hours (plasmids) or 72 hours (siRNA), fixed in ice-cold methanol for 5 minutes, and incubated for 1 hour at room temperature with anti-α-tubulin clone F2C (27), monoclonal anti-γ-tubulin (Sigma), anti-end-binding 1 (EB1; clone 5; BD Biosciences), or anti-acetylated tubulin (clone 6-11B-1; Sigma). Secondary antibodies and fluorescence images capture are described in the Supplementary Methods.

Linescan analyses of α-tubulin and EB1 fluorescence intensity were done (ImageJ) on a 6 μm line along the length of microtubule tip. At least 10 microtubules per cell in 4 separate cells were measured. EB1-comet maximal intensity was obtained by subtracting the intensity value of the EB1-dot (100 a.u.) to the maximal staining intensity.

Analyses of microtubule stability, regrowth, and microtubule dynamic instability are described in the Supplementary Methods.

Statistical analysis

Statistical analyses were done using JMP-7 and GraphPad Prism softwares. Overall survival (OS) curves were plotted according to the method of Kaplan–Meier and compared by the log-rank test. Data in bar graphs (mean +/− SD) were analyzed using 2-tail unpaired Student *t* test. Dot plot analyses were done using Mann–Whitney test. $P < 0.05$ was considered statistically significant.

Results

ATIP3 is a prognostic marker of poor outcome in metastatic breast cancer

The prognostic value of ATIP3 as a marker for metastatic progression and OS was evaluated in 3 independent cohorts of patients with breast cancer. Comparison of *MTUS1* Affymetrix probeset intensities with clinicopathologic data of the patients in a panel of 150 invasive breast carcinomas (Supplementary Table S1) showed that the overall probability of survival is strongly reduced in patients with tumors expressing low as compared with normal ATIP3 transcript levels (Fig. 1A and Supplementary Fig. S1A). Relapse-free survival (RFS) of the patients was also significantly reduced in low ATIP3-expressing tumors (Supplementary Fig. S1B). Similar results were obtained by analyzing *MTUS1* levels in an independent cohort of 162 patients with breast cancer (Fig. 1B and Supplementary Table S2) and in a meta-analysis of 2,898 patients with breast cancer (Fig. 1C and Supplementary Fig. S1C and S1D). Of note, correlation between ATIP3 expression and OS of the patients was independent of the estrogen receptor (ER) status of the tumor (Fig. 1D).

Tumors were then classified according to their metastatic properties and *MTUS1* probeset intensities were compared with the probability of patient survival. As shown in Fig. 1E, the percentage of patients with metastatic disease surviving after 5 years was markedly reduced when tumors expressed low ATIP3 (6.25%) compared with normal ATIP3 levels (31.6%), whereas in patients with nonmetastatic tumors, 5-year survival (Fig. 1E and Supplementary Fig. S1E) and OS rates (Fig. 1F and H) were independent of the levels of ATIP3. Within patients with metastatic disease, OS rates (Fig. 1F and H and Supplementary Fig. S1E) and survival time (Fig. 1G and I) were also reduced when tumors expressed low levels of ATIP3. Thus, ATIP3 expression is an important indicator of clinical outcome for patients with metastatic breast tumors. Correlation between low ATIP3 levels and reduced survival rates among patients with advanced breast cancer suggests major effects of ATIP3 on metastatic progression.

ATIP3 limits breast cancer metastatic colonization *in vivo*

In vivo effects of ATIP3 on the metastatic potential of breast cancer cells were evaluated using a well-defined experimental mouse model of metastasis monitored by intravital bioluminescence imaging (23, 25, 26). Highly metastatic, ATIP3-negative, D3H2LN breast cancer cells were transfected with either GFP or GFP-ATIP3, and independent stable cell clones (Cl3 and Cl6) expressing moderate levels of ATIP3 were selected (Fig. 2A, left). All cell clones exhibited similar levels of luciferase activity (Fig. 2A, right). Metastatic cancer cells were injected intracardiacally into the bloodstream of nude mice to recapitulate the late, rate-limiting, steps of the metastatic process, and examine metastatic dissemination to various organs while avoiding any effect of ATIP3 on primary tumor growth. Four groups of 18 mice were analyzed in two independent experiments. For each animal, the total number of metastatic foci and the number of photons/s were quantified every 2 days for 24 days (Supplementary Table S3). As shown in Fig. 2B, the time-course of metastasis formation was markedly delayed in mice injected with ATIP3-positive as compared with ATIP3-negative cell clones. The number of cancer cells growing at secondary sites increased exponentially from day 17 after injection of ATIP3-positive clones, as compared with day 10 for mice injected with control cells (Fig. 2B). As shown in Fig. 2C, the number of mice developing metastasis was strongly diminished upon ATIP3 expression. Importantly, the number of detectable metastases per mouse was also significantly reduced at all times in the presence of ATIP3 (Fig. 2D). At day 24, the number of mice invaded with large metastases reached 13 of 18 (72.2%) in the control group as compared with 2 of 18 (11.1%) following injection of ATIP3-positive cells (Fig. 2E and F), indicating a prominent effect of ATIP3 on cancer cell growth and colonization at secondary sites. Accordingly, on day 24, the total number of photons/s per mouse was 50- and 25-fold lower following injection with Cl3 and Cl6 clones, respectively, compared with WT (Supplementary Fig. S2A). For ethical reasons, mice had to be sacrificed at day 24, therefore OS of the two groups of mice could not be quantified. Furthermore, *ex-vivo* and histologic analysis of metastatic nodules (Supplementary Fig. S2B) confirmed that bioluminescent signals indeed correspond to metastases of human tumor cells having infiltrated mouse tissues. Metastases were mainly detected in the bones, the lungs, and the brain, which are the most frequent sites of metastatic dissemination of human breast tumors. No preferential location of metastatic nodules in ATIP3-positive versus ATIP3-negative cell types could be observed. Altogether, these results identify ATIP3 as a potent antimetastatic molecule, and support a role for ATIP3 in metastatic growth and colonization *in vivo*.

ATIP3 impairs breast cancer cell proliferation and migration

Metastatic colonization involves cancer cell migration, invasion through the extracellular matrix, and proliferation at the secondary site. As expected from our previous studies (19), cell proliferation was significantly reduced in ATIP3-positive clones Cl3 and Cl6 as compared with control (Supplementary Fig. S3A). In addition, Boyden chambers assays of chemotaxis and invasion revealed more than 90% reduction in the promigratory properties of Cl3 compared with GFP (Fig. 3A). Similar effects were observed using stably transfected MDA-MB-231 cells (Supplementary Fig. S3B). Conversely, ATIP3 silencing in metastatic MDA-MB-468 breast cancer cells expressing endogenous ATIP3 induced a 2- to 2.5-fold increased chemotactic migration (Fig. 3B), suggesting that cancer cells having lost ATIP3 may acquire a promigratory phenotype and may be more prone to develop distant metastasis.

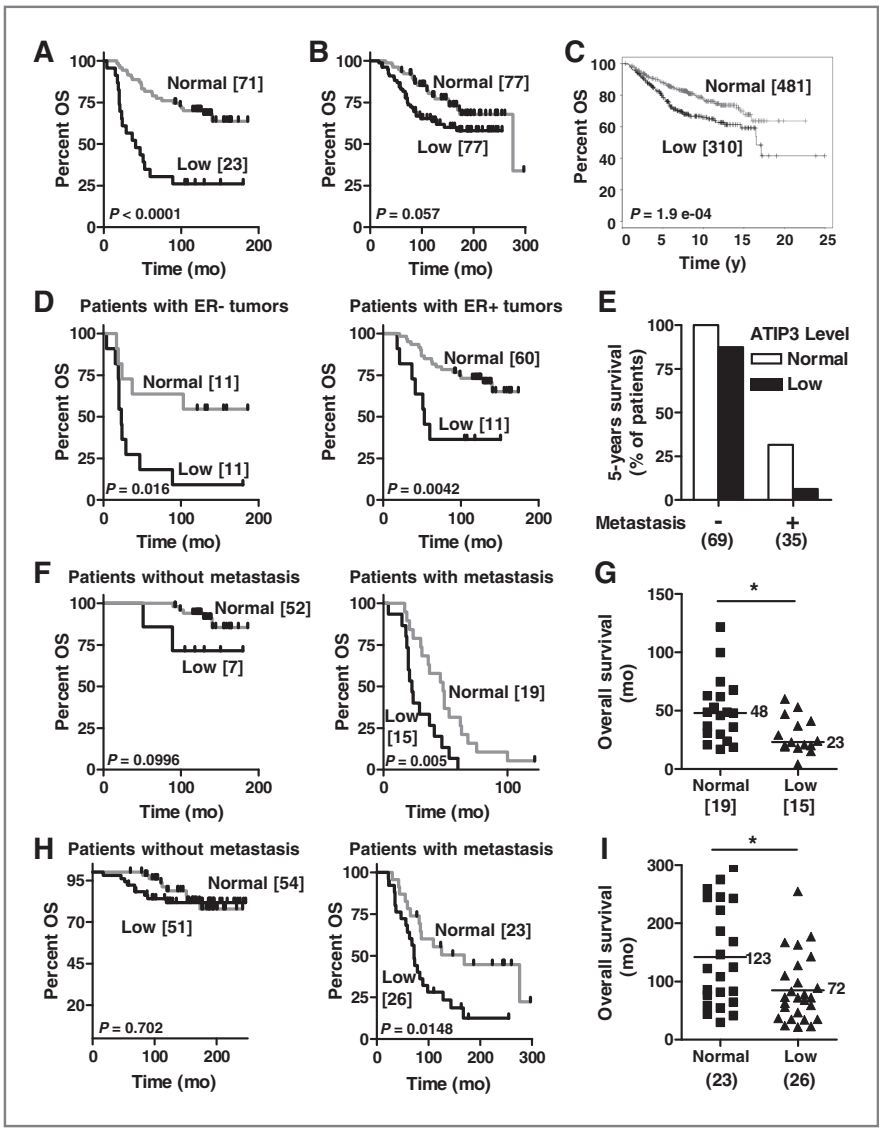

Figure 1. Low levels of ATIP3 predict poor outcome among metastatic tumors. A, OS curves for patients from the Institut Curie cohort, with tumors expressing normal (> 0.5) or low (< 0.3) ATIP3 levels, relative to the median value of *MTUS1* probeset (212096_s_at) in normal tissues. B, OS curves for patients from the IGR cohort, with tumors expressing normal or low ATIP3 levels [inferior or superior to the median value of *MTUS1* probeset (A_23_P347169) intensities in the 162 tumors analyzed]. C, OS curves for patients with tumors expressing normal to high (gray) or low (black) *MTUS1* (212096_s_at) using Kaplan–Meier plotter. The best performing threshold was used as a cutoff. D, OS curves from patients expressing normal or low ATIP3 as in A, among ER negative (ER−, left) and positive (ER+, right) tumors. E, percentage of patients remaining alive after 5 years with nonmetastatic (−) and metastatic (+) tumors expressing ATIP3 levels as in A. F, OS curves for patients with nonmetastatic (left) or metastatic (right) tumors expressing ATIP3 levels as in A. G, OS time (in months) for patients with metastatic tumors expressing ATIP3 levels as in A. Median values are on the right. *, $P = 0.0119$. H, OS curves as in F for patients from the IGR cohort. Nonmetastatic (left) and metastatic (right) tumors were classified according to ATIP3 levels as in B. I, OS time (in months) for patients as in G with metastatic tumors classified as in H. Number of patients is under brackets. *, $P = 0.0172$.

The ability to migrate through a monolayer of endothelial cells (transendothelial migration) was significantly reduced (58 ± 16%) in Cl3 compared with control (Fig. 3C). Adhesion of clones Cl3 and Cl6 to endothelial cells was significantly elevated (3-fold and 2.8-fold, respectively) compared with WT (Fig. 3D), suggesting that increased tumor-endothelial cell adhesion may account for reduced transendothelial migration. Cell adhesion to collagen I was also increased in Cl3 (1.85-fold) and Cl6 (1.93-fold) compared with WT (Fig. 3E). Altogether, these data indicate that ATIP3 concomitantly increases cell adhesion and limits cell migration.

The consequences of ATIP3-silencing on cancer cell motility were analyzed in HeLa cells that express endogenous ATIP3 and are well suited for analyses of wound closure. As shown

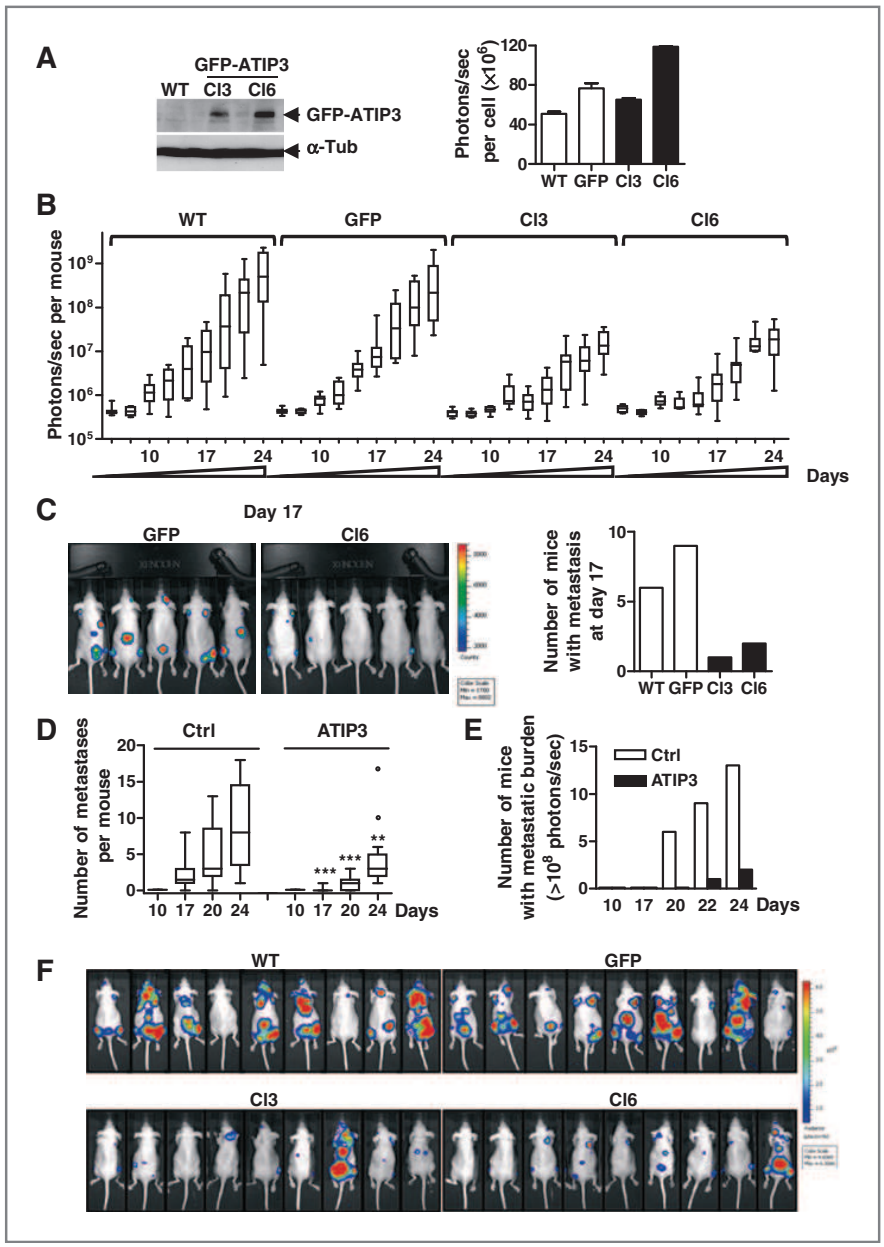

Figure 2. ATIP3 expression slows metastatic progression *in vivo*. A, characterization of stably transfected D3H2LN cell clones. Left, immunoblots of nontransfected (WT) and GFP-ATIP3-expressing D3H2LN clones (Cl3, Cl6) using anti-GFP antibodies, reprobed with anti-α-tubulin (α-tub) antibodies. Right, measurement of luciferase activity per cell ($n = 3$). B, number of photons/s per mouse ($n = 9$) at days 6 to 24 following tumor cell inoculation. C, left, representative pictures of bioluminescence (5/9 mice) at day 17 following intracardiac injection. Scale is on the right. Right, number of mice with at least one detectable metastasis at day 17. D, total number of metastastic sites per mouse at indicated days after inoculation of control (Ctrl, WT and GFP, $n = 18$) and ATIP3 positive (ATIP3, Cl3 and Cl6, $n = 18$) cells. **, $P < 0.01$, ***, $P < 0.001$. E, number of mice with large metastases at different times after inoculation as in D. F, representative pictures (day 24) as in C.

in Fig. 3F, ATIP3 silencing in HeLa cells increased (1.84- to 2.6-fold) directional migration. Conversely, stable ATIP3 expression into D3H2LN (Cl3 and Cl6, Fig. 3G) and MCF7 cells (Supplementary Fig. S3C) significantly reduced wound closure. Time-lapse microscopy (Supplementary Movies S1 and S2) and tracking of D3H2LN-migrating cells further indicated that stable ATIP3 expression impairs both cancer cell velocity (0.34 μm/s and 0.55 μm/s for Cl3 and GFP clones, respectively; ref. Fig. 3H) and directionality (Fig. 3I). Similar results were obtained (Supplementary Fig. S3D and S3E) by analyzing cell tracking following transient transfection of GFP or GFP-ATIP3 into D3H2LN cells (Supplementary Movies S3 and S4). Of note, the number of GFP-ATIP3–positive cells reaching the wound edge was reduced compared with GFP-expressing cells. GFP-ATIP3 expressing cells were overtaken by nontransfected cells reaching the border of the wound (Supplementary Fig. S3F), further confirming the inhibitory effect of ATIP3 on cancer cell migration.

ATIP3 alters microtubule dynamics

We hypothesized that ATIP3, being closely associated with microtubules (19), may limit cell proliferation and migration by

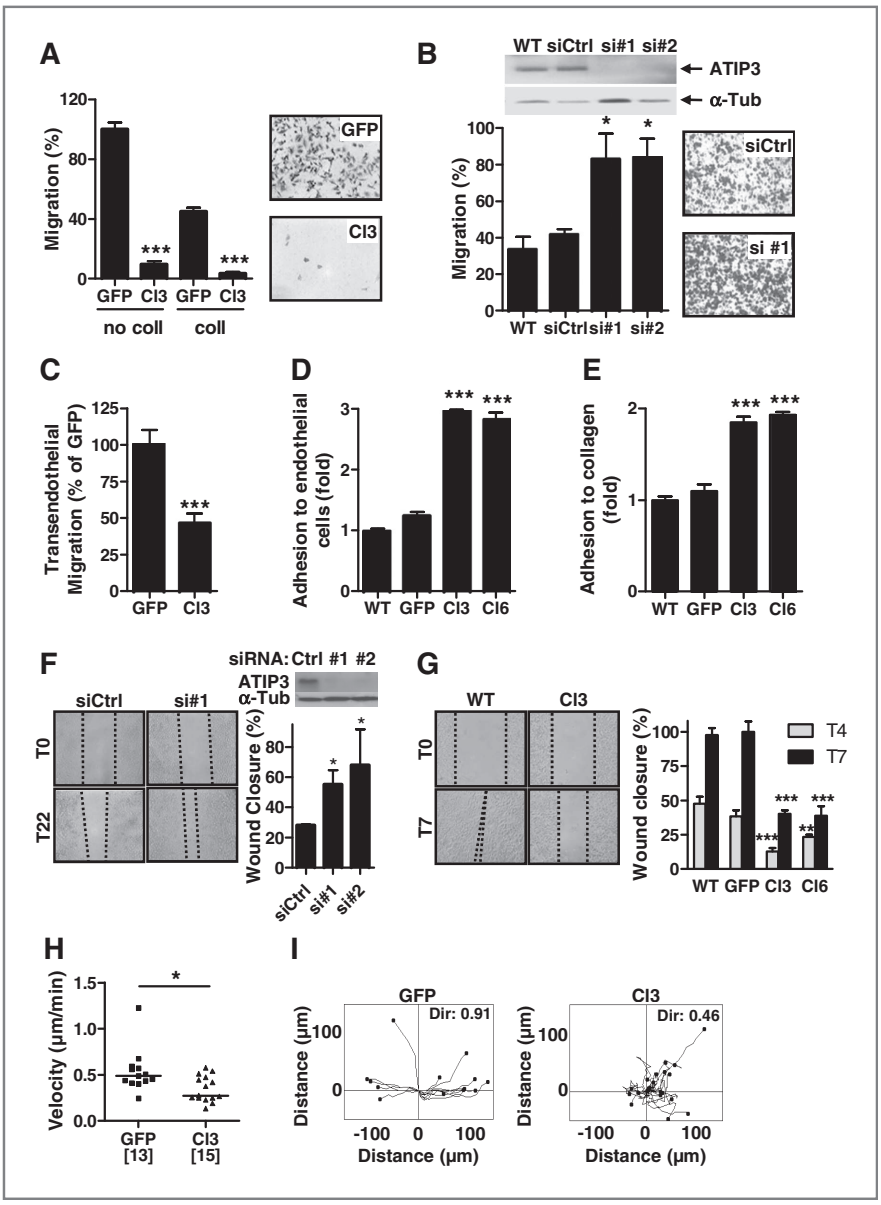

Figure 3. ATIP3 reduces breast cancer cell migration. A, Boyden chamber migration of stable D3H2LN cell clones across filters coated (coll) or not (no coll) with collagen I. Results (percent) are mean ± SEM ($n = 3$). Right, representative picture of cells migrating to the bottom of the well. B, Boyden chamber assay using ATIP3-positive (WT and siCtrl) and ATIP3-negative (si#1 and si#2) MDA-MB-468 cells. Results are shown as in A. Top, immunoblots of MDA-MB-468 cells after siRNA silencing [anti-MTUS1, reprobed with anti-α-tubulin (α-tub) antibodies]. Right, representative pictures of the lower face of the filter. C, transendothelial migration, mean ± SEM ($n = 3$). D and E, cancer cell adhesion (mean ± SEM, $n = 3$) to endothelial cells (D) and collagen (E). F, migration of ATIP3-positive (siCtrl) and ATIP3-silenced (si#1, si#2) HeLa cells ($n = 3$). Left, representative pictures of wound at times T0 and T22. Right, quantification (percent) of wound closure at T22. Results are mean ± SEM ($n = 2$). Top, immunoblots of siRNA-transfected HeLa cells as in B. G, directional migration of stably transfected D3H2LN clones ($n = 4$). Left, representative pictures of wound at times T0 and T7. Right, quantification of wound closure at T4 and T7. Results are mean ± SD ($n = 3$). H and I, cell tracking of D3H2LN stable clones during wound closure. H, cell velocity scattered dot plot. I, diagrams of migration trajectories (12 hours). Number of cells is under brackets. Directionality coefficient (Dir) is inside the graph. A, B, F, and G, magnification, ×100. *, $P < 0.05$; **, $P < 0.001$; ***, $P < 0.0001$.

regulating microtubule dynamics. We first analyzed the consequences of ATIP3 depletion on the sensitivity of microtubules to nocodazole that prevents repolymerization of dynamic microtubules. Stable microtubules that are not affected by nocodazole treatment are typically stained by anti-acetylated tubulin. As shown in Fig. 4A, ATIP3-silenced HeLa cells were highly sensitive to nocodazole. The number of cells retaining stable microtubules was decreased by 51% ± 10 and 53% ± 14 following transfection of siRNA#1 and siRNA#2 compared with control. Conversely, stable transfection of GFP-ATIP3 into MCF7 cells significantly increased the number of cells retaining stable, nocodazole-resistant, microtubules as assessed by anti-acetylated tubulin labeling (Fig. 4B) and immunoblotting (Fig. 4C). ATIP3 expression also significantly delayed microtubule regrowth following nocodazole washout (Fig. 4D). At 5 minutes, microtubule length around the centrosome was reduced by 57 ± 20% in GFP-ATIP3 compared with GFP-transfected clones, supporting the notion that ATIP3 may impair microtubule dynamics.

The effects of ATIP3 on microtubule dynamic instability parameters were further analyzed by measuring EB1 protein accumulation at the microtubule plus tips (13–15, 28, 29) in RPE-1 epithelial cells and lung fibroblasts (MRC5-SV), which have a sparse microtubule array and are well suited for

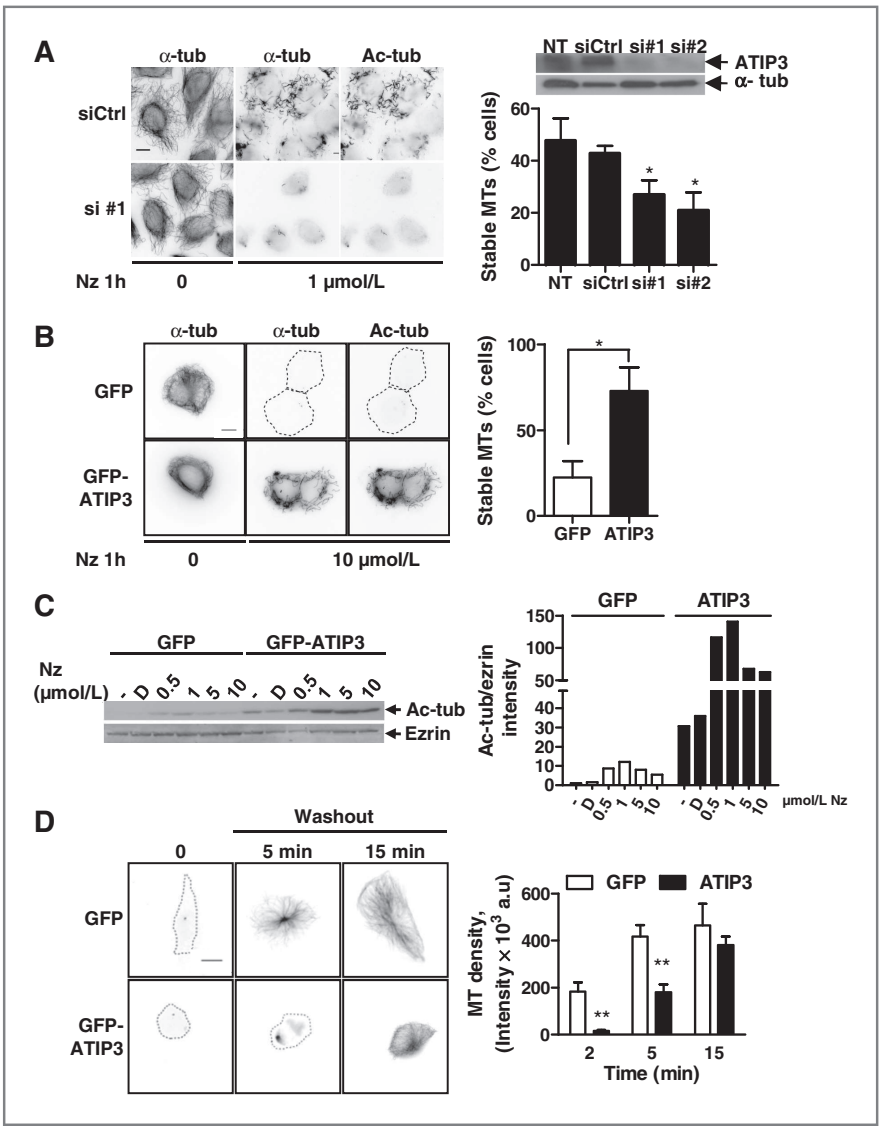

Figure 4. ATIP3 reduces nocodazole sensitivity and microtubule outgrowth. A, immunostaining (anti-α-tubulin (α-tub) and anti-acetylated tubulin [Ac-tub antibodies] of ATIP3-positive (siCtrl) and -negative (si#1) HeLa cells incubated without (0) or with 1 μmol/L nocodazole (Nz). Right, immunoblots of HeLa cells after siRNA silencing (anti-MTUS1, reprobed with antitubulin antibodies). Bottom, quantification (%) of cells retaining stable microtubules, mean ± SEM ($n = 3$). B, immunostaining of stable MCF7 clones incubated with or without 10 μmol/L nocodazole, as in A. Right, quantification as in A, mean ± SEM ($n = 3$). C, immunoblot analysis of acetylated-tubulin (Ac-tub) and ezrin content in stably transfected MCF7 clones, either nontreated (−) or treated with DMSO (D) or increasing concentrations of nocodazole. Right, quantification of the ratio between Ac-tub and ezrin intensity. D, microtubule regrowth in transiently transfected RPE-1 cells ($n = 4$). Shown is α-tubulin staining at indicated times after nocodazole (10 μmol/L) washout. Right, quantification of microtubule density at 4 μm around the centrosome, mean ± SD ($n = 4$ to 10 cells). *, $P < 0.05$; **, $P < 0.001$. Scale bar, 10 μm.

distinguishing individual microtubule tips. As shown in Fig. 5A, ATIP3 expression in RPE-1 cells led to a significant reduction in the number and size of EB1 comets that rather appeared as dots. Decreased accumulation of EB1 at microtubule plus ends was not associated with decreased EB1 expression (Supplementary Fig. S4A). In ATIP3-depleted HeLa cells, significantly more EB1 comets of increased length and intensity were detected compared with control cells (Fig. 5B), suggesting that ATIP3 silencing increases microtubule dynamics. Time-lapse total internal reflection fluorescence (TIRF) videomicroscopy analysis of EB1-GFP comets (Supplementary Movie S5) and subsequent microtubule-tips tracking indicated that microtubule growth episodes were significantly longer in ATIP3-silenced HeLa cells compared with control (Fig. 5C). ATIP3 depletion increased microtubule growth rate and decreased the time spent in pause as well as the frequency of catastrophes (Fig. 5C), accounting for increased microtubule dynamics. Conversely, videomicroscopy of EB3-GFP comets following expression of mCherry-ATIP3 in MRC5-SV cells (Supplementary Movie S6), and corresponding kymographs (Supplementary Fig. S4B), indicated that ATIP3 expression decreases microtubule dynamics and reduces the rate of microtubule growth.

Microtubule stabilization and decreased growth rate at the cell periphery should be responsible for an inhibition of microtubule targeting and capture at the cell cortex (30). As shown in Fig. 5D, in migrating D3H2LN cells, microtubules projected radially toward the cell periphery and microtubule plus ends were close to the cell edge (mean distance 1.43 ± 0.7 μm), whereas in the presence of ATIP3, microtubules

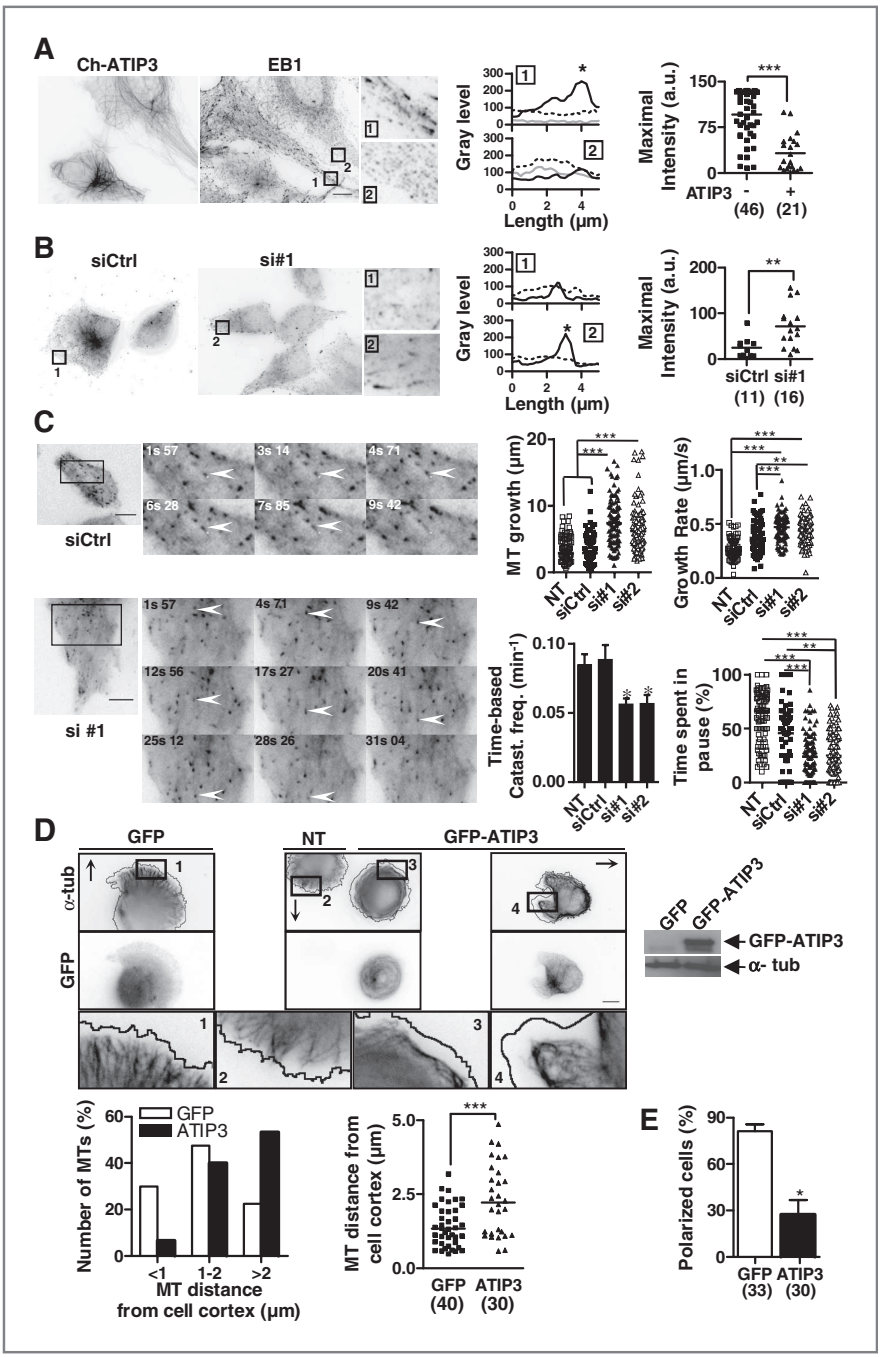

Figure 5. ATIP3 regulates microtubule dynamics. A, immunostaining (anti-EB1, anti-mCherry antibodies) of RPE-1 cells transiently transfected with mCherry-ATIP3 (Ch-ATIP3). Insets, EB1 comet-like structures in ATIP3-negative (1) and positive (2) cells. Distribution of EB1 (black), α-tubulin (dashed) and ATIP3 (gray) at the microtubule tip (linescans) and quantification of comets intensity (scattered dot plot). Number of comets analyzed is under brackets. Shown is 1 experiment out of 5. B, EB1 localization in siRNA-silenced HeLa cells. Insets, EB1 comet-like structures in ATIP3-positive (1) and ATIP3-negative (2) cells. Distribution of EB1 (black) and α-tubulin (dashed) at the microtubule tip (linescans). Quantification of comets intensity as in A. Shown is 1 experiment out of 3. C, time-lapse images of siRNA-silenced HeLa cells expressing EB1-GFP. Arrowhead indicates the position of EB1 comet over time (in seconds). Parameters of microtubule dynamics (EB1-GFP comets) in siRNA-transfected HeLa cells ($n = 100$ comets) are shown in scattered dot plot and histograms. D, immunostaining [anti-α-tubulin (α-tub) and anti-GFP] of transfected D3H2LN in migration. Arrows indicate the direction of migration. Cell margin (black line) is visualized by bright field microscopy. Insets show microtubule array at the cell border of ATIP3-negative (1, 2) and GFP-ATIP3-positive (3, 4) cells. Right, immunoblots (anti-GFP, antitubulin) of transiently transfected D3H2LN cells. Bottom left, quantification of microtubules reaching given distance from the cell cortex in GFP- and GFP-ATIP3- expressing cells. Bottom right, mean distance between microtubules and cell cortex. Number of microtubules analyzed is under brackets. E, quantification (percent) of polarized D3H2LN cells during migration. Number of cells is under brackets. *, $P < 0.05$; **, $P < 0.001$, ***, $P < 0.0001$. A, B, C, and D, scale bar, 10 μm.

were bended and more than 50% of microtubule tips did not reach the cell margin (mean distance 2.31 ± 1.2 μm). Of note, reduced ability of microtubules to reach the cell cortex in migrating ATIP3-positive cells was accompanied by a 34% decrease in cell polarity (Fig. 5E). Taken together, these results suggest that ATIP3-dependent regulation of microtubule dynamics results in decreased ability of microtubules to reach the cell cortex, which contributes to reduced cell polarity and migration.

Microtubule-binding domain D2 recapitulates the functional effects of ATIP3

The ATIP3 polypeptide was cleaved into 3 fragments designated D1, D2, and D3 (Fig. 6A), which were fused to GFP and

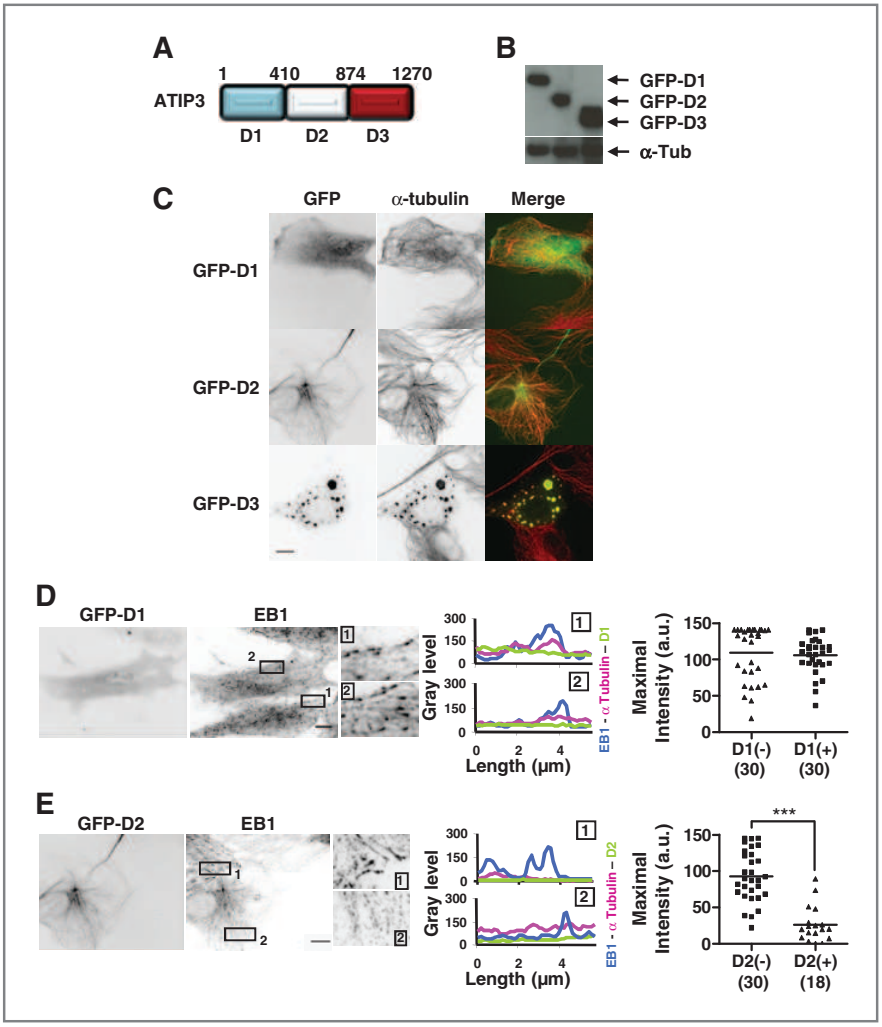

Figure 6. The D2 region of ATIP3 decorates and stabilizes microtubules. A, scheme of ATIP3 regions D1, D2, and D3. Amino acid numbering is according to accession number NP_001001924. B, immunoblots (anti-GFP, antitubulin) of RPE-1 cells transfected (24 hours) with GFP-D1, GFP-D2, and GFP-D3. C, immunostaining (anti-GFP, antitubulin) of RPE-1 cells transiently transfected as in A. D, anti-EB1 immunostaining of GFP-D1–transfected RPE-1 cells. Insets show EB1 comets in GFP-D1-negative (1) and GFP-D1-positive (2) cells. Distribution of EB1 (blue), α-tubulin (pink), and GFP-D1 (green) at the microtubule tip (linescans) and quantification of comets intensity (scattered dot plot). Number of comets is under brackets. E, GFP-D2-transfected RPE-1 cells stained with anti-EB1 antibodies and analyzed as in D. ***, $P < 0.0001$. B, C, and D, scale bar, 10 μm.

expressed in RPE-1 cells (Fig. 6B). As shown in Fig. 6C, the GFP-D1 fusion protein did not associate with microtubules and was rather diffuse in the cytosol. Accordingly, GFP-D1 expression had no significant effect on the number, size, or intensity of EB1 comets (Fig. 6D). In contrast, GFP-D2 clearly colocalized with the microtubule cytoskeleton and centrosome in living cells (Fig. 6C). As for GFP-ATIP3, GFP-D2 was entirely retrieved in the pellet fraction in microtubule cosedimentation assays (Supplementary Fig. S5A). Of interest, upon expression of GFP-D2, accumulation of EB1 as comet-like structures at the microtubule plus ends was strongly impaired (Fig. 6E), indicating that expression of the D2 domain is sufficient to stabilize microtubules. Expression of GFP-D3 (Fig. 6C) led to the formation of large aggregates containing tubulin, probably due to oligomerization of coiled-coil motifs present in the C-terminal region of ATIP3 (31). Because of these aggregates, functional properties of GFP-D3 could not be evaluated further.

Altogether our results identify D2 as the ATIP3 domain able to associate with microtubules and suppress their dynamics. Of importance, the D2 domain also retained the ability of ATIP3 to inhibit cell proliferation (91.6% inhibition for GFP-D2 and GFP-ATIP3 compared with GFP; ref. Fig. 7A). In wound healing assays, cells expressing GFP-D2 showed reduced cell migration and directionality (Fig. 7B). Cell tracking of transient transfectants (Supplementary Movie S7) indicated that similar to GFP-ATIP3, GFP-D2–positive cells mostly remained at the back of the wound and were overtaken by untransfected cells (Fig. 7C and Supplementary Fig. S5B). Thus, the microtubule-binding domain D2 is sufficient to recapitulate the functional features of ATIP3.

Discussion

We report here that ATIP3 is an important prognostic marker for survival of the patients with breast cancer, independently of the ER status of the tumor. Using 3 different patient cohorts, we show that among metastatic breast tumors, low ATIP3 levels correlate with reduced probability for overall survival of the patients, suggesting that ATIP3 may be an important indicator of metastatic progression.

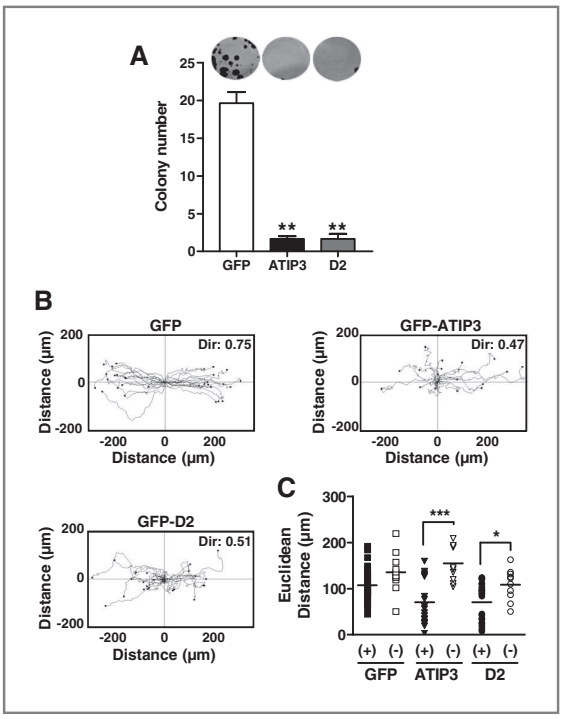

Figure 7. Microtubule-binding domain D2 is the functional domain of ATIP3. A, colony formation of GFP-, GFP-ATIP3-, GFP-D2- transfected MCF7 cells, and quantification (mean ± SD, $n = 4$). Shown is 1 representative experiment out of 3. B, migration trajectories (17 hours) covered by GFP- ($n = 30$), GFP-ATIP3- ($n = 17$), and GFP-D2- ($n = 24$) expressing D3H2LN cells. Directionality coefficient (Dir) is inside the graph. C, aligned dot plots show Euclidean distance covered by untransfected (−) and transfected cells (+) cells as indicated. *, $P < 0.05$; **, $P < 0.001$; ***, $P < 0.0001$.

Examination of ATIP3 levels in breast tumors may contribute to identify a population of patients at high risk of fatal complication, who should be the subject of careful medical follow-up.

Using a bioluminescence-based experimental mouse model for cancer metastasis (23, 25, 26), we showed that restoring ATIP3 expression into highly metastatic ATIP3-deficient D3H2LN breast tumor cells significantly delays the time-course of metastasis and reduces the number of detectable metastases per mouse at all times examined. ATIP3 expression in cancer cells also strongly reduces the size of metastatic foci as well as the number of mice fully invaded with large metastases. These observations, together with above mentioned results on human patients, suggest that ATIP3 may have a prominent effect on metastatic colonization.

Essential steps of metastatic progression include the ability of cancer cells to reach a secondary organ and grow in the new microenvironmental context (3–5). This requires active cell migration and proliferation, two important biologic processes that are significantly increased in breast cancer cells following ATIP3 silencing. By promoting dual effects on cancer cell proliferation and migration, ATIP3 likely regulates both early (tumorigenic) and late (metastatic) stages of cancer development. Beneficial actions of ATIP3 on a wide range of cancer-related processes, including invasion, transendothelial migration, cell migration, and proliferation may explain its potent anti-metastatic effects in preclinical studies.

Other studies have shown that the *MTUS1* gene encoding ATIP3 is significantly downregulated in various types of cancers including from the pancreas (32), ovary (33), head-and-neck (34, 35), colon (36), and bladder (37). Low *MTUS1* levels were also correlated with reduced overall survival of the patients with bladder cancer (37) and oral tongue squamous cell carcinomas (35), highlighting the potential importance of ATIP3 as a new prognostic marker in a variety of solid tumors.

At the molecular level, we show that ATIP3 is a microtubule-associated protein with potent microtubule-stabilizing effects. We propose that by stabilizing microtubules, ATIP3 decreases their dynamics therefore leading to impaired ability of microtubule tips to reach the cell cortex during migration. Microtubule dynamics at the cell cortex is essential for generating a polarized microtubule array, required for cell polarity and migration (30). Reduced microtubule dynamics may thus represent a major mechanism accounting for anti-migratory and anti-metastatic effects of ATIP3 in breast cancer. Accordingly, loss of ATIP3 leads to increased microtubule growth rate, less time spent in pause, and decreased frequency of catastrophes. Alteration of microtubule dynamics parameters in ATIP3-depleted cells may explain uncontrolled cancer cell motility that is associated with increased metastasis and poor prognosis in patients with ATIP3-negative breast cancer. The association of ATIP3 with the microtubule lattice involves an internal basic region designated D2 whose expression is sufficient to recapitulate all effects of the full-length protein on microtubule stabilization, as well as cell proliferation, motility, and directional migration. The microtubule-binding D2 region thus represents the functional domain of ATIP3. Further characterization of this domain and identification of intracellular interacting partners may help deciphering the molecular mechanisms by which ATIP3 limits breast cancer cell migration and hence, metastasis. Our study paves the way to the design of peptides or small molecules able to mimic the effects of ATIP3, which is a prerequisite for the development of targeted therapy. These may be particularly beneficial to the subset of breast tumors that have lost ATIP3 expression and are prone to metastasize.

Disclosure of Potential Conflicts of Interest

No potential conflicts of interest were disclosed.

Authors' Contributions

Conception and design: S. Honoré, M. Di Benedetto, C. Nahmias, S. Rodrigues-Ferreira

Development of methodology: A. Molina, L. Ghouinem, M. Abdelkarim, M. Di Benedetto

Acquisition of data (provided animals, acquired and managed patients, provided facilities, etc.): L. Velot, B.P. Bouchet, A.-C. Luissint, I. Bouhlel, A. Vincent-Salomon, O. Delattre, B. Sigal-Zafrani, F. André, B. Terris, M. Di Benedetto, S. Rodrigues-Ferreira

Analysis and interpretation of data (e.g., statistical analysis, biostatistics, computational analysis): A. Molina, L. Velot, S. Honoré, D. Braguer, N. Gruel, O. Delattre, F. André, B. Terris, A. Akhmanova, M. Di Benedetto, C. Nahmias, S. Rodrigues-Ferreira

Writing, review, and/or revision of the manuscript: A. Molina, L. Velot, A.-C. Luissint, A. Di Tommaso, S. Honoré, B. Sigal-Zafrani, F. André, A. Akhmanova, C. Nahmias, S. Rodrigues-Ferreira
Administrative, technical, or material support (i.e., reporting or organizing data, constructing databases): M. Morel, E. Sapharikas
Study supervision: C. Nahmias, S. Rodrigues-Ferreira

Acknowledgments

The authors thank the Cochin Imaging facility, the Hospital St Louis Animal facility, Nicolas Cagnard (Genomics facility of the University Paris Descartes), Muriel Andrieu, Karine Labroquère (Cybio platform), Maryline Favier, and Corinne Lesaffre (Histology facility) of the Cochin Institute.

Grant Support

This work was supported by the University Paris Descartes, Inserm, CNRS, the Ligue Contre le Cancer-IDF, Inserm-Transfert, the association "Le Cancer du Sein, Parlons-en!", Roche laboratories, the fondation RAJA-Danièle-Marcovici, Odyssea, and Prolific.

The costs of publication of this article were defrayed in part by the payment of page charges. This article must therefore be hereby marked *advertisement* in accordance with 18 U.S.C. Section 1734 solely to indicate this fact.

Received September 10, 2012; revised January 29, 2013; accepted February 4, 2013; published OnlineFirst February 8, 2013.

References

1. Geiger TR, Peeper DS. Metastasis mechanisms. Biochim Biophys Acta 2009;1796:293–308.
2. Chambers AF, Groom AC, MacDonald IC. Dissemination and growth of cancer cells in metastatic sites. Nat Rev Cancer 2002;2:563–72.
3. Bidard FC, Vincent-Salomon A, Sigal-Zafrani B, Rodrigues M, Diéras V, Mignot L, et al. Time to metastatic relapse and breast cancer cells dissemination in bone marrow at metastatic relapse. Clin Exp Metastasis 2008;25:871–5.
4. Hedley BD, Chambers AF. Tumor dormancy and metastasis. Adv Cancer Res 2009;102:67–101
5. Valastyan S, Weinberg RA. Tumor metastasis: molecular insights and evolving paradigms. Cell 2011;147:275–92.
6. Aguirre-Ghiso JA. Models, mechanisms, and clinical evidence for cancer dormancy. Nat Rev Cancer 2007;7:834–46.
7. Perou CM, Sørlie T, Eisen MB, van de Rijn M, Jeffrey SS, Rees CA, et al. Molecular portraits of human breast tumours. Nature 2000;406:747–52.
8. Sørlie T, Perou CM, Tibshirani R, Aas T, Geisler S, Johnsen H, et al. Gene expression patterns of breast carcinomas distinguish tumor subclasses with clinical implications. Proc Natl Acad Sci U S A 2001;98:10869–74.
9. Higgins MJ, Baselga J. Targeted therapies for breast cancer. J Clin Invest 2011;121:3797–803.
10. Cortes J, Vidal M. Beyond taxanes: the next generation of microtubule-targeting agents. Breast Cancer Res Treat 2012;133:821–30.
11. Mitchison T, Kirschner M. Dynamic instability of microtubule growth. Nature 1984;312:237–42.
12. Akhmanova A, Steinmetz MO. Tracking the ends: a dynamic protein network controls the fate of microtubule tips. Nat Rev Mol Cell Biol 2008;9:309–22.
13. Straube A. How to measure microtubule dynamics? Methods Mol Biol 2011;777:1–14.
14. Kamath K, Oroudjev E, Jordan MA. Determination of microtubule dynamic instability in living cells. Methods Cell Biol 2010;97:1–14.
15. Honore S, Braguer D. Investigating microtubule dynamic instability using microtubule-targeting agents. In:Straube A, editor. Methods in molecular biology. Microtubule dynamics: methods and protocols. New York: Springer Press; 2011. p. 245–60.
16. Di Benedetto M, Bièche I, Deshayes F, Vacher S, Nouet S, Collura V, et al. Structural organization and expression of human MTUS1, a candidate 8p22 tumor suppressor gene encoding a family of angiotensin II AT2 receptor-interacting proteins, ATIP. Gene 2006;380:127–36.
17. Rodrigues-Ferreira S, Nahmias C. An ATIPical family of angiotensin II AT2 receptor-interacting proteins. Trends Endocrinol Metab 2010;21:684–90.
18. Molina A, Rodrigues-Ferreira S, Di Tommaso A, Nahmias C. ATIP, a novel superfamily of microtubule-associated proteins. Med Sci (Paris) 2011;27:244–46.
19. Rodrigues-Ferreira S, Di Tommaso A, Dimitrov A, Cazaubon S, Gruel N, Colasson H, et al. 8p22 MTUS1 gene product ATIP3 is a novel anti-mitotic protein underexpressed in invasive breast carcinoma of poor prognosis. PLoS ONE 2009;4:e7239.
20. Reyal F, Stransky N, Bernard-Pierrot I, Vincent-Salomon A, de Rycke Y, Elvin P , et al. Visualizing chromosomes as transcriptome correlation maps: evidence of chromosomal domains containing co-expressed genes–a study of 130 invasive ductal breast carcinomas. Cancer Res 2005;65:1376–83.
21. Gyorffy B, Lanczky A, Eklund AC, Denkert C, Budczies J, Li Q, et al. An online survival analysis tool to rapidly assess the effect of 22,277 genes on breast cancer prognosis using microarray data of 1809 patients. Breast Cancer Res Treat 2010;123:725–31.
22. Kaplan-Meier plotter, 2013 [updated 2013 Feb 2]. Available form: http://www.kmplot.com
23. Rodrigues-Ferreira S, Abdelkarim M, Dillenburg-Pilla P, Luissint AC, di-Tommaso A, Deshayes F, et al. Angiotensin II facilitates breast cancer cell migration and metastasis. PLoS One 2012;7:e35667.
24. Grigoriev I, Splinter D, Keijzer N, Wulf PS, Demmers J, Ohtsuka T, et al. Rab6 regulates transport and targeting of exocytotic carriers. Dev Cell 2007;13:305–14.
25. Jenkins DE, Hornig YS, Oei Y, Dusich J, Purchio T. Bioluminescent human breast cancer cell lines that permit rapid and sensitive *in vivo* detection of mammary tumors and multiple metastases in immune deficient mice. Breast Cancer Res 2005;7:R444–R454.
26. Abdelkarim M, Vintonenko N, Starzec A, Robles A, Aubert J, Martin ML, et al. Invading basement membrane matrix is sufficient for MDA-MB-231 breast cancer cells to develop a stable *in vivo* metastatic phenotype. PLoS ONE 2011;6:e23334.
27. Nizak C, Martin-Lluesma S, Moutel S, Roux A, Kreis TE, Goud B, et al. Recombinant antibodies against subcellular fractions used to track endogenous Golgi protein dynamics *in vivo*. Traffic 2003;4:739–53.
28. Piehl M, Cassimeris L. Organization and dynamics of growing microtubule plus ends during early mitosis. Mol Biol Cell 2003;14:916–25.
29. Salaycik KJ, Fagerstrom CJ, Murthy K, Tulu US, Wadsworth P. Quantification of microtubule nucleation, growth and dynamics in wound-edge cells. J Cell Sci 2005;118:4113–22.
30. Kaverina I, Straube A. Regulation of cell migration by dynamic microtubules. Semin Cell Dev Biol 2011;22:968–74.
31. Nouet S, Amzallag N, Li JM, Louis S, Seitz I, Cui TX, et al. Trans-inactivation of receptor tyrosine kinases by novel angiotensin II AT2 receptor-interacting protein, ATIP. J Biol Chem 2004;279:28989–97.
32. Seibold S, Rudroff C, Weber M, Galle J, Wanner C, Marx M. Identification of a new tumor suppressor gene located at chromosome 8p21.3–22. FASEB J 2003;17:1180–2.
33. Pils D, Horak P, Gleiss A, Sax C, Fabjani G, Moebus VJ, et al. Five genes from chromosomal band 8p22 are significantly down-regulated in ovarian carcinoma: N33 and EFA6R have a potential impact on overall survival. Cancer 2005;104:2417–29.
34. Ye H, Pungpravat N, Huang BL, Muzio LL, Mariggiò MA, Chen Z, et al. Genomic assessments of the frequent loss of heterozygosity region on 8p21.3-p22 in head and neck squamous cell carcinoma. Cancer Genet Cytogenet 2007;176:100–6.
35. Ding X, Zhang N, Cai Y, Li S, Zheng C, Jin Y, et al. Down-regulation of tumor suppressor MTUS1/ATIP is associated with enhanced proliferation, poor differentiation and poor prognosis in oral tongue squamous cell carcinoma. Mol Oncol 2012;6:73–80.
36. Zuern C, Heimrich J, Kaufmann R, Richter KK, Settmacher U, Wanner C, et al. Down-regulation of MTUS1 in human colon tumors. Oncol Rep 2010;23:183–9.
37. Xiao J, Chen JX, Zhu YP, Zhou LY, Shu QA, Chen LW. Reduced expression of MTUS1 mRNA is correlated with poor prognosis in bladder cancer. Oncol Lett 2012;4:113–8.

Supporting Information Materials and Methods

Plasmids constructs and transfections

EB1-GFP and EB3-GFP plasmids were described previously (1). mCherry-ATIP3 plasmid was obtained by subcloning the full-length cDNA insert (3.8 Kb) of GFP-ATIP3 (2) into the XhoI-KpnI cloning sites of pmCherry-C1 vector (Clontech, CA, USA). Plasmids encoding GFP-fused ATIP3 regions D1, D2 and D3 (410, 464 and 396 amino acids, respectively) were obtained by PCR-amplification of full-length ATIP3 sequence using specific oligonucleotides :

5'-CCGCTCGAGCCATGACTGATGATAATTC AGATG-3' (sense) and

5'-CGGGGTACCTCATCCAAATGACGAGCCCACCTTTTG-3' (antisense) for D1;

5'-CCGCTCGAGGACTGACTTGGGATGCAAATGAT-3' (sense) and

5'-CGGGGTACCTCATGCATTAAGAGCTGTAAATAA-3' (antisense) for D2;

5'-CCG CTCGAGCAGTTGAAAAGAGCAGGCAAAAG-3' (sense) and

5'-CGGGGTACCTCAT CTGGGTGAAATGCTGGG-3' (antisense) for D3.

Resulting cDNA insert fragments (1230 bp, 1395 bp and 1188 bp for D1, D2 and D3, respectively) were subcloned into the XhoI and KpnI sites of the pEGFP-C1 vector (Clontech, CA, USA) so that the first codon of each domain is in frame with the carboxy-terminal end of the Green Fluorescent Protein, and entirely sequenced.

Transient and stable transfections of plasmid constructs were performed as described (2).

XCELLigence proliferation assay

For measurement of cell proliferation by XCELLigence technology, D3H2LN cell clones (WT, GFP, Cl3 and Cl6) were seeded in quadruplicate (15,000 cells per well) in 100 µl complete medium on the top of gold electrodes in 96-well E-plates (Roche Diagnostics, France). Electrical impedance was monitored every 15 min during 80 hrs by the RTCA software (Real-time Cell Analyzer) as described (3, 4).

Histological analysis

Sections (5 µm) of metastatic organs were cut from formalin-fixed, paraffin-embedded tissue blocks, counterstained with hematoxylin-eosin and examined under an inverted microscope.

Time-lapse videomicroscopy of wound healing

D3H2LN cells were transfected for 14 hrs with appropriate constructs prior to seeding (100,000 cells/well) for 7 hrs in each compartment of IBIDI culture insert (Biovalley, France). Time-lapse acquisitions were each 5 min (bright field acquisition) and each 30 min (GFP acquisition) for at least 13h in a Zeiss Axiovert 200M microscope and 10X objective lens. Cell tracking was done using the manual tracking plugin of ImageJ. Cell velocity was calculated by a regression analysis of the distance versus time plot. Migratory properties were evaluated by measuring the euclidean distance for each cell at time 8h. Cell directionality was measured by ImageJ chemotaxis and migration tool plugin (Euclidean distance/Accumulated distance). A value of 1 means straight motion and a value of 0 means non-straight motion.

Microtubule stability and regrowth

For analysis of MT stability, HeLa cells transfected with control or ATIP3-specific siRNAs, or stable MCF7 cell clones (2) were treated for 1 hr at 37°C with different doses of

nocodazole and free tubulin was extracted with PEM (PIPES 80 mM, EGTA 2mM, MgCl2 1 mM) Triton X100 0.1% buffer solution. Cells were fixed with cold methanol prior to staining for 1 hr at room temperature with anti-α-tubulin (clone F2C, a kind gift of Dr Franck Perez, Institut Curie, Paris), and anti-acetylated-tubulin (clone 6-11B-1; Sigma) antibodies. Cy2, Cy3 and Cy5 conjugated secondary antibodies were from Jackson Laboratories. Fluorescence images were captured in a Zeiss Axiovert 200M inverted fluorescence microscope equipped with a CCD camera (CoolSNAP HQ, Photometrics) and 100X objective lens. Multi-dimensional acquisitions were performed using Metamorph 7.1.7 software.

For analysis of MT regrowth after nocodazole washout, transiently transfected RPE-1 cells were treated for 1 hr at 4°C with 10μM of nocodazole, then washed with cold PBS and warmed in complete medium to allow MT regrowth for 2, 5 and 15 min prior to fixation in cold methanol and staining as described above. Alpha-tubulin fluorescence intensity was measured in concentric circles of different diameters (2, 4, 6, 8 μm) around the centrosome (stained by anti-γ-tubulin). Values for 2 μm were subtracted from 4, 6 and 8 μm to eliminate fluorescence due to MT nucleation.

Live cell imaging and microtubule dynamics

HeLa cells co-transfected for 48 hrs with (50 nM) siRNA (control or ATIP3-specific) and (2 μg) EB1-GFP were seeded in 35 mm glass bottom dishes (IBIDI) and analyzed with inverted fluorescence microscope using the TIRF module and 60X objective lens. Only cells with low levels of EB1-GFP were chosen. Time-lapse series of 1000 images were acquired with a 157 ms interval using Live Acquisition (TILL Photonics) software. Time-lapse recordings were then reduced to 1 frame each 1.57s and ImageJ manual tracking plugin was used for measurement. At least 10 MTs per cell in 10 separate cells were tracked for each condition. The changes in length of ≥0.5 μm were considered as a growth phase, and movements of <0.5

μm were considered as pause events. MT growth rate was calculated by linear regression analysis of the lifetime history plots and catastrophe frequency based on time and distance were calculated according to the following formula : C^{time-1}: $S_{Catastrophes}/S_{growth + pause\ duration\ until\ catastrophe}$ and $C^{length-1}$: $S_{Catastrophes}/S_{growth\ length\ until\ catastrophe}$ as described (5).

Microtubule cosedimentation assay

Microtubule cosedimentation assay was performed as described (2). Briefly, cells were incubated for 20 min at 4°C in PEM buffer (100 mM PIPES, pH 6.9, 1 mM MgSO4, 1 mM EGTA), scraped and sonicated prior to centrifugation at 15000 rpm for 10 min, 4°C. Clarified samples were incubated with Taxol (20 μM) in the presence of GTP (1 mM) and DTT (1 mM) for 45 min at 37°C and were spun at 70 000 g for 30 min at 30°C through a cushion buffer containing 40% glycerol, 20 μM taxol and 1 mM GTP. The supernatant (S) and pellet (P) fractions were collected separately and subsequently immunoblotted with anti-GFP antibody. Blots were reprobed using anti-alpha-tubulin antibody.

Legends to Supporting Information Movies

Supporting Information Movie 1. Time-lapse videomicroscopy of wound healing assay using GFP-transfected D3H2LN clone

Stably transfected GFP cells were seeded in IBIDI chambers and wound closure was analyzed for 12 hrs by time-lapse videomicroscopy using a wide field Zeiss microscope (10X lens). Shown is 1 image every 20 min.

Supporting Information Movie 2. Time-lapse videomicroscopy of wound healing assay using GFP-ATIP3-transfected D3H2LN clone (Cl3)

GFP-ATIP3-expressing stable clone was analyzed as described for movie 1.

Supporting Information Movie 3. Time-lapse videomicroscopy of wound healing assay using GFP-transiently transfected D3H2LN cells

Transiently transfected GFP cells were seeded in IBIDI chambers and wound closure was analyzed for 12 hrs by time-lapse videomicroscopy using a Zeiss microscope (10X lens). Images were acquired every 5 min (bright field) and every 30 min (GFP filter). Shown is 1 image every hour.

Supporting Information Movie 4. Time-lapse videomicroscopy of wound healing assay using GFP-ATIP3-transiently transfected D3H2LN cells

GFP-ATIP3 transient transfectants were analyzed as described for movie 3.

Supporting Information Movie 5. Time-lapse videomicroscopy of EB1-GFP comets in siRNA-silenced HeLa cells

Cells were co-transfected with EB1-GFP and siRNA (control or ATIP3-specific si#1) for 48 hrs. EB1 comets were analyzed by time-lapse TIRF microscopy (60X lens). Time-lapse series of 1000 images were acquired with a 157 ms interval and shown at 8 frames per second.

Supporting Information Movie 6. Time-lapse videomicroscopy of EB3-GFP comets in wild type and mCherry-ATIP3 transfected MRC5 cells

Cells were transfected for 24 hrs with EB3-GFP-construct without (upper panel) or with (lower panel) mCherry-ATIP3 cDNA. EB3-GFP comets were analyzed by time-lapse videomicroscopy using a spinning disk microscope (CSU-X1-A1; Yokogawa). On the lower panel, movies taken with GFP and mCherry filters are shown on the left and right panels, respectively. Time-lapse series of 500 images were acquired with a 100 ms interval and shown at 8 frames per second.

Supporting Information Movie 7. Time-lapse videomicroscopy of wound healing assay in GFP-D2-transiently transfected D3H2LN cells

GFP-D2 transient transfectants were analyzed as described for movie 3.

Supporting Information References

1. Stepanova T, Slemmer J, Hoogenraad CC, Lansbergen G, Dortland B, De Zeeuw CI, et al. Visualization of Microtubule Growth in Cultured Neurons via the Use of EB3-GFP (End-Binding Protein 3-Green Fluorescent Protein). The Journal of Neuroscience 2003;23(7):2655–64.

2. Rodrigues-Ferreira S, Di Tommaso A, Dimitrov A, Cazaubon S, Gruel N, Colasson H, et al. 8p22 MTUS1 gene product ATIP3 is a novel anti-mitotic protein underexpressed in invasive breast carcinoma of poor prognosis. PLoS One 2009;4: e7239.

3. Ke Y, Wu D, Princen F, Nguyen T, Pang Y, et al. Role of Gab2 in mammary tumorigenesis and metastasis. Oncogene 2007;26(34):4951-60.

4. Stander XX, Stander BA, Joubert AM. In vitro effects of an in silico-modelled 17β-estradiol derivative in combination with dichloroacetic acid on MCF-7 and MCF-12A cells. Cell Prolif 2011;44(6):567-81.

5. Honore S, Braguer D. Investigating Microtubule Dynamic Instability Using Microtubule-Targeting Agents. In: Straube A, editor. Methods in Molecular Biology. vol 777. Microtubule Dynamics: Methods and Protocols. New York: Springer Press; 2011. pp245-60.

6. Gyorffy B, Lanczky A, Eklund AC, Denkert C, Budczies J, Li Q, et al. An online survival analysis tool to rapidly assess the effect of 22,277 genes on breast cancer prognosis using microarray data of 1809 patients. Breast Cancer Res Treat 2010;123(3):725-31.

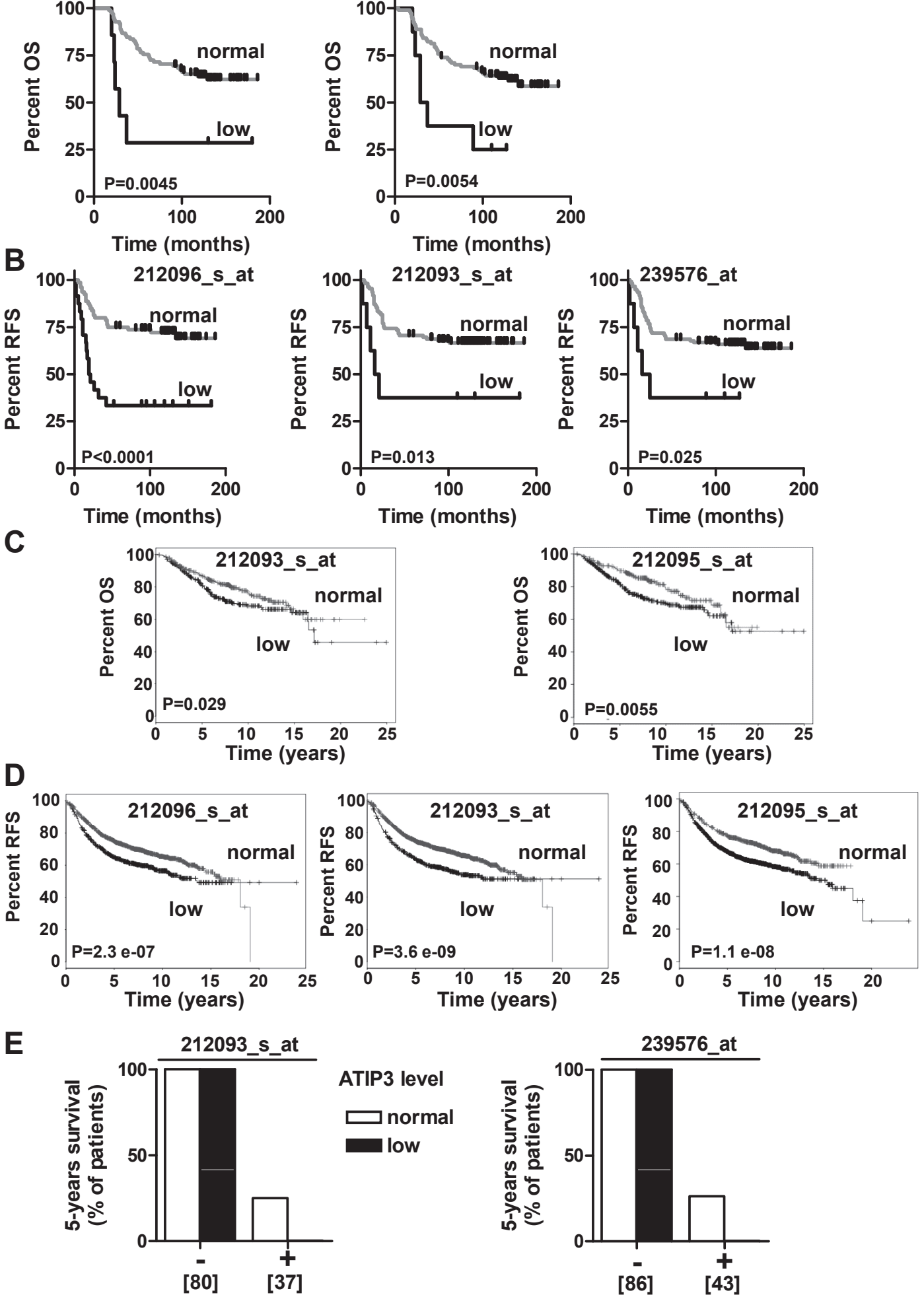

Molina et al, Supporting Information Fig S1

Supporting Information Figure S1. Low levels of ATIP3 associate with decreased overall and relapse-free survival of the patients

(A) Overall survival (OS) curves from patients (n=150) with tumors expressing normal (>0.5, gray line) or low (<0.3, black line) ATIP3 levels, relative to the median value of Affymetrix *MTUS1* probeset intensities in non tumoral tissues. Results shown are from Affymetrix *MTUS1* probesets 212093_s_at and 239576_at on the Institut Curie cohort **(B)** Relapse-free survival (RFS) curves from patients (n=150) with tumors expressing normal or low ATIP3 levels as in (A). Results shown are from Affymetrix *MTUS1* probesets 212096_s_at, 212093_s_at and 239576_at. **(C)** Overall survival (OS, n= 791) curves from patients with tumors expressing normal to high (grey line) or low (black line) *MTUS1* level using Kaplan-Meier plotter (http://www.kmplot.com). All percentiles between the lower and the upper quartiles were automatically computed, and the best performing threshold was used as a cut off. Results shown are from Affymetrix *MTUS1* probesets 212093_s_at and 212095_s_at. **(D)** Relapse-free survival (RFS, n=2898) curves from patients with tumors expressing normal to high (grey line) or low (black line) *MTUS1* level using Kaplan-Meier plotter as in (C). Results shown are from Affymetrix *MTUS1* probesets 212096_s_at, 212093_s_at and 212095_s_at. **(E)** Percentage of patients remaining alive after 5 years with non metastatic (-) and metastastic (+) tumors expressing normal (white bar) or low (black bar) levels of ATIP3, based on Affymetrix *MTUS1* probesets 212093_s_at and 239756_at as in (A). Number of tumors is indicated below under brackets

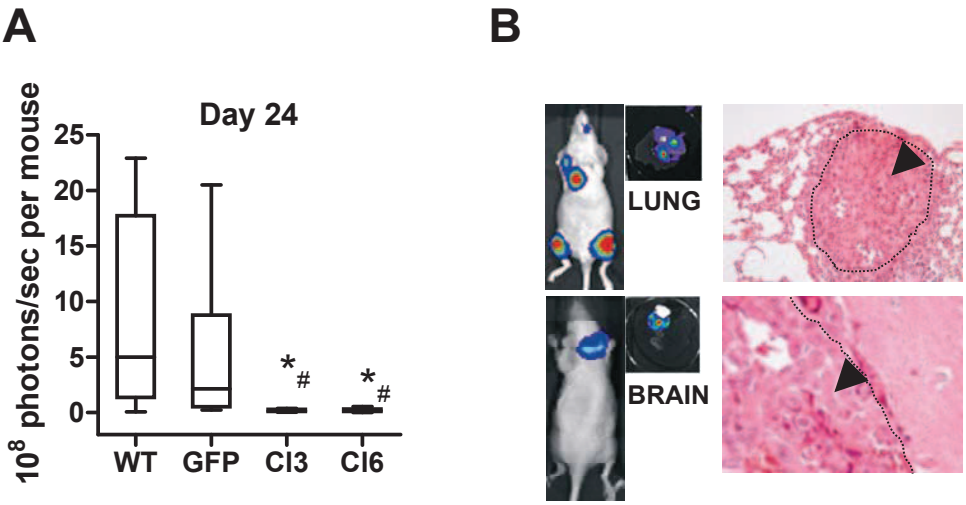

Supporting Information Figure S2. Anti-metastatic effects of ATIP3 *in vivo*

(A) Total number of photons/sec per mouse at day 24. *p<0.05 as compared to WT, #p<0.05 as compared to GFP. **(B)** Histological analysis of metastatic foci at day 24 after H&E coloration. Magnification x100 (lung) and x400 (brain).

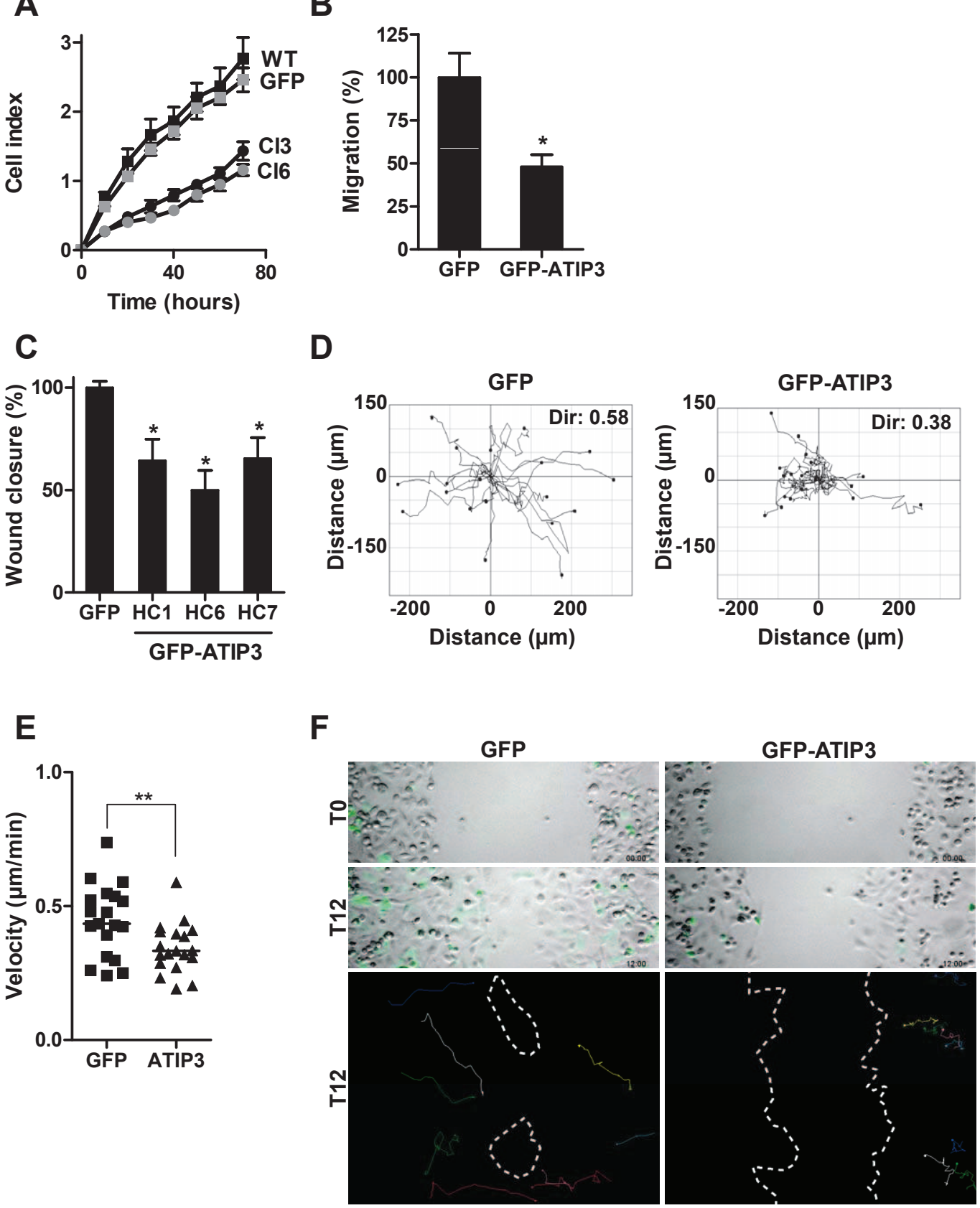

Molina et al, Supporting Information Fig S3

Supporting Information Figure S3. ATIP3 inhibits breast cancer cell proliferation and migration

(A) Real-time measurement of impedance-based cell proliferation of ATIP3-negative (WT, GFP) and ATIP3-positive (Cl3, Cl6) D3H2LN cells as measured by the XCELLigence methodology. Shown is one representative experiment out of 3 performed in quadruplicate. **(B)** Boyden chamber migration assay of ATIP3-negative (GFP-transfected) and GFP-ATIP3-positive MDA-MB-231 cell clones. Cell migration was quantified by densitometry. Results (mean±SD) are expressed as percent of GFP-transfected cells (n=3). **(C)** Quantification of wound closure (in percent) at time T18 in GFP-ATIP3-expressing MCF-7 clones (HC1, HC6, HC7, described in Rodrigues-Ferreira *et al.,* PLoS One 2009;4:e7239) as compared to ATIP3-negative MCF-7 transfected GFP clone (n=2). **(D)** Diagrams representing the migration trajectories covered within 12 hrs by transiently transfected GFP (n=19) and GFP-ATIP3 (n=19) cells. Directionality coefficient (Dir) is indicated inside the graph. **(E)** Scattered dot plot of GFP- (black square) and GFP-ATIP3-expressing (black triangle) cell velocity (n=19 cells for each condition). **(F)** Representative pictures of wound closure (times T0 and T12 after removal of the insert) of D3H2LN transiently transfected with GFP and GFP-ATIP3 constructs. Shown are merge pictures taken in bright field and GFP fluorescence filters. **Lower panel :** cell tracking of fluorescent positive cells at time T12. Dashed lines indicate wound border. *$p<0.05$, **$p<0.001$.

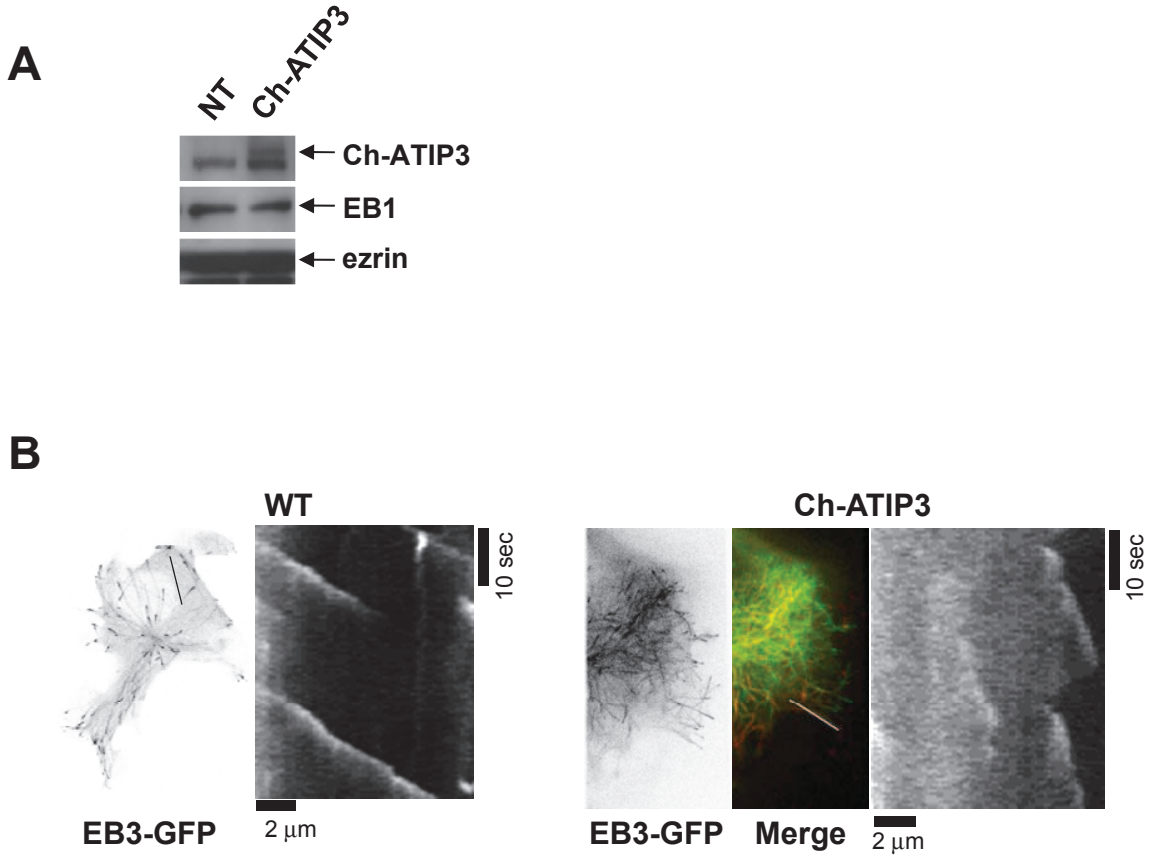

Supporting Information Figure S4. ATIP3 regulates MT dynamics

(A) Western blot analysis of RPE-1 cells either non-transfected (NT) or transfected with mCherry-ATIP3 (Ch-ATIP3) using anti-EB1 antibody. Blots were probed using anti-cherry and anti-ezrin antibodies for control of transfection and loading respectively. **(B)** Kymographs of two microtubules extracted from supplemental movie 6. EB3-GFP labels MT plus end and allows the quantification of dynamic parameters on control (WT, left) and mCherry-ATIP3 expressing cells (Ch-ATIP3, right). Calculated velocity of EB3-GFP comets was 0.5µm/sec for control cells (WT) and 0.2µm/sec for cells co-transfected with Ch-ATIP3.

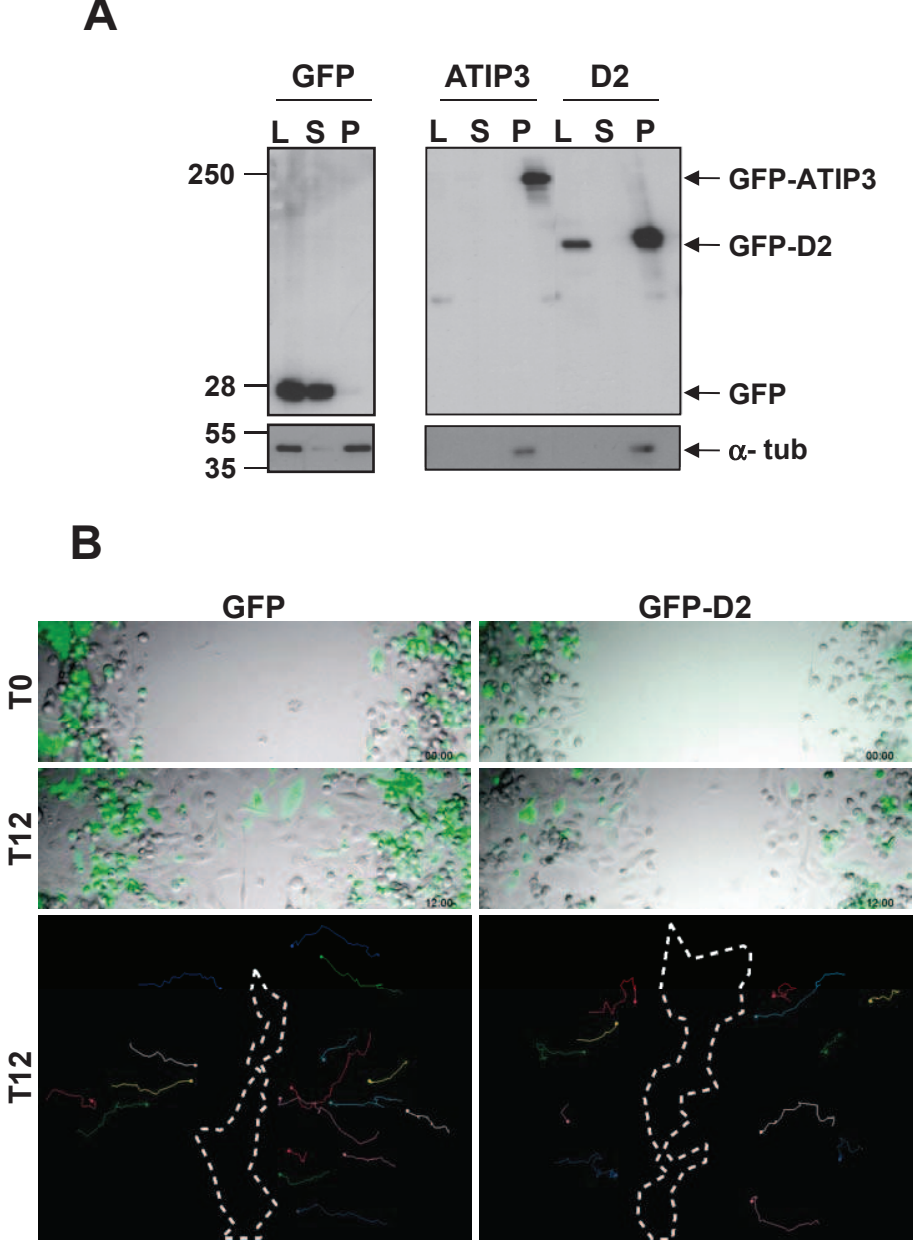

Supporting Information Figure S5. Characterization of ATIP3 domains

(A) Microtubule co-sedimentation assay performed on MCF-7 transfected with GFP, GFP-ATIP3 (ATIP3) or GFP-D2 (D2). Immunoblots were revealed using anti-GFP and reprobed with anti-tubulin antibodies. Molecular weights are indicated on the left. L: total cell lysate; S: supernatant; P: pellet. **(B)** Representative pictures of wound closure of GFP and GFP-D2 transfected D3H2LN cells at times T0 and T12 after removal of the insert. Shown are merge pictures taken in bright field and GFP fluorescence filters. **Lower panel:** cell tracking of fluorescent positive cells at time T12. Dashed lines indicate wound border.

ARTICLE 2:

ATIP3 interacts with End Binding protein EB1 to limit its accumulation at the microtubule plus ends

Results from the Cancer Research paper demonstrate that ATIP3 was able to regulate microtubule (MT) dynamics to, in turn, control cell polarity and cell migration. Thus, the aim of this second submitted article was to investigate how ATIP3 decreases MT dynamic instability parameters.

Analysis of ATIP3 amino acid sequence revealed one SxIP (SAIP) motif in the D3 region and two SxIP-like (KNIP and RPLP) motifs in the D2 region, all surrounded by serine and basic rich residues. To date SxIP motifs are recognized as one of the EB1 interaction motifs and as a Microtubule Tip Localization Signals (MtSL) that confers tip tracking properties. The presence of these three motifs suggest that ATIP3 is a novel EB1 interacting partner.

Cell lysates from MCF7 breast cancer cells transiently transfected with GFP-ATIP3 were incubated with GST-EB1 as an affinity matrix for GST-pull-down experiments. Interestingly, results indicated that GFP-ATIP3 was able to interact with EB1. Experiments using ATIP3-expressing HeLa cells confirmed the first result, showing that endogenous ATIP3 was also interacting with GST-EB1. Finally, co-immunoprecipitation experiments in MCF7 cells co-transfected with mCherry-ATIP3, EB1-GFP, EB3-GFP and GFP-EB3 confirmed the interaction of ATIP3 with EB1 and revealed that ATIP3 was able to interact with EB3 as well.

To further characterize the interaction, GFP-ATIP3 cell lysates were incubated with GST-EB1 comprising the C-terminal or the N-terminal region. As for most of the SxIP-containing EB1 partners, ATIP3 interacts with the C-terminal domain of EB1. The interacting domain of ATIP3 was then investigated by transfecting the D1, D2 and D3 GFP-constructs in MCF7 cells. Cell lysates were then incubated with GST-EB1 and pull-down experiments were performed. Western blot analysis indicate that only the D2 domain was interacting with EB1 and more precisely with the C-terminal domain of EB1, eliminating the SAIP domain present in D3 region of ATIP3 as involved in the interaction with EB1.

To investigate which of the two SxIP-like (KNIP and RPLP) motifs of D2 was interacting with EB1, D2 deletion mutants (D2C terminal and D2N terminal) were constructed and tagged with GFP. Transfection of these constructs on MCF7 cells followed by the incubation of the lysates with GST-EB1 was performed. Results showed that only the D2C domain was able to interact with EB1. Refining of this D2C domain using shorter deletion mutants allowed the identification of a domain, termed CN, capable to interact with EB1. Deletion of the CN domain from the full-length protein and the D2 domain (ATIP3delCN and D2delCN) led to a marked decrease in EB1 interaction. Additionally, deletion of the RPLP motif from the CN domain (CN67delP) also reduces the interaction with EB1.

Fluorescent peptides corresponding to a smaller sequence of the CN, termed CN45 comprising the RPLP motif, and the CC motif that do not interact with EB1, were incubated together with GST-EB1. Results revealed that CN interacts directly with EB1. Altogether these results indicate that ATIP3 directly interacts with EB1 via an SxIP-like domain, RPLP, located in the CN domain.

To investigate if EB1-interaction may contribute to MT-association, examination of cellular localization of D2 deletion mutants was then performed in RPE1 cells stained with anti-GFP and anti-tubulin antibodies after transient transfection of the different constructs. Similar to ATIP3 and D2, D2N, D2C and CN associate with MTs. The CN domain weakly interacts with MTs and remains mostly cytosolic. EB1-interacting domain termed CN67 (which is smaller than the CN but 22 residues longer than CN45) remains completely diffuse at the cytosol. Of note, the D2delCN deletion mutant still decorates MT lattice, even if the EB1-interacting domain was removed. These results indicate that EB1 interaction and MT interaction involve two different regions located in the central functional domain of ATIP3.

As mentioned above, the presence of SxIP motif often confers tip tracking properties. Transiently transfection of low levels of GFP-ATIP3 in RPE1 cells followed by EB1 staining was performed. Immunofluorescence images showed that ATIP3 decorates the MT lattice but does not co-localize with EB1 at the MT plus-end. Time-lapse images of MRC5 cells co-transfected with mCherry-ATIP3 and EB3-GFP were then taken. Analysis of the videos confirmed the previous result, in which ATIP3 does not accumulate at the MT growing-ends, and consequently is not a MT plus-end tracking protein (+TIP). Interestingly, time-lapse videomicroscopy of MCF7 stably expressing GFP-ATIP3 showed that rather than an accumulation at the end of growing MTs, ATIP3 accumulate at the end of shrinking MTs.

As ATIP3 does not interact with EB1 at the MT growing-end, Proximity Ligation Assay (PLA) experiments were design to identify the cellular compartment where the interaction occurs. Two conditions were tested. First, transient transfection of full-length and ATIP3 deletion mutants in RPE1 cells and amplification using anti-GFP and anti-EB1 antibodies, and the second condition using ATIP3-expressing HeLa cells, that were amplified using anti-MTUS1 and anti-EB1 antibodies to reveal the interaction of endogenous proteins. PLA amplification signals (or RCP for rolling circle product) was observed in cells transfected with ATIP3, D2, D2C and CN, as well as in the endogenous condition. Transfection of the full-length and D2 depleted for the CN domain (ATIP3delCN and D2delCN) showed a significant reduction in the PLA amplification signals.

Detailed analysis of PLA immunofluorescence images showed that the interaction happens mostly in the cytosol, which is coherent with the interaction of CN67 domain which is

completely cytosolic and interacts with EB1. Interestingly, some PLA signals were also detected along MT lattice in ATIP3 and D2 transfection and endogenous ATIP3. Altogether these results indicate that ATIP3 interacts with EB1 in intact cells through the CN domain mainly in the cytosol and along the MT lattice.

Cancer Research published results showed that ATIP3 silencing increases MT dynamic instability, and that ATIP3 and D2 re-expression limits EB1 accumulation at the MT growing end. To investigate the consequence of ATIP3-EB1 interaction on EB1 localization at the MT plus-end, D2 deletion mutants were transfected in RPE1 cells and staining of GFP, tubulin and EB1 was performed. Observation of the immunofluorescence images revealed all the EB1-interacting domains (D2C, CN and CN67) impaired EB1 accumulation at the plus-end, whereas domains that do not bind EB1 (CC, D2delCN and CN67delP) had no effect on EB1 comet number and length. Delocalization of EB1 in the cells transfected with D2, D2C and CN from the MT tip to the lattice and cytosol, were in line with PLA results. These data suggest a functional involvement of the EB1-interacting domain of ATIP3 in reducing EB1 accumulation at the MT plus-ends.

Rescue experiments were then design in ATIP3-silenced HeLa cells in which GFP-ATIP3 and deletion mutants were re-introduced at endogenous levels and EB1 immunostaining was performed. Results showed that GFP-ATIP3 restore ATIP3 knock-down phenotype decreasing EB1 comet-like structures. In addition, GFP-D2 and GFP-CN, similar to GFP-ATIP3, restore the impaired accumulation of EB1, whereas GFP-D2delCN does not.

Altogether these results demonstrate that functional ATIP3-EB1 complexes are formed in the cytosol and near to the MT lattice. This interaction may contribute to restrain the accumulation of EB1 at the MT growing end. Given that EB1 play a key role in regulating MT dynamics from the plus-ends, these data may account for decreased MT dynamics in the presence of ATIP3.

The findings reported suggest that altered expression of either ATIP3 or EB1 may modify the number of ATIP3-EB1 molecular complexes and subsequent accumulation of EB1 at the MT plus ends. In order to investigate the functional relevance of these data in human pathology, examination of the prognostic value in respect to ATIP3 and EB1 expression levels in breast cancer was evaluated. Using a panel of 150 breast cancer patients with known clinico-pathological characteristics, DNA microarray probeset values for *MTUS1* (ATIP3) and *MAPRE1* (EB1) genes were compared with overall survival of the patients. Hierarchical clustering of these tumors allowed the classification in four groups according to the expression levels of both genes: group 1, low expression of both genes; group 2, high expression levels of *MTUS1* and low of *MAPRE1*; group 3, low levels of *MTUS1* and high of *MAPRE1*; and group 4, very high levels of *MTUS1* and low levels of *MAPRE1*.

Overall survival curves indicate that tumors from cluster 3 (low ATIP3-high EB1) are associated with significantly reduced overall survival of the patients as compared to all other breast tumors analyzed. In addition, the percent of patients surviving after 5 years was also markedly decreased in tumors from group 3. These analyses indicate that combined information on ATIP3 and EB1 could be considered as a prognostic marker of breast cancer progression and clinical outcome.

To conclude, this work showed that ATIP3 interacts with EB1 and that this interaction may regulate MT dynamics and functions at the growing ends. Of relevance, combined ATIP3/EB1 may represent a novel prognostic marker that should be taken into account for better medical follow up.

ATIP3 interacts with End Binding protein EB1 to limit its accumulation at the microtubule plus ends

Lauriane VELOT#[1,2,3], Angie MOLINA#[1,2,3], Sylvie RODRIGUES-FERREIRA[1,2,3], Benjamin Pierre BOUCHET[4], Marina MOREL[1,2], Anne VINCENT-SALOMON[5], Vanessa BENHAMO[5], Fabrice ANDRE[3], Diane BRAGUER[6,7], Ariel SAVINA[8], Stéphane HONORE[6,7], Clara NAHMIAS*[1,2,3]

#equal contribution

* correspondence to : Dr Clara Nahmias, Inserm U981, Institut Gustave Roussy, 114 rue Edouard Vaillant, 94800 Villejuif. Email : clara.nahmias@inserm.fr

1. Inserm U1016, Université Paris Descartes, 75014 Paris, France.
2. CNRS UMR8104, Institut Cochin, 75014 Paris France.
3. Inserm U981, Université Paris Sud, Institut Gustave Roussy Department of Molecular Medicine, 94800 Villejuif, France.
4. Cell Biology, Faculty of Science, Utrecht University, Padualaan 8, 3584 CH Utrecht, The Netherlands.
5. Inserm U934, Department of Biopathology, Institut Curie, 75248 Paris Cedex 5, France.
6. Aix Marseille Université, Inserm, CRO2 UMR_S 911, 13385 Marseille, France.
7. APHM, Hôpital Timone, 13385 Marseille, France.
8. Scientific Partnerships Roche SAS, Boulogne Billancourt, France.

Running title : ATIP3 interacts with EB1

Keywords: Breast cancer / EB1 / microtubule / MTUS1 / Proximity Ligation Assay

Total count : 51234 characters including spaces

8 Figures, 2 Tables

5 Expanded View Figures, 2 Expanded View Tables, 6 movies

Abstract

Microtubule-associated protein ATIP3 is the major product of candidate tumor suppressor *MTUS1* gene down-regulated in breast cancer. We have previously reported that ATIP3 is a potent microtubule stabilizer whose depletion increases microtubule dynamics, cell proliferation and migration. We show here that ATIP3 directly interacts with End Binding protein 1 (EB1) via an SxIP-like motif but has no tip-tracking properties. Proximity ligation assays reveal that molecular interaction between ATIP3 and EB1 takes place in the cytosol and along the microtubule lattice in living cells. ATIP3-EB1 interaction is functionally involved in regulating EB1 accumulation at the MT plus ends. We propose a novel mechanism by which ATIP3-EB1 molecular complexes may locally reduce the effective concentration of EB1, thereby limiting EB1 diffusion and access to the MT plus ends. This in turn may limit the recruitment of regulatory +TIPs and subsequently decrease MT dynamics. Finally, we provide evidence for reduced clinical outcome in breast cancer patients with low ATIP3 and high EB1 expression levels, illustrating functional relevance of our findings in human pathology.

Introduction

Microtubules (MTs) are highly polarized structures that continuously switch between periods of polymerization (growth) and depolymerization (shrinkage) at their growing (plus) ends (Mitchison and Kirschner, 1984; Desai and Mitchison, 1997; Howard and Hyman, 2003). This process, termed MT dynamic instability, allows rapid reorganization of the MT cytoskeleton during essential cell functions such as cell polarity and migration, mitosis and intracellular transport of proteins and organelles. Alterations in MT dynamic instability parameters lead to defects in mitotic spindle formation and chromosome segregation and are a major cause of cancer initiation and progression.

MT dynamic instability is tightly regulated by microtubule-associated proteins (MAPs) and MT plus end tracking proteins (+TIPs) that accumulate at the MT growing ends (Akhmanova and Steinmetz, 2008). End Binding proteins (EB1, EB2, EB3) are +TIPs that play a pivotal role in the regulation of MT dynamics. EB1 and EB3 can autonomously recognize growing MT ends through binding to GTP-cap structures (Maurer *et al*., 2011, 2012) and have been shown to control persistent MT growth (Komarova *et al*., 2009). EBs interaction with the plus ends is highly dynamic, and rapid exchange of EBs at the MT plus ends requires free diffusion and mobility of the cytosolic pool of EB proteins (Dragestein *et al*., 2008). A major function attributed to EBs is their ability to recruit a variety of regulatory +TIPs at the growing ends to orchestrate MT dynamics in a coordinated fashion. Numerous +TIPs bind to EB1 through a core SxIP motif (Serine - any amino acid – Isoleucine - Proline) embedded in an intrinsically unstructured polypeptide region rich in basic, proline and serine amino acids (Honnappa *et al*., 2009; Galjart, 2010, Slep 2010; Kumar and Wittmann, 2012; Jiang *et al*., 2012). Efficient SxIP-EB1 interaction requires that at least one basic residue, and no acidic residue, is present within the 9 amino acids surrounding the SxIP motif (Buey *et al*., 2012, Jiang *et al.,* 2012). Consensus SxIP motifs have been shown to confer both EB1 binding and tip-tracking properties (Honnappa *et al*., 2009, Buey *et al.,* 2012). Recent high throughput and *in silico* analyses have identified a broad and heterogeneous group of SxIP-containing EB1 partners (Jiang *et al*., 2012). Most of them are localized at the MT plus ends and regulate MT dynamics while others

may connect MT plus ends with cellular compartments, indicating a diversity of functions associated with EB1 interaction (Jiang *et al*., 2012).

The ATIP3 protein is a novel MAP whose expression is markedly decreased in highly proliferative and metastatic breast tumors (Rodrigues-Ferreira *et al*., 2009; Rodrigues-Ferreira and Nahmias, 2010; Molina *et al*., 2013). Restoring ATIP3 expression at normal levels in breast cancer cells significantly reduces cell proliferation and migration, as well as tumor growth and metastasis formation in experimental animal models (Rodrigues-Ferreira *et al*., 2009; Molina *et al*., 2013). Our group has recently shown that ATIP3 is a potent MT-stabilizing protein and that its depletion increases MT dynamics. Accordingly, expression of ATIP3 in breast cancer cells reduces cell migration by decreasing cell polarity and directionality, and impairs the ability of MTs to reach the cell cortex as a consequence of reduced MT dynamics at the plus ends (Molina *et al*., 2013). However, the molecular mechanisms by which ATIP3 regulates MT dynamic instability remain unknown.

ATIP3 is the major product of *MTUS1* gene, a paralog of *MTUS2* gene encoding TIP150 (Du Puy *et al*., 2009; Jiang *et al*., 2009) and the ortholog of Xenopus ICIS (Ohi *et al*., 2003). Of interest, both TIP150 and ICIS localize at MT growing ends where they interact with other +TIPs (Jiang *et al.,* 2009, Ohi *et al.,* 2003). Structural homology between ATIP3, ICIS and TIP150 (Di Benedetto *et al.,* 2006; Rodrigues-Ferreira and Nahmias, 2010) prompted us to investigate whether ATIP3 may regulate MT dynamics through functional interaction with +TIPs.

In the present study, we show that ATIP3 directly interacts with EB1 via an SxIP-like sequence but does not accumulate at the MT plus ends. We provide evidence that ATIP3-EB1 molecular complexes are present in the cytosol and along the MT lattice in intact cells. Our results support the notion that ATIP3-EB1 interaction limits EB1 accumulation at the MT growing ends, which in turn may contribute to the regulation of MT dynamics and function.

Results

ATIP3 interacts with EB1

Close examination of the ATIP3 amino acid sequence revealed three SxIP or SxIP-like motifs, each surrounded by intrinsically unstructured stretches of basic and proline/serine residues (Fig.1A). These features are recognized as hallmarks of EB1 binding and MT tip-tracking (Akhmanova and Steinmetz 2008; Honnappa *et al*., 2009; Galjart 2010; Jiang *et al*., 2012), suggesting that ATIP3 may be a novel cellular partner of EB1.

To investigate whether ATIP3 interacts with EB1, we performed pull-down assays using Gluthation-S-transferase (GST)-EB1 as an affinity matrix to precipitate GFP-ATIP3 proteins expressed in cell lysates. Results indicate that GST-EB1 precipitates GFP-ATIP3 fusion proteins (Fig.1B, 1C) as well as endogenous ATIP3 expressed in HeLa cells (Fig.1C). ATIP3-EB1 complexes were also detected by co-immunoprecipitation using either anti-Cherry or anti-GFP antibodies following co-transfection of Cherry-ATIP3 with EB1-GFP (Fig.1D). Cherry-ATIP3 also co-immunoprecipitated with GFP-EB3 as well as EB3-GFP (Expanded view Fig.E1A) indicating that ATIP3 interacts with End Binding proteins (EBs) in intact cells. Since EB1 is the leader member of the EB family studied in most cell types, we focused here on ATIP3 interaction with EB1.

To map the domain of EB1 that interacts with ATIP3, we used GST-EB1 deletion mutants comprising either the N-terminal (EB1-N) or C-terminal (EB1-C) portion of the molecule (Fig.1E). Similar to what observed for other SxIP-containing +TIPs (Askham *et al*., 2002; Komarova *et al*., 2005; Mimori-Kiyosue *et al*., 2005, Jiang *et al*., 2009), ATIP3 interacts with the C-terminal portion of EB1 (Fig.1F). ATIP3 also binds to EB1 in the presence of microtubule depolymerizing agent nocodazole (Fig.1G) indicating that EB1-ATIP3 interaction does not require an intact microtubule network.

To get further insight into the ATIP3-EB1 interaction, ATIP3 was cleaved into three distinct domains designated D1, D2 and D3 (see Fig.1A) that were fused to GFP and used in GST-EB1 pull-down experiments. As shown in Fig.1H, the central D2 domain clearly interacts with EB1, whereas the N-terminal (D1) and C-terminal (D3) domains of ATIP3 are not retained on GST-EB1 beads. These results indicate that the consensus C-terminal SxIP motif (SAIP, position 1249) present in

the D3 domain of ATIP3 (Fig.1A) is not mainly involved in EB1 interaction. Accordingly, an ATIP3 deletion mutant lacking the last 30 amino acids of the protein (ATIP3delCTer) was still able to bind EB1 (Expanded View Fig.E1B). Furthermore, site-directed mutagenesis of either Ile or Pro residues of the SAIP sequence (positions 1251 and 1252) into Asn or Ala, respectively, did not affect the EB1-binding properties of ATIP3 (Expanded View Fig.E1B). Altogether these results indicate that the central D2 domain is the major EB1-binding domain of ATIP3. As for the whole ATIP3 protein, the D2 domain interacts with the C-terminal part of EB1 and this interaction is not affected by nocodazole treatment (Fig.1I).

As illustrated in Fig.1A, the D2 domain contains two SxIP-related motifs (KNIP and RPLP at positions 462 and 780, respectively), in which a basic amino acid is present instead of the canonical serine residue. To investigate whether one or both of these non-classical motifs may be involved in EB1 binding, we generated D2 deletion mutants tagged with GFP (Fig.2A) and analyzed their ability to interact with EB1 in GST pull-down assays. As shown in Fig.2B, the C-terminal (D2C) fragment containing the RPLP sequence was precipitated by GST-EB1 whereas the N-terminal (D2N) fragment containing the KNIP motif remained unbound. Site-directed mutagenesis of Ile and/or Pro residues (positions 464 and 465) into Asn and/or Ala, respectively, in the KNIP sequence of either ATIP3 or D2 fragment did not abrogate EB1 binding (Expanded View Fig.E1B), confirming minor involvement of the KNIP sequence in EB1 interaction. The presence of an asparagine at position +2 and a negatively charged aspartic acid at position +5 of the KNIP sequence (see Fig.1A) may account for weak interaction of this motif with EB1. In contrast, the sequence surrounding the RPLP motif (see Fig.1A) follows the SxIP-9AA rule (Jiang *et al*., 2012), showing three basic and no acidic amino acid within the nine residues proximal to the SxIP sequence.

By refining the analysis of D2C fragments using shorter deletion mutants, we identified an EB1-interacting sequence of 112 residues (CN) (Fig.2B) that could be further reduced to 67 and 45 amino acids (CN67 and CN45 domains, respectively) (Fig.2C, Table I, Expanded view Fig.E1C). The minimal EB1-interacting fragment CN45 includes the consensus RPLP motif, has a net positive charge and displays significant homology to the EB1-interacting region of TIP150 (Jiang *et al*., 2009) (Expanded View Fig.E1D) as well as high evolutionary conservation (Expanded

View Fig.E1E). Importantly, deletion of the CN sequence in ATIP3 and D2 polypeptides (ATIP3delCN and D2delCN) led to a marked decrease in EB1 interaction (Fig.2D). Deletion of the RPLP sequence (CN67delP mutant) also significantly reduced the ability of CN67 to interact with EB1 (Fig.2D), further indicating major involvement of this SxIP-like motif in EB1-binding.

To investigate whether the ATIP3-EB1 interaction is direct, or whether it requires the presence of intermediate proteins present in the cell lysate, fluorescent peptides corresponding to the sequence of CN45 were synthesized and analyzed in GST-EB1 pull-down assays *in vitro*. The short CC domain that does not bind EB1 (Fig. 2A, 2B) was used as a negative control. As shown in Fig.2E, FITC-CN45 (but not FITC-CC) was specifically retained on GST-EB1 beads, indicating direct interaction between CN45 and EB1.

Altogether, these results demonstrate that ATIP3 directly interacts with EB1 *via* a non-canonical (RPLP) motif present in the C-terminal portion of the D2 domain.

EB1-binding domain is distinct from MT-localization domain

Our studies have shown that D2 is a positively charged domain whose expression is sufficient to recapitulate all functional features of ATIP3, including the ability to associate with MTs (Molina *et al*., 2013). To investigate whether EB1-interaction may require or contribute to MT-association, we examined the cellular localization of GFP-fused D2 deletion mutants in RPE1 cells, that are well-spread and suited for analyzing microtubule arrays and protein localization. Immunofluorescence studies (Fig.3) revealed that both N-terminal (D2N) and C-terminal (D2C) portions of the D2 domain are co-localized with tubulin at the MT lattice. Shorter deletion mutants of D2C (CN and CC fragments) remained mostly cytosolic, suggesting that MT localization involves a conformational recognition motif that requires both parts of the sequence. Of note, the CN fragment retained weak MT-binding (Fig.3, insets). Importantly, the minimal EB1-interacting domain CN67 was diffuse in the cytosol whereas the D2delCN deletion mutant, that has lost EB1 binding, still decorated the MT lattice (Fig.3, Table I). Thus, EB1 interaction and MT localization involve two distinct, although adjacent, regions of ATIP3.

ATIP3 is not a tip-tracking protein

The presence of SxIP motifs, also designated MtLS (microtubule tip localisation signal), often confers tip-tracking properties to EB1 partners (Honnappa *et al*., 2009, Slep, 2010; Buey *et al*., 2012, Jiang *et al*., 2012; Kumar and Wittmann, 2012), leading us to examine whether ATIP3 may accumulate with EB1 at the MT plus ends.

RPE-1 cells were transfected with low levels of GFP-ATIP3 in order to avoid extensive MT stabilization and subsequent loss of EB1 comets due to ATIP3 expression (Molina *et al*., 2013). As shown in Fig.4A, EB1 comet-like structures were still detectable in low GFP-ATIP3-expressing RPE-1 cells. Under these conditions, GFP-ATIP3 localized along the MT lattice but did not accumulate at the MT plus tips together with endogenous EB1. Time-lapse microscopy analysis of co-transfected MRC5 cells (movies 1 to 4; Expanded View Fig.E2) also clearly showed distinct patterns of Cherry-ATIP3 and EB3-GFP localization in living cells and confirmed that ATIP3 does not accumulate at the MT growing ends close to the cell cortex. Thus, ATIP3 is not a +TIP.

Time-lapse images of MCF-7 cells stably expressing moderate levels of GFP-ATIP3 (Fig.4B, movies 5 and 6) further confirmed that ATIP3 localizes along the MT lattice and is not a tip-tracking protein. They also revealed for the first time that ATIP3 accumulates on the plus end of shrinking microtubules in living cells, therefore highlighting its back-tracking properties.

ATIP3-EB1 complexes are present in the cytosol

To identify the cellular compartment in which ATIP3 and EB1 co-localize *in vivo*, we used Proximity Ligation Assay (PLA) technology that allows *in situ* detection of molecular complexes in single cells, at the location where the proteins of interest interact (Soderberg *et al*., 2006; Jarvius *et al*., 2007). RPE-1 cells were transfected with GFP-ATIP3 and molecular proximity between GFP-ATIP3 and endogenous EB1 was assessed by PLA using anti-GFP and anti-EB1 primary antibodies followed by *in situ* detection of fluorescent Rolling Circle Products (RCP). As shown in Fig.5A, PLA amplification signals were detected in cells transfected with GFP-ATIP3 and GFP-D2, but not GFP-D1, indicating that ATIP3 and D2 specifically interact with EB1 in intact cells. No signal was detected in negative control conditions, either following incubation with only one of the two primary

antibodies (Expanded View Fig.E3A) or in the presence of both antibodies in EB1-silenced cells (Expanded View Fig.E3B) or in cells transfected with GFP empty vector (Expanded View Fig.E3C). Specific PLA signals were also detected in Cherry-ATIP3-transfected RPE-1 cells stably expressing EB1-GFP, following incubation with both anti-Cherry and anti-GFP antibodies but not with anti-Cherry alone (Expanded View Fig.E3D).

As shown in Fig.5A and 5B, the number of *in situ* PLA amplification signals was markedly reduced in cells transfected with ATIP3delCN and D2delCN deletion mutants as compared to full-length ATIP3 and D2 domains. These results corroborate our GST-EB1 pull-down assays (see Fig.2D, Table I) and further demonstrate the involvement of the CN domain in the formation of EB1-ATIP3 molecular complexes in intact cells. In line with these results, PLA analyses of D2 deletion domains revealed *in situ* molecular complexes of endogenous EB1 with GFP-D2C and GFP-CN, but not GFP-D2N and GFP-CC domains (Expanded View Fig.E3E).

In all positive cells, individual bright fluorescent signals specifying protein complex formation were distributed throughout the cytosol, indicating cytosolic localization of ATIP3-EB1 complexes (Fig.5A). These results are consistent with GST pull-down experiments performed in the presence of nocodazole (Fig.1G, 1I) indicating that interaction of ATIP3 and D2 with EB1 does not require intact MTs. They are also consistent with the observation that the minimal EB1-interacting domain CN67 has a diffuse localization in the cytosol (Fig.3). Of note, bright PLA signals were also detected along MTs in GFP-ATIP3 and GFP-D2-expressing cells (insets, Fig.5C), indicating that some ATIP3/EB1 molecular complexes may also associate with the MT lattice *in vivo*.

We then sought to investigate the presence of endogenous ATIP3/EB1 complexes in intact cells. PLA experiments were conducted using rabbit anti-MTUS1 and mouse anti-EB1 primary antibodies in HeLa cells that express detectable levels of endogenous ATIP3 (Expanded view Fig.E4A). As shown in Fig.5D, RCP signals specifying interaction between endogenous ATIP3 and EB1 proteins were detected in control conditions, but not following transfection with ATIP3- or EB1-siRNA. No RCP signal was detected in negative control conditions using only anti-MTUS1 primary antibodies (Expanded view Fig.E4B). Endogenous ATIP3/EB1 complexes were located in the cytosol and along the MT lattice (Fig.5D, inset),

comforting previous results obtained in RPE-1 cells transfected with GFP-ATIP3. PLA analysis of several breast cancer cell lines expressing or not ATIP3 (Expanded View E4C) further indicated endogenous interaction between ATIP3 and EB1 in ATIP3-positive (MDA-MB-468 and HCC1143) but not ATIP3-negative (MDA-MB-231, CAL-120) breast cancer cells (Expanded View Fig.E4D).
Altogether, these results provide evidence that ATIP3 interacts with EB1 through its CN domain and that endogenous ATIP3/EB1 molecular complexes are present in the cytosol and along the MT lattice of ATIP3-expressing cells.

ATIP3-EB1 interaction limits EB1 accumulation at the MT plus ends

Our previous studies have shown that ATIP3 silencing increases MT dynamics whereas ATIP3 (and D2 domain) expression limits the accumulation of EB1 comet-like structures at the MT plus ends (Molina *et al.,* 2013). To investigate the consequence of ATIP3-EB1 interaction on EB1 localization at the MT growing ends, we analyzed the effects of D2 deletion mutants on the number and size of EB1 comet-like structures. As shown in Fig.6A, expression of EB1-interacting domains D2C and CN reduced EB1 comet formation to the same extent as D2, whereas CC - that does not bind EB1 - had no significant effect on the number or length of EB1 comets. In cells expressing D2, D2C and CN, EB1 staining was visualized in the cytosol and along MT segments (Fig.6A), in line with previous observations that ATIP3/EB1 complexes are present at the vicinity of the MT lattice. Of importance, deletion mutants (D2delCN and CN67delP) having lost the ability to interact with EB1 were no longer able to reduce EB1 comet number and size (Fig.6B, Table I), highlighting the functional involvement of the EB1-interacting domain of ATIP3 in reducing EB1 accumulation at the MT growing ends.
Rescue experiments were performed on ATIP3-silenced HeLa cells in which GFP-ATIP3 was re-introduced at levels close to endogenous (Expanded view Fig.E5A). As shown in Expanded view Fig.E5B, moderate levels of GFP-ATIP3 were sufficient to fully restore the ATIP3 knock-down phenotype, and abolish EB1 comets number and length. We then investigated whether GFP-D2 and deletion mutants were also able to rescue the phenotype. Expression levels of GFP-D2, GFP-D2delCN and GFP-CN domains were monitored by immunofluorescence (Expanded view Fig.E5C) and shown to be comparable to GFP-ATIP3 levels previously determined to be close to endogenous. As shown in Expanded Views

Fig.E5D and Fig.E5E, moderate expression of GFP-D2 and GFP-CN, but not GFP-D2delCN constructs in ATIP3-silenced HeLa cells was sufficient to restore EB1 comets number and length at levels close to those of wild type cells.

Altogether, our data indicate that functional ATIP3-EB1 complexes are formed in the cytosol and close to the MT lattice *in vivo* and contribute to restraining the accumulation of EB1 at the MT plus ends. Given the pivotal role of EB1 in regulating MT plus ends dynamics, our results may account for decreased MT dynamics in the presence of ATIP3.

Prognostic value of relative ATIP3 and EB1 levels in breast tumors

Our results suggest that altered expression of either ATIP3 or EB1 may modify the number of ATIP3-EB1 molecular complexes and subsequent accumulation of EB1 at the MT plus ends, and be deleterious to essential cell functions. To investigate the functional relevance of these findings in human pathology, we examined the prognostic value of respective ATIP3 and EB1 expression levels in breast cancer, a disease in which loss of ATIP3 correlates with tumor aggressiveness (Rodrigues-Ferreira *et al.,* 2009) and represents a prognostic biomarker of patient survival (Molina *et al.,* 2013). We reasoned that increased levels of EB1 in low ATIP3-expressing tumors may result in poor prognosis as compared to low EB1-expressing tumors.

In a panel of 150 breast cancer patients with known clinico-pathological characteristics, Affymetrix DNA array probeset values for *MTUS1* (ATIP3) and *MAPRE1* (EB1) genes were compared with overall survival of the patients (Expanded View Table E1). Unsupervised classification of the tumors was performed using intensity values for three *MTUS1* (212096_s_at; 212093_s_at; 239576_at) and two *MAPRE1* (200712_s_at ; 200713_s_at) probesets. Results of hierarchical clustering (Fig.7A) allowed us to distinguish four groups of tumors expressing various levels of ATIP3 and EB1.

Tumors from clusters 1 and 3 expressed low levels of ATIP3 (median values 473 and 425, respectively, for probeset 212093_s_at) as compared to those in clusters 2 and 4 (median values of 692 and 1056, respectively) (Fig.7B). In tumors from cluster 3, EB1 levels were significantly increased (median value 1399 for probeset 200713_s_at) as compared to those in clusters 1, 2 and 4 (median values 812, 809 and 910, respectively) (Fig.7C) (Table II).

Kaplan-Meier survival curves (Fig.7D) indicated that tumors from cluster 3 (low ATIP3-high EB1) are associated with significantly reduced overall survival of the patients as compared to all other breast tumors analyzed. As shown in Fig.7E and Table II, the median value for survival times of patients with tumors from cluster 3 was decreased by a factor of two compared to those from clusters 1, 2 and 4. The percent of patients surviving after 5 years was also markedly decreased (36.3%) in group 3 tumors as compared to tumors from other groups (60.8%, 71.4% and 76.2% survival for patients from clusters 1, 2 and 4, respectively) (Fig.7F, Table II). Of note, among tumors expressing low ATIP3 levels (clusters 1 and 3), those showing high EB1 levels (cluster 3) are of poorer outcome, indicating that combined information on ATIP3 and EB1 levels provides a more powerful prognostic marker than considering low ATIP3 levels alone. Furthermore, among tumors expressing similar levels of EB1 (clusters 1, 2 and 4), those showing high ATIP3 levels (clusters 2 and 4) were of better prognosis.

Altogether, these results illustrate the importance of coordinated ATIP3 and EB1 expression levels in breast cancer progression and clinical outcome.

Discussion

Results presented here demonstrate that MT-associated protein ATIP3 directly interacts with EB1 and that functional ATIP3-EB1 complexes present in the cytosol and at the MT lattice in living cells may regulate the accumulation, and hence the function, of EB1 at the MT plus ends.

ATIP3 interacts with EB1 through an RPLP motif surrounded by a positively charged sequence rich in proline and serine/threonine residues. This motif is very similar to the previously described consensus SxIP motif conferring EB1 interaction and tip-tracking properties (Honnappa *et al*., 2009; Buey *et al*., 2012, Kumar and Wittmann 2012; Jiang *et al*., 2012). Other EB1 partners such as SLAIN2 also present a positively charged arginine residue in place of the canonical serine at position +1 of the SxIP-like motif (Van der Vaart *et al*., 2011), suggesting that additional EB1 partners with divergent [S/R-x-I/L-P]-like motifs may be identified in the future. ATIP3 also contains a bona-fide SAIP motif in its C-terminal portion and a SxIP-like (KNIP) motif in its central region. Mutations and deletions of corresponding sequences indicate that these motifs are not necessary for EB1 binding, however they may contribute to stabilizing the interaction, as reported for other EB1-interacting proteins (Jiang *et al*., 2009; Van der Vaart *et al*., 2011).

The amino acid sequence surrounding the RPLP motif of ATIP3 is conserved in different species and is homologous to the EB1-interacting sequence of TIP150 (Jiang *et al*., 2009). TIP150, the major product of *MTUS2* gene (Jiang *et al*., 2009; Du Puy *et al.,* 2009) and ICIS, the Xenopus ortholog of *MTUS1* (Ohi *et al.,* 2003) belong to the same superfamily as ATIP3 (Di Benedetto *et al.,* 2006; Rodrigues-Ferreira and Nahmias, 2010). Both proteins have been shown to interact with +TIPs and they localize at the MT plus ends, either at the cell cortex (TIP150) or at the kinetochore (ICIS). Our results clearly show that although binding to EB1, ATIP3 does not accumulate at the MT plus ends and shows no tip-tracking activity. Time-lapse images of GFP-ATIP3 rather indicate that ATIP3 is mainly associated along the MT lattice in living cells and displays back-tracking properties.

The observation that ATIP3 and EB1 do not accumulate together at the MT plus ends raises the question of the intracellular location at which ATIP3 and EB1 interact in intact cells. Results from Proximity Ligation Assays, that highlight

molecular proximity between two proteins *in situ*, revealed that endogenous ATIP3-EB1 molecular complexes are formed in living cells and are distributed throughout the cytosol. Interestingly, in cells expressing ATIP3 or the D2 domain, molecular complexes were also detected along the MT lattice, in line with immunofluorescence studies showing increased endogenous EB1 staining at the MT lattice in cells transfected with MT-associated proteins ATIP3, D2 and D2C but not ATIP3delCN and D2delCN that associate with MTs but do not bind EB1.

As previously reported (Molina *et al*., 2013), the number and length of EB1 comet-like structures, that are characteristic of EB1 accumulation at the MT growing ends, are strongly reduced in cells expressing ATIP3 and D2. We report here that loss of EB1 comets correlates with the presence of EB1-interacting domain but is not related with MT-association. Of importance, the effect of ATIP3 and D2 domains on EB1 comet formation is lost in cells expressing D2delCN and CN67delP deletion mutants that are unable to bind EB1, therefore indicating that the ATIP3-EB1 interaction is functionally involved in reducing EB1 accumulation at the MT plus ends.

Based on our data, we propose the model shown in Fig.8. In control cells expressing ATIP3, ATIP3/EB1 complexes are formed in the cytosol and retained at close vicinity of the MT lattice, therefore locally reducing the 'efficient concentration' of cytosolic EB1 available to exchange at MT plus-ends. In ATIP3-deficient cells, more cytosolic EB1 is totally free to exchange and accumulate at MT plus-ends, leading to increased MT persistent growth and recruitment of regulatory +TIPs, thereby increasing MT dynamic instability. This in turn might account for the increase in proliferation and migration reported in ATIP3-depleted cells (Rodrigues-Ferreira *et al*., 2009; Molina *et al*., 2013).

According to this model, EB1 localization and function at the MT plus ends should be tightly regulated by the relative expression levels of ATIP3 and EB1. We challenged our hypothesis in the context of human breast cancer, as we have previously reported that loss of ATIP3 in breast tumors is associated with poor prognosis (Molina *et al*., 2013). Using a panel of 150 breast cancer patients, we provide evidence that relative levels of ATIP3 and EB1 in tumors are related with clinical outcome. Among breast tumors with low levels of ATIP3, those showing elevated EB1 levels are associated with significantly reduced overall survival of the patients, probably reflecting higher proportion of free EB1 molecules that do

not interact with ATIP3. This in turn may increase EB1 accumulation at the MT plus ends and subsequent increase in MT dynamics, and may account for increased tumor growth and metastasis in ATIP3-deficient breast tumors. Conversely, among tumors expressing similar levels of EB1, those showing high levels of ATIP3 were associated with better clinical outcome, possibly due to increased formation of ATIP3/EB1 molecular complexes and cytosolic sequestration of EB1. Of note, other groups have reported the poor prognostic value of elevated EB1 expression in hepatocellular carcinoma (Orimo *et al.,* 2008), breast cancer (Dong *et al*., 2010) and colorectal cancer (Sugihara *et al.,* 2012), raising the interest to investigate combined EB1/ATIP3 expression levels in these tumor samples.

Altogether, these results extend our knowledge of EB1 interaction with cellular partners, and depict a novel way to indirectly regulate MT functions at the growing ends through cytosolic interaction of EBs with the ATIP3 protein. A similar mechanism of EB1 sequestration in the cytosol by the MAP1B protein has recently been described in developing neurons (Tortosa *et al*., 2013), suggesting that these findings may be extended to other EB1-interacting MAPs acting in diverse physiopathological situations. Our studies also bring a major milestone in the field of breast cancer, being the first to provide a link between combined ATIP3/EB1 expression levels in tumors and clinical outcome of the patients. We propose that coordinated expression of these two proteins in breast tumors represents a novel prognostic marker that should be taken into account for better handling of the patients and choice of future therapeutic options.

Materials and Methods

Cell lines

Human breast cancer cell line MCF-7 and stable MCF-7 cell line (clone HC7) expressing endogenous levels of GFP-ATIP3, SV-MRC5 lung fibroblasts, as well as HeLa and RPE-1 (h-TERT-immortalized, retinal pigment epithelial) cells were described previously (Rodrigues-Ferreira *et al*., 2009; Molina *et al*., 2013). RPE-1 cells stably expressing EB1-GFP were a kind gift of Dr Matthieu Piel (Institut Curie, Paris, France). All cells were used at passages 2 to 20 after thawing and grown as described (Molina *et al*., 2013). Cells were routinely authenticated by morphologic observation and tested for absence of mycoplasma contamination using MycoAlert Assay detection kit (Lonza, France).

Plasmids constructs and transfections

Plasmids encoding GFP-ATIP3, Cherry-ATIP3 and domains GFP-D1, GFP-D2, GFP-D3 were described elsewhere (Molina *et al*., 2013). GFP-fused D2 subdomains (D2N, D2C, CN, CC, CN67 and CN45) were obtained by PCR-amplification of full-length ATIP3 sequence as described (Molina *et al*., 2013) using specific oligonucleotides shown in Expanded View Table E2A. Deletion mutants (GFP-ATIP3delCN, GFP-D2delCN, and GFP-CN67delP) were obtained by Site-Directed Mutagenesis according to the Quick Change kit (Stratagene) using oligonucleotides shown in Expanded View Table E2B. Procaryotic expression vectors encoding GST-EB1, GST-EB1-C, and GST-EB1-N were kind gifts of Dr Anna Akhmanova (Utrecht University, The Netherlands). EB1-GFP construct was kindly provided by Dr Franck Perez (Institut Curie, Paris, France). EB3-GFP and GFP-EB3 expression constructs were described by Stepanova *et al*. (2003).

Plasmids were transiently transfected into MCF-7, RPE-1 or HeLa cells for 24h using Turbofect (Fermentas GMBH, St Leon Rot, Germany), X-tremeGENE DNA (Roche, Mannheim, Germany) or Dreamfect (Oz-Bioscience, Marseille, France) transfection reagents as described by the manufacturer. ATIP3-specific siRNAs were described previously (Rodrigues-Ferreira *et al.,* 2009). EB1-specific siRNA (on-target plus smart pool, NM_012325) and scrambled siRNA used as a control, were purchased from Dharmacon (ThermoFisher Scientific) and Qiagen SAS,

respectively. All siRNAs (50 nM) were transfected using lipofectamine 2000 (Invitrogen) and silencing efficiency was evaluated by immunoblotting using rabbit anti-MTUS1 polyclonal antibodies (ARP44419; Aviva Systems Biology, San Diego, CA, USA) and rat anti-EB1 (clone KT51; Santa Cruz). For rescue experiments, HeLa cells were transfected with specific ATIP3-siRNA (sens strand UGG CAG AGG UUU AAG GUU A) that targets the 5' untranslated sequence of ATIP3 and allows expression of wild type ATIP3 coding sequence.

GST pull-down assays and immunoprecipitations

Production and purification of GST fusion proteins (GST-EB1, GST-EB1-C, and GST-EB1-N) on gluthatione-agarose beads were performed as described (Komarova *et al*., 2005). Transfected MCF-7 cell lysates or endogenous proteins from HeLa cells were retained on the beads for 1h at room temperature as described (Grigoriev *et al*., 2008). GST pull-down were analyzed by Western blotting using polyclonal anti-MTUS1 antibodies diluted 1:1000 or monoclonal anti-GFP antibodies (clone 7.1/13.1, Roche (Mannheim, Germany), diluted 1:3000) as indicated.

For *in vitro* interaction, chemically synthesized peptides (CN45 and CC) coupled to FITC were purchased from GL Biochem (Shanghai, China). Sequences of FITC-CN45 and FITC-CC correspond to amino acids 755-799 and 816-874 of ATIP3 (accession number NP_001001924), respectively. Purified peptides (10 or 15µg) were incubated for 1 hr at room temperature with GST- or GST-EB1 fusion proteins in 50mM HEPES containing 150mM NaCl, 0.01% Triton X100 (pH 7.4) then washed in the same buffer. Interaction was assessed by FITC fluorescence measurement using Fusion Universal Microplate Analyzer (Packard BioScience Company, Excitation 485nm Fluorescein and Emission 525-530 nm) and with Typhoon™ system (Amersham Biosciences) following 15% SDS-PAGE.

For immunoprecipitation, MCF-7 cells were transfected with appropriate plasmid constructs and cell lysates were incubated for 2 hrs at 4°C with 4µg of mouse monoclonal anti-GFP (Roche), or mouse monoclonal anti-Cherry (Clonetech) antibodies prior to incubation with G protein-sepharose beads. Bound proteins were detected by Western blotting using rabbit anti-MTUS1 antibodies (Aviva Systems Biology) or rabbit anti-GFP (Roche) as described before.

Immunofluorescence

RPE-1 cells were plated on glass coverslips, transfected for 24 hrs with appropriate plasmids, then fixed with ice-cold methanol and incubated as described (Molina *et al*., 2013) with human anti-alpha-tubulin clone F2C (Nizak *et al*., 2003), rat anti-EB1 (clone KT51; Santa Cruz) or mouse anti-GFP (Roche).

Linescan analyses of alpha-tubulin and EB1 fluorescence intensity were performed on a 5 µm line along the length of MT plus end as described (Molina *et al*., 2013). For quantification of comet number, 5 different areas of at least 5 single cells were analyzed.

Live cell imaging

SV-MRC5 co-transfected for 24h with mcherry-ATIP3 and EB3-GFP were imaged by spinning disc confocal microscopy on a Nikon Ti-E (Nikon) with perfect focus system (PFS, Nikon) equipped with a Plan APO VC 60x 1.40 N.A. oil objective, a Yokogawa motorized CSU-X1-A1 confocal head, a Photometrics Evolve 512 EMCCD camera (Roper Scientific) and controlled with MetaMorph 7.5 software (Molecular Devices). For simultaneous excitation of GFP and mCherry we used 491nm 50mW Calypso (Cobolt) and 561nm 50mW Jive (Cobolt) lasers together with a DV2 beam splitter (MAG Biosystems, Roper) equipped with a dichroic filter 565dcxr (Chroma) and a HQ630/50m emission filter (Chroma). To keep cells at 37°C we used a stage top incubator (model INUG2E-ZILCS, Tokai Hit). Images were acquired in a stream mode at 500 ms exposure. Movies are played at 15 frames per second.

For backtracking experiments, GFP-ATIP3 stable MCF-7 clones were imaged on a Nikon Eclipse Ti-E with the PFS, equipped with a Nikon CFI Apo TIRF 100X 1.49 N.A. oil objective (Nikon), a TIRF-E motorized TIRF illuminator modified by Roper Scientific France/PICT-IBiSA, Institut Curie, a stage top incubator (model INUG2E-ZILCS, Tokai Hit) set at 37°C, a Photometrics Evolve 512 EMCCD camera and controlled with MetaMorph 7.7 software. For excitation of GFP we used a Cobolt Calypso 491 nm (100 mW) laser and green fluorescent light was collected via a ET-GFP filter set (Chroma). Images were acquired in a stream mode at 100 ms exposure. Movies are played at 30 frames per second.

Timelapse inset images were denoised using the ImageJ Safir Filter plugin (Kervrann and Boulanger, 2006). Four iterations and a patch size of 1 were used as parameters of the denoising process.

Proximity Ligation Assay

In situ PLA detection was carried out using DUOLINK II In Situ Far Red kit (Sigma-Aldrich, St Louis, USA). RPE-1 cells were plated on glass coverslips at 100,000 cells per well, transfected for 24 hrs with indicated plasmids, then fixed with ice-cold methanol and incubated for 1h at room temperature with rabbit anti-GFP (Roche, 1:10000) and mouse anti-EB1 (clone 5, BD Bioscience, 1:1000) antibodies diluted in PBS-0.2% BSA as a blocking solution. For detection of endogenous ATIP3/EB1 interaction, HeLa cells were either left untreated or transfected with 50 nM appropriate siRNA as indicated, then fixed in ice-cold methanol and incubated for 1hr at room temperature with rabbit anti-MTUS1 (Aviva, 1:300) and mouse anti-EB1 (clone 5, BD Bioscience, 1:1000) antibodies in PBS-0.2% BSA. Following one wash in PBS with gentle shaking, cells were incubated with Duolink PLA Probes anti-mouse PLUS and anti-rabbit MINUS (1:5 dilution in PBS-BSA 0.2%) for 1h at 37°C in a humidified chamber, and then processed for ligation and rolling circle amplification (RCA) in the presence of cy5-labeled oligonucleotide probe according to manufacturer's protocol. Specificity of DUOLINK signals was assessed using only one of each primary antibody in the presence of both Duolink PLA probes and labeled oligonucleotide. For imaging, coverslips were stained with DAPI (1µg/mL) and analyzed by fluorescence microscopy (objective 100X, Zeiss Axiovert 200M inverted fluorescence microscope equipped with a CCD camera (CoolSNAP HQ, Photometrics)). Multi-dimensional acquisitions were performed using Metamorph 7.1.7 software. For quantification of RCP number, 5 different areas of at least 6 single cells were analyzed.

Breast tumor samples and gene arrays

Affymetrix microarray data for a series of 150 infiltrating breast carcinomas from the Institut Curie (Paris, France) and clinical data for the patients were described elsewhere (Rodrigues-Ferreira *et al.,* 2009, Molina *et al*., 2013).

Heat map and hierarchical clustering were performed on MTUS1 (212093_s_at; 212096_s_at; 239576_at) and MAPRE1 (200712_s_at; 200713_s_at) probesets, using JMP7 software. Four main clusters were isolated and the relative expression of *MTUS1* and *MAPRE1* genes in each cluster was evaluated using JMP7 and GraphPad Prism6 softwares. One tumor sample did not fit into any of the 4 clusters identified and was therefore eliminated from our study, that was further conducted on 149 tumors.

Statistical analysis

Statistical analyses were done using GraphPad Prism softwares. Overall survival (OS) curves were plotted according to the method of Kaplan–Meier and compared by the log-rank test. Data in bar graphs (mean +/- SD) and dot plots were analyzed using two-tail unpaired t-test. $p<0.05$ was considered statistically significant.

Acknowledgements

We wish to thank Dr. Anna Akhmanova (Utrecht University, The Netherlands) for kindly providing plasmids encoding GST-EB1, GST-EB1-C and GST-EB1-N fusion proteins and for helpful advice and critical reading of the manuscript. We thank Dr. Matthieu Piel (I. Curie, Paris, France) for the kind gift of RPE-1 cells stably expressing EB1-GFP. We are grateful to Anne Nehlig for excellent technical assistance and to Dr. Celine Lefebvre (Inserm U981, Institut Gustave Roussy, Villejuif, France) for help with bio-informatics analysis. We thank the Institut Cochin imaging facility. This work was supported by the Inserm, the CNRS, the University Paris Descartes, Roche SAS, the association Odyssea, Le cancer du sein, Parlons-en! and Prolific.

Authors contribution

Designed the experiments: LV, AM, SRF, CN

Performed the experiments: LV, AM, SRF, BPB, MM

Discussed and interpretated the data : LV, AM, SRF, BPB, DB, AS, SH, CN

Wrote the paper : LV, AM, SRF, CN

Contributed to essential data : FA, DB, SH, VB, AVS

Conflict of interest

The authors declare that they have no conflict of interest

Expanded View information is available at The EMBO Journal Online.

References

Akhmanova A, Steinmetz MO (2008) Tracking the ends: a dynamic protein network controls the fate of microtubule tips. *Nat Rev Mol Cell Biol* **9**: 309–322

Askham JM, Vaughan KT, Goodson HV, Morrison EE (2002) Evidence that an interaction between EB1 and p150(Glued) is required for the formation and maintenance of a radial microtubule array anchored at the centrosome. *Mol Biol Cell* **13**:3627-3645

Buey RM, Sen I, Kortt O, Mohan R, Gfeller D, Veprintsev D, Kretzschmar I, Scheuermann J, Neri D, Zoete V, Michielin O, de Pereda JM, Akhmanova A, Volkmer R, Steinmetz MO (2012) Sequence determinants of a microtubule tip localization signal (MtLS). *J Biol Chem* **287**:28227-28242

Desai A, Mitchison TJ (1997) Microtubule polymerization dynamics. *Annu Rev Cell Dev Biol* **13**:83-117

Di Benedetto M, Bièche I, Deshayes F, Vacher S, Nouet S, Collura V, Seitz I, Louis S, Pineau P, Amsellem-Ouazana D, Couraud PO, Strosberg AD, Stoppa-Lyonnet D, Lidereau R, Nahmias C (2006) Structural organization and expression of human MTUS1, a candidate 8p22 tumor suppressor gene encoding a family of angiotensin II AT2 receptor-interacting proteins, ATIP. *Gene* **380:**127-136

Dragestein KA, van Cappellen WA, van Haren J, Tsibidis GD, Akhmanova A, Knoch TA, Grosveld F, Galjart N (2008) Dynamic behavior of GFP-CLIP-170 reveals fast protein turnover on microtubule plus ends. *J Cell Biol* **180:** 729–737

Du Puy L, Beqqali A, Monshouwer-Kloots J, Haagsman HP, Roelen BA, Passier R (2009) CAZIP, a novel protein expressed in the developing heart and nervous system. *Dev Dyn* **238**:2903-2911

Dong X, Liu F, Sun L, Liu M, Li D, Su D, Zhu Z, Dong JT, Fu L, Zhou J (2010) Oncogenic function of microtubule end-binding protein 1 in breast cancer. *J Pathol* **220**:361-369

Galjart N (2010) Plus-end-tracking proteins and their interactions at microtubule ends. *Curr Biol* **20**:R528-537

Grigoriev I, Gouveia SM, van der Vaart B, Demmers J, Smyth JT, Honnappa S, Splinter D, Steinmetz MO, Putney JW Jr, Hoogenraad CC, Akhmanova A (2008) STIM1 is a MT-plus-end-tracking protein involved in remodeling of the ER. *Curr Biol* **18:**177-182

Honnappa S, Gouveia SM, Weisbrich A, Damberger FF, Bhavesh NS, Jawhari H, Grigoriev I, van Rijssel FJ, Buey RM, Lawera A, Jelesarov I, Winkler FK, Wüthrich K, Akhmanova A, Steinmetz MO (2009) An EB1-binding motif acts as a microtubule tip localization signal. *Cell* **138**:366-376

Howard J, Hyman AA (2003) Dynamics and mechanics of the microtubule plus end. *Nature* **422**:753-758

Jarvius M, Paulsson J, Weibrecht I, Leuchowius KJ, Andersson AC, Wählby C, Gullberg M, Botling J, Sjöblom T, Markova B, Ostman A, Landegren U, Söderberg O (2007) In situ detection of phosphorylated platelet-derived growth factor receptor beta using a generalized proximity ligation method. *Mol Cell Proteomics* **6**:1500-1509

Jiang K, Wang J, Liu J, Ward T, Wordeman L, Davidson A, Wang F, Yao X (2009) TIP150 interacts with and targets MCAK at the microtubule plus ends. *EMBO Rep* **10**:857-865

Jiang K, Toedt G, Montenegro Gouveia S, Davey NE, Hua S, van der Vaart B, Grigoriev I, Larsen J, Pedersen LB, Bezstarosti K, Lince-Faria M, Demmers J, Steinmetz MO, Gibson TJ, Akhmanova A (2012) A Proteome-wide screen for mammalian SxIP motif-containing microtubule plus-end tracking proteins. *Curr Biol* **22**:1800-1807

Kervrann C, Boulanger J (2006) Optimal spatial adaptation for patch-based image denoising. *IEEE Trans. Image Processing* **15**:2866-2878

Komarova Y, Lansbergen G, Galjart N, Grosveld F, Borisy GG, Akhmanova A (2005) EB1 and EB3 control CLIP dissociation from the ends of growing microtubules. *Mol Biol Cell* **16**: 5334–5345

Komarova Y, De Groot CO, Grigoriev I, Gouveia SM, Munteanu EL, Schober JM, Honnappa S, Buey RM, Hoogenraad CC, Dogterom M, Borisy GG, Steinmetz MO, Akhmanova A (2009) Mammalian end binding proteins control persistent microtubule growth. *J Cell Biol* **184**: 691–706

Kumar P, Wittmann T (2012) +TIPs: SxIPping along microtubule ends. *Trends Cell Biol* **22**:418-428

Maurer SP, Bieling P, Cope J, Hoenger A, Surrey T (2011) GTPgammaS microtubules mimic the growing microtubule end structure recognized by end-binding proteins (EBs). *Proc Natl Acad Sci U S A* **108:**3988-3993

Maurer SP, Fourniol FJ, Bohner G, Moores CA, Surrey T (2012) EBs recognize a nucleotide-dependent structural cap at growing microtubule ends. *Cell* **149**:371-382

Mimori-Kiyosue Y, Grigoriev I, Lansbergen G, Sasaki H, Matsui C, Severin F, Galjart N, Grosveld F, Vorobjev I, Tsukita S, Akhmanova A (2005) CLASP1 and CLASP2 bind to EB1 and regulate microtubule plus-end dynamics at the cell cortex. *J Cell Biol* **168**:141-153

Mitchison T, Kirschner M (1984) Dynamic instability of microtubule growth. *Nature* **312**:237-242

Molina A, Rodrigues-Ferreira S, Di Tommaso A, Nahmias C (2011) ATIP, a novel superfamily of microtubule-associated proteins. *Med Sci (Paris)* **27**:244-246

Molina A, Velot L, Ghouinem L, Abdelkarim M, Bouchet BP, Luissint AC, Bouhlel I, Morel M, Sapharikas E, Di Tommaso A, Honoré S, Braguer D, Gruel N, Vincent-Salomon A, Delattre O, Sigal-Zafrani B, André F, Terris B, Akhmanova A, Di Benedetto M, Nahmias C, Rodrigues-Ferreira S (2013) ATIP3, a novel prognostic marker of breast cancer patient survival, limits cancer cell migration

and slows metastatic progression by regulating microtubule dynamics. *Cancer Res* **73:**2905-2915

Nizak C, Martin-Lluesma S, Moutel S, Roux A, Kreis TE, Goud B, Perez F (2003) Recombinant antibodies against subcellular fractions used to track endogenous Golgi protein dynamics in vivo. *Traffic* **4**:739-753

Ohi R, Coughlin ML, Lane WS, Mitchison TJ (2003) An inner centromere protein that stimulates the microtubule depolymerizing activity of a KinI kinesin. *Dev Cell* 5:309-321

Orimo T, Ojima H, Hiraoka N, Saito S, Kosuge T, Kakisaka T, Yokoo H, Nakanishi K, Kamiyama T, Todo S, Hirohashi S, Kondo T (2008) Proteomic profiling reveals the prognostic value of adenomatous polyposis coli-end-binding protein 1 in hepatocellular carcinoma. *Hepatology* **48:**1851-1863

Rodrigues-Ferreira S, Di Tommaso A, Dimitrov A, Cazaubon S, Gruel N, Colasson H, Nicolas A, Chaverot N, Molinié V, Reyal F, Sigal-Zafrani B, Terris B, Delattre O, Radvanyi F, Perez F, Vincent-Salomon A, Nahmias C (2009) 8p22 MTUS1 gene product ATIP3 is a novel anti-mitotic protein underexpressed in invasive breast carcinoma of poor prognosis. *PLoS One* **4(10):**e7239

Rodrigues-Ferreira S, Nahmias C (2010) An ATIPical family of Angiotensin II AT2 receptor interacting proteins. *Trends Endocrinol Metab* **21**:684-690

Slep KC (2010) Structural and mechanistic insights into microtubule end-binding proteins. *Curr Opin Cell Biol* **22**: 88–95

Söderberg O, Gullberg M, Jarvius M, Ridderstråle K, Leuchowius KJ, Jarvius J, Wester K, Hydbring P, Bahram F, Larsson LG, Landegren U (2006) Direct observation of individual endogenous protein complexes in situ by proximity ligation. *Nat Methods* **3:**995-1000

Stepanova T, Slemmer J, Hoogenraad CC, Lansbergen G, Dortland B, De Zeeuw CI, Grosveld F, van Cappellen G, Akhmanova A, Galjart N (2003) Visualization

of microtubule growth in cultured neurons via the use of EB3-GFP (end-binding protein 3-green fluorescent protein). *J Neurosci* **23**:2655-2664

Sugihara Y, Taniguchi H, Kushima R, Tsuda H, Kubota D, Ichikawa H, Sakamoto K, Nakamura Y, Tomonaga T, Fujita S, Kondo T (2012) Proteomic-based identification of the APC-binding protein EB1 as a candidate of novel tissue biomarker and therapeutic target for colorectal cancer. *J Proteomics* **75**:5342-5355.

Tortosa E, Galjart N, Avila J, Sayas CL (2013) MAP1B regulates microtubule dynamics by sequestering EB1/3 in the cytosol of developing neuronal cells. *EMBO J.* **32**:1293-1306

Van der Vaart B, Franker MA, Kuijpers M, Hua S, Bouchet BP, Jiang K, Grigoriev I, Hoogenraad CC, Akhmanova A (2011) Microtubule plus-end tracking proteins SLAIN1/2 and ch-TOG promote axonal development. *J Neurosci* **32:**14722-14728

Figure legends

Figure 1. ATIP3 interacts with EB1

(A). Schematic representation of ATIP3 protein and domains (D1, D2, D3) showing microtubule (MT)-binding domain (in grey) and coiled-coil (CC) motifs (in blue). Positions of KNIP, RPLP and SAIP motifs (residues 462, 780 and 1249, respectively) are shown in red. Amino acid numbering is from Accession number NP_001001924. Lower panel: ATIP3 amino acid sequence surrounding each motif. Basic residues are indicated in red. Acidic residues (blue) are bold and underlined. SxIP and SxIP-like motifs are boxed.

(B). GST pull-down analysis showing specific interaction between GFP-ATIP3 expressed in MCF-7 cell lysates and purified GST–EB1 agarose beads. Blots were probed with anti-GFP antibodies. Polypeptides corresponding to GFP-ATIP3 and GFP are indicated on the right. A star indicates cleavage product of GFP-ATIP3.

(C). Purified GST-EB1 beads were used to precipitate GFP-ATIP3 (210 KDa) and endogenous ATIP3 (180 KDa) expressed in HeLa cells. Blots were probed with anti-ATIP (MTUS1) antibodies.

(D). Co-immunoprecipitation of Cherry-ATIP3 (Ch-ATIP3) and/or EB1-GFP transfected in MCF-7 cells, using anti-GFP or anti-Cherry (Ch) antibodies as indicated below. Western blots were probed with anti-GFP and anti-ATIP antibodies to reveal EB1-GFP (55 KDa) and Ch-ATIP3 (210 KDa), as indicated on the right. IgH: Immunoglobulin heavy chain.

(**E).** Schematic drawing of EB1 deletion mutants. Amino acid positions at domain boundaries are indicated.

(F). Pull-down analysis of MCF-7 cell lysates expressing GFP-ATIP3 using indicated purified GST-fusion proteins. Blots were probed using anti-GFP antibodies.

(G). MCF-7 cell lysates expressing GFP-ATIP3 were treated or not (Ctrl) with 10 µm nocodazole (Nz) for 1 hr at 4°C, then incubated with GST-EB1 beads as in B.

(H). GST-EB1 pull-down assays on MCF-7 cell lysates expressing GFP-D1, GFP-D2 or GFP-D3, performed as in B.

(I). GST pull-down assays on MCF-7 cell lysates expressing GFP-D2, performed as in F and G.

Figure 2. Minimal interacting domain of ATIP3

(A). Schematic drawing of deletion mutants and their ability to bind EB1 (+) or not (-).

(B). Pull-down analysis of GFP-D2 domain and GFP-fused deletion mutants (D2N, D2C, CN, CC) using GST or GST-EB1 agarose beads, as indicated in Fig.1B. Blots were probed with anti-GFP antibodies**.** Molecular weights are indicated in KDa on the left.

(C) Pull-down analysis of GFP-fused deletion mutants (D2C, CN67, CN45) as indicated in B.

(D) Pull-down analysis of deletion mutants lacking the CN domain (D2delCN) or RPLP motif (CN67delP), as indicated in B.

(E). *In vitro* pull-down assay using purified GST (white bars) or GST-EB1 (black bars) and 10 or 15µg of synthetic fluorescent peptides (CN45 and CC coupled to FITC) as indicated below. Upper panel: fluorescence intensity (arbitrary units) in the precipitates was measured using Fusion fluorimeter. Lower panel: samples before (input) and after GST pull-down were resolved on 15% SDS-PAGE and fluorescent peptides were detected using Typhoon scanner.

Figure 3. Cellular localization of D2 deletion mutants.

Immunofluorescence imaging of RPE-1 cells expressing GFP-D2 domain and GFP-tagged deletion mutants as indicated. Cells were fixed and stained with anti-GFP (green), anti-alpha-tubulin (red) antibodies and DAPI (blue). Enlarged portions of the selected areas are shown in the insets. Red arrowheads show MT-localization of GFP-fusion proteins. Scale bar, 10μm.

Figure 4. ATIP3 is not a +TIP

(A). RPE-1 cells transfected with low amounts of GFP-ATIP3 were fixed and stained with anti-GFP (green) and anti-EB1 (red) antibodies. Insets show that EB1 comet-like structures at plus ends are not stained by GFP-ATIP3. Magnification 100X. Scale bar, 10μm.

(B). Time-lapse images of HC7 (MCF-7 cell clone stably expressing GFP-ATIP3 at endogenous levels, described in Rodrigues-Ferreira *et al*., 2009). GFP-ATIP3 stains the MT lattice and the ends of shrinking MTs (arrowheads) in living cells, indicating backtracking properties. Scale bar, 10μm.

Figure 5. *In situ* interaction between ATIP3 and EB1

(A). Proximity Ligation Assays were performed in RPE-1 cells transfected with GFP-tagged constructs and deletion mutants as indicated on the left. Molecular complexes were analyzed using rabbit anti-GFP and mouse anti-EB1 primary antibodies and corresponding secondary DUO-LINK antibodies. *In situ* molecular interaction is revealed by red bright signals of rolling circle amplification products (RCP) stained with cy5-labeled oligonucleotide probe. Shown are merge pictures of GFP (green), RCP (red) and nuclei (DAPI, blue) staining. Scale bar 10μm.

(B). Quantification of the number of RCP signals per square (100 μm^2 area). Number of squares analyzed is under brackets. *** $p<0.0001$.

(C). Enlarged portions of selected areas in (A) are shown in the insets. Arrowheads illustrate alignment of RCP signals along the MT lattice.

(D). Proximity Ligation Assays revealing *in situ* molecular interaction between endogenous ATIP3 and EB1 in HeLa cells transfected with control siRNA (SiCtrl), ATIP3-specific siRNA (siATIP3) or EB1-specific siRNA (siEB1) as indicated. Endogenous complexes were analyzed using rabbit anti-MTUS1 and mouse anti-EB1 primary antibodies and corresponding secondary DUO-LINK antibodies. Cells were stained with anti-tubulin F2C antibodies and secondary antibodies conjugated to Cy3. Shown are merge pictures of tubulin (green), RCP (red) and nuclei (DAPI, blue) staining. Scale bar 10µm. Inset shows enlarged portion of a selected area from siCtrl-transfected cell. The arrowhead illustrates alignment of RCP signals along the MT lattice.

(E). Silencing efficiency was assessed by immunoblotting with anti-MTUS1 (ATIP3) and anti-EB1 antibodies. Blots were reprobed using anti-tubulin antibodies for internal control.

(F). Quantification of the number of RCP signals per square in PLA conditions shown in (D) (100 μm^2 area). Number of squares analyzed is under brackets. *** $p<0.0001$.

Figure 6. Effect of D2 deletion mutants on EB1 comet formation

Anti-EB1 (green) and anti-tubulin (red) immunostaining of RPE-1 cells transiently transfected with GFP-D2 and GFP-tagged domains **(A)** and GFP-D2 deletion mutants **(B).** Insets show EB1 comet-like structures in enlarged portions of selected areas. Red arrowheads illustrate EB1 staining along the MT lattice. Right panels show distribution of EB1 (green) and alpha-tubulin (red) at the microtubule plus ends (linescans), quantification of comet length (scattered dot plot) and number of comets (per 62μm^2 area). Number of comets analyzed is under brackets. Scale bar, 10µm. *** $p<0.0001$.

Figure 7. Prognostic value of combined ATIP3 and EB1 expression levels in breast tumors.

(A). Heat map and hierarchical clustering of 150 breast tumor samples based on the intensities of *MTUS1* (212096_s_at; 212093_s_at; 239576_at) and *MAPRE1*

(200712_s_at ; 200713_s_at) probesets. Heat map illustrates relative expression profiles of *MTUS1* and *MAPRE1* (column) for each tumor sample (line) in continuous color scale from low (green) to high (red) expression. Dendogram of the four selected tumor groups is shown on the right.

(B). Box plot comparison of MTUS1 (ATIP3) intensities (Raw Mas 5) in each of the four selected tumor clusters based from dendogram shown in (A). *p<0.05; ***p<0.0001.

(C). Box plot comparison of MAPRE1 (EB1) intensities (GCMRA) in each of the four selected tumor clusters based from dendogram shown in (A). ***p<0.0001.

(D). Overall survival curves for patients with breast tumors classified into four groups based from dendogram shown in (A). p=0.0011 between clusters 3 and 4.

(E). Overall survival (in months) for patients classified according to tumor groups shown in (D). Scattered dot plot and median values are shown for each tumor cluster. Number of patients is in brackets. *p<0.05; **p<0.001.

(F). Percentage of patients remaining alive after 5 years with tumors classified into four groups as in (D). Number of patients is in brackets.

Figure 8. Proposed mechanism for regulation of EB1 localization by interaction with ATIP3.

In control cells, ATIP3-EB1 complexes are present in the cytosol and at the vicinity of the microtubule lattice and limit the binding of EB1 to MT plus ends. In ATIP3-deficient cancer cells, free diffusion of cytosolic EB1 results in enhanced accumulation of EB1 at the plus ends of MTs and subsequent increase in MT dynamics at the growing ends.

Table I. Characterization of ATIP3 domains and deletion mutants

Domain	Positions (AA)	Length (AA)	EB1 binding	MT localization	Loss of EB1 comets
ATIP3	1-1270	1270	+	+	+
D2	410-874	465	+	+	+
D2N	410-634	225	-	+	nd
D2C	705-874	170	+	+	+
CN	705-816	112	+	+/-	+
CC	817-874	58	-	-	-
CN67	743-809	67	+	-	+
CN45	755-799	45	+	-	+
CN67delP	[743-777]+[783-809]	61	-	-	-
ATIP3delCN	[1-704]+[817-1270]	1158	-	+	nd
ATIP3delCC1	[1-816]+[869-1270]	1218	+	nd	nd
ATIP3delCC2	[1-867]+[875-1270]	1263	+	nd	nd
ATIP3delCTer	1-1240	1240	+	nd	nd
D2delCN	[410-704]+[817-874]	353	-	+	-
D2delCC1	[410-816]+[867-874]	413	+	nd	nd

AA: amino acids. Positions are according to accession number NP_001001924; nd: not determined.

Table II. ATIP3-EB1 expression levels in breast tumor clusters and overall survival of the patients.

cluster	nb of tumors	median value MTUS1 (212093_s_at)	median value MAPRE1 (200713_s_at)	Expression ATIP3-EB1	median survival (months)	5-y survival % patients (n)
1	46	473,2 (166,7 - 740,9)	811,8 (515,6 - 1201)	L-L	105,8 (4,43 - 180,6)	60,8% (28/46)
2	49	692 (445,8 - 1321)	809 (413 - 1541)	H-L	129,5 (17,37 - 174)	71,4% (35/49)
3	33	424,9 (148,2 - 862,8)	1399 (1010- 2539)	L-H	53,7 (19,53 - 145,3)	36,3% (12/33)
4	21	1057 (603,1 - 1518)	910,2 (526,4 - 1596)	VH-L	126,5 (49,27 - 186,1)	76,2% (16/21)

For each tumor cluster, shown is : number (nb) of tumors, median values for Affymetrix *MTUS1* probeset 212093_s_at (raw mas5) and *MAPRE1* probeset 200713_s_at (GCMRA), corresponding expression levels for ATIP3 and EB1, median survival in months and percent of patients surviving after 5 years. Range values are in parenthesis. L: low; H: high; VH: very high.

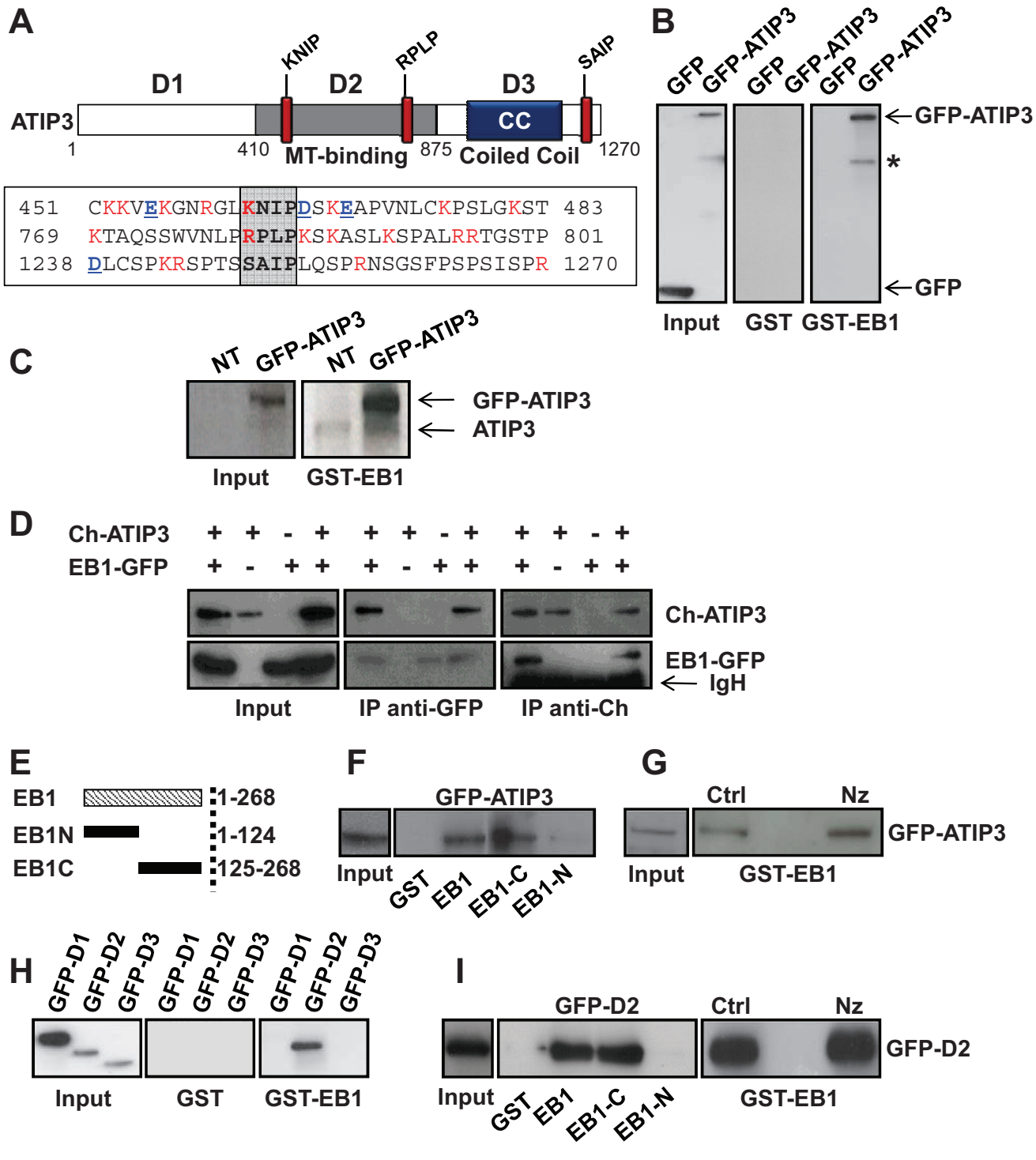

Velot, Molina et al., Fig.1

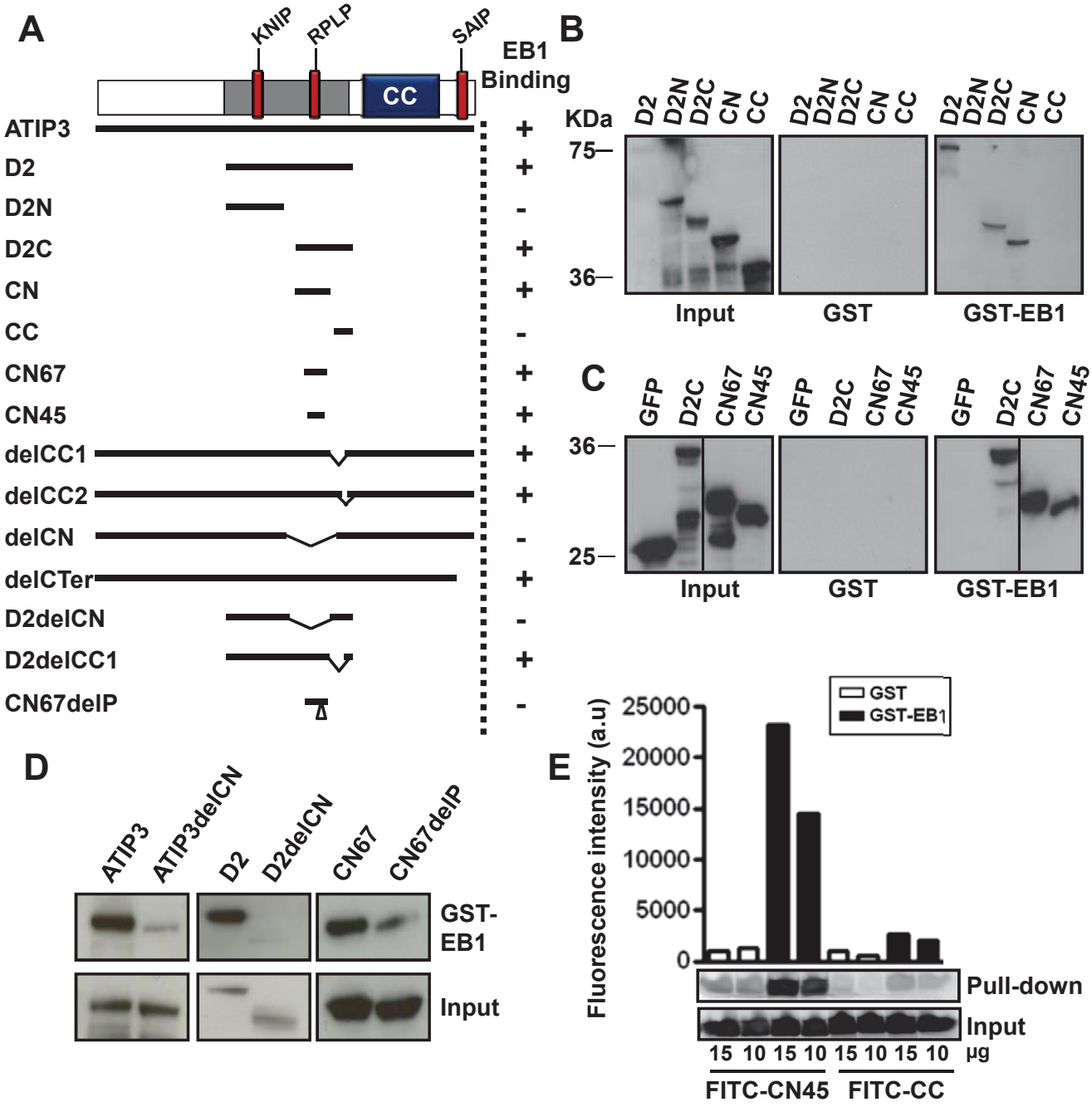

Velot, Molina et al., Fig.2

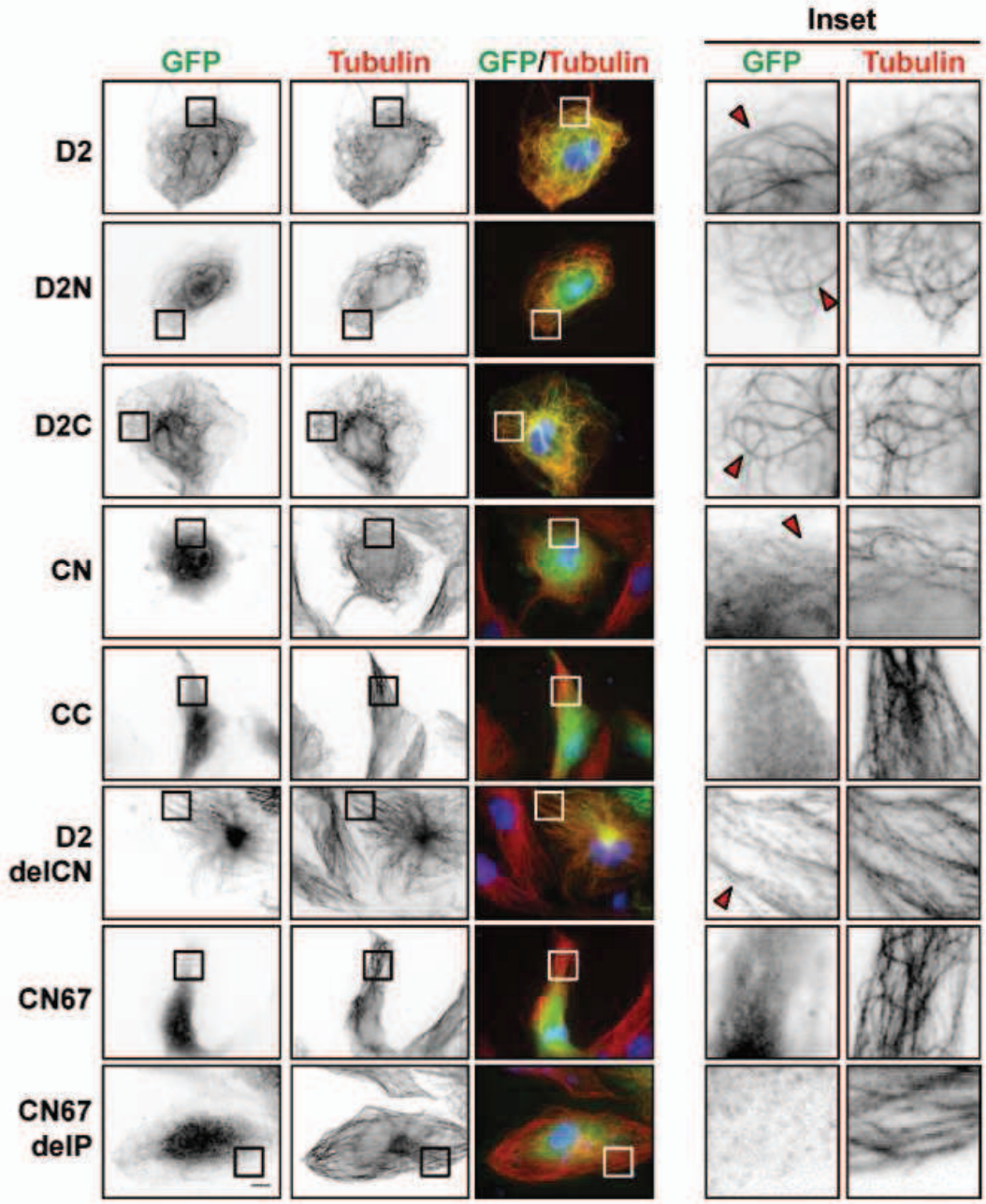

Velot, Molina et al., Fig.3

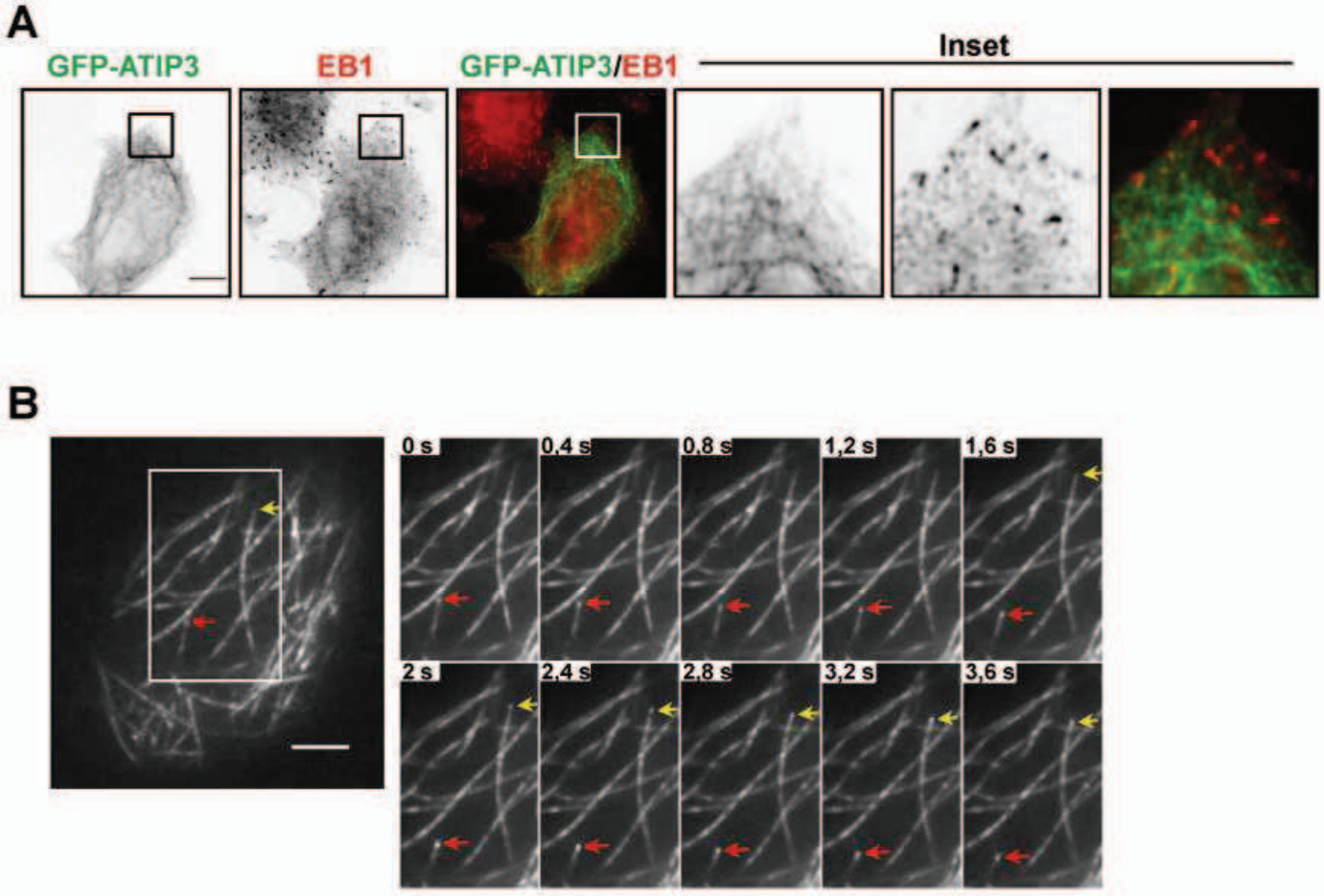

Velot, Molina et al., Fig.4

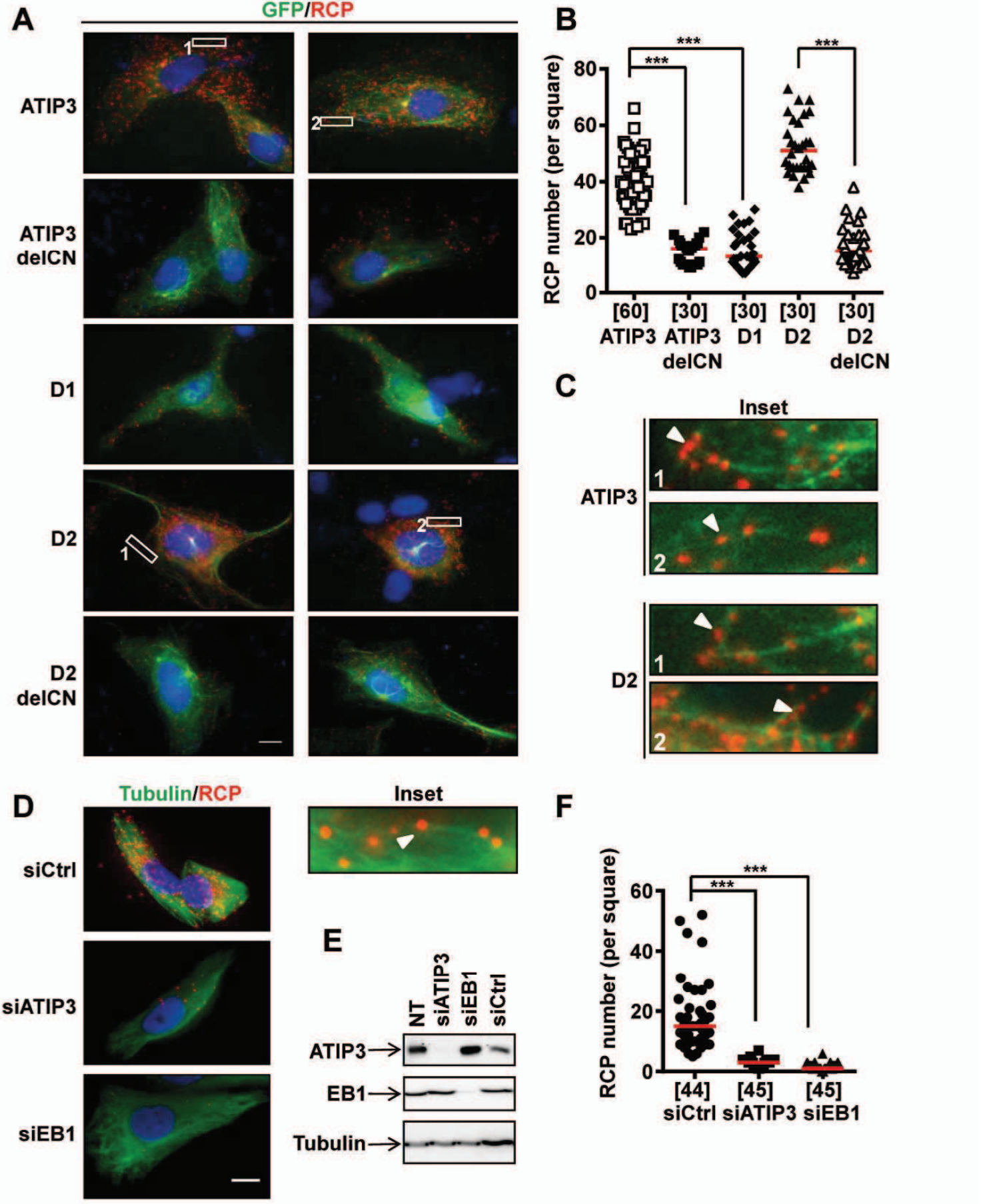

Velot, Molina et al., Fig.5

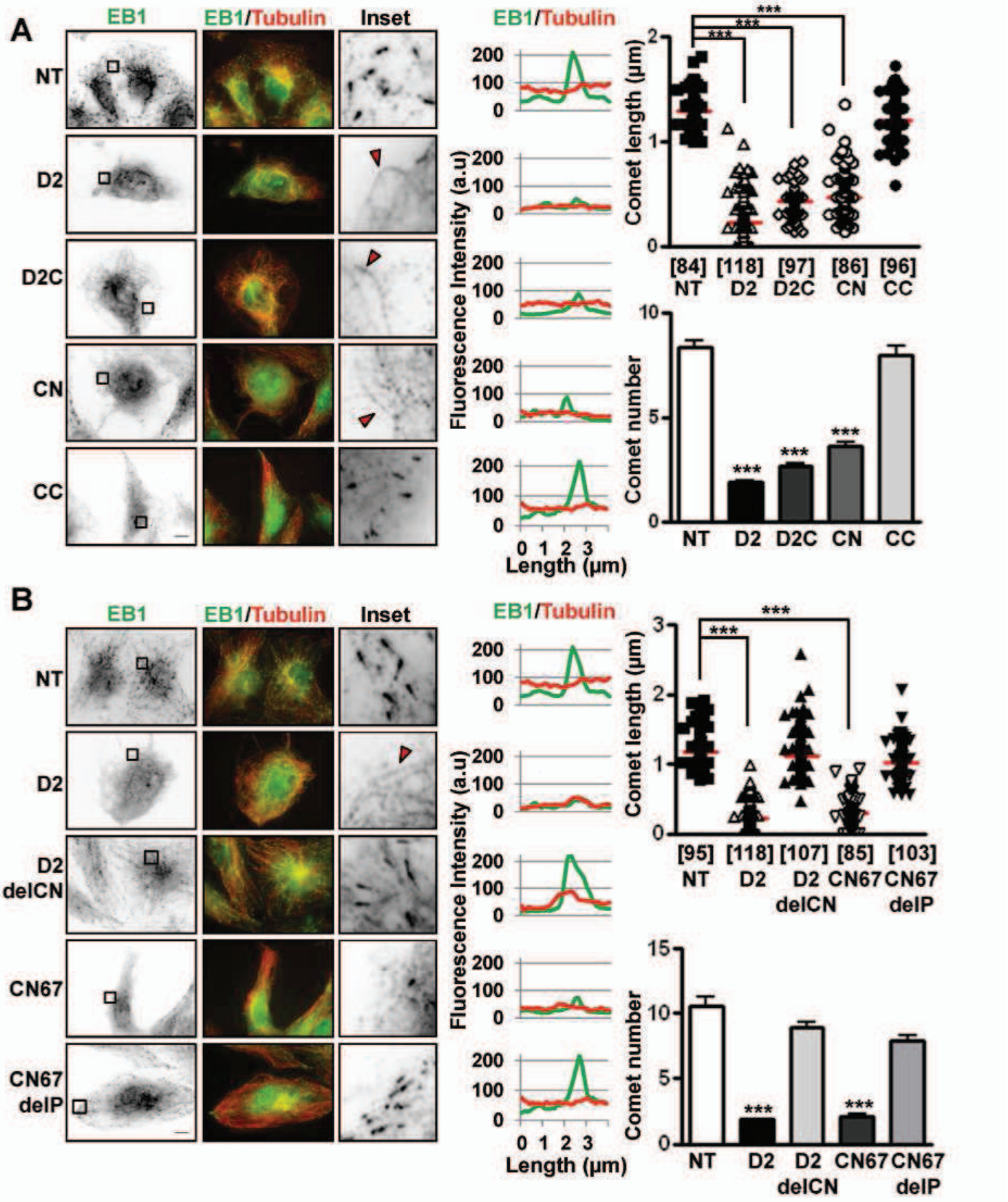

Velot, Molina et al., Fig.6

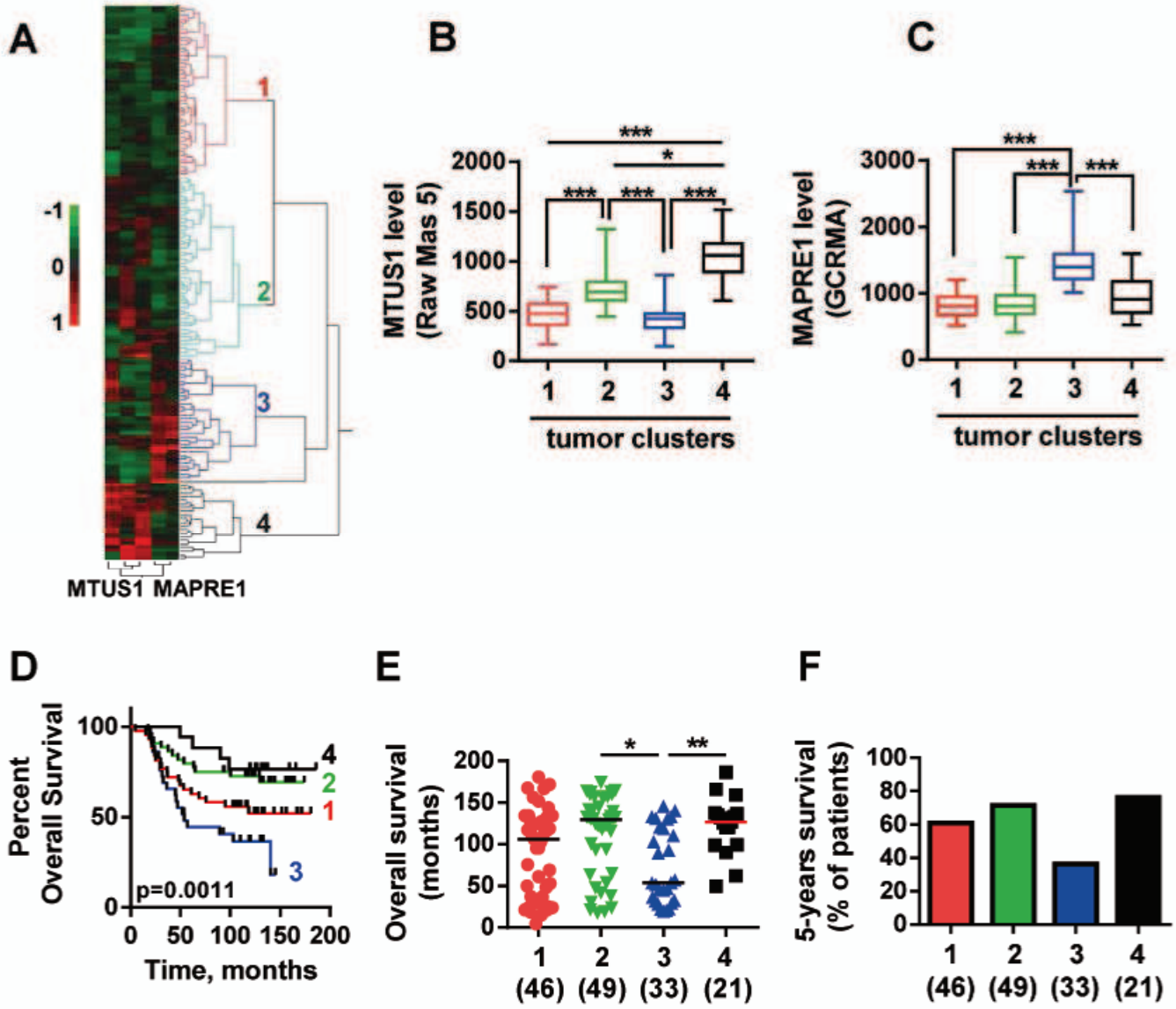

Velot, Molina et al., Fig.7

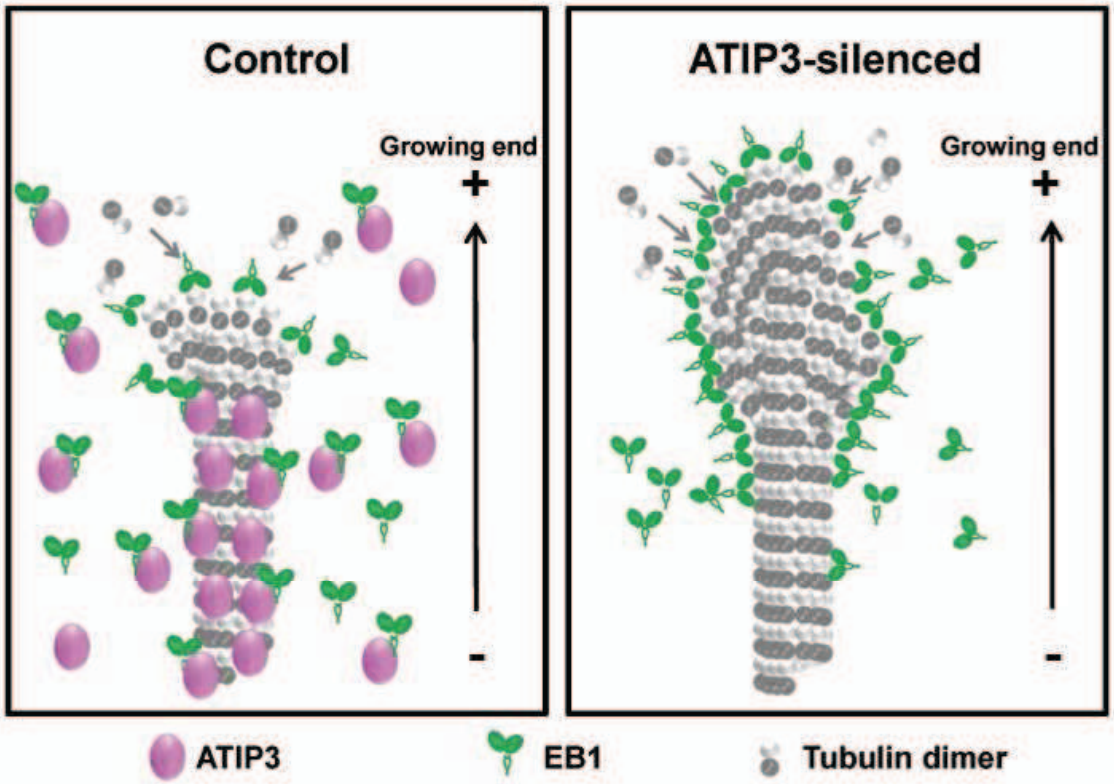

Velot, Molina et al., Fig.8

Manuscript Title : ATIP3 interacts with End Binding protein EB1 to limit its accumulation at the microtubule plus ends

Expanded View Material and Methods

Human breast cancer cell lines

Triple-negative breast cancer cell lines expressing (MDA-MB-468) or not (MDA-MB-231-D3H2LN) endogenous ATIP3 were described previously (Rodrigues-Ferreira *et al.,* 2009; Molina *et al.,* 2013). HCC1143 and CAL-120 breast cancer cell lines were a kind gift of Dr. S. Alsafadi (Institut Gustave Roussy, Villejuif, France). All cell lines were tested for absence of mycoplasma contamination using MycoAlert Assay detection kit (Lonza, France), used at passages 2 to 20 after thawing and grown as described by the provider.

Proximity Ligation Assay

In situ PLA detection was carried out using DUOLINK II In Situ Far Red kit (Sigma-Aldrich, St Louis, USA). RPE-1 cells stably expressing EB1-GFP were transfected for 24 hrs with Cherry-ATIP3 construct as described in the Materials and Methods. Cells were fixed with ice-cold methanol and incubated for 1h at room temperature with rabbit anti-Cherry (1:500) and mouse anti-GFP (Roche, 1:200) antibodies diluted in PBS-0.2% BSA as a blocking solution. Incubation with PLA probes and RCP analysis was performed as described in the Materials and Methods.

Legends to Expanded View Figures

Expanded View Figure E1. ATIP3 interacts with EB1

(A). Co-immunoprecipitation of Cherry-ATIP3 or Cherry and/or indicated constructs (EB1-GFP, GFP-EB3, EB3-GFP or GFP) transfected in MCF-7 cells, using anti-GFP antibodies. Western blots were probed with anti-GFP and anti-MTUS1 antibodies as indicated on the right, to reveal EB1/3-GFP (55 KDa) and Ch-ATIP3 (210 KDa), respectively.

(B). GST pull-down analysis showing interaction between GFP-ATIP3 and GFP-D2 mutants as indicated and purified GST-EB1 agarose beads. Blots were probed with anti-GFP antibodies.

(C). GST-EB1 pull-down assays as in B, performed on MCF-7 cell lysates expressing indicated GFP-ATIP3 or GFP-D2 deletion mutants described in Fig.2A and Table I.

(D). Amino acid sequence alignment of EB1-binding domains of ATIP3 (CN45) and TIP150. Basic residues are highlighted in red and underlined. The SxIP motif (RPLP) is boxed. Stars indicate identical residues. Gaps have been introduced to maximize homology.

(E). Amino acid sequence alignment of ATIP3 polypeptides from different species. The RPLP motif is boxed and stars indicate conserved residues. Hs, *Homo sapiens*, Bt, *Bos taurus*, Rn, *Rattus norvegicus*, Mm, *Mus musculus*.

Expanded View Figure E2. ATIP3 is not a +TIP

Images from fluorescent microscopy of MRC5 living cells co-transfected with Cherry-ATIP3 (Ch-ATIP3) and EB3-GFP. Note that EB3 is enriched at the plus ends and weakly stains the MT lattice. Inset shows that ATIP3 is along the MT lattice and does not accumulate with EB3 at the plus ends. Scale bar 10 µm.

Expanded View Figure E3. *In situ* interaction between ATIP3 and EB1

(A). Proximity Ligation Assays were performed in RPE-1 cells transfected with GFP-ATIP3 or GFP-D2 as indicated on the left. Molecular complexes were analyzed using rabbit anti-GFP and/or mouse anti-EB1 primary antibodies (as indicated above) and corresponding secondary DUO-LINK antibodies. *In situ* molecular interaction is

revealed by red bright signals of rolling circle amplification products (RCP) stained with cy5-labeled oligonucleotide probe. Shown are merge pictures of GFP (green), RCP (red) and nuclei (DAPI) staining.

(B). PLA assay in RPE-1 cells transfected with GFP-ATIP3 in the presence or not of EB1-specific siRNA as indicated above. Shown are merge pictures as in A.

(C). PLA assay in RPE-1 cells transfected with GFP and analyzed as in B.

(D). PLA assay in RPE-1 cells stably expressing EB1-GFP and transfected with Cherry-ATIP3. Molecular complexes were analyzed using rabbit anti-Cherry (Ch) and/or mouse anti-GFP primary antibodies and corresponding secondary DUO-LINK antibodies as indicated on the left. *In situ* molecular interaction is revealed by red bright signals of rolling circle amplification products (RCP) stained with cy5-labeled oligonucleotide probe. Shown are merge pictures of Cherry (yellow), RCP (red) and nuclei (DAPI) staining.

(E). PLA assay in RPE-1 cells transfected with GFP-D2C, D2N, CN and CC constructs.

(A-E) Magnification x100. Scale bar 10µm.

Expanded View Figure E4. Endogenous interaction between ATIP3 and EB1

(A). Western blot analysis of endogenous ATIP3 expression in non-tumoral human mammary epithelial cells (HMEC), HeLa cells and non-transformed MCF10A cells, using anti-MTUS1 antibodies, and reprobed with anti-tubulin antibodies for internal control.

(B). Proximity Ligation Assays performed in non transfected HeLa cells using rabbit anti-MTUS1 and mouse anti-EB1 primary antibodies, or anti-MTUS1 antibodies alone as negative control. Endogenous molecular interaction is revealed by red bright signals of rolling circle amplification products (RCP) stained with cy5-labeled oligonucleotide probe. Shown are merge pictures of RCP (red) and nuclei (DAPI, blue) staining. Scale bar 10µm.

(C). Western blot analysis of endogenous ATIP3 expression levels in human breast cancer cell lines using anti-MTUS1 antibodies (upper panel) and reprobed with anti-tubulin antibodies (lower panel).

(D). PLA assays performed using rabbit anti-MTUS1 and mouse anti-EB1 primary antibodies as in (B), showing endogenous ATIP3/EB1 interaction in ATIP3-positive

MDA-MB-468 and HCC1143 breast cancer cell lines but not in ATIP3-negative MDA-MB-231 and CAL-120 cell lines. MDA-MB-231 cells were previously demonstrated to be ATIP3-negative (Rodrigues-Ferreira et al., 2009). Shown are merge pictures of RCP (red) and nuclei (DAPI, blue) staining. Scale bar 10µm.

Expanded View Figure E5. Rescue of ATIP3-silenced phenotype

(A). Western blot analysis comparing expression of GFP-ATIP3 with that of endogenous ATIP3. HeLa cells were either left non-transfected (NT), or transfected for 72hrs with ATIP3-specific siRNA and for 24 hrs with plasmids encoding GFP (0.5 µg) or GFP-ATIP3 (2 µg) as indicated. Blots were probed with anti-MTUS1 antibodies to reveal endogenous ATIP3 (180 KDa) and transfected GFP-ATIP3 (210 KDa), and then reprobed with anti-tubulin antibodies for internal control.

(B). ATIP3-silenced HeLa cells were transfected with GFP-ATIP3 plasmid (2 µg) as in (A), then labeled with anti-GFP (green) and anti-EB1 (red) antibodies. Insets show EB1 comet-like structures in enlarged portions of selected areas (insets 1 and 2 show non-transfected and transfected cells, respectively). Right panel : Quantification of comet length (scattered dot plot) and number of comets (per 62µm^2 area). Fifty comets were analyzed for each condition. Scale bar, 10µm. *** $p<0.0001$.

(C). ATIP3-silenced HeLa cells were transfected with plasmids encoding GFP-ATIP3 (2 µg), GFP-D2 (2 µg), GFP-D2delCN (1µg) or GFP-CN (0.5 µg) as indicated. Fluorescence intensity of GFP immunostaining indicates similar levels of expression for all fusion proteins. Scale bar : 10 µm.

(D). ATIP3-silenced HeLa cells were transfected for 24 hrs with indicated plasmids in conditions of moderate expression as shown in (C), then labelled with anti-GFP (green) anti-EB1 (red) antibodies. Insets show EB1 comet-like structures in enlarged portions of selected areas as in (B). Scale bar, 10µm.

(E). Quantification of comet length (scattered dot plot) and number of comets (per 62µm^2 area) in HeLa cells transfected with control siRNA (left) or ATIP3-specific siRNA (right panel) then transfected with GFP fusion proteins at levels close to endogenous as in (C). Number of comets analyzed is under brackets. *** $p<0.0001$.

Legends to Expanded View Movies

Movies 1 and 2. Time-lapse microscopy of MRC5-SV cells co-transfected with Cherry-ATIP3 and EB3-GFP

EB3-GFP (left) and Cherry-ATIP3 (right) MRC5-SV-coexpressing cells were imaged by spinning disk confocal microscopy (60X lens).Time-lapse series of 100 images were acquired in a stream mode and shown at 15 frames per second.

Movies 3 and 4. Time-lapse microscopy of MRC5-SV cells co-transfected with Cherry-ATIP3 (red) and EB3-GFP (green). Inset.

Cherry-ATIP3 (red) and EB3-GFP (green) MRC5-SV-coexpressing cells were imaged by spinning disk confocal microscopy as for movies 1 and 2. A zone of 1900 μm^2 at the cell periphery is shown.

Movies 5 and 6. Time-lapse microscopy of MCF-7 cells stably expressing moderate levels of GFP-ATIP3.

Stably transfected GFP-ATIP3 cells were analyzed by time-lapse TIRF microscopy (100X lens). Time-lapse series of 500 images were acquired in a stream mode and shown at 30 frames per second.

Expanded View Table E2. Oligonucleotides used for PCR-amplification of ATIP3 domains (A) and site-directed mutagenesis (B).

Expanded View Table E2.A

Name	Primers (5' → 3')	Number	Size (bp)
D2	F : CCGCTCGAGGA CTGACTTGGGATGCAAATGAT R : CGGGGTACCTCATGCATTAAGAGCTGTAAATAA	C 206 C 208	1395
D2N	F : CCG CTCGAGGACTGACTTGGGATGCAAATGAT R : CGGGGTACCTCAAAACAACGCAGAAACGGACCCGGT	C 206 C 304	675
D2C	F : CCGCTCGAGCAACCACCTCAGGTAGGAATATATCC R : CGGGGTACCTCATGCATTAAGAGCTGTAAATAA	C 306 C 208	510
CN	F : CCGCTCGAGCAACCACCTCAGGTAGGAATATATCC R : CGGCGGGGTACCTCAATTGTTGCTGTAAGTGCTCAGCTC	C 746 C 791	336
CC	F : GGCCCGCTCGAGGATCTGGTAATGCCGCTGTCATC R : CGGGGTACCTCATGCATTAAGAGCTGTAAATAA	C 793 C 208	174
CN67	F : GCCCCGCTCGAGGAAGAAATCCCAGTGCTGATCGAGCC R : CGGCGGGGTACCTCACTCACTGTGGGTGCTGGCTATTGA	C 987 C 988	201
CN45	F : GGCCCGCTCGAGGAAGGATCAGGCGTGTGTCCAG R : CGGCGGGGTACCTCAGCTTCCTGTCCTCCGCAGCGC	C 1022 C 1023	135

F : Forward ; R : Reverse

Expanded View Table E2.B

Name	Primers (5' → 3')	Number	Size (bp)
CN67 delP	F : GCACAGTCGTCATGGGTGAATAAATCCAAAGCATCTTTG R : CAAAGATGCTTTGGATTTATTCACCCATGACGACTGTGC	C 1030 C 1031	183
ATIP3 delCN	F : GGGCTCTGCTTCAAAAACAACGTCTGGTAATGCCGCTGTC R : GACAGCGGCATTACCAGACGTTGTTTTTGAAGCAGAGCCC	C 928 C 929	3474
ATIP3 delCC1	F : AGCTGAGCACTTACAGCAACAATGGTCCTTCGAGA R : TCTCGAAGGACCATTGTTGCTGTAAGTGCTCAGCT	C 724 C 725	3654
ATIP3 delCC2	F : GATGAAAACTCCTCCAAAAGTTGAAAAGAGCAGGCAAAAG R : CTTTTGCCTGCTCTTTTCAACTTTTGGAGGAGTTTTCATC	C 91 C 92	3789
ATIP3 delCTer	F : CCGCTCGAGCCATGACTGATGATAATTCAGATG R : CGGGGTACCTCAACACAGGTCCCCATTGTGCAG	C 70 C 209	3721
D2 delCN	F : GGGCTCTGCTTCAAAAACAACGTCTGGTAATGCCGCTGTC R : GACAGCGGCATTACCAGACGTTGTTTTTGAAGCAGAGCCC	C 928 C 929	1059
D2 delCC1	F : AGCTGAGCACTTACAGCAACAATGGTCCTTCGAGA R : TCTCGAAGGACCATTGTTGCTGTAAGTGCTCAGCT	C 724 C 725	1239

F : Forward ; R : Reverse

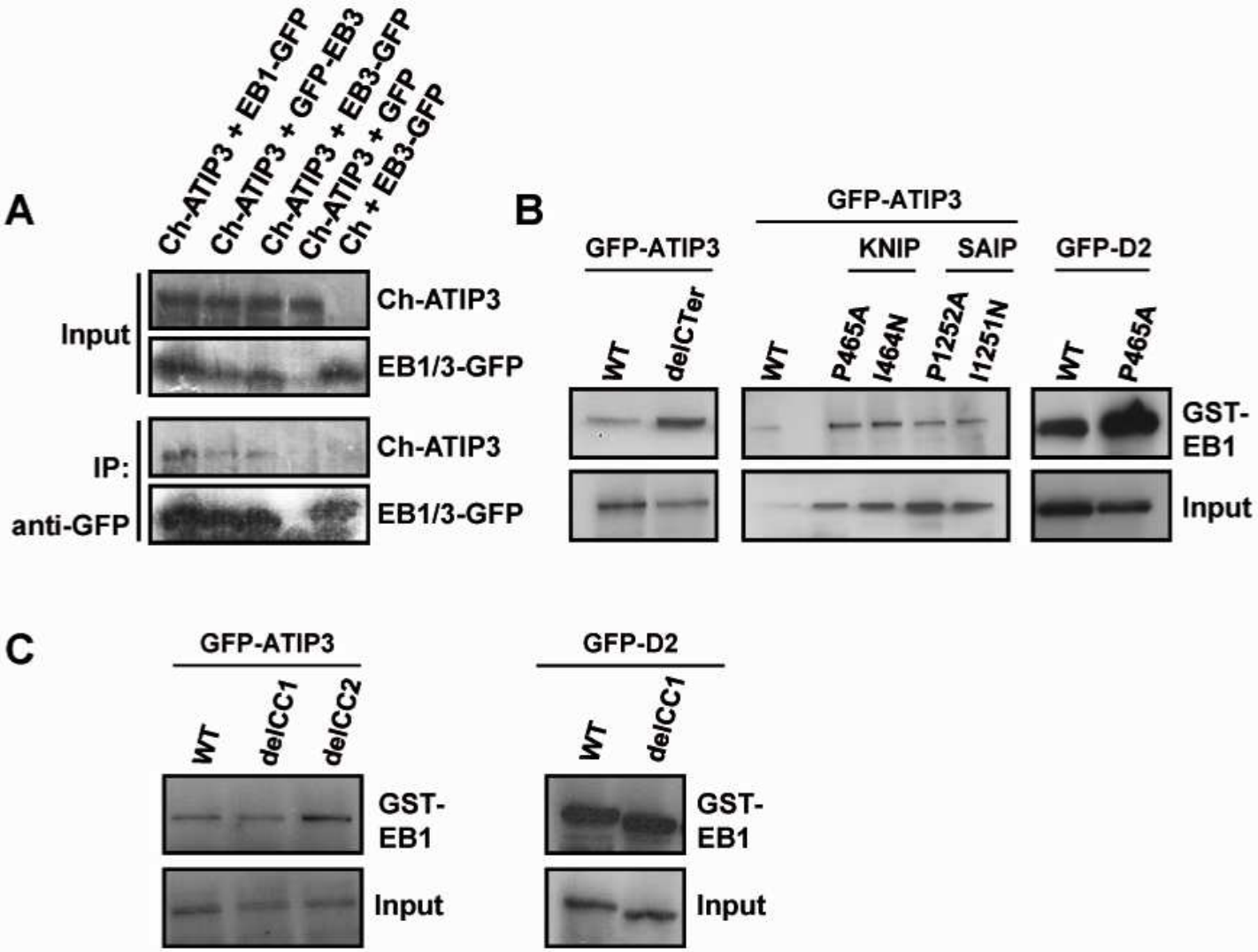

Velot, Molina et al., Expanded View Fig.E1

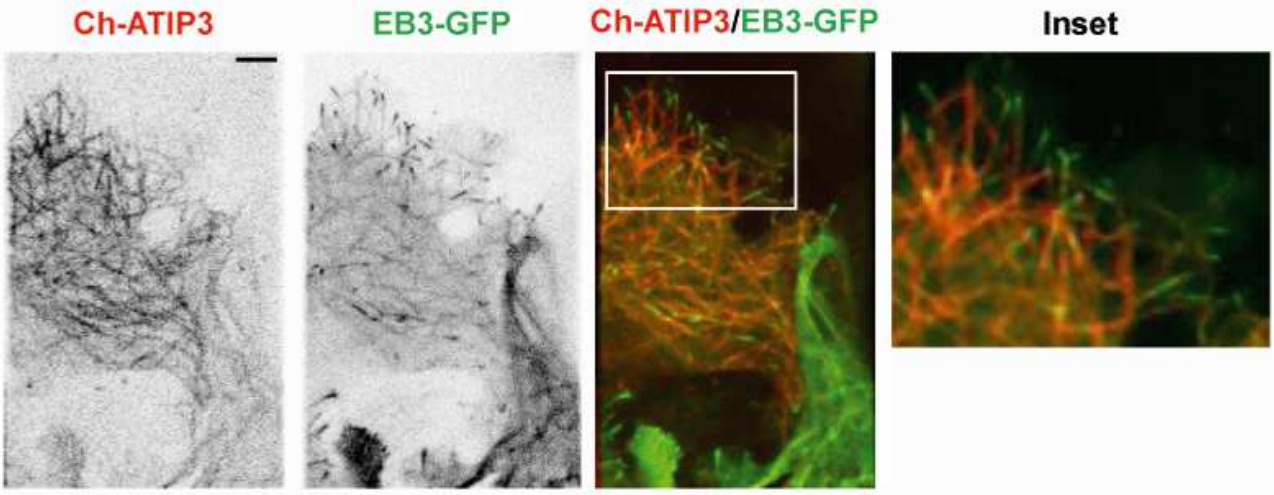

Velot, Molina et al., Expanded View Fig.E2

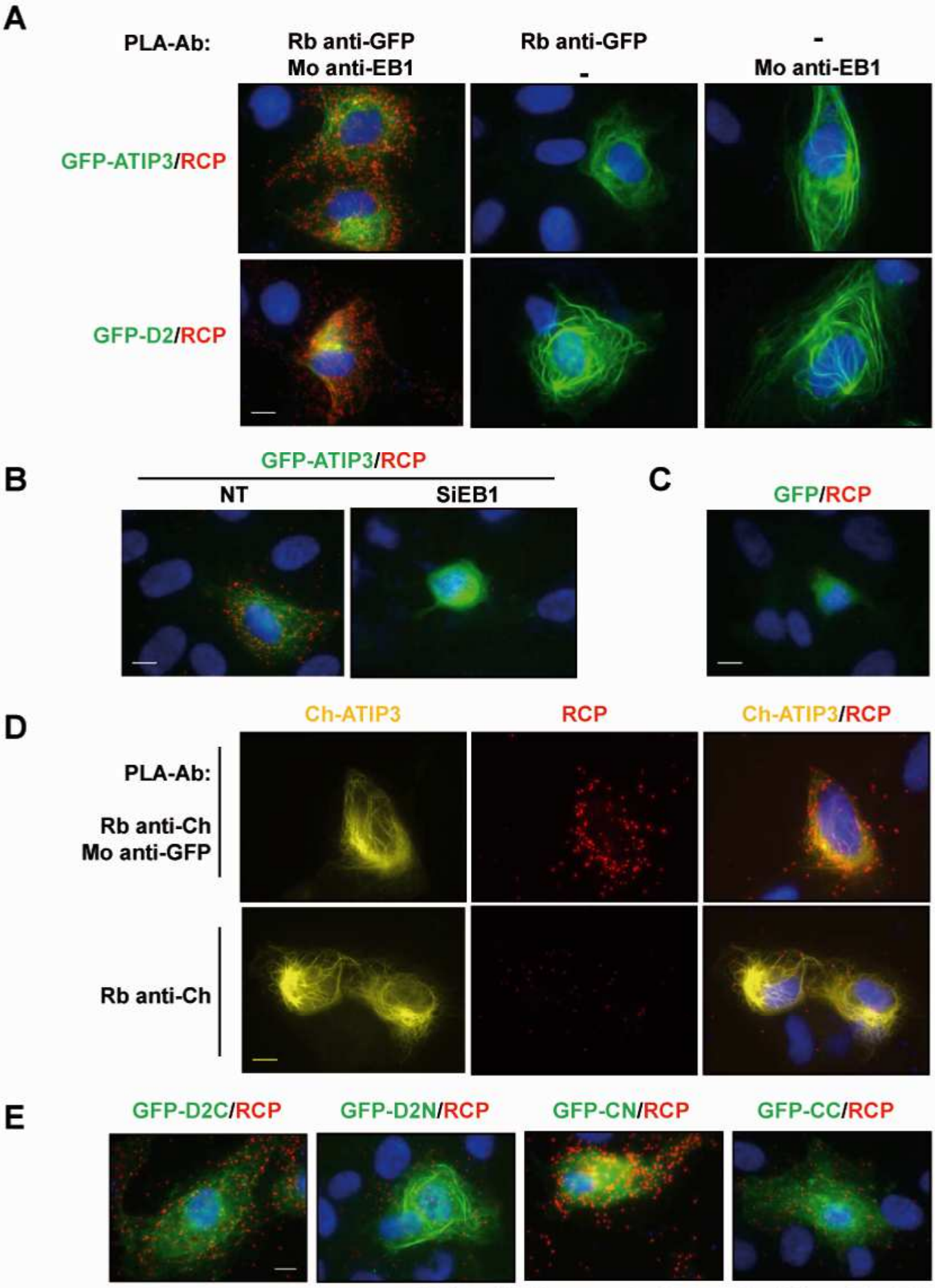

Velot, Molina et al., Expanded View Fig.E3

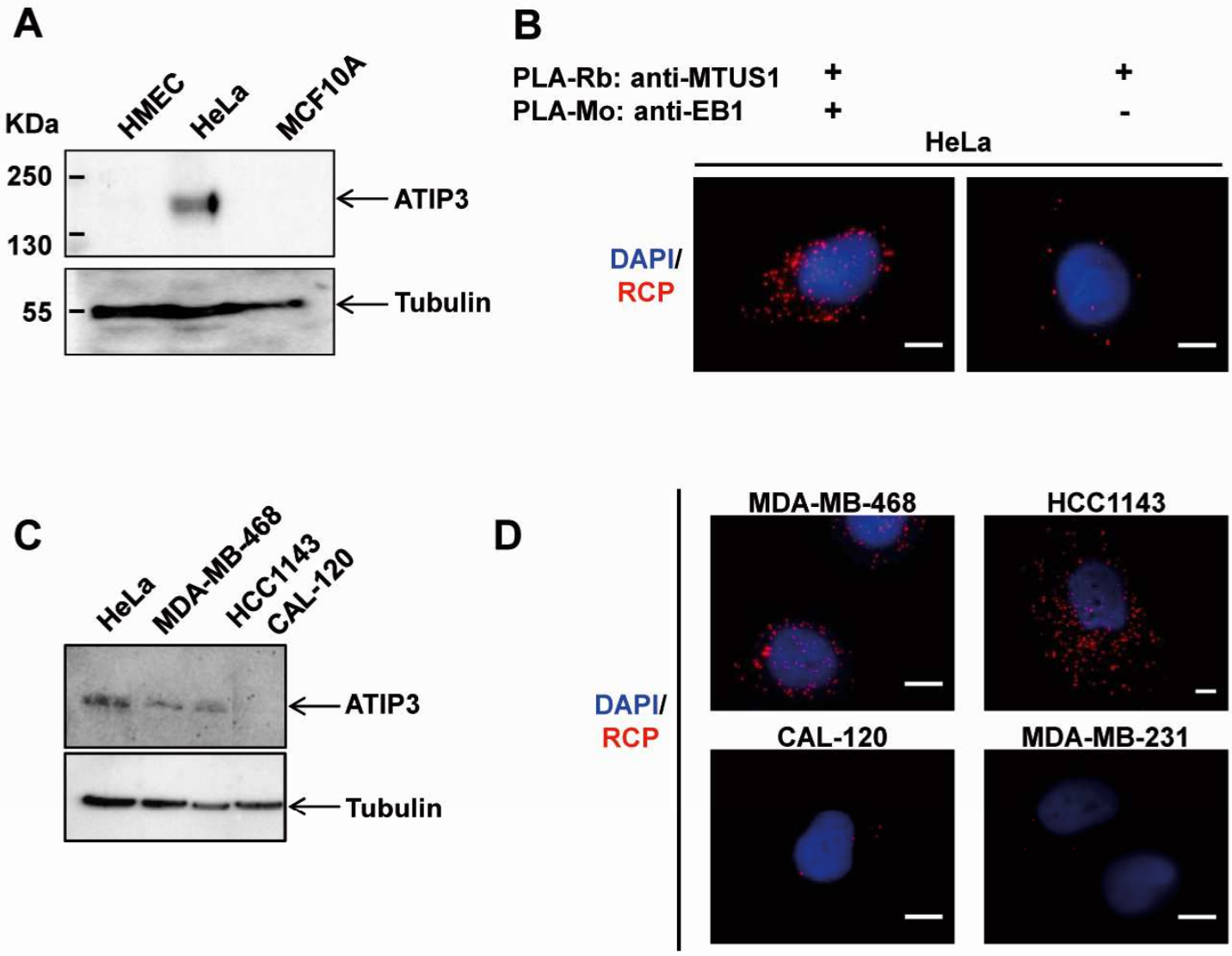

Velot, Molina et al., Expanded View Fig.E4

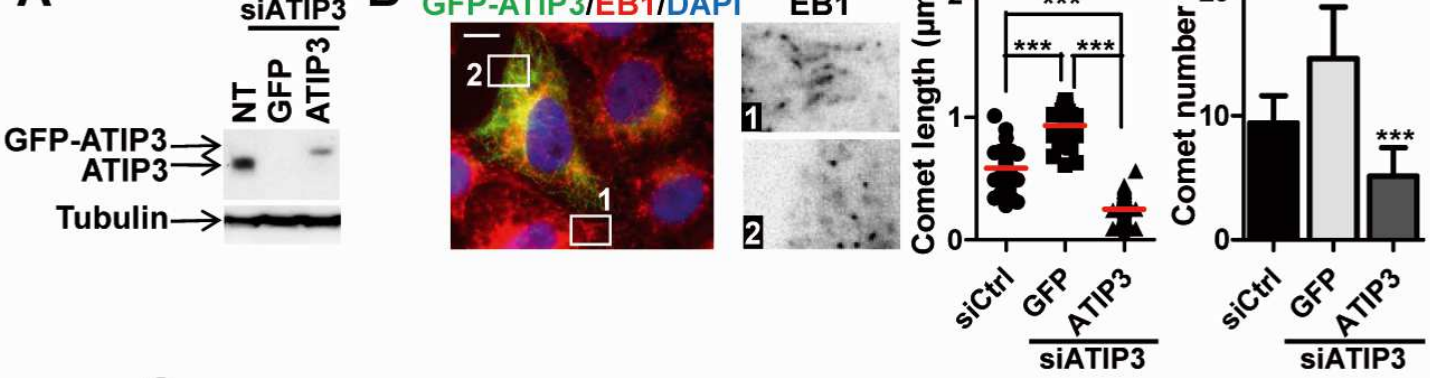

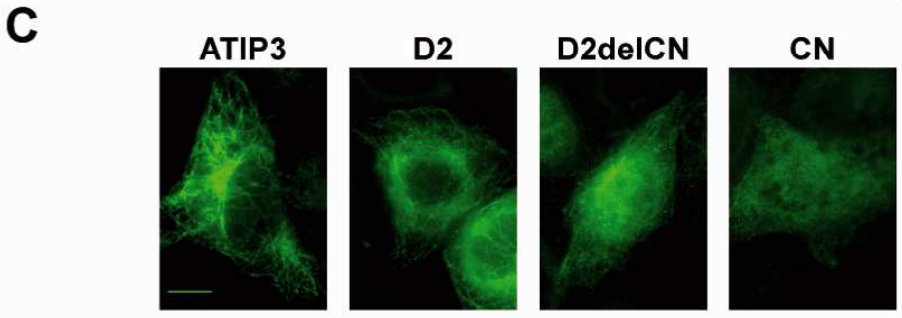

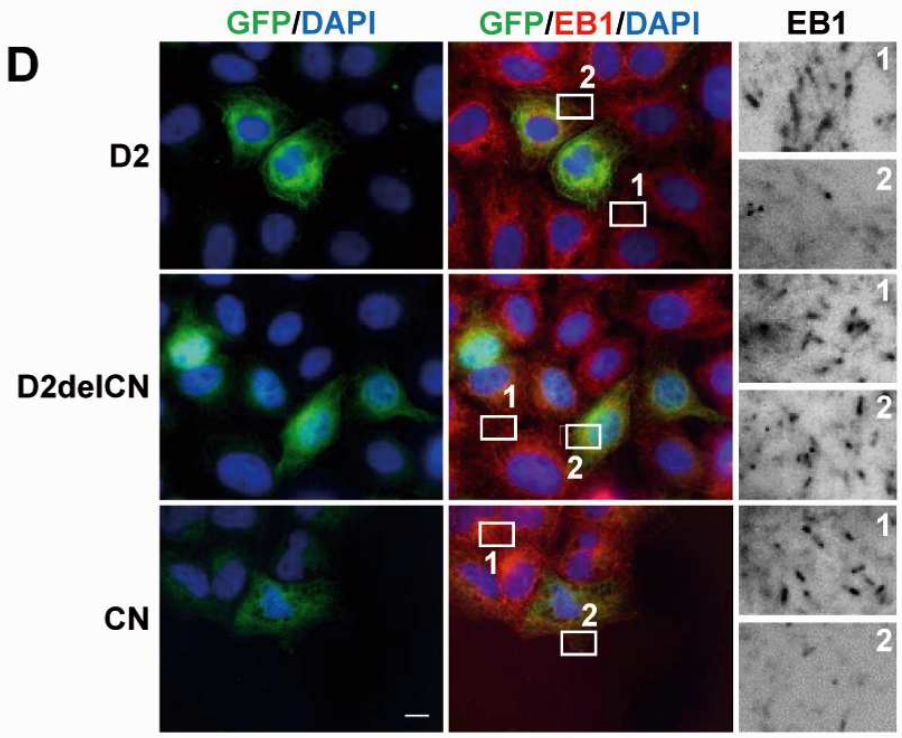

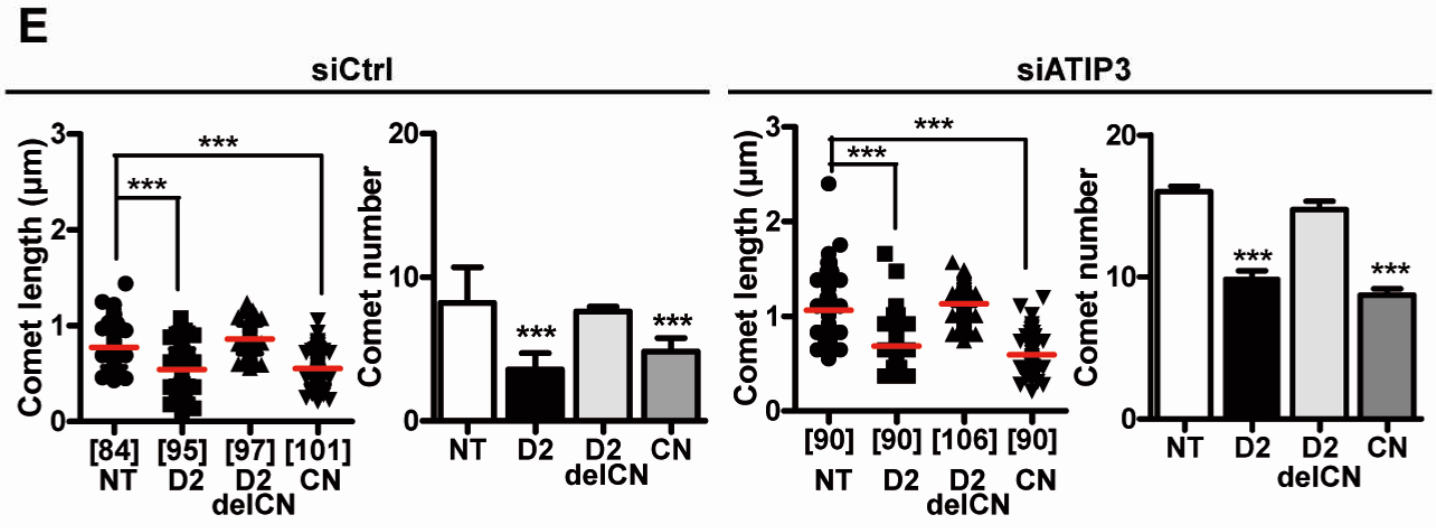

Velot, Molina et al., Expanded View Fig.E5

Unpublished Results

1. New ATIP3 interacting partners

1.1. ATIP3 interacts with MCAK and regulates its localization at the MT plus-ends

As mentioned in the introduction, microtubules are highly dynamic structures whose regulation depends (at least in large part) on the plus-end tracking proteins (+TIPs). A potent MT destabilizer is the EB1-interacting protein MCAK. MCAK (Mitotic Centromere-Associated Kinesin) is a MT plus-end tracking kinesin able to change MT plus-end structure to induce its depolymerization.

Our previous results have shown that ATIP3 regulates MT dynamic instability possibly by its interaction with EB1. However, whether ATIP3 participates in a complex with other MT regulators is an unknown question. Of note, the ATIP3 paralog TIP150, which also interacts with EB1, is able to associate with MCAK to form a complex (together with EB1) that will accumulate at the MT plus-ends (Jiang K *et al*. 2009). Additionally, the ATIP3 *Xenopus* ortholog ICIS also associates with MCAK to stimulate its MT-destabilizing activity (Ohi R *et al*. 2003). Given this information we hypothesized that ATIP3 could interact with MCAK to regulate MT dynamics.

In order to define whether ATIP3 interacts with MCAK, co-immunoprecipitation assays were performed in ATIP3-deficient MCF7 cells co-transfected with Myc-MCAK (Unpublished Figure 1A) and full-length ATIP3. As shown in Unpublished Figure 1B, GFP-ATIP3 and positive control EB1-GFP, and not GFP, are able to co-precipitate with Myc-MCAK (lines 1, 2 and 3). To get further insight into the ATIP3-MCAK interaction, ATIP3 deletion mutants were also tested for an interaction with MCAK. Interestingly, EB1-interacting domains of ATIP3 (D2, D2C, D2CN) interact with the kinesin (Unpublished Figure 1B lines 4, 5 and 6). This indicates that ATIP3 interacts with MCAK via the CN domain, which is the same domain of interaction with EB1.

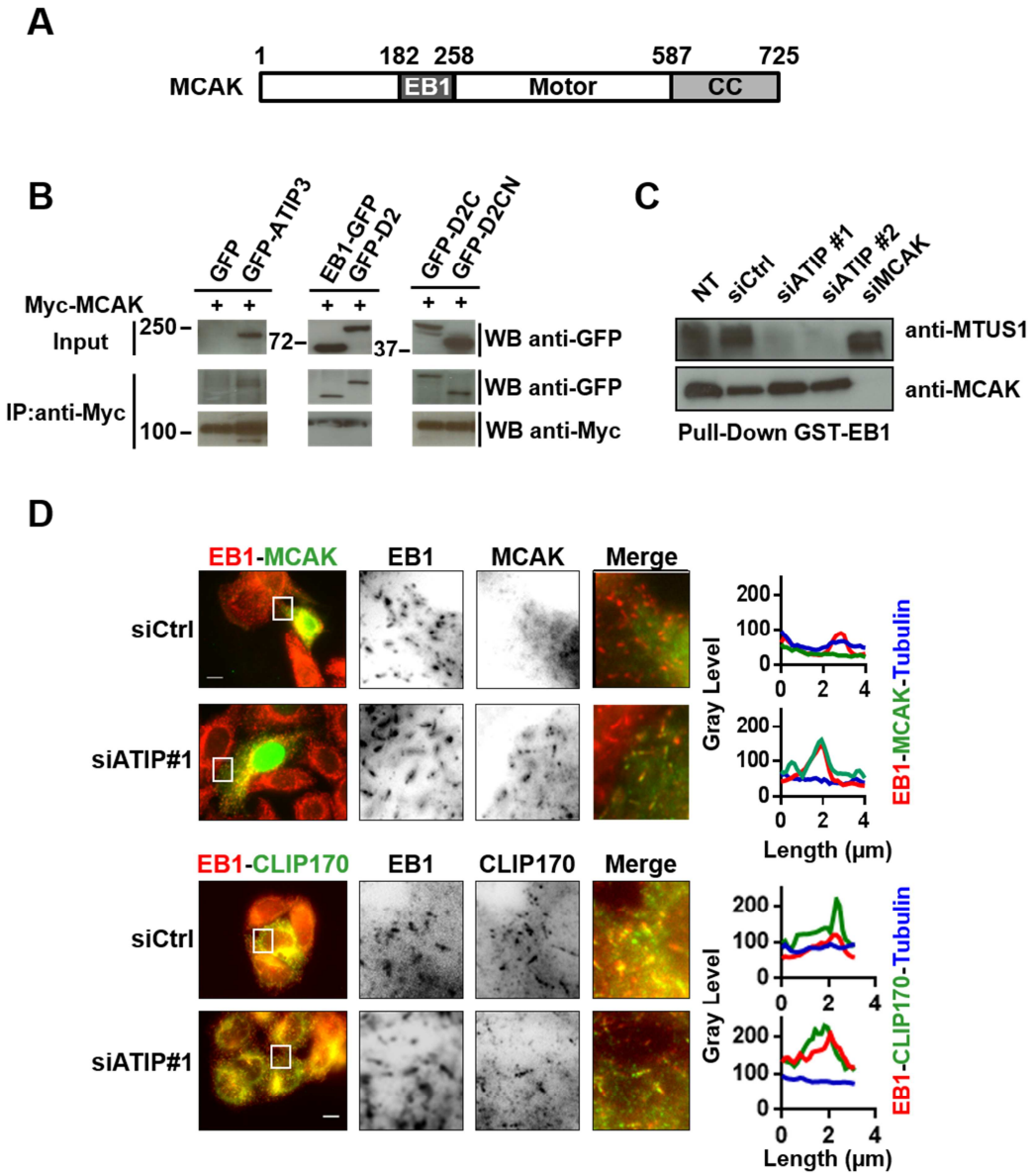

Unpublished Figure 1. ATIP3 interacts with MCAK. **(A)** Schematic representation of MCAK protein. EB1 domain (dark gray) contains the EB1 binding site; CC domain (gray) the coiled-coil motifs. Amino acids are shown on the top. **(B)** Co-immunoprecipitation of Myc-MCAK and GFP, EB1-GFP or GFP-ATIP3 indicated constructs (GFP-ATIP3, GFP-D2, GFP-D2C or GFP-D2CN) transfected in MCF7 cells, using anti-Myc antibodies. Western blots were probed with anti-GFP and anti-Myc antibodies as indicated on the right. Molecular weights are indicated in KDa on the left. **(C)** GST pull-down analysis in HeLa cells non-transfected or transfected with control siRNA (siCtrl), ATIP3-specific siRNA (siATIP #1 and siATIP #2) or MCAK-specific siRNA (siMCAK) as indicated, using GST-EB1 agarose beads. Blots were probed with anti-ATIP (MTUS1) and anti-MCAK antibodies. **(D)** Immunostaining (anti-EB1, anti-GFP antibodies) of siRNA-silenced HeLa cells transfected with GFP-MCAK or GFP-CLIP170. Insets: EB1, MCAK and CLIP170 comet-like structures in ATIP3-positive (siCtrl) and ATIP3-negative (siATIP#1) cells. Distribution of EB1 (red), α-tubulin (blue) and GFP-MCAK or GFP-CLIP170 (green) at the MT plus-end (linescan) is shown. Scale Bar, 10 µm.

Given that ATIP3 interacts with MCAK and EB1 through the CN domain, and that ATIP3 and MCAK interact with the C-terminal portion of EB1, two possibilities can be extracted from the results concerning the interaction domains. Either, ATIP3, EB1 and MCAK are in the same macromolecular complex and cooperate to maintain the interaction or conversely ATIP3-EB1, MCAK-EB1 and ATIP3-MCAK interactions are independent and compete for the interaction with each other. In order to test a possible competition between these proteins, ATIP3-depleted or MCAK-depleted HeLa cells lysates were incubated with GST-EB1 and pull-down experiments were performed. Unpublished Figure 1C shows that silencing of ATIP3 does not alter the interaction of MCAK with EB1; as well as MCAK silencing does not change ATIP3 interaction with EB1. Thus, neither ATIP3 nor MCAK compete to interact with EB1.

Previous results indicate that ATIP3 interacts with EB1 and delocalize it from the MT growing ends. As ATIP3 also interacts with MCAK, the localization of this +TIP was then evaluated by immunofluorescence imaging. HeLa cells co-transfected with control or ATIP3-specific siRNAs and GFP-MCAK were then stained with anti-GFP and anti-EB1 antibodies. Unpublished Figure 1D (top panels) revealed that MCAK does not accumulate at the plus-ends and rather it stays diffuse in the cytosol when ATIP3 is expressed. Conversely, in ATIP3-silenced cells, MCAK comet-like structures were detected, as wells as EB1's. These results suggest that ATIP3 impairs EB1 and EB1-interacting proteins accumulation at the MT growing end. To test this hypothesis, HeLa cells co-transfected with siRNAs (control or ATIP3-specific) and GFP-CLIP170 were stained with anti-GFP and anti-EB1 antibodies (as for MCAK experiment). Interestingly, unlike EB1 and MCAK, CLIP170 accumulates at the plus-end, in a comet-like fashion, independently of ATIP3 expression (Unpublished Figure 1D, lower panels). Of note, CLIP170 binds EB1 via a CAP-Gly domain and not via an SxIP motif as MCAK.

All these data provide evidence that ATIP3 interacts with MCAK via the CN domain. However, the elucidation of a macromolecular complex would be necessary to explain if the delocalization effect seen for EB1 and MCAK is specific to these proteins or if it is rather a consequence of EB1 delocalization.

1.2. ATIP3 interacts with APC

The importance of stable MTs for cell migration was shown for the first time by Wen Y *et al*. (2004). In this study, they demonstrated that EB1 and APC worked as a capture complex to stabilize MT ends near the cell cortex.

Given that ATIP3 is a stabilizing MAP, that its expression is related to a higher content of acetylated (stable) MTs and a reduction of cell migration, we sought to investigate if the effects of ATIP3 were due to a possible complex with APC and EB1, as demonstrated for mDia. Thus, to examine if ATIP3 interacts with APC, pull-down experiments were performed using GST-APC deletion mutants comprising either the MT and EB1 binding domains (APC-EZ), the MT binding domain (APC-basic) or the EB1 binding domain (APC-C) (Unpublished Figure 2A). These three fusion proteins were incubated with GFP, GFP-ATIP3 or GFP-D2 transfected MCF7 cell lysates and GST-pull-down experiments were analyzed by western blot.

As shown in Unpublished Figure 2B, ATIP3 strongly interacts with APC-EZ and weakly with APC-C and APC-basic. Similarly, the central D2 domain of ATIP3 was able to interact both with APC-EZ and APC-C, and with less affinity to APC-basic.

Altogether, these results indicate that ATIP3 interacts with APC via its central domain D2, which is the functional domain of ATIP3, also involved in EB1 interaction.

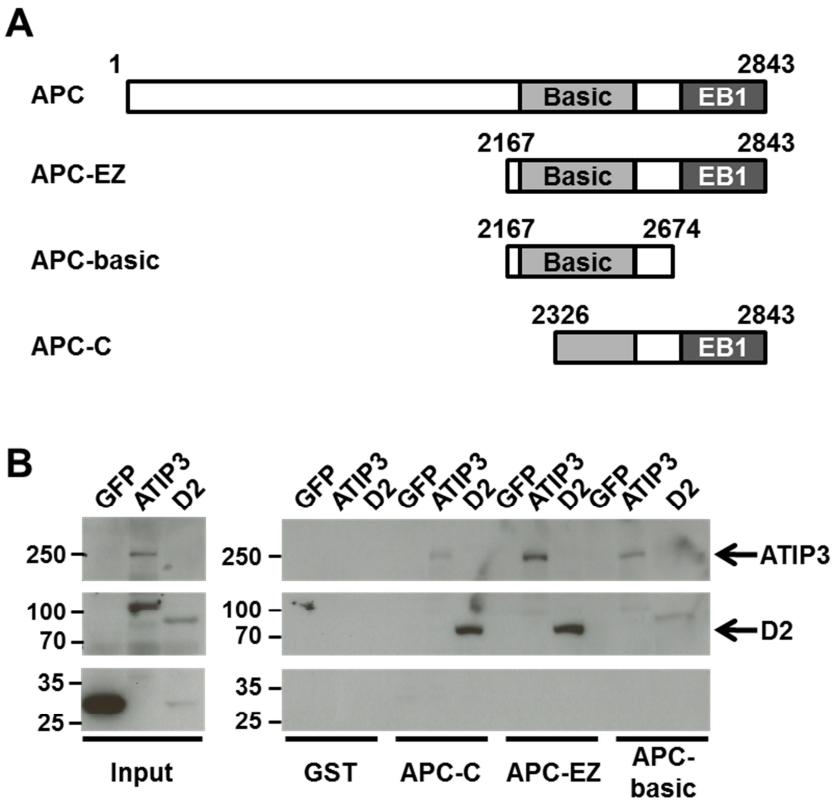

Unpublished Figure 2. ATIP3 interacts with APC. **(A)** Schematic representation of APC proteins and deletion mutants APC-EZ, APC-basic and APC-C. Basic domain (gray) contains the MT binding region; EB1 domain (dark gray) EB1 binding site. **(B)** Pull-down analysis of GFP, GFP-ATIP3 and GFP-D2 using GST, GST-APC-C, GST-APC-EZ or GST-APC-basic agarose beads. Blots were probed with anti-GFP antibodies. Molecular weights are indicated in KDa on the left.

2. ATIP3 role in ciliogenesis

Given that ATIP3 associates with MTs and regulates its dynamics, an interesting question that must be addressed is, does ATIP3 has a role in the assembly or in the function of MT-based structures, such as the primary cilium?

The primary cilium is an antenna-like structure (composed by stable MTs) which is anchored to the cell by the basal body (which develops from a centriole) in a manner that is regulated within the cell cycle. This structure works as a sensory organelle which receives signals from the environment and transmits them to the nucleus. Few studies have investigated the involvement of primary cilia in cancer cells, but most of them have associated a decrease in the incidence of primary cilia with multiples types of cancer (Yuan K *et al*. 2010). Recently, Emoto K and coworkers (2014) showed that primary cilia can be detected in human pancreatic cell lines and in cancer cells of pancreatic ductal carcinoma patients. Interestingly, they correlated the presence of the primary cilia with a higher frequency of lymph node metastasis and decreased overall survival, considering the presence of primary cilia as a prognostic indicator.

As ATIP3 stabilizes MTs, we hypothesize that it will decorate the primary cilium, as VHL protein. RPE1 cells, which are a suitable model for ciliogenesis, were growth until confluence before transfection with GFP, GFP-ATIP3 and GFP-D2 constructs. Immunostaining with anti-acetylated tubulin, anti-EB1 and anti-GFP was performed. Wide field images revealed that in ATIP3- and D2-expressing cells the incidence of primary cilia was markedly reduced (Unpublished Figure 3). Same results were obtained by staining another component of the cilium, the GTPase Arl13B, suggesting that ATIP3 could regulate the ciliogenesis.

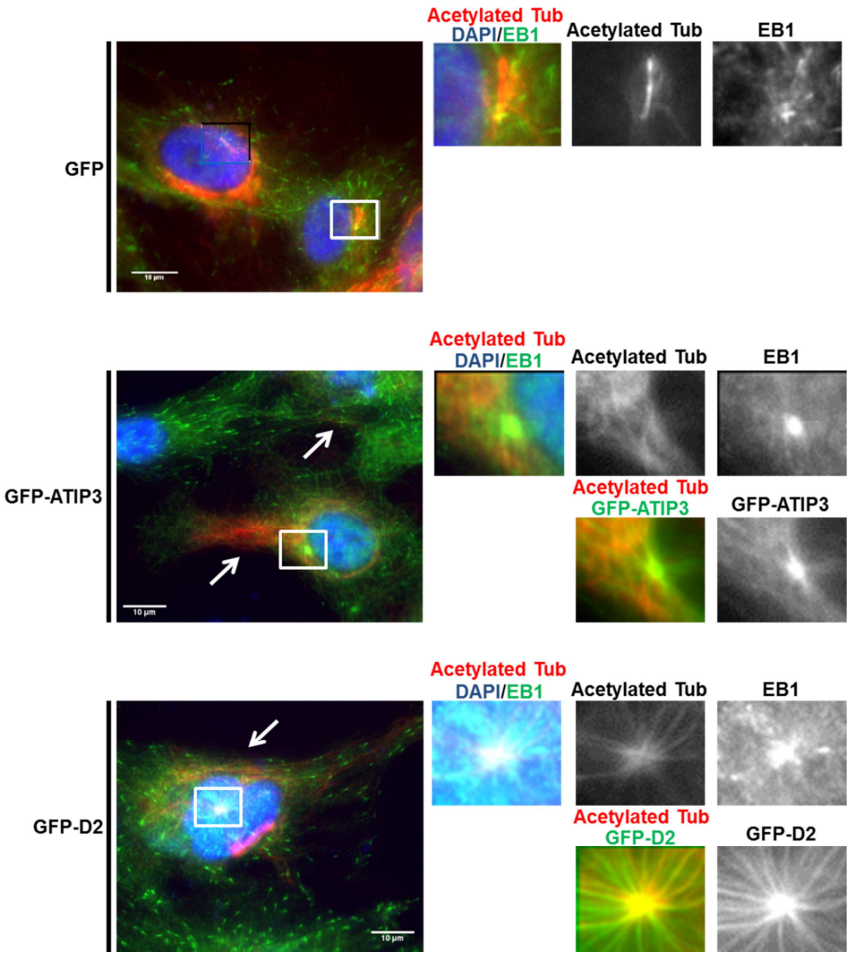

Unpublished Figure 3. ATIP3 impairs primary cilia formation. Immunostaining (anti-acetylated tubulin, anti-EB1 and anti-GFP) of RPE1 cells transiently transfected with GFP, GFP-ATIP3 and GFP-D2. Upper insets, merge, acetylated tubulin and EB1; lower insets, merge (acetylated tubulin and GFP) and GFP images near the basal body. Arrows indicate GFP-ATIP3 and GFP-D2 transfected cells. Scale bar, 10µm.

Whether ATIP3 inhibits or delays ciliogenesis from the basal body, as well it decreases MT regrowth from the centrosome, should be investigated. For this aim, a cell model capable to assemble cilia and which expresses ATIP3 should be used and transfected with control and ATIP3-specific siRNA in order to quantify and compare the number of ciliated cells and the size of the cilia in ATIP3-expressing and depleted cells.

3. *MTUS1* gene mutations in breast cancer

Previous mutational analysis of *MTUS1* performed in the laboratory, in a series of 30 primary breast carcinoma and 10 breast carcinoma cell lines, identified five non-conservative nucleotide alterations. Amino acid replacements were located on positions T186S, M418R, P503R, K644Q and R1003Q. Of note, variations T186S, M418R, P503R, K644Q reside in exon 1 and consequently are specific for ATIP3. More precisely, M418R, P503R, K644Q are located in D2 (Colasson H and Kheddache S, unpublished results). Transfections of GFP-ATIP3 constructs carrying these alterations were performed in RPE1 and D3H2LN cells in order to analyze EB1 accumulation and wound healing time-lapse images, respectively. As shown in Unpublished Table 1, ATIP3-mutations did not differ from the wild-type protein in both EB1 accumulation, and migration directionality.

Unpublished Table 1. Characterization of ATIP amino acid sequence variations.

Domain	MT localization	Loss of EB1 comets	Directionality coefficient*
ATIP3	+	+	0.39
T186S	+	+	0.49
M418R	+	+	0.51
P503R	+	+	0.55
K644Q	+	+	0.49
R1003Q	+	+	0.60

* GFP transfected cells had a coefficient of directionality of 0.85

These results, along with previous data showing that ATIP3 mutations did not alter MT-association and co-sedimentation, neither the ability to inhibit cell proliferation (Colasson H, unpublished results) nor the capacity to interact with EB1 (Velot L, unpublished results), suggest that the five alterations may be passenger mutations that are not essential for tumoral development. Interestingly, a mutational analysis of *MTUS1* gene in hepatocellular carcinoma identified five different nucleotide alterations, of which four are located in ATIP3 exons (Di Benedetto M *et al*. 2006b). However, no functional experiments were performed to verify the importance of these mutations on cancer progression.

Further *in vitro* experiments, as MT dynamics measurements, as well as an extensive mutational DNA analysis using different patient cohorts or data bases as the TCGA (the cancer genome atlas) would be of relevance to investigate the presence of driver mutations implicated in the carcinogenesis process that would confirmed the tumor suppressor function of ATIP3.

III. CONCLUSIONS

Based on previous data from the laboratory showing ATIP3 as a novel Microtubule-Associated Protein (MAP) which is down-regulated in invasive and metastatic breast tumors, and with inhibitory effects on breast cancer cell proliferation *in vitro* and tumor growth *in vivo*, one of the goals of this thesis was to elucidate whether ATIP3 was involved in breast cancer metastasis and if, besides tumor cell proliferation, this tumor suppressor was also impairing some other steps of the metastatic process such as invasion, migration, extravasation and colonization.

Using three independent patient cohorts it was possible to demonstrate that ATIP3 is a prognostic marker for survival of the patients with breast cancer. Furthermore, we showed that ATIP3 may be an indicator of metastatic progression and high risk of fatal complication because its low expression correlates with reduced overall survival of patients with metastatic disease.

The role of ATIP3 on breast cancer metastasis was then evaluated by means of a bioluminescence-based experimental mouse model for cancer metastasis. Results show that restoration of ATIP3 in highly invasive D3H2LN breast tumor cells decreases the metastatic colonization (time course and the number and size of metastatic foci). Analysis of the different steps of the metastatic process indicate that ATIP3 reduces cell migration and transendothelial migration (extravasation), and increases adhesion to endothelial cells and to collagen. Analysis of GFP and GFP-ATIP3 migrating stable clones show that the tumor suppressor reduces cell velocity and cell directionality during wound-induced migration. These data indicate that ATIP3 limits early (growth) and late (dissemination) phases of metastasis development.

As cell migration is a process that somewhat depends on microtubule (MT) network and MT dynamics, a second objective of this work was to determine whether ATIP3 may be able to modulate MT dynamics, as described for almost all MAPs. Different experimental data let to the conclusion that ATIP3 is a stabilizing MAP that increases the acetylation content of interphase MTs, preventing MT depolymerization induced by cold or nocodazole treatment and reducing MT regrowth after nocodazole washout. Moreover, time-lapse analysis of EB1-GFP showed that loss of ATIP3 increases MT dynamic instability by increasing MT growth rate and MT growth episodes and decreasing MT time spent in pause and MT catastrophe frequency.

The asymmetric distribution of stable microtubules is suggested to be amongst the initial events that occur in response to migration signals. The effect of ATIP3 on MT dynamic instability parameters leads to a marked reduction of polarized MTs. Thus, in ATIP3-deficient cells MTs near the cell cortex were radially organized with their plus-ends anchoring at the cell margin, while in ATIP3-expressing cells MT plus-ends do not reach

the cell edge, due to MTs bending before reaching the cell cortex. Furthermore, analysis of acetylated tubulin (marker of stable MT) indicated that ATIP3 induces a global stabilization of MTs that will result in the absence of cell polarization.

ATIP3 can be divided in three regions according to the isoelectric point of each of these parts: D1, the N-terminal part of the protein is characterized by its acidic behavior; D2, the central domain of the protein is rich in basic residues; and D3, the C-terminal region, has a neutral charge and is involved in protein dimerization due to the presence of four coiled-coil domains. Experiments conducted in order to identify the functional domain of the full-length protein revealed that D2, and not D1 or D3, was able to co-sediment with tubulin and to localize with MTs after immunofluorescence staining. Besides binding to MTs, clonogenicity experiments and wound-healing tests confirmed D2 as the functional domain of ATIP3. D2 reduces cell proliferation *in vitro* and impairs directionality during migration, just like ATIP3. This indicates that the central part of the protein (D2) contains the MT binding domain and the functional properties of full-length ATIP3.

Microtubule dynamics are accurately regulated by MAPs. EB1, the core of +TIPs functions, has an important role in MT dynamics. Immunostaining images of mCherry-ATIP3 indicated a reduction of EB1 localization at the MT growing end, that is restored once ATIP3 is not expressed. The aim of this part of my thesis was to investigate if ATIP3 interacts with EB1 to impair its localization at the plus-ends.

Sequence analysis of the ATIP3 polypeptide reveals three possible EB1 interacting motifs: one SxIP (SAIP) located in the C-terminal region of the protein and two SxIP-like (KNIP and RPLP) located in the central domain D2. By means of GST pull-down and co-immunoprecipitation, we showed that ATIP3 interacts with EB1. Detailed analysis of EB1 interaction domains of ATIP3 show that only the RPLP (located in a region termed CN) directly interacts with the C-terminal domain of EB1.

A large number of studies have shown that SxIP-containing proteins accumulate at the MT growing end together with EB1. In spite of evidence suggesting that ATIP3 may be a new plus-end tracking protein via EB1 interaction, immunostaining and time-lapse imaging of ATIP3 and EB1 demonstrate that ATIP3 does not accumulate at the growing end of the MTs. ATIP3 rather remains attached to the MT lattice and surprisingly, tracks shrinking MT ends.

By means of Proximity Ligation Assay (PLA) experiments using endogenous ATIP3 and EB1 antibodies, the *in situ* interaction between these two proteins was revealed: they mostly interact in the cytosol. Interestingly, some complexes were also detected along the MT lattice. This last localization is coherent with immunofluorescence images showing a

reduction at plus-end but a partial MT lattice localization of EB1 in ATIP3-expressing cells. Subsequent experiments, indicated that that impaired accumulation of EB1 at the MT growing end was correlated with the presence of the EB1-interacting domain (CN) and was independent of the association with MTs. Together these results indicate that ATIP3 interacts with EB1 and that it may retain EB1 at the cytosol and MT lattice, decreasing the free available cytosolic pool of EB1 that can accumulate at the plus-ends.

Clinical relevance of this interaction was then evaluated by the analysis of *MTUS1* (ATIP3 gene) and *MAPRE1* (EB1 gene) expression levels in a cohort of 150 breast cancer patients, followed by the comparison with clinicopathologic data. Results showed that relative expression levels of both proteins in breast tumors are related with patient clinical outcome. Indeed, among tumors with low levels of ATIP3 and high levels of EB1 a reduced overall survival of patients was found. Inversely, a better clinical outcome resulted from tumors with low levels of EB1 and high or very high ATIP3 expression levels. These last results highlight the importance of coordinated ATIP3 and EB1 expression levels in breast cancer progression and clinical outcome.

IV. DISCUSSION AND FUTURE DIRECTIONS

Major achievements in this work include the identification of ATIP3 as a new biomarker of metastasis in breast cancer patients and a regulator of MT dynamics which reduces MT dynamic instability. Although a remarkable progress has been done in understanding ATIP3's effects in essential cellular functions, there is still much more to explore.

1. ATIP3 decreases MT dynamic instability

Evidence that ATIP3 reduces EB1 accumulation at the MT growing ends was provided in this work. EB1 reduction at the plus-end has been usually recognized as a hallmark of MT dynamics reduction. However, future TIRF time-lapse videomicroscopy experiments using mCherry-tubulin stable clones transfected with low levels of GFP-ATIP3 (or GFP-D2) and GFP-ATIP3delCN (or GFP-D2delCN), which does not interact with EB1, should be performed to measure dynamic instability parameters that would elucidate the importance of EB1-ATIP3 interaction in MT dynamics.

How does ATIP3 reduce EB1 accumulation at the MT plus-ends? Reduction may be due to (i) EB1 degradation, (ii) post-translational modifications of EB1 that reduces its affinity for the plus ends, (iii) reduction of the free available cytoplasmic EB1, (iv) induction of a conformational change of the MT dynamic end and (v) suppression of the MT growing events.

To date our data have excluded the hypothesis of EB1 degradation induced by ATIP3. Additionally, a conformational change of the MT growing ends by ATIP3 is very unlikely given that association with MTs is independent to the reduction of EB1 accumulation (concerns different protein binding domains). However it should be interesting to evaluate if ATIP3 expression or depletion causes a change in the tubulin-GTP cap (using for example anti-GTP-tubulin antibodies (Dimitrov A *et al*. 2008) or electronic microscopy images of the MT plus-ends).

Thus, EB1 post-translational modifications and cytosolic EB1 retention are the most probable hypotheses that may explain EB1 reduction at the MT growing ends by ATIP3. Recently, Rovini A and coworkers suggested that alteration of the C-terminal tyrosine of EB1 may affect its accumulation at the growing ends, as well as its functions in MT dynamic regulation (Rovini A *et al*. 2013). Additionally, they demonstrated that migration was increased in cells containing detyrosinated EB1, suggesting a potential role of EB1 detyrosination in cancer progression. EB1 tyrosination/detyrosination cycle will be evaluated using anti-tyrosinated and anti-detyrosinated EB1 antibodies (Bosson A *et al*. 2012).

Even if it has not been demonstrated that acetylation of EB1 reduces its accumulation at the plus-ends, evaluation of this post-translational modification would be interesting in ATIP3-depleted cells given that persistent acetylation of EB1 perturbs chromosome alignment in metaphase (Xia P *et al*. 2012).

An alternative option is the possible retention of EB1 by ATIP3. Considering that a diffusible cytosolic pool of EB1 is necessary to allow the dynamic accumulation at the growing end (Dragestein KA *et al*. 2008), ATIP3 interaction with EB1 may limit its dynamic turnover and thus, a reduction of EB1 at the growing end would be observed. In 2003 Tortosa E and coworkers proposed a model for the classical MAP MAP1B. They showed that MAP1B directly interacted with EB3 in the cytosol, reducing its accumulation at the MT plus-ends and consequently regulating MT dynamics. In line with this model and due to the direct interaction of ATIP3 with EB1, one might think that ATIP3 would retain EB1, decreasing the free available pool that can accumulate at the plus-ends. Thus, in ATIP3-deficient cells, more EB1 would accumulate at the growing end, therefore increasing MT dynamics, +TIPs interactions, and consequently cell proliferation and cell migration. However, experiments to evaluate this model are necessary. For instance, comparison of EB1-GFP turnover dynamics at the plus-ends in ATIP3-expressing and depleted cells could be measured through FRAP (Fluorescence Recovery After Photobleaching) videomicroscopy experiments.

Additionally, a comparative and quantitative global proteomic approach (Deracinois B *et al*. 2013) to identify the amount of ATIP3 and EB1 in a normal epithelial cell would be important to elucidate if there is enough ATIP3 proteins to retain EB1 in the cell.

2. ATIP3 molecular complexes

Results from this work showed that ATIP3 interacts with MCAK. Whether this interaction requires EB1 is still unknown, but so far it has been elucidated that CN domain of ATIP3 interacts with C-terminal EB1, as well as with MCAK; and that MCAK interacts with the same C-terminal domain of EB1, suggesting a possible macromolecular complex.

Co-immunoprecipitation assays using ATIP3 and MCAK deletion mutants that do not contain the EB1-interacting domain (ATIP3delCN or D2delCN on ATIP3 and MCAK-3E or MCAK-NN on MCAK (Honnappa S *et al*. 2009)), as well as EB1-specific siRNA transfection must be performed to revealed if the interaction of ATIP3 with MCAK involves EB1. Additionally, if ATIP3, MCAK and EB1 form a complex, should be demonstrated if they are cooperating to stabilize the interaction. With this aim, GST-EB1 pull-down experiments should be performed using increasing amounts of GFP-ATIP3 or increasing amounts of

GFP-MCAK, to elucidate if interaction of MCAK or ATIP3 increases when the concentration of the other protein also increases.

In line with increased EB1 accumulation at the growing ends in ATIP3-depleted cells, observation of GFP-MCAK revealed the same effect for this +TIP. The question that arises is whether ATIP3 is indirectly impairing the accumulation of all EB1-interacting partners at the plus-end. Immunostaining analysis of GFP-CLIP170 revealed that this protein accumulates at the plus-ends independently of ATIP3 expression, suggesting that loss of ATIP3 does not increase dynamics of all MTs, but just a subset where possibly EB1 and MCAK are localized. Of note, CLIP170 contains a CAP-Gly domain that allows to tip-track by hitchhiking on EB1, but as well by MT end recognition and/or by copolymerization with tubulin. Future experiments analyzing other SxIP-containing proteins that do not interact with ATIP3 would help to answer this question and clarify if the effect of ATIP3 on MCAK localization is specific or a direct consequence of EB1 delocalization.

Interaction of ATIP3 with EB1 and MCAK may be involved in MT dynamics regulation given that these two proteins have a key role in MT dynamic instability, being EB1 involved in the polymerization and MCAK in the depolymerization of MTs. Interestingly, the *Xenopus* ortholog of ATIP3, ICIS also interacts with MCAK to stimulate its MT-depolymerizing activity supporting our hypothesis describing a MT regulatory complex.

ATIP3 also interacts with APC. APC and ATIP3 share a large number of characteristics since both are members of the MATSP superfamily of tumor suppressor proteins that bind and regulate MT dynamics. In addition, ATIP3 and APC interact with EB1 and MCAK. It has been reported that interaction of APC with EB1 plays an important role in cell migration (Wen Y *et al*. 2004), whereas its interaction with MCAK is relevant for cell proliferation (Bahmanyar S *et al*. 2009).

Weak interaction of ATIP3 with APC was found in the absence of EB1 binding domain (APC-basic), suggesting that EB1 may be not required for this interaction but for the stabilization. Nevertheless, additional GST pull-down experiments should be performed to confirm this hypothesis using EB1-specific siRNA or ATIP3 or D2 deletion mutants lacking the CN domain. In addition, further experiments aiming to determine ATIP3 domain of interaction with APC should be performed. Deletion of this domain from full-length protein must be tested in functional assays, such as cell migration to define if the effect of ATIP3 on MT polarity and thus cell polarity and migration are due to its interaction with APC.

Where is the interaction between ATIP3 and APC happening? As APC is an SxIP-containing protein, its localization (in ATIP3-expressing and depleted cells) is important to verify

whether an accumulation at the MT plus-ends of APC is induced by the loss of ATIP3, as observed for EB1 and MCAK. Furthermore, considering that Louie RK *et al*. (2004) showed that APC and EB1 co-localize at the mother centriole, and that ATIP3 also localized at the centrosome, super resolution images should be taken to determine the exact position of ATIP3 and to define if it co-localizes with EB1 and APC complexes.

In addition, PLA experiments aiming to identify the *in situ* localization of ATIP3 and APC (and as well ATIP3 and MCAK) should be performed to characterize the interaction between these proteins. Finally, and as for MCAK, it should be investigated if ATIP3, APC and EB1 form a complex to regulate MT behavior during cell migration.

3. ATIP3 is not a +TIP

In 2009, Honnappa S and coworkers revealed that some +TIPs contain repeated SxIP motifs (such as mammalian CLASP2) and show enhanced affinity for MT growing ends, suggesting that multiple SxIP motifs may cooperate to enhance MT tip tracking (Honnappa S *et al*. 2009). Considering that ATIP3 contains three SxIP motifs and that it interacts with three +TIPs (EB1, MCAK and APC), this strongly suggest that ATIP3 is a MT plus-end interacting protein (+TIP). However, ATIP3 does not track the end of growing MTs but instead the MT lattice and the end of shrinking MTs.

In 2012, Jiang K and coworkers identified some SxIP-containing proteins that interacted with EB1 but did not showed tip-tracking behavior. Two interesting proteins were tastin and DDA3. By means of time-lapse videomicroscopy, these two proteins were described as back-tracking proteins, similar to ATIP3. Nevertheless, nothing is known about the mechanism by which these two proteins track depolymerizing MT ends. Backtracking proteins have been described in budding yeast (Salmon ED, 2005), Drosophila (Mennella V *et al*. 2005) and in humans (Langford KJ *et al*. 2006). In Drosophila, KLP59C (KIF2C/MCAK ortholog) remains associated with shrinking MTs and perpetuates their depolymerization by suppressing rescue. Although the mechanism by which this protein is retained at depolymerizing MT ends remains unclear, it has been suggested that differential affinity for the MT lattice versus the ends may be involved in KLP59C backtracking behavior (Sharp DJ *et al*. 2005). Of interest, APC was also described as a backtracking protein; however, no mechanism of action was associated with this localization (Langford KJ *et al*. 2006).

How does ATIP3 track the end of a depolymerizing MT? A possible explanation for ATIP3 accumulation and tracking of shrinking MTs may be a strong interaction of this protein with the MT lattice that will result in the slow dissociation of ATIP3 and the apparent accumulation at the depolymerizing end. However, future experiments like FRAP analyses

to measure the dynamics of GFP-ATIP3 association/dissociation with tubulin at the MT lattice would be interesting to test this hypothesis.

4. ATIP3 impairs cell polarity and cell migration

Several studies have shown that coupling of MTs at the front edge is relevant to sustain cell polarization and involves MTs plus-ends tracking proteins (+TIPs) such as EB1, APC, mDia, CLIP170, CLASP1, CLASP2, MACF/ACF7 and IQGAP. As mentioned above ATIP3 interacts with EB1 and APC, but the role of this interaction on cell migration must be evaluated.

It has been reported that cell polarization through APC includes the activation of Par proteins, especially Par6, the atypical PKCζ and GS3Kβ (Etienne-Manneville S *et al*. 2005). Evaluation of the activation of these proteins in ATIP3-expressing and depleted cells will allow to elucidate the effect of ATIP3 in the pathways that mediates MT and cell polarization.

Cell polarity mostly depends on actin rearrangement which in turn depends on activation of Rho GTPases. In accordance, the relevance of Rho pathway in ATIP3 effects should be tested using Rho inhibitors (as the toxin B or the C3 exoenzyme) or Rho Kinases (ROCK) inhibitors (like Y-27632). Additionally, actin dynamics in ATIP3-expressing and depleted cells during migration can be elucidated by means of TIRF (Total Internal Reflection Fluorescence) time-lapse videomicroscopy and will provide some clues to unravel the molecular mechanism of ATIP3 in cell polarity.

Impaired MT polarization results in a defect on cell polarity and subsequent cell migration. Tracking of phase contrast time-lapse images revealed an alteration of cell directionality that was accompanied with a difference in cell morphology. While highly invasive D3H2LN GFP cells formed a clear lamellipodium in the front of the cell near the wound and a trailing edge at the rear, ATIP3-positive cells exhibited various protrusions in different directions that do not persist over time. This unsustained cell shape during migration results in the failure of ATIP3-expressing cells to develop a polarized morphology that is instrumental for migration of adherent cells.

Time-lapse images also revealed a difference in the way GFP- or GFP-ATIP3-expressing cells migrate. D3H2LN GFP-expressing cells exhibit a collective cell migration where confluence cells remain attached and the cell monolayer moves coordinately to close the wound. Conversely, ATIP3-expressing cells do not form a compact monolayer and single cells move independently of their neighbors without a direction, confirming the defect on cell polarity. The change in morphology observed raises the hypothesis that loss of ATIP3

might induce a mesenchymal-epithelial transition (MET), where spindle-shaped cells become an array of polarized cells. Even if little is known about the role of MET in cancer and metastatic progression, it has been reported that it participates in the establishment and the stabilization of distant metastasis by allowing cancerous cells to regain epithelial properties and integrate into distant organs (Thiery JP, 2002; Brabletz T *et al*. 2005).

This observation should be verified by immunostaining of E-cadherin and N-cadherin, β-catenin, APC, intermediate filaments and other proteins involved in the transition, in both ATIP3-expressing and depleted cells. Additionally, ATIP3 introduction at low levels in cysts to evaluate a possible disruption of the structure, loss of polarity, and a switch between epithelial to mesenchymal markers would be important. This experiment should be performed as well with ATIP3-expressing cells where the protein will be silenced using specific siRNAs.

5. Clinical relevance of ATIP3

At the clinical level, this work allowed the identification of a new prognostic marker of the clinical outcome and an indicator of metastatic progression and high risk of fatal complication. Interestingly, two independent studies have shown that low expression of *MTUS1* is associated with low overall survival of patients with bladder cancer (Xiao J *et al*. 2012) and oral tongue squamous cell carcinoma (Ding X *et al*. 2012). The identification of ATIP3 as the *MTUS1* splice variant down-regulated in these two human cancers will permit the extrapolation of our results in human tumors other than breast cancer. Additionally, the evaluation of ATIP3 status in those cancers where *MTUS1* expression levels have been reported as reduced (pancreas, ovary, colon, head-and-neck, bladder and gastric) it would be of importance.

This work provides evidence that the combined evaluation of ATIP3 and EB1 gene expression profiles predicts the clinical outcome of breast cancer patients. Reduction of EB1 accumulation at the MT growing ends and alteration of its functions will depend on the relative expression levels of EB1 and ATIP3. In normal conditions, combined EB1/ATIP3 levels will maintain the equilibrium between the oncoprotein functions and the tumor suppressor functions. In contrast, an increase of EB1 or a decrease of ATIP3 will end in a deregulation of the balance, thus tumors with high levels of EB1 or low levels of ATIP3 may have an increase MT dynamics, tumor growth, tumor metastasis and consequently patients would have a worst prognosis.

It will be interesting to extend this first analysis including more patients' cohorts or using data bases (as the Kaplan-Meier plotter) to confirm the result obtained, and to evaluate

the clinical importance of a group that was not present in this first gene expression analysis: high levels of both proteins. Furthermore, the evaluation of ATIP3 relative expression levels in those human cancers where EB1 has been reported as overexpressed (Fujii K *et al*. 2005; Nishigaki R *et al*. 2005; Wang Y *et al*. 2005; Orimo T *et al*. 2008; Stypula-Cyrus Y *et al*. 2014) will allow to extend the correlation seen in breast cancer. Additionally, the implement of PLA experiments (using anti-MTUS1 and anti-EB1 antibodies in tumor and normal tissue) as clinic test may be of diagnostic value.

How could we translate these results in an ATIP3 targeted therapy? Different strategies (such as nanoparticles, cell-penetrating peptides or CPPs, or injection of naked DNA) have been reported as options for a personalized treatment (Bolhassani A *et al*. 2011; Sanchez C *et al*. 2014; Bu X *et al*. 2014; Fioretti D *et al*. 2014). However, given that ATIP3 is a large protein (1270 amino acids) is difficult its introduction in cancer cells. Which is why, the identification of a functional domain is important. D2 (465 amino acids) seems a good candidate as it retains all the full-length functions. Subsequent reduction of this domain showed that D2C and CN (170 and 112 amino acids, respectively) retained all of the functions tested as the interaction with EB1, the co-localization with MTs (CN with less affinity) and impairment of EB1 localization at the MT growing end. Future experiments should validate the effect of D2 deletion mutants in cellular processes, such as cell proliferation and cell migration, and metastatic progression to determine if these domains are fully functional and suitable for further use as a targeted therapy.

Results from this work allowed the identification of patients with high risk of fatal complication. The design and modelization of peptides that mimic the effects of ATIP3 and impede the accumulation of EB1 at the plus-ends (CN, par example), should be considered as an important therapeutic tool, against tumors that have lost ATIP3 and overexpress EB1, that has to be still developed.

V. REFERENCES

Akhmanova, A., Hoogenraad, C.C., Drabek, K., Stepanova, T., Dortland, B., Verkerk, T., Vermeulen, W., Burgering, B.M., De Zeeuw, C.I., Grosveld, F., Galjart, N., 2001. Clasps are CLIP-115 and -170 associating proteins involved in the regional regulation of microtubule dynamics in motile fibroblasts. Cell 104, 923–935.

Akhmanova, A., Steinmetz, M.O., 2008. Tracking the ends: a dynamic protein network controls the fate of microtubule tips. Nature Reviews Molecular Cell Biology 9, 309–322. doi:10.1038/nrm2369

Al-Bassam, J., Kim, H., Brouhard, G., van Oijen, A., Harrison, S.C., Chang, F., 2010. CLASP promotes microtubule rescue by recruiting tubulin dimers to the microtubule. Dev. Cell 19, 245–258. doi:10.1016/j.devcel.2010.07.016

Allen, C., Borisy, G.G., 1974. Structural polarity and directional growth of microtubules of Chlamydomonas flagella. J. Mol. Biol. 90, 381–402.

Amos, L., Klug, A., 1974. Arrangement of subunits in flagellar microtubules. J. Cell. Sci. 14, 523–549.

Amos, L.A., 2008. The tektin family of microtubule-stabilizing proteins. Genome Biology 9, 229. doi:10.1186/gb-2008-9-7-229

Aoki, K., Taketo, M.M., 2007. Adenomatous polyposis coli (APC): a multi-functional tumor suppressor gene. J. Cell. Sci. 120, 3327–3335. doi:10.1242/jcs.03485

Arnal, I., Heichette, C., Diamantopoulos, G.S., Chrétien, D., 2004. CLIP-170/tubulin-curved oligomers coassemble at microtubule ends and promote rescues. Curr. Biol. 14, 2086–2095. doi:10.1016/j.cub.2004.11.055

Arnette, C., Efimova, N., Zhu, X., Clark, G.J., Kaverina, I., 2014. Microtubule segment stabilization by RASSF1A is required for proper microtubule dynamics and Golgi integrity. Mol. Biol. Cell 25, 800–810. doi:10.1091/mbc.E13-07-0374

Baas, P.W., Slaughter, T., Brown, A., Black, M.M., 1991. Microtubule dynamics in axons and dendrites. J. Neurosci. Res. 30, 134–153. doi:10.1002/jnr.490300115

Bacac, M., Stamenkovic, I., 2008. Metastatic Cancer Cell. Annual Review of Pathology: Mechanisms of Disease 3, 221–247. doi:10.1146/annurev.pathmechdis.3.121806.151523

Bahmanyar, S., Nelson, W.J., Barth, A.I.M., 2009. Role of APC and its binding partners in regulating microtubules in mitosis. Adv. Exp. Med. Biol. 656, 65–74.

Barros, T.P., Kinoshita, K., Hyman, A.A., Raff, J.W., 2005. Aurora A activates D-TACC–Msps complexes exclusively at centrosomes to stabilize centrosomal microtubules. J Cell Biol 170, 1039–1046. doi:10.1083/jcb.200504097

Bartolini, F., Gundersen, G.G., 2010. Formins and microtubules. Biochimica et Biophysica Acta (BBA) - Molecular Cell Research, Includes Special Section on Formins 1803, 164–173. doi:10.1016/j.bbamcr.2009.07.006

Belmont, L., Mitchison, T., Deacon, H.W., 1996. Catastrophic revelations about Op18/stathmin. Trends Biochem. Sci. 21, 197–198.

Berrueta, L., Kraeft, S.K., Tirnauer, J.S., Schuyler, S.C., Chen, L.B., Hill, D.E., Pellman, D., Bierer, B.E., 1998. The adenomatous polyposis coli-binding protein EB1 is associated with cytoplasmic and spindle microtubules. Proc. Natl. Acad. Sci. U.S.A. 95, 10596–10601.

Bieling, P., Kandels-Lewis, S., Telley, I.A., van Dijk, J., Janke, C., Surrey, T., 2008. CLIP-170 tracks growing microtubule ends by dynamically recognizing composite EB1/tubulin-binding sites. J. Cell Biol. 183, 1223–1233. doi:10.1083/jcb.200809190

Bieling, P., Laan, L., Schek, H., Munteanu, E.L., Sandblad, L., Dogterom, M., Brunner, D., Surrey, T., 2007. Reconstitution of a microtubule plus-end tracking system in vitro. Nature 450, 1100–1105. doi:10.1038/nature06386

Bienz, M., 2002. The subcellular destinations of apc proteins. Nat Rev Mol Cell Biol 3, 328–338. doi:10.1038/nrm806

Bignell, G.R., Warren, W., Seal, S., Takahashi, M., Rapley, E., Barfoot, R., Green, H., Brown, C., Biggs, P.J., Lakhani, S.R., Jones, C., Hansen, J., Blair, E., Hofmann, B., Siebert, R., Turner, G., Evans, D.G., Schrander-Stumpel, C., Beemer, F.A., van Den Ouweland, A., Halley, D., Delpech, B., Cleveland, M.G., Leigh, I., Leisti, J., Rasmussen, S., 2000. Identification of the familial cylindromatosis tumour-suppressor gene. Nat. Genet. 25, 160–165. doi:10.1038/76006

Blanchoin, L., Boujemaa-Paterski, R., Sykes, C., Plastino, J., 2014. Actin dynamics, architecture, and mechanics in cell motility. Physiol. Rev. 94, 235–263. doi:10.1152/physrev.00018.2013

Bolhassani, A., Safaiyan, S., Rafati, S., 2011. Improvement of different vaccine delivery systems for cancer therapy. Mol. Cancer 10, 3. doi:10.1186/1476-4598-10-3

Bornens, M., 2008. Organelle positioning and cell polarity. Nat Rev Mol Cell Biol 9, 874–886. doi:10.1038/nrm2524

Bosc, C., Andrieux, A., Job, D., 2003. STOP proteins. Biochemistry 42, 12125–12132. doi:10.1021/bi0352163
Bosson, A., Soleilhac, J.-M., Valiron, O., Job, D., Andrieux, A., Moutin, M.-J., 2012. Cap-Gly Proteins at Microtubule Plus Ends: Is EB1 Detyrosination Involved? PLoS One 7. doi:10.1371/journal.pone.0033490
Brabletz, T., Hlubek, F., Spaderna, S., Schmalhofer, O., Hiendlmeyer, E., Jung, A., Kirchner, T., 2005. Invasion and Metastasis in Colorectal Cancer: Epithelial-Mesenchymal Transition, Mesenchymal-Epithelial Transition, Stem Cells and β-Catenin. Cells Tissues Organs 179, 56–65. doi:10.1159/000084509
Bré, M.H., Pepperkok, R., Hill, A.M., Levilliers, N., Ansorge, W., Stelzer, E.H., Karsenti, E., 1990. Regulation of microtubule dynamics and nucleation during polarization in MDCK II cells. J. Cell Biol. 111, 3013–3021.
Brinkley, W.B.R., 1997. Microtubules: A Brief Historical Perspective. Journal of Structural Biology 118, 84–86. doi:10.1006/jsbi.1997.3854
Bu, W., Su, L.-K., 2003. Characterization of functional domains of human EB1 family proteins. J. Biol. Chem. 278, 49721–49731. doi:10.1074/jbc.M306194200
Bu, X., Zhu, T., Ma, Y., Shen, Q., 2014. Co-administration with cell penetrating peptide enhances the oral bioavailability of docetaxel-loaded nanoparticles. Drug Dev Ind Pharm. doi:10.3109/03639045.2014.902465
Buey, R.M., Mohan, R., Leslie, K., Walzthoeni, T., Missimer, J.H., Menzel, A., Bjelic, S., Bargsten, K., Grigoriev, I., Smal, I., Meijering, E., Aebersold, R., Akhmanova, A., Steinmetz, M.O., 2011. Insights into EB1 structure and the role of its C-terminal domain for discriminating microtubule tips from the lattice. Mol Biol Cell 22, 2912–2923. doi:10.1091/mbc.E11-01-0017
Bulinski, J.C., Gundersen, G.G., 1991. Stabilization of post-translational modification of microtubules during cellular morphogenesis. Bioessays 13, 285–293. doi:10.1002/bies.950130605
Califano, D., Pignata, S., Pisano, C., Greggi, S., Laurelli, G., Losito, N.S., Ottaiano, A., Gallipoli, A., Pasquinelli, R., De Simone, V., Cirombella, R., Fusco, A., Chiappetta, G., 2010. FEZ1/LZTS1 protein expression in ovarian cancer. J. Cell. Physiol. 222, 382–386. doi:10.1002/jcp.21962
Cancer Help UK, 2012. Breast Cancer Types.
Caplow, M., Ruhlen, R.L., Shanks, J., 1994. The free energy for hydrolysis of a microtubule-bound nucleotide triphosphate is near zero: all of the free energy for hydrolysis is stored in the microtubule lattice. J. Cell Biol. 127, 779–788.
Carey, L.A., Dees, E.C., Sawyer, L., Gatti, L., Moore, D.T., Collichio, F., Ollila, D.W., Sartor, C.I., Graham, M.L., Perou, C.M., 2007. The Triple Negative Paradox: Primary Tumor Chemosensitivity of Breast Cancer Subtypes. Clin Cancer Res 13, 2329–2334. doi:10.1158/1078-0432.CCR-06-1109
Carlier, M.-F., Pantaloni, D., 2007. Control of Actin Assembly Dynamics in Cell Motility. J. Biol. Chem. 282, 23005–23009. doi:10.1074/jbc.R700020200
Carvalho, P., Tirnauer, J.S., Pellman, D., 2003. Surfing on microtubule ends. Trends in Cell Biology 13, 229–237. doi:10.1016/S0962-8924(03)00074-6
Cassimeris, L., 1993. Regulation of microtubule dynamic instability. Cell Motil. Cytoskeleton 26, 275–281. doi:10.1002/cm.970260402
Cassimeris, L.U., Walker, R.A., Pryer, N.K., Salmon, E.D., 1987. Dynamic instability of microtubules. Bioessays 7, 149–154. doi:10.1002/bies.950070403
Chambers, A.F., Groom, A.C., MacDonald, I.C., 2002. Metastasis: Dissemination and growth of cancer cells in metastatic sites. Nat Rev Cancer 2, 563–572. doi:10.1038/nrc865
Chaudhuri, A.R., Khan, I.A., Prasad, V., Robinson, A.K., Ludueña, R.F., Barnes, L.D., 1999. The tumor suppressor protein Fhit. A novel interaction with tubulin. J. Biol. Chem. 274, 24378–24382.
Chen, L., Zhu, Z., Sun, X., Dong, X.-Y., Wei, J., Gu, F., Sun, Y.-L., Zhou, J., Dong, J.-T., Fu, L., 2009. Down-regulation of tumor suppressor gene FEZ1/LZTS1 in breast carcinoma involves promoter methylation and associates with metastasis. Breast Cancer Res. Treat. 116, 471–478. doi:10.1007/s10549-008-0147-6
Chernov, K.G., Mechulam, A., Popova, N.V., Pastre, D., Nadezhdina, E.S., Skabkina, O.V., Shanina, N.A., Vasiliev, V.D., Tarrade, A., Melki, J., Joshi, V., Baconnais, S., Toma, F., Ovchinnikov, L.P., Curmi, P.A., 2008. YB-1 promotes microtubule assembly in vitro through interaction with tubulin and microtubules. BMC Biochemistry 9, 23. doi:10.1186/1471-2091-9-23
Choi, Y.P., Lee, J.H., Gao, M.-Q., Kim, B.G., Kang, S., Kim, S.H., Cho, N.H., 2014. Cancer-associated fibroblast promote transmigration through endothelial brain cells in three-dimensional in vitro models. Int. J. Cancer n/a–n/a. doi:10.1002/ijc.28848

Chrétien, D., Fuller, S.D., Karsenti, E., 1995. Structure of growing microtubule ends: two-dimensional sheets close into tubes at variable rates. J Cell Biol 129, 1311–1328. doi:10.1083/jcb.129.5.1311

Cooper, J., Giancotti, F.G., 2014. Molecular insights into NF2/Merlin tumor suppressor function. FEBS Letters. doi:10.1016/j.febslet.2014.04.001

Cooper, J.R., Wordeman, L., 2009. The diffusive interaction of microtubule binding proteins. Curr. Opin. Cell Biol. 21, 68–73. doi:10.1016/j.ceb.2009.01.005

Cooper, S.A.P., 1840. On the anatomy of the breast, volume I.

Coquelle, F.M., Caspi, M., Cordelières, F.P., Dompierre, J.P., Dujardin, D.L., Koifman, C., Martin, P., Hoogenraad, C.C., Akhmanova, A., Galjart, N., Mey, J.R.D., Reiner, O., 2002. LIS1, CLIP-170's Key to the Dynein/Dynactin Pathway. Mol. Cell. Biol. 22, 3089–3102. doi:10.1128/MCB.22.9.3089-3102.2002

Cortes, J., Montero, A.J., Glück, S., 2012. Eribulin mesylate, a novel microtubule inhibitor in the treatment of breast cancer. Cancer Treatment Reviews 38, 143–151. doi:10.1016/j.ctrv.2011.03.006

Dallol, A., Agathanggelou, A., Fenton, S.L., Ahmed-Choudhury, J., Hesson, L., Vos, M.D., Clark, G.J., Downward, J., Maher, E.R., Latif, F., 2004. RASSF1A interacts with microtubule-associated proteins and modulates microtubule dynamics. Cancer Res. 64, 4112–4116. doi:10.1158/0008-5472.CAN-04-0267

Dallol, A., Agathanggelou, A., Tommasi, S., Pfeifer, G.P., Maher, E.R., Latif, F., 2005. Involvement of the RASSF1A tumor suppressor gene in controlling cell migration. Cancer Res. 65, 7653–7659. doi:10.1158/0008-5472.CAN-05-0247

Dehmelt, L., Halpain, S., 2005. The MAP2/Tau family of microtubule-associated proteins. Genome Biol. 6, 204. doi:10.1186/gb-2004-6-1-204

Deracinois, B., Flahaut, C., Duban-Deweer, S., Karamanos, Y., 2013. Comparative and Quantitative Global Proteomics Approaches: An Overview. Proteomes 1, 180–218. doi:10.3390/proteomes1030180

Desai, A., Mitchison, T.J., 1997. Microtubule Polymerization Dynamics. Annual Review of Cell and Developmental Biology 13, 83–117. doi:10.1146/annurev.cellbio.13.1.83

Desai, A., Verma, S., Mitchison, T.J., Walczak, C.E., 1999. Kin I kinesins are microtubule-destabilizing enzymes. Cell 96, 69–78.

Di Benedetto, M., Bièche, I., Deshayes, F., Vacher, S., Nouet, S., Collura, V., Seitz, I., Louis, S., Pineau, P., Amsellem-Ouazana, D., Couraud, P.O., Strosberg, A.D., Stoppa-Lyonnet, D., Lidereau, R., Nahmias, C., 2006a. Structural organization and expression of human MTUS1, a candidate 8p22 tumor suppressor gene encoding a family of angiotensin II AT2 receptor-interacting proteins, ATIP. Gene 380, 127–136. doi:10.1016/j.gene.2006.05.021

Di Benedetto, M., Pineau, P., Nouet, S., Berhouet, S., Seitz, I., Louis, S., Dejean, A., Couraud, P.O., Strosberg, A.D., Stoppa-Lyonnet, D., Nahmias, C., 2006b. Mutation analysis of the 8p22 candidate tumor suppressor gene ATIP/MTUS1 in hepatocellular carcinoma. Molecular and Cellular Endocrinology 252, 207–215. doi:10.1016/j.mce.2006.03.014

Diamantopoulos, G.S., Perez, F., Goodson, H.V., Batelier, G., Melki, R., Kreis, T.E., Rickard, J.E., 1999. Dynamic localization of CLIP-170 to microtubule plus ends is coupled to microtubule assembly. J. Cell Biol. 144, 99–112.

Dimitrov, A., Quesnoit, M., Moutel, S., Cantaloube, I., Poüs, C., Perez, F., 2008. Detection of GTP-tubulin conformation in vivo reveals a role for GTP remnants in microtubule rescues. Science 322, 1353–1356. doi:10.1126/science.1165401

Ding, X., Zhang, N., Cai, Y., Li, S., Zheng, C., Jin, Y., Yu, T., Wang, A., Zhou, X., 2012. Down-regulation of tumor suppressor MTUS1/ATIP is associated with enhanced proliferation, poor differentiation and poor prognosis in oral tongue squamous cell carcinoma. Mol Oncol 6, 73–80. doi:10.1016/j.molonc.2011.11.002

Dong, X., Liu, F., Sun, L., Liu, M., Li, D., Su, D., Zhu, Z., Dong, J.-T., Fu, L., Zhou, J., 2009. Oncogenic function of microtubule end-binding protein 1 in breast cancer. The Journal of Pathology n/a–n/a. doi:10.1002/path.2662

Dougherty, G.W., Adler, H.J., Rzadzinska, A., Gimona, M., Tomita, Y., Lattig, M.C., Merritt, R.C., Kachar, B., 2005. CLAMP, a novel microtubule-associated protein with EB-type calponin homology. Cell Motil. Cytoskeleton 62, 141–156. doi:10.1002/cm.20093

Drabek, K., van Ham, M., Stepanova, T., Draegestein, K., van Horssen, R., Sayas, C.L., Akhmanova, A., Ten Hagen, T., Smits, R., Fodde, R., Grosveld, F., Galjart, N., 2006. Role of CLASP2 in microtubule stabilization and the regulation of persistent motility. Curr. Biol. 16, 2259–2264. doi:10.1016/j.cub.2006.09.065

Dragestein, K.A., van Cappellen, W.A., van Haren, J., Tsibidis, G.D., Akhmanova, A., Knoch, T.A., Grosveld, F., Galjart, N., 2008. Dynamic behavior of GFP-CLIP-170 reveals fast protein turnover on microtubule plus ends. J. Cell Biol. 180, 729–737. doi:10.1083/jcb.200707203

Drechsel, D.N., Hyman, A.A., Cobb, M.H., Kirschner, M.W., 1992. Modulation of the dynamic instability of tubulin assembly by the microtubule-associated protein tau. Mol. Biol. Cell 3, 1141–1154.

Du Puy, L., Beqqali, A., Monshouwer-Kloots, J., Haagsman, H.P., Roelen, B.A.J., Passier, R., 2009. CAZIP, a novel protein expressed in the developing heart and nervous system. Dev. Dyn. 238, 2903–2911. doi:10.1002/dvdy.22107

Dupin, I., Etienne-Manneville, S., 2011. Nuclear positioning: mechanisms and functions. Int. J. Biochem. Cell Biol. 43, 1698–1707. doi:10.1016/j.biocel.2011.09.004

Emoto, K., Masugi, Y., Yamazaki, K., Effendi, K., Tsujikawa, H., Tanabe, M., Kitagawa, Y., Sakamoto, M., 2014. Presence of primary cilia in cancer cells correlates with prognosis of pancreatic ductal adenocarcinoma. Human Pathology 45, 817–825. doi:10.1016/j.humpath.2013.11.017

Ems-McClung, S.C., Walczak, C.E., 2010. Kinesin-13s in mitosis: Key players in the spatial and temporal organization of spindle microtubules. Semin. Cell Dev. Biol. 21, 276–282. doi:10.1016/j.semcdb.2010.01.016

Erickson, H.P., O'Brien, E.T., 1992. Microtubule dynamic instability and GTP hydrolysis. Annu Rev Biophys Biomol Struct 21, 145–166. doi:10.1146/annurev.bb.21.060192.001045

Etienne-Manneville, S., 2013. Microtubules in cell migration. Annu. Rev. Cell Dev. Biol. 29, 471–499. doi:10.1146/annurev-cellbio-101011-155711

Etienne-Manneville, S., Hall, A., 2001. Integrin-mediated activation of Cdc42 controls cell polarity in migrating astrocytes through PKCzeta. Cell 106, 489–498.

Etienne-Manneville, S., Manneville, J.-B., Nicholls, S., Ferenczi, M.A., Hall, A., 2005. Cdc42 and Par6-PKCzeta regulate the spatially localized association of Dlg1 and APC to control cell polarization. J. Cell Biol. 170, 895–901. doi:10.1083/jcb.200412172

Fan, J., Griffiths, A.D., Lockhart, A., Cross, R.A., Amos, L.A., 1996. Microtubule minus ends can be labelled with a phage display antibody specific to alpha-tubulin. J. Mol. Biol. 259, 325–330. doi:10.1006/jmbi.1996.0322

Fant, X., Merdes, A., Haren, L., 2004. Cell and Molecular Biology of Spindle Poles and NuMA, in: International Review of Cytology. Academic Press, pp. 1–57.

Ferlay, J., Soerjomataram, I., Ervik,, M., Dikshit, R., Eser, S., Mathers, C., Rebelo, M., Parkin, D., Forman, D., Bray, F., 2013. GLOBOCAN 2012 v1.0, Cancer Incidence and Mortality Worldwide: IARC CancerBase No. 11 [Internet]. Lyon, France: International Agency for Research on Cancer.

Fioretti, D., Iurescia, S., Rinaldi, M., 2014. Recent Advances in Design of Immunogenic and Effective Naked DNA Vaccines Against Cancer. Recent Patents on Anti-Cancer Drug Discovery 9, 66–82.

Fojo, A.T., Adelberg, D.E., 2010. Microtubule Targeting Agents, in: Drug Management of Prostate Cancer.

Folker, E.S., Baker, B.M., Goodson, H.V., 2005. Interactions between CLIP-170, tubulin, and microtubules: implications for the mechanism of Clip-170 plus-end tracking behavior. Mol. Biol. Cell 16, 5373–5384. doi:10.1091/mbc.E04-12-1106

Fong, K.-W., Choi, Y.-K., Rattner, J.B., Qi, R.Z., 2008. CDK5RAP2 is a pericentriolar protein that functions in centrosomal attachment of the gamma-tubulin ring complex. Mol. Biol. Cell 19, 115–125. doi:10.1091/mbc.E07-04-0371

Foulkes, W.D., Shuen, A.Y., 2013. In Brief: BRCA1 and BRCA2. The Journal of Pathology 230, 347–349. doi:10.1002/path.4205

Foulkes, W.D., Smith, I.E., Reis-Filho, J.S., 2010. Triple-Negative Breast Cancer. New England Journal of Medicine 363, 1938–1948. doi:10.1056/NEJMra1001389

Fourniol, F., Perderiset, M., Houdusse, A., Moores, C., 2013. Structural studies of the doublecortin family of MAPs. Academic Press.

Frank, B., Bermejo, J.L., Hemminki, K., Sutter, C., Wappenschmidt, B., Meindl, A., Kiechle-Bahat, M., Bugert, P., Schmutzler, R.K., Bartram, C.R., Burwinkel, B., 2007. Copy number variant in the candidate tumor suppressor gene MTUS1 and familial breast cancer risk. Carcinogenesis 28, 1442–1445. doi:10.1093/carcin/bgm033

Friedl, P., Alexander, S., 2011. Cancer Invasion and the Microenvironment: Plasticity and Reciprocity. Cell 147, 992–1009. doi:10.1016/j.cell.2011.11.016

Friedl, P., Gilmour, D., 2009. Collective cell migration in morphogenesis, regeneration and cancer. Nat Rev Mol Cell Biol 10, 445–457. doi:10.1038/nrm2720

Friedl, P., Locker, J., Sahai, E., Segall, J.E., 2012. Classifying collective cancer cell invasion. Nat Cell Biol 14, 777–783. doi:10.1038/ncb2548

Friedl, P., Noble, P.B., Walton, P.A., Laird, D.W., Chauvin, P.J., Tabah, R.J., Black, M., Zänker, K.S., 1995. Migration of Coordinated Cell Clusters in Mesenchymal and Epithelial Cancer Explants in Vitro. Cancer Res 55, 4557–4560.

Friedl, P., Wolf, K., 2003. Tumour-cell invasion and migration: diversity and escape mechanisms. Nature Reviews Cancer 3, 362–374. doi:10.1038/nrc1075

Fu, N., Lindeman, G.J., Visvader, J.E., 2014. The mammary stem cell hierarchy. Curr. Top. Dev. Biol. 107, 133–160. doi:10.1016/B978-0-12-416022-4.00005-6

Fujii, K., Kondo, T., Yokoo, H., Yamada, T., Iwatsuki, K., Hirohashi, S., 2005. Proteomic study of human hepatocellular carcinoma using two-dimensional difference gel electrophoresis with saturation cysteine dye. Proteomics 5, 1411–1422. doi:10.1002/pmic.200401004

Fujita, T., Mogi, M., Min, L.-J., Iwanami, J., Tsukuda, K., Sakata, A., Okayama, H., Iwai, M., Nahmias, C., Higaki, J., Horiuchi, M., 2009. Attenuation of cuff-induced neointimal formation by overexpression of angiotensin II type 2 receptor-interacting protein 1. Hypertension 53, 688–693. doi:10.1161/HYPERTENSIONAHA.108.128140

Fukata, M., Watanabe, T., Noritake, J., Nakagawa, M., Yamaga, M., Kuroda, S., Matsuura, Y., Iwamatsu, A., Perez, F., Kaibuchi, K., 2002. Rac1 and Cdc42 capture microtubules through IQGAP1 and CLIP-170. Cell 109, 873–885.

Fumoleau, P., Guiu, S., 2012. New Vinca Alkaloids in Clinical Development. Current Breast Cancer Reports 5, 69–72. doi:10.1007/s12609-012-0096-2

Gaglio, T., Saredi, A., Compton, D., 1995. NuMA is required for the organization of microtubules into aster-like mitotic arrays. J Cell Biol 131, 693–708.

Gao, J., Huo, L., Sun, X., Liu, M., Li, D., Dong, J.-T., Zhou, J., 2008. The Tumor Suppressor CYLD Regulates Microtubule Dynamics and Plays a Role in Cell Migration. Journal of Biological Chemistry 283, 8802–8809. doi:10.1074/jbc.M708470200

Gelfand, V.I., Bershadsky, A.D., 1991. Microtubule dynamics: mechanism, regulation, and function. Annu. Rev. Cell Biol. 7, 93–116. doi:10.1146/annurev.cb.07.110191.000521

Ghosh, D.K., Dasgupta, D., Guha, A., 2012. Models, Regulations, and Functions of Microtubule Severing by Katanin. ISRN Molecular Biology 2012, e596289. doi:10.5402/2012/596289

Gleeson, J.G., Lin, P.T., Flanagan, L.A., Walsh, C.A., 1999. Doublecortin Is a Microtubule-Associated Protein and Is Expressed Widely by Migrating Neurons. Neuron 23, 257–271. doi:10.1016/S0896-6273(00)80778-3

Goldhirsch, A., Wood, W.C., Coates, A.S., Gelber, R.D., Thürlimann, B., Senn, H.-J., Panel members, 2011. Strategies for subtypes--dealing with the diversity of breast cancer: highlights of the St. Gallen International Expert Consensus on the Primary Therapy of Early Breast Cancer 2011. Ann. Oncol. 22, 1736–1747. doi:10.1093/annonc/mdr304

Gomes, E.R., Jani, S., Gundersen, G.G., 2005. Nuclear Movement Regulated by Cdc42, MRCK, Myosin, and Actin Flow Establishes MTOC Polarization in Migrating Cells. Cell 121, 451–463. doi:10.1016/j.cell.2005.02.022

Goshima, G., Nédélec, F., Vale, R.D., 2005. Mechanisms for focusing mitotic spindle poles by minus end-directed motor proteins. J. Cell Biol. 171, 229–240. doi:10.1083/jcb.200505107

Goss, K.H., Groden, J., 2000. Biology of the Adenomatous Polyposis Coli Tumor Suppressor. JCO 18, 1967–1979.

Green, R.A., Wollman, R., Kaplan, K.B., 2005. APC and EB1 function together in mitosis to regulate spindle dynamics and chromosome alignment. Mol. Biol. Cell 16, 4609–4622. doi:10.1091/mbc.E05-03-0259

Grigoriev, I., Gouveia, S.M., van der Vaart, B., Demmers, J., Smyth, J.T., Honnappa, S., Splinter, D., Steinmetz, M.O., Putney, J.W., Jr, Hoogenraad, C.C., Akhmanova, A., 2008. STIM1 is a MT-plus-end-tracking protein involved in remodeling of the ER. Curr. Biol. 18, 177–182. doi:10.1016/j.cub.2007.12.050

Guillaud, L., Bosc, C., Fourest-Lieuvin, A., Denarier, E., Pirollet, F., Lafanechère, L., Job, D., 1998. STOP proteins are responsible for the high degree of microtubule stabilization observed in neuronal cells. J. Cell Biol. 142, 167–179.

Guise, T., 2010. Examining the Metastatic Niche: Targeting the Microenvironment. Seminars in Oncology 37, S2–S14. doi:10.1053/j.seminoncol.2010.10.007

Gundersen, G.G., Bulinski, J.C., 1988. Selective stabilization of microtubules oriented toward the direction of cell migration. Proc. Natl. Acad. Sci. U.S.A. 85, 5946–5950.

Gundersen, G.G., Gomes, E.R., Wen, Y., 2004. Cortical control of microtubule stability and polarization. Current Opinion in Cell Biology 16, 106–112. doi:10.1016/j.ceb.2003.11.010

Gupta, G.P., Massagué, J., 2006. Cancer Metastasis: Building a Framework. Cell 127, 679–695. doi:10.1016/j.cell.2006.11.001

Haddad, N.M.N., Cavallerano, J.D., Silva, P.S., 2013. Von hippel-lindau disease: a genetic and clinical review. Semin Ophthalmol 28, 377–386. doi:10.3109/08820538.2013.825281

Hammond, J.W., Cai, D., Verhey, K.J., 2008. Tubulin modifications and their cellular functions. Curr. Opin. Cell Biol. 20, 71–76. doi:10.1016/j.ceb.2007.11.010

Hanahan, D., Weinberg, R.A., 2011. Hallmarks of Cancer: The Next Generation. Cell 144, 646–674. doi:10.1016/j.cell.2011.02.013

Hanson, C.A., Miller, J.R., 2005. Non-traditional roles for the Adenomatous Polyposis Coli (APC) tumor suppressor protein. Gene 361, 1–12. doi:10.1016/j.gene.2005.07.024

Hassiotou, F., Geddes, D., 2013. Anatomy of the human mammary gland: Current status of knowledge. Clinical Anatomy 26, 29–48. doi:10.1002/ca.22165

Hayashi, I., Ikura, M., 2003. Crystal structure of the amino-terminal microtubule-binding domain of end-binding protein 1 (EB1). J. Biol. Chem. 278, 36430–36434. doi:10.1074/jbc.M305773200

Hayashi, I., Wilde, A., Mal, T.K., Ikura, M., 2005. Structural basis for the activation of microtubule assembly by the EB1 and p150Glued complex. Mol. Cell 19, 449–460. doi:10.1016/j.molcel.2005.06.034

Hegerfeldt, Y., Tusch, M., Bröcker, E.-B., Friedl, P., 2002. Collective Cell Movement in Primary Melanoma Explants Plasticity of Cell-Cell Interaction, β1-Integrin Function, and Migration Strategies. Cancer Res 62, 2125–2130.

Helenius, J., Brouhard, G., Kalaidzidis, Y., Diez, S., Howard, J., 2006. The depolymerizing kinesin MCAK uses lattice diffusion to rapidly target microtubule ends. Nature 441, 115–119. doi:10.1038/nature04736

Hergovich, A., Lisztwan, J., Barry, R., Ballschmieter, P., Krek, W., 2002. Regulation of microtubule stability by the von Hippel-Lindau tumour suppressor protein pVHL. Nature Cell Biology 5, 64–70. doi:10.1038/ncb899

Himes, R.H., 1991. Interactions of the catharanthus (Vinca) alkaloids with tubulin and microtubules. Pharmacol. Ther. 51, 257–267.

Holy, T.E., Leibler, S., 1994. Dynamic instability of microtubules as an efficient way to search in space. Proc. Natl. Acad. Sci. U.S.A. 91, 5682–5685.

Honnappa, S., Gouveia, S.M., Weisbrich, A., Damberger, F.F., Bhavesh, N.S., Jawhari, H., Grigoriev, I., van Rijssel, F.J.A., Buey, R.M., Lawera, A., Jelesarov, I., Winkler, F.K., Wüthrich, K., Akhmanova, A., Steinmetz, M.O., 2009. An EB1-binding motif acts as a microtubule tip localization signal. Cell 138, 366–376. doi:10.1016/j.cell.2009.04.065

Honnappa, S., John, C.M., Kostrewa, D., Winkler, F.K., Steinmetz, M.O., 2005. Structural insights into the EB1-APC interaction. EMBO J. 24, 261–269. doi:10.1038/sj.emboj.7600529

Honnappa, S., Okhrimenko, O., Jaussi, R., Jawhari, H., Jelesarov, I., Winkler, F.K., Steinmetz, M.O., 2006. Key interaction modes of dynamic +TIP networks. Mol. Cell 23, 663–671. doi:10.1016/j.molcel.2006.07.013

Honore, S., Pasquier, E., Braguer, D., 2005. Understanding microtubule dynamics for improved cancer therapy. Cellular and Molecular Life Sciences 62, 3039–3056. doi:10.1007/s00018-005-5330-x

Hoogenraad, C.C., Akhmanova, A., Grosveld, F., De Zeeuw, C.I., Galjart, N., 2000. Functional analysis of CLIP-115 and its binding to microtubules. J. Cell. Sci. 113 (Pt 12), 2285–2297.

Horio, T., Hotani, H., 1986. Visualization of the dynamic instability of individual microtubules by dark-field microscopy. Nature 321, 605–607. doi:10.1038/321605a0

Hortobágyi, G.N., 1997. Anthrazykline in der Krebstherapie: Ein Überblick. Drugs 54, 1–7. doi:10.2165/00003495-199700544-00003

Hotani, H., Horio, T., 1988. Dynamics of microtubules visualized by darkfield microscopy: treadmilling and dynamic instability. Cell Motil. Cytoskeleton 10, 229–236. doi:10.1002/cm.970100127

Howard, J., Hyman, A.A., 2003. Dynamics and mechanics of the microtubule plus end. Nature 422, 753–758. doi:10.1038/nature01600

Howell, B., Deacon, H., Cassimeris, L., 1999a. Decreasing oncoprotein 18/stathmin levels reduces microtubule catastrophes and increases microtubule polymer in vivo. J. Cell. Sci. 112 (Pt 21), 3713–3722.

Howell, B., Larsson, N., Gullberg, M., Cassimeris, L., 1999b. Dissociation of the tubulin-sequestering and microtubule catastrophe-promoting activities of oncoprotein 18/stathmin. Mol. Biol. Cell 10, 105–118.

Hsu, L.C., White, R.L., 1998. BRCA1 is associated with the centrosome during mitosis. Proc. Natl. Acad. Sci. U.S.A. 95, 12983–12988.

Hubbert, C., Guardiola, A., Shao, R., Kawaguchi, Y., Ito, A., Nixon, A., Yoshida, M., Wang, X.-F., Yao, T.-P., 2002. HDAC6 is a microtubule-associated deacetylase. Nature 417, 455–458. doi:10.1038/417455a

Hunter, A.W., Caplow, M., Coy, D.L., Hancock, W.O., Diez, S., Wordeman, L., Howard, J., 2003. The kinesin-related protein MCAK is a microtubule depolymerase that forms an ATP-hydrolyzing complex at microtubule ends. Mol. Cell 11, 445–457.

Hunter, K.W., Crawford, N.P.S., Alsarraj, J., 2008. Mechanisms of metastasis. Breast Cancer Res. 10 Suppl 1, S2. doi:10.1186/bcr1988

Hyman, A.A., Salser, S., Drechsel, D.N., Unwin, N., Mitchison, T.J., 1992. Role of GTP hydrolysis in microtubule dynamics: information from a slowly hydrolyzable analogue, GMPCPP. Mol. Biol. Cell 3, 1155–1167. doi:10.1091/mbc.3.10.1155

Ignatiadis, M., Sotiriou, C., 2013. Luminal breast cancer: from biology to treatment. Nat Rev Clin Oncol 10, 494–506. doi:10.1038/nrclinonc.2013.124

Ishii, H., Baffa, R., Numata, S.I., Murakumo, Y., Rattan, S., Inoue, H., Mori, M., Fidanza, V., Alder, H., Croce, C.M., 1999. The FEZ1 gene at chromosome 8p22 encodes a leucine-zipper protein, and its expression is altered in multiple human tumors. Proc. Natl. Acad. Sci. U.S.A. 96, 3928–3933.

Ishii, H., Vecchione, A., Murakumo, Y., Baldassarre, G., Numata, S., Trapasso, F., Alder, H., Baffa, R., Croce, C.M., 2001. FEZ1/LZTS1 gene at 8p22 suppresses cancer cell growth and regulates mitosis. Proc. Natl. Acad. Sci. U.S.A. 98, 10374–10379. doi:10.1073/pnas.181222898

Janke, C., Bulinski, J.C., 2011. Post-translational regulation of the microtubule cytoskeleton: mechanisms and functions. Nature Reviews Molecular Cell Biology 12, 773–786. doi:10.1038/nrm3227

Janke, C., Kneussel, M., 2010. Tubulin post-translational modifications: encoding functions on the neuronal microtubule cytoskeleton. Trends in Neurosciences 33, 362–372. doi:10.1016/j.tins.2010.05.001

Janosi, I.M., Chretien, D., Flyvbjerg, H., 2002. Structural microtubule cap: stability, catastrophe, rescue, and third state. Biophys J 83, 1317–1330.

Jaulin, F., Kreitzer, G., 2010. KIF17 stabilizes microtubules and contributes to epithelial morphogenesis by acting at MT plus ends with EB1 and APC. J. Cell Biol. 190, 443–460. doi:10.1083/jcb.201006044

Jiang, K., Toedt, G., Montenegro Gouveia, S., Davey, N.E., Hua, S., van der Vaart, B., Grigoriev, I., Larsen, J., Pedersen, L.B., Bezstarosti, K., Lince-Faria, M., Demmers, J., Steinmetz, M.O., Gibson, T.J., Akhmanova, A., 2012. A Proteome-wide screen for mammalian SxIP motif-containing microtubule plus-end tracking proteins. Curr. Biol. 22, 1800–1807. doi:10.1016/j.cub.2012.07.047

Jiang, K., Wang, J., Liu, J., Ward, T., Wordeman, L., Davidson, A., Wang, F., Yao, X., 2009. TIP150 interacts with and targets MCAK at the microtubule plus ends. EMBO Rep. 10, 857–865. doi:10.1038/embor.2009.94

Jimbo, T., Kawasaki, Y., Koyama, R., Sato, R., Takada, S., Haraguchi, K., Akiyama, T., 2002. Identification of a link between the tumour suppressor APC and the kinesin superfamily. Nat. Cell Biol. 4, 323–327. doi:10.1038/ncb779

Jing, F., Mogi, M., Min, L.-J., Ohshima, K., Nakaoka, H., Tsukuda, K., Wang, X., Iwanami, J., Horiuchi, M., 2013. Effect of angiotensin II type 2 receptor-interacting protein on adipose tissue function via modulation of macrophage polarization. PLoS ONE 8, e60067. doi:10.1371/journal.pone.0060067

Jordan, M.A., Thrower, D., Wilson, L., 1992. Effects of vinblastine, podophyllotoxin and nocodazole on mitotic spindles. Implications for the role of microtubule dynamics in mitosis. J. Cell. Sci. 102 (Pt 3), 401–416.

Kaverina, I., Straube, A., 2011. Regulation of cell migration by dynamic microtubules. Seminars in Cell & Developmental Biology 22, 968–974. doi:10.1016/j.semcdb.2011.09.017

Kawasaki, Y., Sato, R., Akiyama, T., 2003. Mutated APC and Asef are involved in the migration of colorectal tumour cells. Nat. Cell Biol. 5, 211–215. doi:10.1038/ncb937

Kawasaki, Y., Senda, T., Ishidate, T., Koyama, R., Morishita, T., Iwayama, Y., Higuchi, O., Akiyama, T., 2000. Asef, a link between the tumor suppressor APC and G-protein signaling. Science 289, 1194–1197.

Keller, P.J., Pampaloni, F., Stelzer, E.H.K., 2007. Three-dimensional preparation and imaging reveal intrinsic microtubule properties. Nat. Methods 4, 843–846. doi:10.1038/nmeth1087

Kennecke, H., Yerushalmi, R., Woods, R., Cheang, M.C.U., Voduc, D., Speers, C.H., Nielsen, T.O., Gelmon, K., 2010. Metastatic behavior of breast cancer subtypes. J. Clin. Oncol. 28, 3271–3277. doi:10.1200/JCO.2009.25.9820

Kim, Y., Heuser, J.E., Waterman, C.M., Cleveland, D.W., 2008. CENP-E combines a slow, processive motor and a flexible coiled coil to produce an essential motile kinetochore tether. J. Cell Biol. 181, 411–419. doi:10.1083/jcb.200802189

Kinjo, T., Isomura, M., Iwamasa, T., Nakamura, Y., 2000. Molecular cloning and characterization of two novel genes on chromosome 8p21.3. J. Hum. Genet. 45, 12–17. doi:10.1007/s100380050003

Kirschner, M., Mitchison, T., 1986. Beyond self-assembly: from microtubules to morphogenesis. Cell 45, 329–342.

Kita, K., Wittmann, T., Näthke, I.S., Waterman-Storer, C.M., 2006. Adenomatous polyposis coli on microtubule plus ends in cell extensions can promote microtubule net growth with or without EB1. Mol. Biol. Cell 17, 2331–2345. doi:10.1091/mbc.E05-06-0498

Knowlton, A.L., Vorozhko, V.V., Lan, W., Gorbsky, G.J., Stukenberg, P.T., 2009. ICIS and Aurora B coregulate the microtubule depolymerase Kif2a. Curr. Biol. 19, 758–763. doi:10.1016/j.cub.2009.03.018

Kobayashi, T., Murayama, T., 2009. Cell cycle-dependent microtubule-based dynamic transport of cytoplasmic dynein in mammalian cells. PLoS ONE 4, e7827. doi:10.1371/journal.pone.0007827

Kodama, A., Karakesisoglou, I., Wong, E., Vaezi, A., Fuchs, E., 2003. ACF7: an essential integrator of microtubule dynamics. Cell 115, 343–354.

Komarova, Y., De Groot, C.O., Grigoriev, I., Gouveia, S.M., Munteanu, E.L., Schober, J.M., Honnappa, S., Buey, R.M., Hoogenraad, C.C., Dogterom, M., Borisy, G.G., Steinmetz, M.O., Akhmanova, A., 2009. Mammalian end binding proteins control persistent microtubule growth. J. Cell Biol. 184, 691–706. doi:10.1083/jcb.200807179

Komarova, Y., Lansbergen, G., Galjart, N., Grosveld, F., Borisy, G.G., Akhmanova, A., 2005. EB1 and EB3 Control CLIP Dissociation from the Ends of Growing Microtubules. Mol Biol Cell 16, 5334–5345. doi:10.1091/mbc.E05-07-0614

Komarova, Y.A., Akhmanova, A.S., Kojima, S.-I., Galjart, N., Borisy, G.G., 2002a. Cytoplasmic linker proteins promote microtubule rescue in vivo. J. Cell Biol. 159, 589–599. doi:10.1083/jcb.200208058

Komarova, Y.A., Vorobjev, I.A., Borisy, G.G., 2002b. Life cycle of MTs: persistent growth in the cell interior, asymmetric transition frequencies and effects of the cell boundary. J. Cell. Sci. 115, 3527–3539.

Konzack, S., Thies, E., Marx, A., Mandelkow, E.-M., Mandelkow, E., 2007. Swimming against the tide: mobility of the microtubule-associated protein tau in neurons. J. Neurosci. 27, 9916–9927. doi:10.1523/JNEUROSCI.0927-07.2007

Krylyshkina, O., Anderson, K.I., Kaverina, I., Upmann, I., Manstein, D.J., Small, J.V., Toomre, D.K., 2003. Nanometer targeting of microtubules to focal adhesions. J Cell Biol 161, 853–859. doi:10.1083/jcb.200301102

Kumar, P., Wittmann, T., 2012. +TIPs: SxIPping along microtubule ends. Trends Cell Biol. 22, 418–428. doi:10.1016/j.tcb.2012.05.005

Kwok, B.H., Kapitein, L.C., Kim, J.H., Peterman, E.J.G., Schmidt, C.F., Kapoor, T.M., 2006. Allosteric inhibition of kinesin-5 modulates its processive directional motility. Nat. Chem. Biol. 2, 480–485. doi:10.1038/nchembio812

Lafanechère, L., Job, D., 2000. The third tubulin pool. Neurochem. Res. 25, 11–18.

Lam, S.W., Jimenez, C.R., Boven, E., 2014. Breast cancer classification by proteomic technologies: Current state of knowledge. Cancer Treatment Reviews 40, 129–138. doi:10.1016/j.ctrv.2013.06.006

Langford, K.J., Askham, J.M., Lee, T., Adams, M., Morrison, E.E., 2006. Examination of actin and microtubule dependent APC localisations in living mammalian cells. BMC Cell Biol 7, 3. doi:10.1186/1471-2121-7-3

Langlands, F.E., Horgan, K., Dodwell, D.D., Smith, L., 2013. Breast cancer subtypes: response to radiotherapy and potential radiosensitisation. British Journal of Radiology 86, 20120601–20120601. doi:10.1259/bjr.20120601

Lansbergen, G., Akhmanova, A., 2006. Microtubule plus end: a hub of cellular activities. Traffic 7, 499–507. doi:10.1111/j.1600-0854.2006.00400.x

Lawrence, C.J., Dawe, R.K., Christie, K.R., Cleveland, D.W., Dawson, S.C., Endow, S.A., Goldstein, L.S.B., Goodson, H.V., Hirokawa, N., Howard, J., Malmberg, R.L., McIntosh, J.R., Miki, H., Mitchison, T.J., Okada, Y., Reddy, A.S.N., Saxton, W.M., Schliwa, M., Scholey, J.M., Vale, R.D., Walczak, C.E., Wordeman, L., 2004. A standardized kinesin nomenclature. J. Cell Biol. 167, 19–22. doi:10.1083/jcb.200408113

Lee, S., Bang, S., Song, K., Lee, I., 2006. Differential expression in normal-adenoma-carcinoma sequence suggests complex molecular carcinogenesis in colon. Oncol. Rep. 16, 747–754.

Lee, T., Langford, K.J., Askham, J.M., Brüning-Richardson, A., Morrison, E.E., 2008. MCAK associates with EB1. Oncogene 27, 2494–2500. doi:10.1038/sj.onc.1210867

Li, D., Gao, J., Yang, Y., Sun, L., Suo, S., Luo, Y., Shui, W., Zhou, J., Liu, M., 2014. CYLD coordinates with EB1 to regulate microtubule dynamics and cell migration. Cell Cycle 13, 974–983. doi:10.4161/cc.27838

Li, J.-M., Mogi, M., Tsukuda, K., Tomochika, H., Iwanami, J., Min, L.-J., Nahmias, C., Iwai, M., Horiuchi, M., 2007. Angiotensin II-induced neural differentiation via angiotensin II type 2 (AT2) receptor-MMS2 cascade involving interaction between AT2 receptor-interacting protein and Src homology 2 domain-containing protein-tyrosine phosphatase 1. Mol. Endocrinol. 21, 499–511. doi:10.1210/me.2006-0005

Li, S., Han, B., Liu, G., Li, S., Ouellet, J., Labrie, F., Pelletier, G., 2010. Immunocytochemical localization of sex steroid hormone receptors in normal human mammary gland. J. Histochem. Cytochem. 58, 509–515. doi:10.1369/jhc.2009.954644

Li, X., Liu, H., Yu, T., Dong, Z., Tang, L., Sun, X., 2014. Loss of MTUS1 in gastric cancer promotes tumor growth and metastasis. Neoplasma 61, 128–135. doi:10.4149/neo_2014_018

Ligon, L.A., Shelly, S.S., Tokito, M.K., Holzbaur, E.L.F., 2006. Microtubule binding proteins CLIP-170, EB1, and p150Glued form distinct plus-end complexes. FEBS Lett. 580, 1327–1332. doi:10.1016/j.febslet.2006.01.050

Lim, E., Vaillant, F., Wu, D., Forrest, N.C., Pal, B., Hart, A.H., Asselin-Labat, M.-L., Gyorki, D.E., Ward, T., Partanen, A., Feleppa, F., Huschtscha, L.I., Thorne, H.J., Fox, S.B., Yan, M., French, J.D., Brown, M.A., Smyth, G.K., Visvader, J.E., Lindeman, G.J., 2009. Aberrant luminal progenitors as the candidate target population for basal tumor development in BRCA1 mutation carriers. Nat Med 15, 907–913. doi:10.1038/nm.2000

Liu, L., Tommasi, S., Lee, D.-H., Dammann, R., Pfeifer, G.P., 2003. Control of microtubule stability by the RASSF1A tumor suppressor. Oncogene 22, 8125–8136. doi:10.1038/sj.onc.1206984

Lolkema, M.P., Mehra, N., Jorna, A.S., van Beest, M., Giles, R.H., Voest, E.E., 2004. The von Hippel-Lindau tumor suppressor protein influences microtubule dynamics at the cell periphery. Exp. Cell Res. 301, 139–146. doi:10.1016/j.yexcr.2004.07.016

Lomakin, A.J., Semenova, I., Zaliapin, I., Kraikivski, P., Nadezhdina, E., Slepchenko, B.M., Akhmanova, A., Rodionov, V., 2009. CLIP-170-dependent capture of membrane organelles by microtubules initiates minus-end directed transport. Dev. Cell 17, 323–333. doi:10.1016/j.devcel.2009.07.010

Long, J.B., Bagonis, M., Lowery, L.A., Lee, H., Danuser, G., Vactor, D.V., 2013. Multiparametric Analysis of CLASP-Interacting Protein Functions during Interphase Microtubule Dynamics. Mol. Cell. Biol. 33, 1528–1545. doi:10.1128/MCB.01442-12

Lotti, L.V., Ottini, L., D'Amico, C., Gradini, R., Cama, A., Belleudi, F., Frati, L., Torrisi, M.R., Mariani-Costantini, R., 2002. Subcellular localization of the BRCA1 gene product in mitotic cells. Genes Chromosom. Cancer 35, 193–203. doi:10.1002/gcc.10105

Louie, R.K., Bahmanyar, S., Siemers, K.A., Votin, V., Chang, P., Stearns, T., Nelson, W.J., Barth, A.I.M., 2004. Adenomatous polyposis coli and EB1 localize in close proximity of the mother centriole and EB1 is a functional component of centrosomes. J Cell Sci 117, 1117–1128. doi:10.1242/jcs.00939

Lowery, L.A., Stout, A., Faris, A.E., Ding, L., Baird, M.A., Davidson, M.W., Danuser, G., Vactor, D.V., 2013. Growth cone-specific functions of XMAP215 in restricting microtubule dynamics and promoting axonal outgrowth. Neural Development 8, 22. doi:10.1186/1749-8104-8-22

Lyle, K., Kumar, P., Wittmann, T., 2009a. SnapShot: Microtubule Regulators I. Cell 136, 380, 380.e1. doi:10.1016/j.cell.2009.01.010

Lyle, K., Kumar, P., Wittmann, T., 2009b. SnapShot: Microtubule regulators II. Cell 136, 566, 566.e1. doi:10.1016/j.cell.2009.01.011

Lynch, H.T., Silva, E., Snyder, C., Lynch, J.F., 2008. Hereditary breast cancer: part I. Diagnosing hereditary breast cancer syndromes. Breast J 14, 3–13. doi:10.1111/j.1524-4741.2007.00515.x

Maiato, H., DeLuca, J., Salmon, E.D., Earnshaw, W.C., 2004. The dynamic kinetochore-microtubule interface. J. Cell. Sci. 117, 5461–5477. doi:10.1242/jcs.01536

Maiato, H., Sampaio, P., Lemos, C.L., Findlay, J., Carmena, M., Earnshaw, W.C., Sunkel, C.E., 2002. MAST/Orbit has a role in microtubule-kinetochore attachment and is essential for chromosome alignment and maintenance of spindle bipolarity. J. Cell Biol. 157, 749–760. doi:10.1083/jcb.200201101

Maiato, H., Sampaio, P., Sunkel, C.E., 2004. Microtubule-associated proteins and their essential roles during mitosis. Int. Rev. Cytol. 241, 53–153. doi:10.1016/S0074-7696(04)41002-X

Mandelkow, E.M., Mandelkow, E., 1985. Unstained microtubules studied by cryo-electron microscopy. Substructure, supertwist and disassembly. J. Mol. Biol. 181, 123–135.

Mandelkow, E.M., Mandelkow, E., Milligan, R.A., 1991. Microtubule dynamics and microtubule caps: a time-resolved cryo-electron microscopy study. J. Cell Biol. 114, 977–991.

Maney, T., Wagenbach, M., Wordeman, L., 2001. Molecular dissection of the microtubule depolymerizing activity of mitotic centromere-associated kinesin. J. Biol. Chem. 276, 34753–34758. doi:10.1074/jbc.M106626200

Mannello, F., Tonti, G.A., Canestrari, F., 2008. Nutrients and nipple aspirate fluid composition: the breast microenvironment regulates protein expression and cancer aetiology. Genes Nutr 3, 77–85. doi:10.1007/s12263-008-0087-0

Manneville, J.-B., Jehanno, M., Etienne-Manneville, S., 2010. Dlg1 binds GKAP to control dynein association with microtubules, centrosome positioning, and cell polarity. J. Cell Biol. 191, 585–598. doi:10.1083/jcb.201002151

Manning, A.L., Compton, D.A., 2008. SnapShot: Nonmotor Proteins in Spindle Assembly. Cell 134, 694–694.e1. doi:10.1016/j.cell.2008.08.001

Margolis, R.L., Wilson, L., 1978. Opposite end assembly and disassembly of microtubules at steady state in vitro. Cell 13, 1–8.

Margolis, R.L., Wilson, L., 1998. Microtubule treadmilling: what goes around comes around. Bioessays 20, 830–836. doi:10.1002/(SICI)1521-1878(199810)20:10<830::AID-BIES8>3.0.CO;2-N

Massoumi, R., 2011. CYLD: a deubiquitination enzyme with multiple roles in cancer. Future Oncology 7, 285–297. doi:10.2217/fon.10.187

Maxwell, C.A., Keats, J.J., Crainie, M., Sun, X., Yen, T., Shibuya, E., Hendzel, M., Chan, G., Pilarski, L.M., 2003. RHAMM Is a Centrosomal Protein That Interacts with Dynein and Maintains Spindle Pole Stability. Mol. Biol. Cell 14, 2262–2276. doi:10.1091/mbc.E02-07-0377

Mayr, M.I., Hümmer, S., Bormann, J., Grüner, T., Adio, S., Woehlke, G., Mayer, T.U., 2007. The Human Kinesin Kif18A Is a Motile Microtubule Depolymerase Essential for Chromosome Congression. Current Biology 17, 488–498. doi:10.1016/j.cub.2007.02.036

McNally, F.J., 1996. Modulation of microtubule dynamics during the cell cycle. Curr. Opin. Cell Biol. 8, 23–29.

McNally, F.J., Okawa, K., Iwamatsu, A., Vale, R.D., 1996. Katanin, the microtubule-severing ATPase, is concentrated at centrosomes. J. Cell. Sci. 109 (Pt 3), 561–567.

Melki, R., Carlier, M.F., Pantaloni, D., Timasheff, S.N., 1989. Cold depolymerization of microtubules to double rings: geometric stabilization of assemblies. Biochemistry 28, 9143–9152.

Mennella, V., Rogers, G.C., Rogers, S.L., Buster, D.W., Vale, R.D., Sharp, D.J., 2005. Functionally distinct kinesin-13 family members cooperate to regulate microtubule dynamics during interphase. Nat Cell Biol 7, 235–245. doi:10.1038/ncb1222

Mimori-Kiyosue, Y., Grigoriev, I., Lansbergen, G., Sasaki, H., Matsui, C., Severin, F., Galjart, N., Grosveld, F., Vorobjev, I., Tsukita, S., Akhmanova, A., 2005. CLASP1 and CLASP2 bind to EB1 and regulate microtubule plus-end dynamics at the cell cortex. J. Cell Biol. 168, 141–153. doi:10.1083/jcb.200405094

Mimori-Kiyosue, Y., Shiina, N., Tsukita, S., 2000. The dynamic behavior of the APC-binding protein EB1 on the distal ends of microtubules. Curr. Biol. 10, 865–868.

Mimori-Kiyosue, Y., Tsukita, S., 2001. Where is APC going? J. Cell Biol. 154, 1105–1109. doi:10.1083/jcb.200106113

Mimori-Kiyosue, Y., Tsukita, S., 2003. “Search-and-Capture” of Microtubules through Plus-End-Binding Proteins (+TIPs). J Biochem 134, 321–326. doi:10.1093/jb/mvg148

Min, L.-J., Mogi, M., Iwanami, J., Jing, F., Tsukuda, K., Ohshima, K., Horiuchi, M., 2012. Angiotensin II type 2 receptor-interacting protein prevents vascular senescence. J Am Soc Hypertens 6, 179–184. doi:10.1016/j.jash.2012.01.006

Mishima, M., Maesaki, R., Kasa, M., Watanabe, T., Fukata, M., Kaibuchi, K., Hakoshima, T., 2007. Structural basis for tubulin recognition by cytoplasmic linker protein 170 and its autoinhibition. Proc. Natl. Acad. Sci. U.S.A. 104, 10346–10351. doi:10.1073/pnas.0703876104

Mitchison, T., Kirschner, M., 1984. Dynamic instability of microtubule growth. Nature 312, 237–242.

Mitchison, T.J., 1993. Localization of an exchangeable GTP binding site at the plus end of microtubules. Science 261, 1044–1047.

Moore, A.T., Rankin, K.E., von Dassow, G., Peris, L., Wagenbach, M., Ovechkina, Y., Andrieux, A., Job, D., Wordeman, L., 2005. MCAK associates with the tips of polymerizing microtubules. J. Cell Biol. 169, 391–397. doi:10.1083/jcb.200411089

Moores, C.A., Cooper, J., Wagenbach, M., Ovechkina, Y., Wordeman, L., Milligan, R.A., 2006. The role of the kinesin-13 neck in microtubule depolymerization. Cell Cycle 5, 1812–1815.

Moores, C.A., Milligan, R.A., 2006. Lucky 13-microtubule depolymerisation by kinesin-13 motors. J. Cell. Sci. 119, 3905–3913. doi:10.1242/jcs.03224

Morris, P.G., McArthur, H.L., Hudis, C.A., 2009. Therapeutic options for metastatic breast cancer. Expert Opinion on Pharmacotherapy 10, 967–981. doi:10.1517/14656560902834961

Morrison, E.E., Wardleworth, B.N., Askham, J.M., Markham, A.F., Meredith, D.M., 1998. EB1, a protein which interacts with the APC tumour suppressor, is associated with the microtubule cytoskeleton throughout the cell cycle. Oncogene 17, 3471–3477. doi:10.1038/sj.onc.1202247

Moseley, J.B., Bartolini, F., Okada, K., Wen, Y., Gundersen, G.G., Goode, B.L., 2007. Regulated binding of adenomatous polyposis coli protein to actin. J. Biol. Chem. 282, 12661–12668. doi:10.1074/jbc.M610615200

Munemitsu, S., Souza, B., Müller, O., Albert, I., Rubinfeld, B., Polakis, P., 1994. The APC gene product associates with microtubules in vivo and promotes their assembly in vitro. Cancer Res. 54, 3676–3681.

Muranen, T., Grönholm, M., Lampin, A., Lallemand, D., Zhao, F., Giovannini, M., Carpén, O., 2007. The tumor suppressor merlin interacts with microtubules and modulates Schwann cell microtubule cytoskeleton. Hum. Mol. Genet. 16, 1742–1751. doi:10.1093/hmg/ddm122

Nabeshima, K., Inoue, T., Shimao, Y., Kataoka, H., Koono, M., 1999. Cohort migration of carcinoma cells: differentiated colorectal carcinoma cells move as coherent cell clusters or sheets. Histol. Histopathol. 14, 1183–1197.

Nabeshima, K., Inoue, T., Shimao, Y., Okada, Y., Itoh, Y., Seiki, M., Koono, M., 2000. Front-cell-specific expression of membrane-type 1 matrix metalloproteinase and gelatinase A during cohort migration of colon carcinoma cells induced by hepatocyte growth factor/scatter factor. Cancer Res. 60, 3364–3369.

Nagase, H., Nakamura, Y., 1993. Mutations of the APC (adenomatous polyposis coli) gene. Hum. Mutat. 2, 425–434. doi:10.1002/humu.1380020602

Nahmias, C., Rodrigues-Ferreira, S., 2014. Angiotensin II in breast cancer metastasis: strategy, tools and models towards new cancer therapies., in: Breast, Cervical and Prostate Cancer.

Nakagawa, H., Koyama, K., Murata, Y., Morito, M., Akiyama, T., Nakamura, Y., 2000. EB3, a novel member of the EB1 family preferentially expressed in the central nervous system, binds to a CNS-specific APC homologue. Oncogene 19, 210–216. doi:10.1038/sj.onc.1203308

Nakamura, M., Zhou, X.Z., Lu, K.P., 2001. Critical role for the EB1 and APC interaction in the regulation of microtubule polymerization. Curr. Biol. 11, 1062–1067.

Nakano, A., Kato, H., Watanabe, T., Min, K.-D., Yamazaki, S., Asano, Y., Seguchi, O., Higo, S., Shintani, Y., Asanuma, H., Asakura, M., Minamino, T., Kaibuchi, K., Mochizuki, N., Kitakaze, M., Takashima, S., 2010. AMPK controls the speed of microtubule polymerization and directional cell migration through CLIP-170 phosphorylation. Nat. Cell Biol. 12, 583–590. doi:10.1038/ncb2060

Nelson, C.M., Bissell, M.J., 2006. Of extracellular matrix, scaffolds, and signaling: tissue architecture regulates development, homeostasis, and cancer. Annu. Rev. Cell Dev. Biol. 22, 287–309. doi:10.1146/annurev.cellbio.22.010305.104315

Neville, M.C., Daniel, C.W., 1987. The mammary gland. Development, regulation and function. Plenum Press.

Newton, C.N., Wagenbach, M., Ovechkina, Y., Wordeman, L., Wilson, L., 2004. MCAK, a Kin I kinesin, increases the catastrophe frequency of steady-state HeLa cell microtubules in an ATP-dependent manner in vitro. FEBS Lett. 572, 80–84. doi:10.1016/j.febslet.2004.06.093

Niethammer, P., Bastiaens, P., Karsenti, E., 2004. Stathmin-tubulin interaction gradients in motile and mitotic cells. Science 303, 1862–1866. doi:10.1126/science.1094108

Nishigaki, R., Osaki, M., Hiratsuka, M., Toda, T., Murakami, K., Jeang, K.-T., Ito, H., Inoue, T., Oshimura, M., 2005. Proteomic identification of differentially-expressed genes in human gastric carcinomas. Proteomics 5, 3205–3213. doi:10.1002/pmic.200401307

Nogales, E., Wolf, S.G., Downing, K.H., 1998. Structure of the alpha beta tubulin dimer by electron crystallography. Nature 391, 199–203. doi:10.1038/34465

Nonaka, D., Fabbri, A., Roz, L., Mariani, L., Vecchione, A., Moore, G.W., Tavecchio, L., Croce, C.M., Sozzi, G., 2005. Reduced FEZ1/LZTS1 expression and outcome prediction in lung cancer. Cancer Res. 65, 1207–1212. doi:10.1158/0008-5472.CAN-04-3461

Nouet, S., Amzallag, N., Li, J.-M., Louis, S., Seitz, I., Cui, T.-X., Alleaume, A.-M., Benedetto, M.D., Boden, C., Masson, M., Strosberg, A.D., Horiuchi, M., Couraud, P.-O., Nahmias, C., 2004. Trans-inactivation of Receptor Tyrosine Kinases by Novel Angiotensin II AT2 Receptor-interacting Protein, ATIP. J. Biol. Chem. 279, 28989–28997. doi:10.1074/jbc.M403880200

Nyhan, M.J., O'Sullivan, G.C., McKenna, S.L., 2008. Role of the VHL (von Hippel-Lindau) gene in renal cancer: a multifunctional tumour suppressor. Biochem. Soc. Trans. 36, 472–478. doi:10.1042/BST0360472

O'Brien, K.M., Cole, S.R., Tse, C.-K., Perou, C.M., Carey, L.A., Foulkes, W.D., Dressler, L.G., Geradts, J., Millikan, R.C., 2010. Intrinsic breast tumor subtypes, race, and long-term survival in the Carolina Breast Cancer Study. Clin. Cancer Res. 16, 6100–6110. doi:10.1158/1078-0432.CCR-10-1533

Ogawa, T., Nitta, R., Okada, Y., Hirokawa, N., 2004. A common mechanism for microtubule destabilizers-M type kinesins stabilize curling of the protofilament using the class-specific neck and loops. Cell 116, 591–602.

Ohi, R., Coughlin, M.L., Lane, W.S., Mitchison, T.J., 2003. An inner centromere protein that stimulates the microtubule depolymerizing activity of a KinI kinesin. Dev. Cell 5, 309–321.

Onken, M.D., Worley, L.A., Harbour, J.W., 2008. A Metastasis Modifier Locus on Human Chromosome 8p in Uveal Melanoma Identified by Integrative Genomic Analysis. Clin Cancer Res 14, 3737–3745. doi:10.1158/1078-0432.CCR-07-5144

Ono, K., Uzawa, K., Nakatsuru, M., Shiiba, M., Mochida, Y., Tada, A., Bukawa, H., Miyakawa, A., Yokoe, H., Tanzawa, H., 2003. Down-regulation of FEZ1/LZTS1 gene with frequent loss of heterozygosity in oral squamous cell carcinomas. Int. J. Oncol. 23, 297–302.

Ookata, K., Hisanaga, S., Bulinski, J.C., Murofushi, H., Aizawa, H., Itoh, T.J., Hotani, H., Okumura, E., Tachibana, K., Kishimoto, T., 1995. Cyclin B interaction with microtubule-associated protein 4 (MAP4) targets p34cdc2 kinase to microtubules and is a potential regulator of M-phase microtubule dynamics. J. Cell Biol. 128, 849–862.

Oosawa, F., 1970. Size distribution of protein polymers. J. Theor. Biol. 27, 69–86.

Orimo, T., Ojima, H., Hiraoka, N., Saito, S., Kosuge, T., Kakisaka, T., Yokoo, H., Nakanishi, K., Kamiyama, T., Todo, S., Hirohashi, S., Kondo, T., 2008. Proteomic profiling reveals the prognostic value of adenomatous polyposis coli-end-binding protein 1 in hepatocellular carcinoma. Hepatology 48, 1851–1863. doi:10.1002/hep.22552

Pagano, A., Honoré, S., Mohan, R., Berges, R., Akhmanova, A., Braguer, D., 2012. Epothilone B inhibits migration of glioblastoma cells by inducing microtubule catastrophes and affecting EB1 accumulation at microtubule plus ends. Biochem. Pharmacol. 84, 432–443. doi:10.1016/j.bcp.2012.05.010

Paget, S., 1889. The Distribution of Secondary Growths in Cancer of the Breast. The Lancet, Originally published as Volume 1, Issue 3421 133, 571–573. doi:10.1016/S0140-6736(00)49915-0

Palazzo, A.F., Cook, T.A., Alberts, A.S., Gundersen, G.G., 2001. mDia mediates Rho-regulated formation and orientation of stable microtubules. Nat Cell Biol 3, 723–729. doi:10.1038/35087035

Palazzo, A.F., Joseph, H.L., Chen, Y.J., Dujardin, D.L., Alberts, A.S., Pfister, K.K., Vallee, R.B., Gundersen, G.G., 2001. Cdc42, dynein, and dynactin regulate MTOC reorientation independent of Rho-regulated microtubule stabilization. Curr. Biol. 11, 1536–1541.

Perez, F., Diamantopoulos, G.S., Stalder, R., Kreis, T.E., 1999. CLIP-170 Highlights Growing Microtubule Ends In Vivo. Cell 96, 517–527. doi:10.1016/S0092-8674(00)80656-X

Peris, L., Thery, M., Fauré, J., Saoudi, Y., Lafanechère, L., Chilton, J.K., Gordon-Weeks, P., Galjart, N., Bornens, M., Wordeman, L., Wehland, J., Andrieux, A., Job, D., 2006. Tubulin tyrosination is a major factor affecting the recruitment of CAP-Gly proteins at microtubule plus ends. J. Cell Biol. 174, 839–849. doi:10.1083/jcb.200512058

Perou, C.M., Sørlie, T., Eisen, M.B., van de Rijn, M., Jeffrey, S.S., Rees, C.A., Pollack, J.R., Ross, D.T., Johnsen, H., Akslen, L.A., Fluge, O., Pergamenschikov, A., Williams, C., Zhu, S.X., Lønning, P.E., Børresen-Dale, A.L., Brown, P.O., Botstein, D., 2000. Molecular portraits of human breast tumours. Nature 406, 747–752. doi:10.1038/35021093

Pfister, A.S., Hadjihannas, M.V., Röhrig, W., Schambony, A., Behrens, J., 2012. Amer2 protein interacts with EB1 protein and adenomatous polyposis coli (APC) and controls microtubule stability and cell migration. J. Biol. Chem. 287, 35333–35340. doi:10.1074/jbc.M112.385393

Piehl, M., Cassimeris, L., 2003. Organization and Dynamics of Growing Microtubule Plus Ends during Early Mitosis. Mol. Biol. Cell 14, 916–925. doi:10.1091/mbc.E02-09-0607

Pierre, P., Scheel, J., Rickard, J.E., Kreis, T.E., 1992. CLIP-170 links endocytic vesicles to microtubules. Cell 70, 887–900.

Pietras, K., Östman, A., 2010. Hallmarks of cancer: Interactions with the tumor stroma. Experimental Cell Research, Special Issue Celebrating the 60-Year Anniversary of ECR and the 200-Year Anniversary of the Karolinska Institute 316, 1324–1331. doi:10.1016/j.yexcr.2010.02.045

Pils, D., Horak, P., Gleiss, A., Sax, C., Fabjani, G., Moebus, V.J., Zielinski, C., Reinthaller, A., Zeillinger, R., Krainer, M., 2005. Five genes from chromosomal band 8p22 are significantly down-regulated in ovarian carcinoma: N33 and EFA6R have a potential impact on overall survival. Cancer 104, 2417–2429. doi:10.1002/cncr.21538

Piperno, G., LeDizet, M., Chang, X.J., 1987. Microtubules containing acetylated alpha-tubulin in mammalian cells in culture. J. Cell Biol. 104, 289–302.

Polakis, P., 1997. The adenomatous polyposis coli (APC) tumor suppressor. Biochimica et Biophysica Acta (BBA) - Reviews on Cancer 1332, F127–F147. doi:10.1016/S0304-419X(97)00008-5

Portschy, P.R., Marmor, S., Nzara, R., Virnig, B.A., Tuttle, T.M., 2013. Trends in incidence and management of lobular carcinoma in situ: a population-based analysis. Ann. Surg. Oncol. 20, 3240–3246. doi:10.1245/s10434-013-3121-4

Poste, G., Fidler, I.J., 1980. The pathogenesis of cancer metastasis. Nature 283, 139–146.

Prat, A., Perou, C.M., 2009. Mammary development meets cancer genomics. Nat. Med. 15, 842–844. doi:10.1038/nm0809-842

Pryer, N.K., Walker, R.A., Skeen, V.P., Bourns, B.D., Soboeiro, M.F., Salmon, E.D., 1992. Brain microtubule-associated proteins modulate microtubule dynamic instability in vitro. Real-time observations using video microscopy. J. Cell. Sci. 103 (Pt 4), 965–976.

Putkey, F.R., Cramer, T., Morphew, M.K., Silk, A.D., Johnson, R.S., McIntosh, J.R., Cleveland, D.W., 2002. Unstable Kinetochore-Microtubule Capture and Chromosomal Instability Following Deletion of CENP-E. Developmental Cell 3, 351–365. doi:10.1016/S1534-5807(02)00255-1

Raemaekers, T., Ribbeck, K., Beaudouin, J., Annaert, W., Camp, M.V., Stockmans, I., Smets, N., Bouillon, R., Ellenberg, J., Carmeliet, G., 2003. NuSAP, a novel microtubule-associated protein involved in mitotic spindle organization. J Cell Biol 162, 1017–1029. doi:10.1083/jcb.200302129

Rakha, E.A., Reis-Filho, J.S., Baehner, F., Dabbs, D.J., Decker, T., Eusebi, V., Fox, S.B., Ichihara, S., Jacquemier, J., Lakhani, S.R., Palacios, J., Richardson, A.L., Schnitt, S.J., Schmitt, F.C., Tan, P.-H., Tse, G.M., Badve, S., Ellis, I.O., 2010. Breast cancer prognostic classification in the molecular era: the role of histological grade. Breast Cancer Research 12, 207. doi:10.1186/bcr2607

Reis-Filho, J.S., Westbury, C., Pierga, J.-Y., 2006. The impact of expression profiling on prognostic and predictive testing in breast cancer. J. Clin. Pathol. 59, 225–231. doi:10.1136/jcp.2005.028324

Ren, X.D., Kiosses, W.B., Schwartz, M.A., 1999. Regulation of the small GTP-binding protein Rho by cell adhesion and the cytoskeleton. EMBO J. 18, 578–585. doi:10.1093/emboj/18.3.578

Rexer, B.N., Arteaga, C.L., 2012. Intrinsic and acquired resistance to HER2-targeted therapies in HER2 gene-amplified breast cancer: mechanisms and clinical implications. Crit Rev Oncog 17, 1–16.

Richter, A.M., Pfeifer, G.P., Dammann, R.H., 2009. The RASSF proteins in cancer; from epigenetic silencing to functional characterization. Biochimica et Biophysica Acta (BBA) - Reviews on Cancer 1796, 114–128. doi:10.1016/j.bbcan.2009.03.004

Rickard, J.E., Kreis, T.E., 1990. Identification of a novel nucleotide-sensitive microtubule-binding protein in HeLa cells. J. Cell Biol. 110, 1623–1633.

Ridley, A.J., Schwartz, M.A., Burridge, K., Firtel, R.A., Ginsberg, M.H., Borisy, G., Parsons, J.T., Horwitz, A.R., 2003. Cell migration: integrating signals from front to back. Science 302, 1704–1709. doi:10.1126/science.1092053

Riehemann, K., Sorg, C., 1993. Sequence homologies between four cytoskeleton-associated proteins. Trends Biochem. Sci. 18, 82–83.

Rodionov, V.I., Borisy, G.G., 1997. Microtubule treadmilling in vivo. Science 275, 215–218.

Rodrigues-Ferreira, S., Di Tommaso, A., Dimitrov, A., Cazaubon, S., Gruel, N., Colasson, H., Nicolas, A., Chaverot, N., Molinié, V., Reyal, F., Sigal-Zafrani, B., Terris, B., Delattre, O., Radvanyi, F., Perez, F., Vincent-Salomon, A., Nahmias, C., 2009. 8p22 MTUS1 Gene Product ATIP3 Is a Novel Anti-Mitotic Protein Underexpressed in Invasive Breast Carcinoma of Poor Prognosis. PLoS ONE 4, e7239. doi:10.1371/journal.pone.0007239

Rodrigues-Ferreira, S., le Rouzic, E., Pawlowski, T., Srivastava, A., Margottin-Goguet, F., Nahmias, C., 2013. AT2 Receptor-Interacting Proteins ATIPs in the Brain. International Journal of Hypertension 2013, 1–6. doi:10.1155/2013/513047

Rodrigues-Ferreira, S., Nahmias, C., 2010. An ATIPical family of angiotensin II AT2 receptor-interacting proteins. Trends in Endocrinology & Metabolism 21, 684–690. doi:10.1016/j.tem.2010.08.009

Rogers, S.L., Rogers, G.C., Sharp, D.J., Vale, R.D., 2002. Drosophila EB1 is important for proper assembly, dynamics, and positioning of the mitotic spindle. J. Cell Biol. 158, 873–884. doi:10.1083/jcb.200202032

Rogler, A., Hoja, S., Giedl, J., Ekici, A.B., Wach, S., Taubert, H., Goebell, P.J., Wullich, B., Stöckle, M., Lehmann, J., Petsch, S., Hartmann, A., Stoehr, R., 2014. Loss of MTUS1/ATIP expression is associated with adverse outcome in advanced bladder carcinomas: data from a retrospective study. BMC Cancer 14, 214. doi:10.1186/1471-2407-14-214

Rong, R., Jin, W., Zhang, J., Sheikh, M.S., Huang, Y., 2004. Tumor suppressor RASSF1A is a microtubule-binding protein that stabilizes microtubules and induces G2/M arrest. Oncogene 23, 8216–8230. doi:10.1038/sj.onc.1207901

Rosell, R., Perez-Roca, L., Sanchez, J.J., Cobo, M., Moran, T., Chaib, I., Provencio, M., Domine, M., Sala, M.A., Jimenez, U., Diz, P., Barneto, I., Macias, J.A., de Las Peñas, R., Catot, S., Isla, D., Sanchez, J.M., Ibeas, R., Lopez-Vivanco, G., Oramas, J., Mendez, P., Reguart, N., Blanco, R., Taron, M., 2009. Customized treatment in non-small-cell lung cancer based on EGFR mutations and BRCA1 mRNA expression. PLoS ONE 4, e5133. doi:10.1371/journal.pone.0005133

Roussos, E.T., Balsamo, M., Alford, S.K., Wyckoff, J.B., Gligorijevic, B., Wang, Y., Pozzuto, M., Stobezki, R., Goswami, S., Segall, J.E., Lauffenburger, D.A., Bresnick, A.R., Gertler, F.B., Condeelis, J.S., 2011. Mena invasive (MenaINV) promotes multicellular streaming motility and transendothelial migration in a mouse model of breast cancer. J. Cell. Sci. 124, 2120–2131. doi:10.1242/jcs.086231

Rovini, A., Gauthier, G., Berges, R., Kruczynski, A., Braguer, D., Honore, S., 2013. Anti-Migratory Effect of Vinflunine in Endothelial and Glioblastoma Cells Is Associated with Changes in EB1 C-Terminal Detyrosinated/Tyrosinated Status. PLoS One 8. doi:10.1371/journal.pone.0065694

Rowe, R.G., Weiss, S.J., 2008. Breaching the basement membrane: who, when and how? Trends Cell Biol. 18, 560–574. doi:10.1016/j.tcb.2008.08.007

Russell, P.A., Pharoah, P.D., De Foy, K., Ramus, S.J., Symmonds, I., Wilson, A., Scott, I., Ponder, B.A., Gayther, S.A., 2000. Frequent loss of BRCA1 mRNA and protein expression in sporadic ovarian cancers. Int. J. Cancer 87, 317–321.

Salaycik, K.J., Fagerstrom, C.J., Murthy, K., Tulu, U.S., Wadsworth, P., 2005. Quantification of microtubule nucleation, growth and dynamics in wound-edge cells. J. Cell. Sci. 118, 4113–4122. doi:10.1242/jcs.02531

Salmon, E.D., 2005. Microtubules: A Ring for the Depolymerization Motor. Current Biology 15, R299–R302. doi:10.1016/j.cub.2005.04.005

Sanchez, C., El Hajj Diab, D., Connord, V., Clerc, P., Meunier, E., Pipy, B., Payré, B., Tan, R.P., Gougeon, M., Carrey, J., Gigoux, V., Fourmy, D., 2014. Targeting a G-protein-coupled receptor overexpressed in endocrine tumors by magnetic nanoparticles to induce cell death. ACS Nano 8, 1350–1363. doi:10.1021/nn404954s

Sapir, T., Elbaum, M., Reiner, O., 1997. Reduction of microtubule catastrophe events by LIS1, platelet-activating factor acetylhydrolase subunit. The EMBO Journal 16, 6977–6984. doi:10.1093/emboj/16.23.6977

Scarpace, S.L., 2012. Eribulin Mesylate (E7389): Review of Efficacy and Tolerability in Breast, Pancreatic, Head and Neck, and Non–Small Cell Lung Cancer. Clinical Therapeutics 34, 1467–1473. doi:10.1016/j.clinthera.2012.06.003

Schedin, P., Hovey, R.C., 2010. Editorial: The mammary stroma in normal development and function. J Mammary Gland Biol Neoplasia 15, 275–277. doi:10.1007/s10911-010-9191-z

Schmeichel, K.L., Weaver, V.M., Bissell, M.J., 1998. Structural cues from the tissue microenvironment are essential determinants of the human mammary epithelial cell phenotype. J Mammary Gland Biol Neoplasia 3, 201–213.

Schnitt, S.J., 2010. Classification and prognosis of invasive breast cancer: from morphology to molecular taxonomy. Mod Pathol 23, S60–S64. doi:10.1038/modpathol.2010.33

Schober, J.M., Cain, J.M., Komarova, Y.A., Borisy, G.G., 2009. Migration and actin protrusion in melanoma cells are regulated by EB1 protein. Cancer Lett. 284, 30–36. doi:10.1016/j.canlet.2009.04.007

Schrøder, J.M., Schneider, L., Christensen, S.T., Pedersen, L.B., 2007. EB1 is required for primary cilia assembly in fibroblasts. Curr. Biol. 17, 1134–1139. doi:10.1016/j.cub.2007.05.055

Schuyler, S.C., Pellman, D., 2001. Microtubule "plus-end-tracking proteins": The end is just the beginning. Cell 105, 421–424.

Scully, O.J., Bay, B.-H., Yip, G., Yu, Y., 2012. Breast cancer metastasis. Cancer Genomics Proteomics 9, 311–320.

Seibold, S., Rudroff, C., Weber, M., Galle, J., Wanner, C., Marx, M., 2003. Identification of a new tumor suppressor gene located at chromosome 8p21.3-22. The FASEB Journal. doi:10.1096/fj.02-0934fje

Sharp, D.J., Mennella, V., Buster, D.W., 2005. KLP10A and KLP59C: the dynamic duo of microtubule depolymerization. Cell Cycle 4, 1482–1485.

Shelden, E., Wadsworth, P., 1993. Observation and quantification of individual microtubule behavior in vivo: microtubule dynamics are cell-type specific. J. Cell Biol. 120, 935–945.

Smal, I., Grigoriev, I., Akhmanova, A., Niessen, W.J., Meijering, E., 2009. Accurate estimation of microtubule dynamics using kymographs and variable-rate particle filters. Conf Proc IEEE Eng Med Biol Soc 2009, 1012–1015. doi:10.1109/IEMBS.2009.5333350

Smith, K.J., Levy, D.B., Maupin, P., Pollard, T.D., Vogelstein, B., Kinzler, K.W., 1994. Wild-type but not mutant APC associates with the microtubule cytoskeleton. Cancer Res. 54, 3672–3675.

Smole, Z., Thoma, C.R., Applegate, K.T., Duda, M., Gutbrodt, K.L., Danuser, G., Krek, W., 2014. Tumor Suppressor NF2/Merlin Is a Microtubule Stabilizer. Cancer Res 74, 353–362. doi:10.1158/0008-5472.CAN-13-1334

Sorlie, T., Perou, C.M., Tibshirani, R., Aas, T., Geisler, S., Johnsen, H., Hastie, T., Eisen, M.B., van de Rijn, M., Jeffrey, S.S., Thorsen, T., Quist, H., Matese, J.C., Brown, P.O., Botstein, D., Lonning, P.E., Borresen-Dale, A.-L., 2001. Gene expression patterns of breast carcinomas distinguish tumor subclasses with clinical implications. Proceedings of the National Academy of Sciences 98, 10869–10874. doi:10.1073/pnas.191367098

Sorlie, T., Tibshirani, R., Parker, J., Hastie, T., Marron, J.S., Nobel, A., Deng, S., Johnsen, H., Pesich, R., Geisler, S., Demeter, J., Perou, C.M., L?nning, P.E., Brown, P.O., B?rresen-Dale, A.-L., Botstein, D., 2003. Repeated observation of breast tumor subtypes in independent gene expression data sets. Proc Natl Acad Sci U S A 100, 8418–8423. doi:10.1073/pnas.0932692100

Spencer, J.A., Eliazer, S., Ilaria, R.L., Richardson, J.A., Olson, E.N., 2000. Regulation of Microtubule Dynamics and Myogenic Differentiation by Murf, a Striated Muscle Ring-Finger Protein. J Cell Biol 150, 771–784. doi:10.1083/jcb.150.4.771

Spiegelman, B.M., Penningroth, S.M., Kirschner, M.W., 1977. Turnover of tubulin and the N site GTP in Chinese hamster ovary cells. Cell 12, 587–600.

Steffen, W., Linck, R.W., 1988. Evidence for tektins in centrioles and axonemal microtubules. PNAS 85, 2643–2647.

Stegmeier, F., Sowa, M.E., Nalepa, G., Gygi, S.P., Harper, J.W., Elledge, S.J., 2007. The tumor suppressor CYLD regulates entry into mitosis. Proceedings of the National Academy of Sciences 104, 8869–8874. doi:10.1073/pnas.0703268104

Steinmetz, M.O., Akhmanova, A., 2008. Capturing protein tails by CAP-Gly domains. Trends Biochem. Sci. 33, 535–545. doi:10.1016/j.tibs.2008.08.006

Stypula-Cyrus, Y., Mutyal, N.N., Dela Cruz, M., Kunte, D.P., Radosevich, A.J., Wali, R., Roy, H.K., Backman, V., 2014. End-binding protein 1 (EB1) up-regulation is an early event in colorectal carcinogenesis. FEBS Letters 588, 829–835. doi:10.1016/j.febslet.2014.01.046

Su, L.K., Burrell, M., Hill, D.E., Gyuris, J., Brent, R., Wiltshire, R., Trent, J., Vogelstein, B., Kinzler, K.W., 1995. APC binds to the novel protein EB1. Cancer Res. 55, 2972–2977.

Su, L.K., Qi, Y., 2001. Characterization of human MAPRE genes and their proteins. Genomics 71, 142–149. doi:10.1006/geno.2000.6428

Summers, K., Kirschner, M.W., 1979. Characteristics of the polar assembly and disassembly of microtubules observed in vitro by darkfield light microscopy. J. Cell Biol. 83, 205–217.

Sung, M., Giannakakou, P., 2014. BRCA1 regulates microtubule dynamics and taxane-induced apoptotic cell signaling. Oncogene 33, 1418–1428. doi:10.1038/onc.2013.85

Sütterlin, C., Colanzi, A., 2010. The Golgi and the centrosome: building a functional partnership. J. Cell Biol. 188, 621–628. doi:10.1083/jcb.200910001

Tanaka, H., Iguchi, N., Toyama, Y., Kitamura, K., Takahashi, T., Kaseda, K., Maekawa, M., Nishimune, Y., 2004. Mice deficient in the axonemal protein Tektin-t exhibit male infertility and immotile-cilium syndrome due to impaired inner arm dynein function. Mol. Cell. Biol. 24, 7958–7964. doi:10.1128/MCB.24.18.7958-7964.2004

Tanenbaum, M.E., Galjart, N., van Vugt, M.A.T.M., Medema, R.H., 2006. CLIP-170 facilitates the formation of kinetochore-microtubule attachments. EMBO J. 25, 45–57. doi:10.1038/sj.emboj.7600916

Thiery, J.P., 2002. Epithelial–mesenchymal transitions in tumour progression. Nat Rev Cancer 2, 442–454. doi:10.1038/nrc822

Thoma, C.R., Matov, A., Gutbrodt, K.L., Hoerner, C.R., Smole, Z., Krek, W., Danuser, G., 2010. Quantitative image analysis identifies pVHL as a key regulator of microtubule dynamic instability. J. Cell Biol. 190, 991–1003. doi:10.1083/jcb.201006059

Thoma, C.R., Toso, A., Gutbrodt, K.L., Reggi, S.P., Frew, I.J., Schraml, P., Hergovich, A., Moch, H., Meraldi, P., Krek, W., 2009. VHL loss causes spindle misorientation and chromosome instability. Nat. Cell Biol. 11, 994–1001. doi:10.1038/ncb1912

Thompson, S.L., Bakhoum, S.F., Compton, D.A., 2010. Mechanisms of Chromosomal Instability. Current Biology 20, R285–R295. doi:10.1016/j.cub.2010.01.034

Tirnauer, J.S., Bierer, B.E., 2000. EB1 proteins regulate microtubule dynamics, cell polarity, and chromosome stability. J. Cell Biol. 149, 761–766.

Tirnauer, J.S., Canman, J.C., Salmon, E.D., Mitchison, T.J., 2002a. EB1 targets to kinetochores with attached, polymerizing microtubules. Mol. Biol. Cell 13, 4308–4316. doi:10.1091/mbc.E02-04-0236

Tirnauer, J.S., Grego, S., Salmon, E.D., Mitchison, T.J., 2002b. EB1-microtubule interactions in Xenopus egg extracts: role of EB1 in microtubule stabilization and mechanisms of targeting to microtubules. Mol. Biol. Cell 13, 3614–3626. doi:10.1091/mbc.E02-04-0210

Tobin, Dusheck, 2001. Asking About Life.

Toyoshima, F., Nishida, E., 2007. Integrin-mediated adhesion orients the spindle parallel to the substratum in an EB1- and myosin X-dependent manner. EMBO J. 26, 1487–1498. doi:10.1038/sj.emboj.7601599

Tran, P.T., Joshi, P., Salmon, E.D., 1997. How tubulin subunits are lost from the shortening ends of microtubules. J. Struct. Biol. 118, 107–118. doi:10.1006/jsbi.1997.3844

Tsvetkov, A.S., Samsonov, A., Akhmanova, A., Galjart, N., Popov, S.V., 2007. Microtubule-binding proteins CLASP1 and CLASP2 interact with actin filaments. Cell Motil. Cytoskeleton 64, 519–530. doi:10.1002/cm.20201

Tzima, E., Kiosses, W.B., del Pozo, M.A., Schwartz, M.A., 2003. Localized cdc42 activation, detected using a novel assay, mediates microtubule organizing center positioning in endothelial cells in response to fluid shear stress. J. Biol. Chem. 278, 31020–31023. doi:10.1074/jbc.M301179200

Vale, R.D., Reese, T.S., Sheetz, M.P., 1985. Identification of a novel force-generating protein, kinesin, involved in microtubule-based motility. Cell 42, 39–50.

Valiron, O., Caudron, N., Job, D., 2001. Microtubule dynamics. Cell. Mol. Life Sci. 58, 2069–2084.

Van der Vaart, B., Manatschal, C., Grigoriev, I., Olieric, V., Gouveia, S.M., Bjelić, S., Demmers, J., Vorobjev, I., Hoogenraad, C.C., Steinmetz, M.O., Akhmanova, A., 2011. SLAIN2 links microtubule plus end–tracking proteins and controls microtubule growth in interphase. J Cell Biol 193, 1083–1099. doi:10.1083/jcb.201012179

Van der Weyden, L., Arends, M.J., Dovey, O.M., Harrison, H.L., Lefebvre, G., Conte, N., Gergely, F.V., Bradley, A., Adams, D.J., 2008. Loss of Rassf1a cooperates with ApcMin to accelerate intestinal tumourigenesis. Oncogene 27, 4503–4508. doi:10.1038/onc.2008.94

Vaughan, K.T., Tynan, S.H., Faulkner, N.E., Echeverri, C.J., Vallee, R.B., 1999. Colocalization of cytoplasmic dynein with dynactin and CLIP-170 at microtubule distal ends. J. Cell. Sci. 112 (Pt 10), 1437–1447.

Vaughan, P.S., Miura, P., Henderson, M., Byrne, B., Vaughan, K.T., 2002. A role for regulated binding of p150(Glued) to microtubule plus ends in organelle transport. J. Cell Biol. 158, 305–319. doi:10.1083/jcb.200201029

Vecchione, A., Ishii, H., Baldassarre, G., Bassi, P., Trapasso, F., Alder, H., Pagano, F., Gomella, L.G., Croce, C.M., Baffa, R., 2002. FEZ1/LZTS1 is down-regulated in high-grade bladder cancer, and its restoration suppresses tumorigenicity in transitional cell carcinoma cells. Am. J. Pathol. 160, 1345–1352. doi:10.1016/S0002-9440(10)62561-8

Vecchione, A., Ishii, H., Shiao, Y.H., Trapasso, F., Rugge, M., Tamburrino, J.F., Murakumo, Y., Alder, H., Croce, C.M., Baffa, R., 2001. Fez1/lzts1 alterations in gastric carcinoma. Clin. Cancer Res. 7, 1546–1552.

Verhey, K.J., Gaertig, J., 2007. The tubulin code. Cell Cycle 6, 2152–2160.

Vicente-Manzanares, M., Horwitz, A.R., 2011. Cell Migration: An Overview, in: Wells, C.M., Parsons, M. (Eds.), Cell Migration. Humana Press, Totowa, NJ, pp. 1–24.

Vidi, P.-A., Bissell, M.J., Lelièvre, S.A., 2013. Three-dimensional culture of human breast epithelial cells: the how and the why. Methods Mol. Biol. 945, 193–219. doi:10.1007/978-1-62703-125-7_13

Visvader, J.E., 2009. Keeping abreast of the mammary epithelial hierarchy and breast tumorigenesis. Genes Dev. 23, 2563–2577. doi:10.1101/gad.1849509

Visvader, J.E., 2011. Cells of origin in cancer. Nature 469, 314–322. doi:10.1038/nature09781

Vitre, B., Coquelle, F.M., Heichette, C., Garnier, C., Chrétien, D., Arnal, I., 2008. EB1 regulates microtubule dynamics and tubulin sheet closure in vitro. Nat. Cell Biol. 10, 415–421. doi:10.1038/ncb1703

Wade, R.H., 2009. On and around microtubules: an overview. Mol. Biotechnol. 43, 177–191. doi:10.1007/s12033-009-9193-5

Walczak, C.E., Gan, E.C., Desai, A., Mitchison, T.J., Kline-Smith, S.L., 2002. The microtubule-destabilizing kinesin XKCM1 is required for chromosome positioning during spindle assembly. Curr. Biol. 12, 1885–1889.

Wali, A., 2010. FHIT: doubts are clear now. ScientificWorldJournal 10, 1142–1151. doi:10.1100/tsw.2010.110

Wali, A., Srinivasan, R., Shabnam, M.S., Majumdar, S., Joshi, K., Behera, D., 2006. Loss of fragile histidine triad gene expression in advanced lung cancer is consequent to allelic loss at 3p14 locus and promoter methylation. Mol. Cancer Res. 4, 93–99. doi:10.1158/1541-7786.MCR-05-0070

Walker, R.A., O'Brien, E.T., Pryer, N.K., Soboeiro, M.F., Voter, W.A., Erickson, H.P., Salmon, E.D., 1988. Dynamic instability of individual microtubules analyzed by video light microscopy: rate constants and transition frequencies. J. Cell Biol. 107, 1437–1448.

Wang, Y., Zhou, X., Zhu, H., Liu, S., Zhou, C., Zhang, G., Xue, L., Lu, N., Quan, L., Bai, J., Zhan, Q., Xu, N., 2005. Overexpression of EB1 in human esophageal squamous cell carcinoma (ESCC) may promote cellular growth by activating beta-catenin/TCF pathway. Oncogene 24, 6637–6645. doi:10.1038/sj.onc.1208819

Ward, T., Wang, M., Liu, X., Wang, Z., Xia, P., Chu, Y., Wang, X., Liu, L., Jiang, K., Yu, H., Yan, M., Wang, J., Hill, D.L., Huang, Y., Zhu, T., Yao, X., 2013. Regulation of a dynamic interaction between two microtubule-binding proteins, EB1 and TIP150, by the mitotic p300/CBP-associated factor (PCAF) orchestrates kinetochore microtubule plasticity and chromosome stability during mitosis. J. Biol. Chem. 288, 15771–15785. doi:10.1074/jbc.M112.448886

Warner, F.D., Satir, P., 1973. The Substructure of Ciliary Microtubules. J Cell Sci 12, 313–326.

Watanabe, T., Noritake, J., Kaibuchi, K., 2005. Regulation of microtubules in cell migration. Trends in Cell Biology 15, 76–83. doi:10.1016/j.tcb.2004.12.006

Watanabe, T., Wang, S., Noritake, J., Sato, K., Fukata, M., Takefuji, M., Nakagawa, M., Izumi, N., Akiyama, T., Kaibuchi, K., 2004. Interaction with IQGAP1 links APC to Rac1, Cdc42, and actin filaments during cell polarization and migration. Dev. Cell 7, 871–883. doi:10.1016/j.devcel.2004.10.017

Waterman-Storer, C.M., Salmon, E.D., 1997. Microtubule dynamics: treadmilling comes around again. Curr. Biol. 7, R369–372.

Waterman-Storer, C.M., Worthylake, R.A., Liu, B.P., Burridge, K., Salmon, E.D., 1999. Microtubule growth activates Rac1 to promote lamellipodial protrusion in fibroblasts. Nat. Cell Biol. 1, 45–50. doi:10.1038/9018

Wei, J., Costa, C., Ding, Y., Zou, Z., Yu, L., Sanchez, J.J., Qian, X., Chen, H., Gimenez-Capitan, A., Meng, F., Moran, T., Benlloch, S., Taron, M., Rosell, R., Liu, B., 2011. mRNA expression of BRCA1, PIAS1, and PIAS4 and survival after second-line docetaxel in advanced gastric cancer. J. Natl. Cancer Inst. 103, 1552–1556. doi:10.1093/jnci/djr326

Weigelt, B., Baehner, F.L., Reis-Filho, J.S., 2010. The contribution of gene expression profiling to breast cancer classification, prognostication and prediction: a retrospective of the last decade. The Journal of Pathology n/a–n/a. doi:10.1002/path.2648

Weigelt, B., Peterse, J.L., van't Veer, L.J., 2005. Breast cancer metastasis: markers and models. Nature Reviews Cancer 5, 591–602. doi:10.1038/nrc1670

Weigelt, B., Reis-Filho, J.S., 2009. Histological and molecular types of breast cancer: is there a unifying taxonomy? Nature Reviews Clinical Oncology 6, 718–730. doi:10.1038/nrclinonc.2009.166

Weisenberg, R.C., 1972. Microtubule formation in vitro in solutions containing low calcium concentrations. Science 177, 1104–1105.

Wen, Y., Eng, C.H., Schmoranzer, J., Cabrera-Poch, N., Morris, E.J.S., Chen, M., Wallar, B.J., Alberts, A.S., Gundersen, G.G., 2004. EB1 and APC bind to mDia to stabilize microtubules downstream of Rho and promote cell migration. Nat. Cell Biol. 6, 820–830. doi:10.1038/ncb1160

Westermann, S., Weber, K., 2003. Post-translational modifications regulate microtubule function. Nature Reviews Molecular Cell Biology 4, 938–948. doi:10.1038/nrm1260

Wilson, R., 2006. Normal Histlogy of the Breast.

Wittmann, T., Bokoch, G.M., Waterman-Storer, C.M., 2004. Regulation of Microtubule Destabilizing Activity of Op18/Stathmin Downstream of Rac1. J. Biol. Chem. 279, 6196–6203. doi:10.1074/jbc.M307261200

Wloga, D., Gaertig, J., 2010. Post-translational modifications of microtubules. J Cell Sci 123, 3447–3455. doi:10.1242/jcs.063727

Wolf, K., Wu, Y.I., Liu, Y., Geiger, J., Tam, E., Overall, C., Stack, M.S., Friedl, P., 2007. Multi-step pericellular proteolysis controls the transition from individual to collective cancer cell invasion. Nat. Cell Biol. 9, 893–904. doi:10.1038/ncb1616

Wruck, C.J., Funke-Kaiser, H., Pufe, T., Kusserow, H., Menk, M., Schefe, J.H., Kruse, M.L., Stoll, M., Unger, T., 2005. Regulation of transport of the angiotensin AT2 receptor by a novel membrane-associated Golgi protein. Arterioscler. Thromb. Vasc. Biol. 25, 57–64. doi:10.1161/01.ATV.0000150662.51436.14

Wu, X., Xiang, X., Hammer III, J.A., 2006. Motor proteins at the microtubule plus-end. Trends in Cell Biology 16, 135–143. doi:10.1016/j.tcb.2006.01.004

Wu, X.S., Tsan, G.L., Hammer, J.A., 3rd, 2005. Melanophilin and myosin Va track the microtubule plus end on EB1. J. Cell Biol. 171, 201–207. doi:10.1083/jcb.200503028

Xia, P., Wang, Z., Liu, X., Wu, B., Wang, J., Ward, T., Zhang, L., Ding, X., Gibbons, G., Shi, Y., Yao, X., 2012. EB1 acetylation by P300/CBP-associated factor (PCAF) ensures accurate kinetochore-microtubule interactions in mitosis. Proc Natl Acad Sci U S A 109, 16564–16569. doi:10.1073/pnas.1202639109

Xiao, J., Chen, J.-X., Zhu, Y.-P., Zhou, L.-Y., Shu, Q.-A., Chen, L.-W., 2012. Reduced expression of MTUS1 mRNA is correlated with poor prognosis in bladder cancer. Oncol Lett 4, 113–118. doi:10.3892/ol.2012.673

Xu, H.M., Gutmann, D.H., 1998. Merlin differentially associates with the microtubule and actin cytoskeleton. J. Neurosci. Res. 51, 403–415.

Yan, X., Habedanck, R., Nigg, E.A., 2006. A complex of two centrosomal proteins, CAP350 and FOP, cooperates with EB1 in microtubule anchoring. Mol. Biol. Cell 17, 634–644. doi:10.1091/mbc.E05-08-0810

Yang, H., Ganguly, A., Cabral, F., 2010. Inhibition of Cell Migration and Cell Division Correlates with Distinct Effects of Microtubule Inhibiting Drugs. Journal of Biological Chemistry 285, 32242–32250. doi:10.1074/jbc.M110.160820

Yang, Q., Yoshimura, G., Sakurai, T., Kakudo, K., 2002. The Fragile Histidine Triad gene and breast cancer. Med. Sci. Monit. 8, RA140–144.

Yang, Y., Bauer, C., Strasser, G., Wollman, R., Julien, J.-P., Fuchs, E., 1999. Integrators of the Cytoskeleton that Stabilize Microtubules. Cell 98, 229–238. doi:10.1016/S0092-8674(00)81017-X

Yang, Y., Liu, M., Li, D., Ran, J., Gao, J., Suo, S., Sun, S.-C., Zhou, J., 2014. CYLD regulates spindle orientation by stabilizing astral microtubules and promoting dishevelled-NuMA-dynein/dynactin complex formation. PNAS 111, 2158–2163. doi:10.1073/pnas.1319341111

Yao, X., Abrieu, A., Zheng, Y., Sullivan, K.F., Cleveland, D.W., 2000. CENP-E forms a link between attachment of spindle microtubules to kinetochores and the mitotic checkpoint. Nat Cell Biol 2, 484–491. doi:10.1038/35019518

Ye, H., Pungpravat, N., Huang, B.-L., Muzio, L.L., Mariggiò, M.A., Chen, Z., Wong, D.T., Zhou, X., 2007. Genomic assessments of the frequent loss of heterozygosity region on 8p21.3-p22 in head and neck squamous cell carcinoma. Cancer Genet. Cytogenet. 176, 100–106. doi:10.1016/j.cancergencyto.2007.04.003

Yi, H., Ku, N.-O., 2013. Intermediate filaments of the lung. Histochem. Cell Biol. 140, 65–69. doi:10.1007/s00418-013-1105-x

Yilmaz, M., Christofori, G., Lehembre, F., 2007. Distinct mechanisms of tumor invasion and metastasis. Trends in Molecular Medicine 13, 535–541. doi:10.1016/j.molmed.2007.10.004

Yu, J., Liu, X., Ye, H., Zhou, X., 2009. Genomic characterization of the human mitochondrial tumor suppressor gene 1 (MTUS1): 5' cloning and preliminary analysis of the multiple gene promoters. BMC Res Notes 2, 109. doi:10.1186/1756-0500-2-109

Yuan, K., Serra, R., Frost, A.R., 2010. Primary Cilia in the Breast and Breast Cancer. The Open Breast Cancer Journal 2, 101–107.

Zhang, D., Rogers, G.C., Buster, D.W., Sharp, D.J., 2007. Three microtubule severing enzymes contribute to the "Pacman-flux" machinery that moves chromosomes. J. Cell Biol. 177, 231–242. doi:10.1083/jcb.200612011

Zuern, C., Heimrich, J., Kaufmann, R., Richter, K.K., Settmacher, U., Wanner, C., Galle, J., Seibold, S., 2010. Down-regulation of MTUS1 in human colon tumors. Oncol. Rep. 23, 183–189.

Zumbrunn, J., Kinoshita, K., Hyman, A.A., Näthke, I.S., 2001. Binding of the adenomatous polyposis coli protein to microtubules increases microtubule stability and is regulated by GSK3 beta phosphorylation. Curr. Biol. 11, 44–49.

VI. ANNEXES

ARTICLE 3:

ATIP, a Novel Superfamily of Microtubule-Associated Proteins

ATIP, une nouvelle superfamille de protéines associées aux microtubules

Angie Molina, Sylvie Rodrigues-Ferreira, Anne Di Tommaso, Clara Nahmias

Inserm, U1016, Institut Cochin, Paris, France ;
Cnrs, UMR8104, Paris, France ;
Université Paris Descartes, Paris, France.
Département EMC,
22, rue Méchain, 75014 Paris, France.
clara.nahmias@inserm.fr

› Les microtubules, formés de l'assemblage dynamique de dimères d'alpha et de bêta-tubuline, jouent un rôle essentiel dans l'homéostasie cellulaire. Dans les cellules en interphase, le cytosquelette de microtubules intervient dans le maintien de l'architecture cellulaire, la migration et le trafic intracellulaire de protéines et d'organites ; en mitose, il se réorganise pour former le fuseau mitotique qui permet une répartition correcte des chromosomes [1]. La dynamique de polymérisation des microtubules, essentielle à leur fonction, est sous le contrôle d'un ensemble de protéines agissant de concert : les MAP (*microtubule-associated proteins*) dont l'activité est finement régulée dans l'espace et le temps [1, 2]. Les altérations de la structure ou de la régulation des MAP peuvent avoir des répercussions considérables dans de nombreuses situations physiopathologiques, comme c'est le cas par exemple pour la protéine APC (*adenomatous polyposis coli*) dans le cancer du côlon, ou la protéine Tau dans la maladie d'Alzheimer.

ATIP3, un régulateur de mitose associé aux microtubules

Notre équipe a récemment mis en évidence une nouvelle protéine associée aux microtubules dénommée ATIP3 *(AT2-interacting protein 3)* [3], codée par le gène candidat suppresseur de tumeurs *MTUS1* (*microtubule-associated tumor suppressor*)[1] [4, 5]. La molécule ATIP3 est localisée au centrosome et le long des microtubules dans les cellules en interphase. Au cours de la division cellulaire, elle s'associe au fuseau mitotique à tous les stades de la mitose et au pont intercellulaire lors de la cytokinèse *(Figure 1)*. En accord avec cette localisation particulière, nos travaux ont montré un effet régulateur d'ATIP3 sur la mitose. En effet, ATIP3 freine la prolifération cellulaire et prolonge le temps de division en maintenant les cellules au stade métaphase [3].

L'étude moléculaire de la protéine ATIP3 revêt un intérêt fondamental quand on sait que son expression est diminuée dans le cancer du sein, et ce de façon d'autant plus marquée que la tumeur est plus agressive et de grade histologique élevé, métastatique ou du sous-type triple négatif, pour lequel il n'existe pas à ce jour de thérapie ciblée. Ainsi ATIP3 constitue un nouveau biomarqueur des tumeurs de sein de mauvais pronostic. De plus, ses effets antimitotiques *in vitro* et antitumoraux *in vivo* en font une cible privilégiée pour l'élaboration de nouvelles thérapies moléculaires contre le cancer du sein [3].

Bien que les mécanismes d'action d'ATIP3 demeurent inconnus à ce jour, des études récentes réalisées sur deux protéines (ICIS et TIP150) qui lui sont structuralement apparentées, ouvrent des perspectives intéressantes dans le domaine du cancer. La protéine ICIS (codée par le gène orthologue *MTUS1* de Xénope) a été décrite comme une nouvelle MAP localisée aux

1 Le gène *MTUS1* a initialement été nommé *mitochondrial tumor suppressor* , sur la base des résultats de Seibold *et al.* [11]. En 2010, lorsqu'il s'est avéré qu'ATIP3, ICIS et TIP150, produits des gènes *MTUS1* et *MTUS2,* sont associés aux microtubules [3, 7, 8], le comité de nomenclature de la base de données NCBI (*National center for biotechnolog y information*) a renommé *MTUS1* : *microtubule-associated tumor suppressor*.

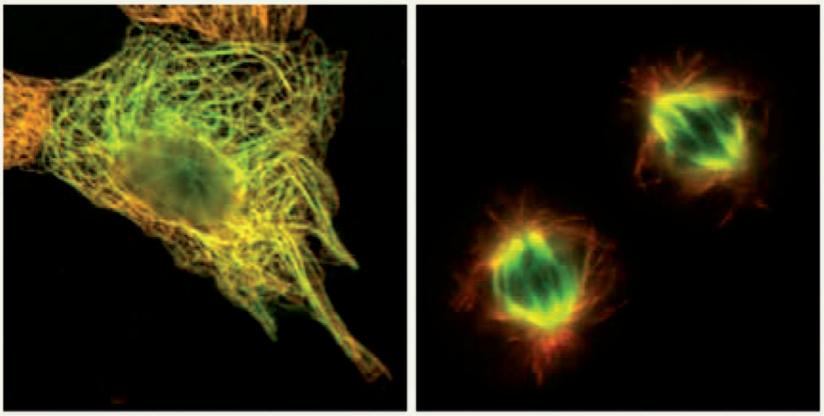

Figure 1. ***Localisation de la protéine ATIP3 aux microtubules dans les cellules de carcinome pulmonaire SK-MES en interphase (à gauche) et en mitose (à droite).*** L'image d'immunofluorescence est obtenue après immunomarquage de la protéine ATIP3 endogène (en vert) et de l'alpha-tubuline (en rouge).

Article disponible sur le site http://www.medecinesciences.org ou http://dx.doi.org/10.1051/medsci/2011273244

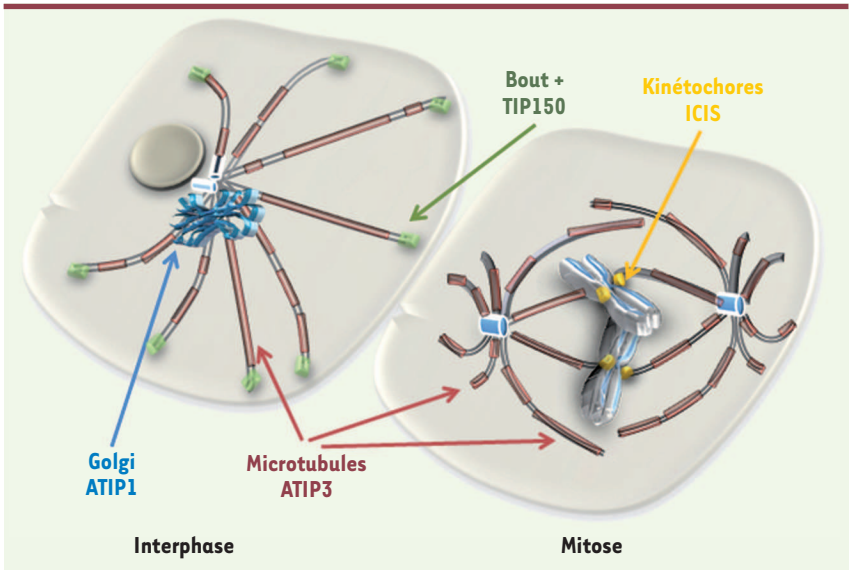

Figure 2. ***Localisation cellulaire des protéines ATIP et de leurs analogues structuraux ICIS et TIP150.*** Schéma représentant l'association d'ATIP3, ICIS et TIP150 avec les microtubules dans une cellule en interphase (à gauche) ou en mitose (stade métaphase, à droite). En interphase, ATIP3 (en rose) est localisée tout le long des microtubules alors que TIP150 (en vert) est exclusivement présente aux extrémités des microtubules (bout +). ATIP1 (en bleu) est localisée au Golgi. Dans une cellule en mitose, on retrouve ATIP3 (en rose) le long des microtubules du fuseau mitotique et ICIS (en jaune) au niveau des kinétochores.

kinétochores [6], structure qui relie les centromères aux microtubules lors de la mitose *(Figure 2)*. ICIS interagit avec la kinésine MCAK (*mitotic centromere-activating kinesin*) et contribue à la dépolymérisation des microtubules et donc à la dynamique du fuseau mitotique essentiel à la ségrégation des chromosomes [6]. Plus récemment, la mise en évidence d'une interaction entre ICIS et une autre kinésine 13 (Kif2A) conforte le rôle de cette protéine dans la dépolymérisation des microtubules [7]. D'autre part, la protéine TIP150 (produit du gène paralogue *MTUS2*) a récemment été identifiée comme une MAP interagissant avec EB1 (*end binding protein 1*) et MCAK aux bouts « plus » des microtubules *(Figure 2)* pour favoriser leur dépolymérisation [8]. Ainsi, par analogie avec ses homologues ICIS et TIP150, on peut avancer l'hypothèse d'un rôle d'ATIP3 dans la dynamique des microtubules *via* l'activation de kinésines de la famille MCAK.

Fonctions des autres membres de la famille ATIP

Qu'en est-il des autres membres de la famille ATIP ? L'épissage alternatif du gène *MTUS1* génère en effet deux autres protéines - ATIP1 et ATIP4 - identiques à ATIP3 dans leur portion carboxy-terminale [4, 5, 9] mais dont le lien avec le cytosquelette de microtubules n'a pas encore été évalué. ATIP1, initialement identifié comme partenaire d'interaction du récepteur AT2 de l'angiotensine II - ce qui lui a d'ailleurs valu son nom d'*AT2 receptor-interacting protein* - est un acteur privilégié des voies de signalisation de ce récepteur, impliqué dans l'inhibition de la prolifération cellulaire, la différenciation neuronale et le remodelage vasculaire [4].

Outre son rôle central dans la signalisation de l'AT2, ATIP1 contribue aussi à l'adressage du récepteur à la membrane [10]. De façon intéressante, ATIP1 a été décrite comme étant localisée dans les mitochondries [11] ou le Golgi [10], deux compartiments cellulaires étroitement associés aux microtubules. La colocalisation d'ATIP1 avec ces deux organites et ses effets sur le trafic intracellulaire du récepteur AT2 suggèrent qu'ATIP1 pourrait interagir avec les microtubules et s'associer à des moteurs moléculaires pour permettre le transport intracellulaire d'organites ou de récepteurs. Bien que purement spéculative, cette hypothèse mérite d'être examinée. La protéine ATIP4 n'a pas encore été isolée à ce jour. Au-delà de son domaine d'interaction avec le récepteur AT2, cette protéine présente deux caractéristiques particulières - la présence d'un domaine transmembranaire et un profil d'expression exclusivement restreint au système nerveux central - qui en font un médiateur potentiel des effets de l'AT2 dans le cerveau [4]. On peut noter que les 400 acides aminés carboxy-terminaux d'ATIP4 sont identiques à ceux d'ATIP1 et ATIP3 et fortement conservés dans les séquences des protéines ICIS et TIP150, ce qui pose la question de l'association potentielle d'ATIP4 avec le cytosquelette de microtubules *via* son domaine carboxy-terminal intracellulaire.

En conclusion

Les protéines de la famille ATIP ont récemment été impliquées dans diverses fonctions, allant de la différenciation neuronale au remodelage vasculaire et à la prolifération tumorale. Cette revue pose l'hypothèse selon laquelle ces protéines pourraient, avec leurs analogues structuraux ICIS et TIP150, constituer une nouvelle superfamille de protéines associées aux microtubules. Localisées dans différents compartiments intracellulaires, les protéines ATIP pourraient contribuer aux fonctions essentielles de la cellule (mitose, trafic, signalisation) en régulant la dynamique des microtubules. L'étude moléculaire des membres de cette superfamille devrait permettre de révéler de nouveaux aspects du rôle des microtubules aux niveaux cérébral, cardiovasculaire et tumoral. ◊

ATIP, a novel superfamily of microtubule-associated proteins

CONFLIT D'INTERÊTS

Les auteurs déclarent n'avoir aucun conflit d'intérêt concernant les données publiées dans cet article.

RÉFÉRENCES

1. Arnal I, Sassoon I, Tournebize R. Dynamique du fuseau : vers une cible anti-cancéreuse. *Med Sci (Paris)* 2002 ; 18 : 1227-35.
2. Etienne-Manneville S. From signaling pathways to microtubule dynamics: the key players. *Curr Opin Cell Biol* 2010 ; 22 : 104-11.
3. Rodrigues-Ferreira S, Di Tommaso A, Dimitrov A, *et al*. 8p22 MTUS1 gene product ATIP3 is a novel anti-mitotic protein underexpressed in invasive breast carcinoma of poor prognosis. *PLoS One* 2009 ; 4 : e7239.
4. Rodrigues-Ferreira S, Nahmias C. An ATIPical family of angiotensin II AT2 receptor-interacting proteins. *Trends Endocrinol Metab* 2010 ; 21 : 684-90.
5. Di Benedetto M, Bièche I, Deshayes F, *et al*. Structural organization and expression of human MTUS1, a candidate 8p22 tumor suppressor gene encoding a family of angiotensin II AT2 receptor-interacting proteins, ATIP. *Gene* 2006 ; 380 : 127-36.
6. Ohi R, Coughlin ML, Lane WS, Mitchison TJ. An inner centromere protein that stimulates the microtubule depolymerizing activity of a KinI kinesin. *Dev Cell* 2003 ; 5 : 309-21.
7. Knowlton AL, Vorozhko VV, Lan W, *et al*. ICIS and Aurora B coregulate the microtubule depolymerase Kif2a. *Curr Biol* 2009 ; 19 : 758-63.
8. Jiang K, Wang J, Liu J, *et al*. TIP150 interacts with and targets MCAK at the microtubule plus ends. *EMBO Rep* 2009 ; 10 : 857-65.
9. Nouet S, Amzallag N, Li JM, *et al*. Trans-inactivation of receptor tyrosine kinases by novel angiotensin II AT2 receptor-interacting protein, ATIP. *J Biol Chem* 2004 ; 279 : 28989-97.
10. Wruck C, Funke-Kaiser H, Pufe T, *et al*. Regulation of transport of the angiotensin AT2 receptor by a novel membrane-associated golgi protein. *Arterioscler Thromb Vasc Biol* 2005 ; 25 : 57-64.
11. Seibold S, Rudroff C, Weber M, *et al*. Identification of a new tumor suppressor gene located at chromosome 8p21.3-22. *FASEB J* 2003 ; 17 : 1180-2.

NOUVELLE

Les cinq couleurs de la chromatine de drosophile

Guillaume Filion

The Netherlands cancer institute,
Gene regulation (B4),
Plesmanlaan 121,
1066CX Amsterdam,
Pays Bas.
g.filion@nki.nl

La chromatine et ses dérivés

Depuis son apparition en 1882 [1], le terme « chromatine » a changé de définition à de nombreuses reprises. Ces définitions ont toutes eu pour fonction de mettre un nom sur un objet dont la nature, la structure, les propriétés et les fonctions n'ont jamais été parfaitement comprises. Par exemple, la dichotomie entre euchromatine et hétérochromatine, initialement établie par microscopie électronique, désignait l'hétérochromatine comme la fraction compacte du matériel nucléaire d'une cellule en interphase. La définition actuelle obéit aux exigences de la génomique : l'hétérochromatine est volontiers définie par sa nature répétitive ou l'absence d'expression des gènes qui y sont codés. Ainsi, chacune des deux définitions élude les mécanismes fondamentaux de la propriété sur laquelle elle est basée.

Malgré la nature éminemment floue du concept de chromatine, la communauté scientifique ne fait preuve ni de dogmatisme, ni de naïveté quant à son usage. Le terme garde son aspect indéfini avant tout pour des raisons expérimentales. Il est clair depuis plus d'une quinzaine d'années que la dichotomie naïve entre euchromatine et hétérochromatine est le fruit de l'inefficacité des méthodes utilisées pour interroger les propriétés du matériel nucléaire *in vivo* . Il n'est donc pas surprenant que les termes changent à nouveau de sens avec l'essor des analyses *in vivo* à l'échelle du génome.

Grâce aux technologies récentes, nous avons cartographié les sites de liaison de 53 protéines de la chromatine sur le génome de la drosophile [2]. Pour cela nous avons utilisé un modèle uniforme de cellules en culture et une méthode de cartographie *in vivo* appelée DamID. Le principe de la méthode repose sur l'activité de l'enzyme Dam (*DNA adenine methyltransferase*). Dam dépose une empreinte sur l'ADN, absente des génomes eucaryotes, qui peut être détectée par des enzymes de restriction. En fusionnant une protéine à Dam, il est possible de restreindre la méthylation de l'ADN aux sites de liaison de cette protéine *in vivo*, ce qui permet ensuite de les identifier *(Figure 1)*. Donnant des résultats comparables à ceux de la précipitation de la chromatine (ChIP), la technologie DamID jouit d'un avantage : elle peut être appliquée de façon systématique sans recours au développement d'anticorps spécifiques, ce qui permet une augmentation conséquente du débit. Les cartes de liaison à haute résolution de ces 53 protéines nous ont permis de donner le premier aperçu de la chromatine à cette échelle dans une cellule eucaryote.

Hétérogénéité et simplicité de la chromatine de drosophile

La première surprise de cette étude est l'hétérogénéité de la chromatine de drosophile. On pourrait s'attendre à une répartition plus ou moins uniforme des évènements de liaison sur la molécule d'ADN. Or, la majeure partie du génome est liée par un petit nombre de protéines très abondantes, telles que l'histone H1, alors qu'une petite fraction du génome est liée par un très grand nombre de protéines différentes. La seconde surprise est la faible complexité de la

ARTICLE 4:

Angiotensin II facilitates breast cancer cell migration and metastasis.

OPEN ACCESS Freely available online

PLoS one

Angiotensin II Facilitates Breast Cancer Cell Migration and Metastasis

Sylvie Rodrigues-Ferreira[1,2,3], Mohamed Abdelkarim[4,5], Patricia Dillenburg-Pilla[1,2,3,6], Anny-Claude Luissint[1,2,3], Anne di-Tommaso[1,2,3], Frédérique Deshayes[1,2,3], Carmen Lucia S. Pontes[7], Angie Molina[1,2,3], Nicolas Cagnard[1,2,3], Franck Letourneur[1,2,3], Marina Morel[1,2,3], Rosana I. Reis[6], Dulce E. Casarini[8], Benoit Terris[1,2,3], Pierre-Olivier Couraud[1,2,3], Claudio M. Costa-Neto[6], Mélanie Di Benedetto[4,5], Clara Nahmias[1,2,3]*

1 Inserm, Institut Cochin, Paris, France, **2** CNRS, Paris, France, **3** Université Paris Descartes, Paris, France, **4** Université Paris 13, Bobigny, France, **5** CNRS, UMRS 940, IGM, Paris, France, **6** Department of Biochemistry and Immunology, Faculty of Medicine at Ribeirão Preto, University of São Paulo, Ribeirão Preto, Brazil, **7** Department of Physiological Sciences, Federal University of São Carlos, São Carlos, São Paulo, Brazil, **8** Department of Medicine, Nephrology Division, Federal University of Saõ Paulo, São Paulo, São Paulo, Brazil

Abstract

Breast cancer metastasis is a leading cause of death by malignancy in women worldwide. Efforts are being made to further characterize the rate-limiting steps of cancer metastasis, i.e. extravasation of circulating tumor cells and colonization of secondary organs. In this study, we investigated whether angiotensin II, a major vasoactive peptide both produced locally and released in the bloodstream, may trigger activating signals that contribute to cancer cell extravasation and metastasis. We used an experimental *in vivo* model of cancer metastasis in which bioluminescent breast tumor cells (D3H2LN) were injected intra-cardiacally into nude mice in order to recapitulate the late and essential steps of metastatic dissemination. Real-time intravital imaging studies revealed that angiotensin II accelerates the formation of metastatic foci at secondary sites. Pre-treatment of cancer cells with the peptide increases the number of mice with metastases, as well as the number and size of metastases per mouse. In vitro, angiotensin II contributes to each sequential step of cancer metastasis by promoting cancer cell adhesion to endothelial cells, trans-endothelial migration and tumor cell migration across extracellular matrix. At the molecular level, a total of 102 genes differentially expressed following angiotensin II pre-treatment were identified by comparative DNA microarray. Angiotensin II regulates two groups of connected genes related to its precursor angiotensinogen. Among those, up-regulated MMP2/MMP9 and ICAM1 stand at the crossroad of a network of genes involved in cell adhesion, migration and invasion. Our data suggest that targeting angiotensin II production or action may represent a valuable therapeutic option to prevent metastatic progression of invasive breast tumors.

Citation: Rodrigues-Ferreira S, Abdelkarim M, Dillenburg-Pilla P, Luissint A-C, di-Tommaso A, et al. (2012) Angiotensin II Facilitates Breast Cancer Cell Migration and Metastasis. PLoS ONE 7(4): e35667. doi:10.1371/journal.pone.0035667

Editor: Adam I. Marcus, Emory University, United States of America

Received January 18, 2012; **Accepted** March 19, 2012; **Published** April 20, 2012

Funding: This work was supported by the University Paris Descartes, the Inserm, the Centre National de la Recherche Scientifique, the Ligue Contre le Cancer-Comité Ile de France, the Association pour la Recherche contre le Cancer (ARC), the Fondation RAJA, and the association Prolific. S.R-F was supported by a fellowship from ARC. The funders had no role in study design, data collection and analysis, decision to publish, or preparation of the manuscript.

Competing Interests: The authors have declared that no competing interests exist.

* E-mail: clara.nahmias@inserm.fr

Introduction

The occurrence of distant metastasis is a critical event that limits the survival of patients with breast cancer. While targeted molecular therapies have considerably improved the management of primary breast tumors, these remain poorly effective for the treatment of distant metastases. The identification of molecular agents that may contribute to breast cancer cell dissemination is therefore essential for future development of new anti-metastatic therapeutic strategies.

Metastasis is an inefficient process. Among the large number of cancer cells that detach from the primary tumor and invade adjacent tissues to reach the bloodstream, most remain quiescent or die in the circulation [1–3]. Only few circulating tumor cells are able to cross the blood barrier and colonize distant organs to form micrometastases [3–5]. There is increasing evidence that, in addition to intrinsic metastasis gene signatures that predict the ability of tumor cells to colonize distant tissues [6], close interactions between circulating tumor cells and the host microenvironment are critical to the establishment of cancer cells at secondary sites [7–9]. Diffusible molecules such as cytokines or chemokines (CXCL12, CCL2) play a seminal role in breast cancer metastasis [10,11]. We reasoned that other small molecules such as vasoactive peptides, either produced locally or released in the blood flow, may trigger activating signals contributing in an autocrine or paracrine manner to cancer cell extravasation, colonization and metastasis.

Angiotensin II (AngII) is the biologically active peptide of the renin-angiotensin system (RAS) involved in blood pressure control, tissue remodeling and angiogenesis as well as in vascular and inflammatory pathologies. Of interest, major functions attributed to AngII (inflammation, angiogenesis and migration) are also related to cancer progression [12,13]. Most components of the RAS including angiotensinogen, angiotensin converting enzyme

(ACE) and angiotensin receptors are expressed locally in a wide variety of tumors, including in breast tumors [13–15]. Local production of AngII in gastric cancer has been shown to facilitate tumor progression and lymph node metastasis [16,17]. Furthermore, blockers of the RAS (either ACE inhibitors or angiotensin receptor blockers ARBs) were shown to efficiently reduce tumor growth, angiogenesis and metastasis in mouse experimental models *in vivo* [12,13,18,19]. However, anti-metastatic properties of RAS inhibitors were mainly associated with effects on the host microenvironment, including infiltration of tumor-associated macrophages or tumor-related angiogenesis [20,21], and to date there has been no report on potential metastatic effects of AngII through direct cancer cell activation.

In this study, we aimed to investigate whether AngII may act directly on tumor cells to modify their metastatic properties. We demonstrate that pre-treatment of breast cancer cells by AngII triggers rapid development of metastatic foci at secondary sites in an experimental mouse model *in vivo* and potentiates cancer cell motility and transendothelial migration.

Results

Angiotensin II accelerates the development of metastases *in vivo*

An experimental mouse model of cancer metastasis was developed to investigate the effects of AngII on the metastatic potential of breast cancer cells *in vivo*. Highly metastatic human breast cancer cells D3H2LN (an *in vivo*-selected subclone of MDA-MB-231 cells expressing luciferase [22]) were exposed to AngII (100 nM) for 24 hrs (or vehicle for control group) and injected intra-cardiacally into the bloodstream of nude mice in order to recapitulate the late and essential steps of cancer metastasis, i.e. extravasation and colonization [22,23]. Such strategy allowed us to evaluate the effects of AngII on cancer cells while avoiding any direct effect of the peptide on the host microenvironment.

The establishment of tumor micrometastases in various organs was evaluated every two days by intravital bioluminescent imaging on anesthetized animals. Fourteen mice injected with AngII-treated cells were compared to 15 control mice, in two independent experiments. As shown in Fig. 1A, mice from both groups showed detectable micrometastases as early as day 7 post-injection and all of them harbored metastases at day 19, illustrating high aggressiveness of the D3H2LN cell line. However, tumor cells exposed to AngII acquired a more aggressive behavior, showing at least one metastatic site in 50% (7/14) of the animals at day 7 as compared to 26,7% (4/15) of control mice. At day 9 of the experiment, 86% (12/14) of the mice that received AngII-treated cells presented at least one detectable metastatic nodule, compared to 40% (6/15) for control mice (Fig. 1A). Notably, AngII pre-treatment not only increased the percentage of mice with metastasis, but also increased the number of detectable metastatic foci per mouse (Fig. 1B) as well as the total number of tumor cells disseminated in the whole body, as assessed by quantification of bioluminescence (Fig. 1C). *Ex-vivo* analysis of bioluminescence in isolated organs (not shown) and subsequent histological analysis (Fig. 1D) on the last day of the experiment confirmed the presence of tumor cells in the brain, lung and bone samples that had been identified as luciferase-positive in the whole animal.

The most significant differences between AngII-pretreated and control groups were observed shortly after cell injection, as illustrated by pictures of 5 representative mice taken at (Fig. 1E). Indeed, breast cancer cells treated with AngII developed three times more metastatic foci per mouse at day 9 compared to control cells (Fig. 1B, Fig. S1A). In agreement, the number of disseminated cancer cells was significantly increased in the AngII-treated group as compared to control (median 1.155 and 0.525×10^6 of photons/s respectively, at day 9 post-injection) (Fig. 1C, Fig. S1B). Our results thus indicate that invasive D3H2LN breast cancer cells exposed to AngII show increased metastatic potential *in vivo* and are more prone to rapidly establish at distant organs.

Angiotensin II increases breast cancer cell adhesion and migration

Metastatic dissemination of circulating cancer cells involves several sequential steps, among which tumor cell adhesion to the vascular endothelium, migration across the endothelial barrier and subsequent invasion across the extracellular matrix to reach a secondary site. In order to evaluate the consequences of AngII activation on cancer cell adhesion and migration, the properties of MDA-MB-231 and D3H2LN breast cancer cells were analyzed *in vitro* following pre-treatment with AngII. As shown in Fig. 2A, AngII stimulation for 24 hrs significantly increased (1.7 fold) the adhesion of cancer cells to a monolayer of human endothelial cells. Cancer cell adhesion following AngII stimulation was also increased (2 fold) when endothelial cells were pre-activated for 24 hrs with pro-inflammatory cytokines (IFNγ and TNFα). To note, short-term exposure (30 min or 6 hrs) of breast cancer cells to AngII was not sufficient to promote increased adhesion to the endothelial monolayer (data not shown), suggesting that AngII-increased cancer cell adhesion may involve transcriptional regulation of target genes rather than activation of intracellular trafficking or signaling pathways – that generally occur within minutes.

We next evaluated the effects of AngII on breast cancer cell migration. As shown in Fig. 2B, pre-treatment of breast cancer cells with AngII for 24 hrs significantly increased (1.5 fold) their ability to migrate in Boyden chamber assays using FCS as chemoattractant. Similar results were obtained in invasion assays using filters coated with matrigel® that mimics the extracellular matrix (Fig. 2C). The pro-migratory effects of AngII on breast cancer cells were further confirmed in wound healing assays (Fig. 2D, E) showing significant increase (1.64 fold) in cell migration and wound closure at 16 hrs following pre-treatment with AngII. To note, AngII-pre-treatment had no significant effect on cell proliferation (Fig. S2), ruling out the possibility that increased cell number may account for increased wound closure. Finally, exposure of breast cancer cells to AngII induced a 2.7 fold-increase in trans-endothelial migration, i.e. the ability to migrate through a monolayer of human endothelial cells (Fig. 2F), which is a hallmark of cancer cell extravasation *in vitro*.

Thus, AngII contributes to each step of breast cancer cell extravasation including tumor cell adhesion to endothelial cells, motility, invasion and trans-endothelial migration.

Angiotensin II regulates a panel of connected target genes

To get further insight into the mechanisms by which AngII increases breast cancer cell migration and metastasis, we searched for downstream molecular targets that may be regulated following exposure of MDA-MB-231 cells to AngII for 24 hrs. Comparative DNA microarray (Affymetrix U133A) studies revealed a panel of 123 differentially expressed genes (more than 1.4-fold, $p<0.05$). Among those, 102 genes (63 up-regulated and 39 down-regulated) were associated with known functions (Tables S1 and S2) including cell proliferation and apoptosis (32%), cell adhesion

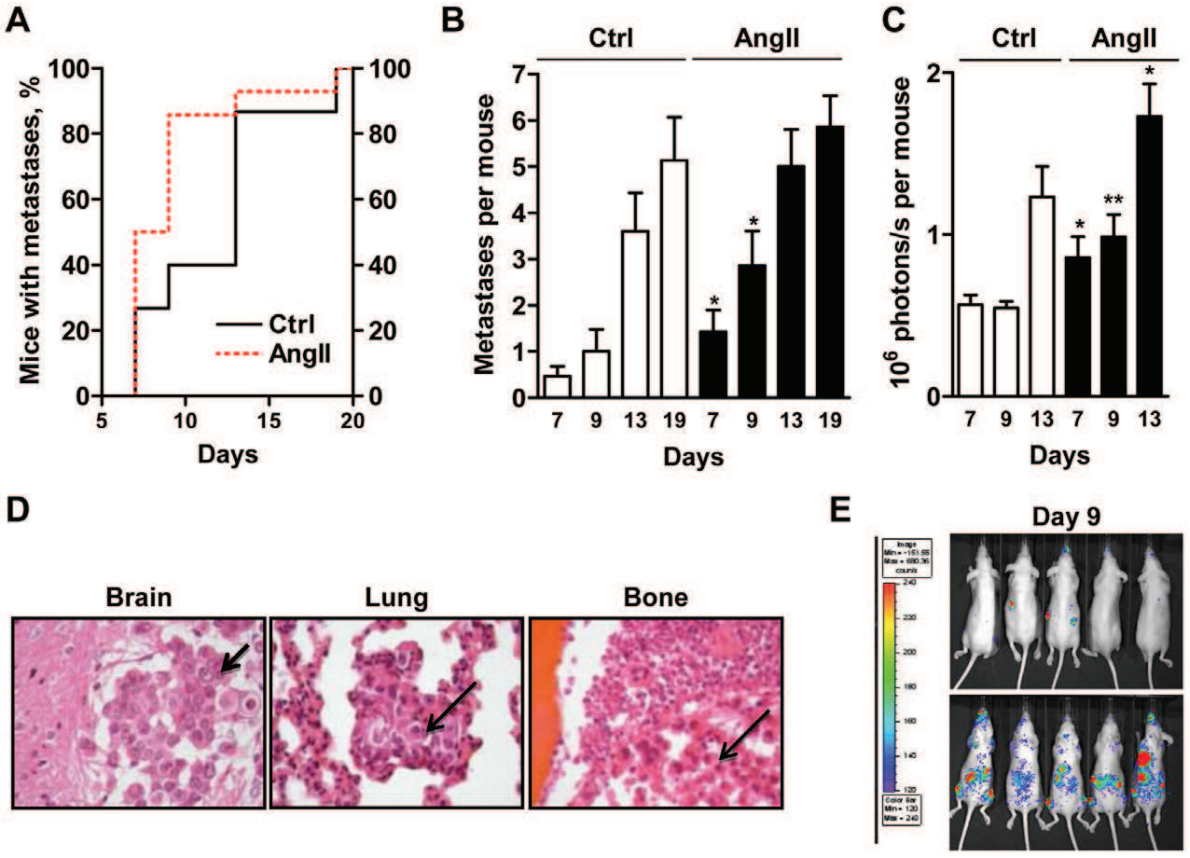

Figure 1. AngII increases the time-course, incidence and number of metastases in an experimental model *in vivo*. (**A**). Percentage of mice showing at least one detectable metastasis over time after intracardiac injection of D3H2LN cells treated with AngII (red dotted line, n = 14) or vehicle (black line, n = 15). (**B**). Number of metastases per mouse at indicated days. Results are mean +/− SEM of 15 control (white bar) and 14 AngII-treated (black bar) groups. (**C**). Number of photons/s per mouse at indicated days. Results are expressed as in B. (**D**). Histological analysis of metastases developing at the brain (left panel), the lung (middle panel) and the bone (right panel), obtained from 3 µm sections of formalin-fixed, paraffin-embedded tissue blocks stained with hematoxylin/eosin. Arrows indicate tumor cells. Magnification, 200x. (**E**). Representative pictures of 5 mice taken at day 9 after injection of control cells (upper panel) or AngII-treated cells (lower panel). * $p<0.05$, ** $p<0.01$.
doi:10.1371/journal.pone.0035667.g001

and migration (27%) and inflammation (18%) (Table S3). Accordingly, these genes were found to contribute to intracellular protein kinase pathways (21%) or small GTPase signaling (17%) (Table S4). Of interest, a large number of differentially regulated genes (25%) were also related to cell metabolism, a finding that opens new areas of investigation regarding the effects of AngII in cancer cells.

Except for one up-regulated gene (encoding anti-apoptotic molecule ATAD3A), differential regulation by AngII at 24 hrs did not exceed a factor of 3 (Table S1), suggesting that AngII may induce fine-tuned modulation of a wide number of genes involved in various signaling pathways, rather than strong activation or inhibition of a restricted set of specific genes. Ingenuity Pathway Analysis (IPA) software revealed a network of genes centered around angiotensinogen (AGT), the precursor of AngII (Fig. 3A). Remarkably, two main groups of regulated genes could be distinguished, one being related to MAP kinase (MAPK1) a major effector of cell proliferation and inflammation (comprising MAPK1, MAP2K7, MKNK2, PAWR, ARHGEF12, IGF1R, RASGRF1 and DOK1), the other one being connected to matrix metalloproteases MMP2 and MMP9 (also comprising ICAM1, ITGB2, BSG, CDKN1, ANAPC10, SMAD2, RASGRF1 and DOK1), well-known mediators of cell invasion and matrix remodeling (Fig. 3A). Notably, RASGFR1 and DOK1 belong to both groups of connected genes.

To note, microarray studies indeed revealed an increase in MMP2 and MMP9 expression levels in response to AngII stimulation, although results did not reach significance due to heterogeneity of probesets hybridization. The pivotal position of these genes within the network of AngII-regulated targets prompted us to further investigate their differential expression by RT-PCR. As shown in Fig. 3B and 3C, AngII dose-dependently increases the mRNA levels of MMP2 (2-fold) and MMP9 (3-fold) but not MMP3 nor MMP1 (not shown). Lipopolysaccharide (LPS), as well-known potent inducer of MMPs expression and activity, was used as a positive control for AngII efficiency. Dose-dependent activation of MMP9 enzymatic (gelatinase) activity, reaching a 2-fold increase at 100 nM AngII, was further confirmed by zymography analysis (Fig. 3D). Of interest, Intercellular Adhesion Molecule (ICAM-1), a major player in cell-cell adhesion and trans-endothelial migration, also stands at the crossroad between AGT, MMPs and integrins (Fig. 3A). In agreement with gene array studies showing up-regulation of ICAM-1 mRNA (1.48 fold) by AngII (Table S1), FACS analyses (Fig. 3E) further confirmed up-regulation (1.8-fold) of ICAM-1 protein levels at the plasma

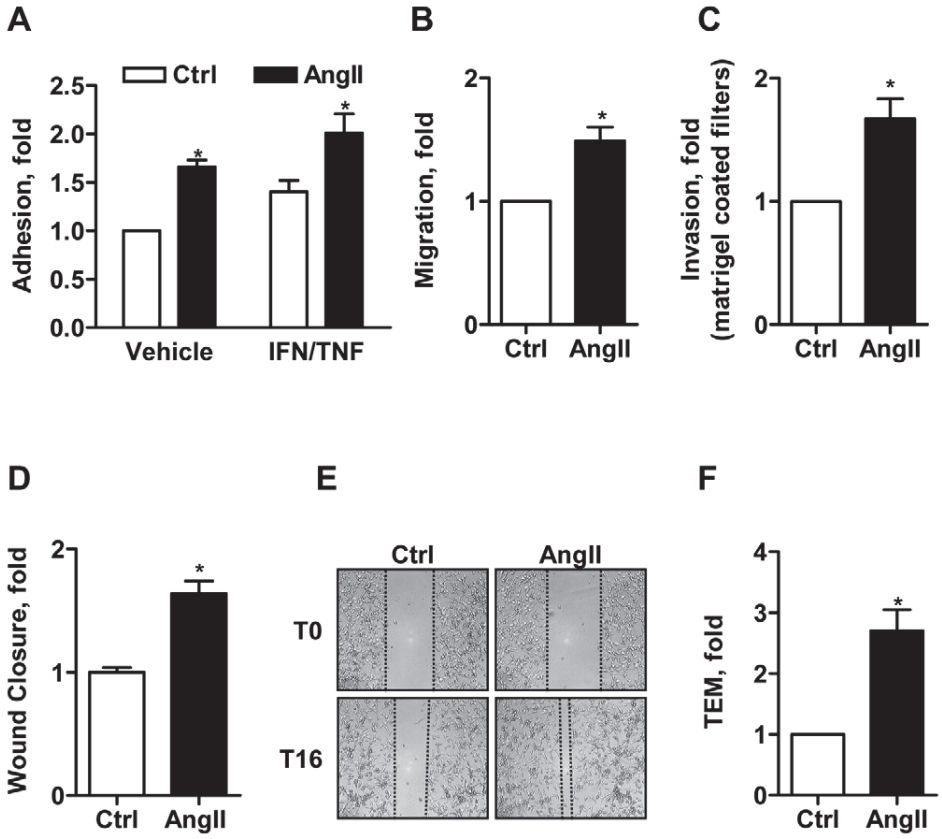

Figure 2. AngII increases breast cancer cell adhesion and migration. (**A**). MDA-MB-231 breast cancer cell adhesion to HCMEC/D3 endothelial cells monolayer following exposure of cancer cells to AngII (100 nM) for 24 hrs. Results are means +/− SEM of 7 independent experiments performed in quadruplicate, and expressed as fold increase of untreated cells (control, Ctrl). *$p<0.05$. (**B, C**). Boyden chamber assays of tumor cell migration across 8 μm-pore filters either non coated (B) or coated with matrigel to mimic cell invasion (C). Results are means +/− SEM of 3 separate experiments performed in triplicate, and expressed as fold increase of control. *$p<0.05$. (**D, E**). Wound healing assay. Results are from 2 independent experiments performed in quintuplicate, and expressed as fold increase of wound closure at time 16 hrs (T16) compared to control (vehicle-treated cells). *$p<0.05$. (E). Representative pictures of wounds from control and AngII-treated cells (100 nM, 24 hrs) at T0 and T16. Magnification, 100x. (**F**). Trans-endothelial migration. Results are mean +/− SEM of 3 independent experiments performed in triplicate, and expressed as fold increase of control. *$p<0.05$.
doi:10.1371/journal.pone.0035667.g002

membrane of MDA-MB-231 cells following 24 hrs treatment with AngII.

Discussion

Pro-metastatic effects of AngII in various experimental models *in vivo* have been attributed to its actions on the host microenvironment [12,13,20,21]. We show here for the first time that direct exposure of breast cancer cells to AngII contributes to increased tumor-endothelial cell adhesion, trans-endothelial migration and motility, and accelerates metastatic progression in an experimental mouse model *in vivo*. AngII is a potent vasoactive peptide that can be both released in the bloodstream and generated locally by endothelial, stromal and/or cancer cells. We propose that autocrine or paracrine effects of AngII, either present in the circulation or in the microenvironment of secondary tissue, may trigger an activating signal facilitating the dissemination and establishment of micrometastases in target organs.

Cancer cell extravasation and metastatic colonization are rate-limiting steps that involve reciprocal interactions between tumor cells and the host stroma [24]. Extravasation requires cancer-endothelial cell adhesion and subsequent trans-endothelial migration. Colonization in turn necessitates remodeling of the extracellular matrix to invade and adapt to the new microenvironment [25], as well as activation of pro-survival pathways that allow maintenance of cancer cells and their growth as micrometastases [24,26]. Data presented here provide evidence that AngII transcriptionally modulates a wide range of coordinated genes that contribute to cell adhesion/migration and proliferation/survival through connection to matrix metalloprotease and MAP kinase pathways, respectively. These observations are in support of the functional studies reported here and suggest that AngII may contribute to both extravasation and colonization of metastatic breast cancer cells.

At the molecular level, previous studies have extensively documented AngII-mediated regulation of MAP kinase pathways in various cell types, in relation with mitogenic and anti-apoptotic effects of the peptide [27]. We show here that AngII up-regulates MMP2 and MMP9 gene expression and enzymatic activity in breast cancer cells, in agreement with studies conducted in the gastric cancer cell line MNK-28 [28]. Notably, we also report here that AngII up-regulates the expression of Intercellular Adhesion Molecule ICAM-1 at the mRNA and protein level. ICAM-1 is well-known to trigger leukocyte adhesion to the endothelium and

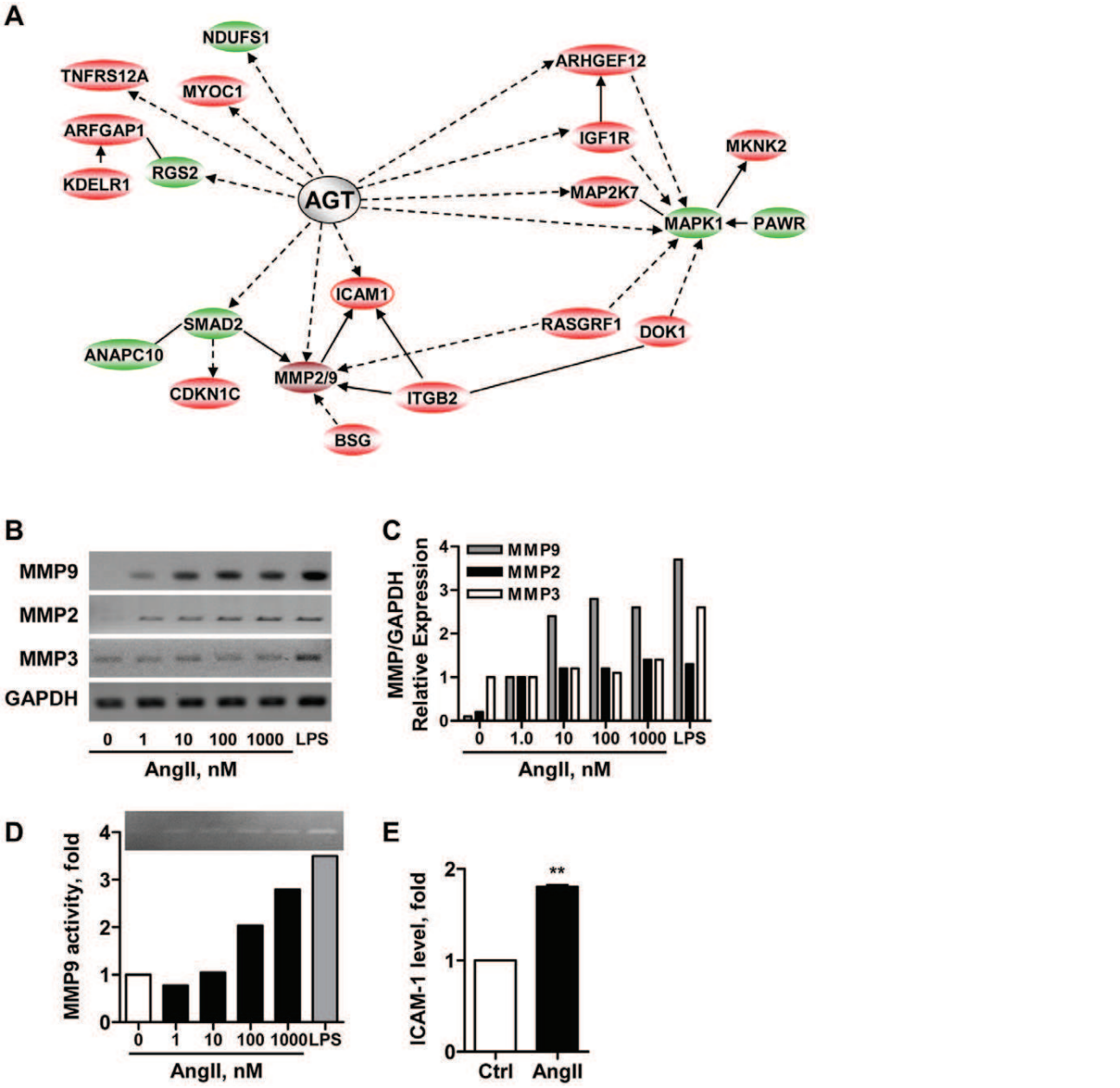

Figure 3. AngII transcriptionally regulates a panel of connected genes. (**A**). Gene networks differentially regulated by AngII. Up- and down-regulated genes related to angiotensinogen (AGT) are indicated in red and green, respectively. Filled lines indicate direct interactions, filled and dashed arrows indicate direct and indirect regulations, respectively. Note two groups of connected genes centered around MAPK1 and MMP2/9, respectively. (**B**). RT-PCR analysis of MMP9, MMP2 and MMP3 mRNA expression in MDA-MB-231 cells treated for 24 hrs with increasing doses of AngII as indicated, or LPS (Lipopolysaccharide, 100 ng/ml) as a positive control. GAPDH amplification was used as internal control. Shown is one out of 3 to 5 independent experiments performed in duplicate. (**C**). Quantification (Image J software) of PCR amplification of MMP9, MMP2 and MMP3 relative to GAPDH and normalized to expression levels in cells treated with 1 nM AngII. (**D**). Gelatin-based zymography analysis of MMP9 activity in conditioned medium of cells treated as in B. Shown is one representative out of 3 independent experiments (Upper panel). Quantification (ImageJ software) of results normalized to the quantity of proteins in cell lysate and expressed relative to control (lower panel). (**E**). FACS analysis of ICAM-1 expression at the plasma membrane of MDA-MB-231 cells treated with AngII (100 nM) or vehicle for 24 hrs. Results are means +/− SEM of 3 independent experiments and expressed as fold-increase of the control. **p<0.01.
doi:10.1371/journal.pone.0035667.g003

subsequent diapedesis, and its expression in endothelial cells has been shown to be increased by AngII in inflammatory situations [29]. Our results show for the first time that ICAM-1 is up-regulated in breast tumor cells in response to AngII treatment. Relevance of this finding to human disease is supported by a recent report showing that increased levels of ICAM-1 in breast tumors are associated with a more aggressive phenotype [30], and by studies highlighting the importance of vascular cell adhesion molecules in the establishment of breast cancer cells at the secondary site [31]. Other genes encoding adhesion molecules

(ITGB2) or metabolic pathways (FUT4) were also significantly up-regulated by AngII (1.5 and 1.7 fold, respectively) (Table S1). Of interest, FUT4 encodes fucosyltransferase which is involved in the synthesis of sialyl-Lewis X, a well-known ligand of selectins adhesion molecules, suggesting an indirect effect of AngII on the selectin–selectin ligand axis.

We propose here a model in which direct stimulation of circulating cancer cells by locally-produced AngII may regulate a set of genes that ultimately influence the host microenvironment to facilitate cancer cell extravasation, adaptation to the soil and subsequent metastatic colonization. This model supports the notion that targeting AngII production or action using ACE inhibitors or ARBs, respectively, may represent an interesting therapeutic option to prevent metastatic progression of invasive breast tumors. In patients however, the question of whether RAS blockers may have beneficial effects in cancer remains contradictory [12,13,32–35], a finding that might reflect tumor heterogeneity in terms of RAS expression and local levels of AngII production. Future prospective studies analyzing expression of RAS components and AngII production in breast cancer may lead to the identification of a subpopulation of tumors that respond to ACE inhibitors and/or ARBs. Such agents being largely used in the clinics as antihypertensive agents with mild side effects may constitute a major breakthrough for personalized therapy of metastatic breast tumors.

Materials and Methods

Cell lines

MDA-MB-231-Luc-D3H2LN luciferase-positive breast cancer cells (referred here as D3H2LN) were obtained from Caliper Life Science (Xenogen, MA, USA) and grown as described previously [23]. These cells were derived from a spontaneous lymph node metastasis of the MDA-MB-231 adenocarcinoma cell line expressing luciferase, as described [22]. Metastatic MDA-MB-231 breast tumor cells were obtained and grown as described previously [36]. Human vascular endothelial HCMEC/D3 cells were immortalized from brain microcapillaries and grown as described [37].

Animal studies

Intracardiac experimental mouse model of metastasis *in vivo* was conducted as described [22,23]. Briefly, female nude mice of 8–0 weeks (Janvier, France) were anesthetized by intraperitoneal injection of 120 mg/kg ketamine and 6 mg/kg xylazine. D3H2LN cells expressing luciferase were pre-treated with 100 nM AngII (Sigma, France) or vehicle in serum-free medium for 24 hrs prior to injection (100.000 cells in 100 µl sterile PBS) into the left ventricle of the heart by non surgical means. Anesthetized mice were placed in the IVIS^{TM} Imaging System (Xenogen, Caliper Life Science, MA, USA) and imaged from both dorsal and ventral views five minutes after intraperitoneal injection of D-luciferin (Caliper Life Science). A successful intracardiac injection was indicated on day 0 by systemic bioluminescence distributed throughout the animal. Only mice with evidence of successful injection were included in the experiment. Assessment of subsequent metastasis was monitored by imaging using the IVIS^{TM} Imaging System (Caliper Life Science), every 3–4 days for up to 24 days on mice anesthetized by exposure to 1–3% isoflurane. Experiments were carried out with the approval of the Département d'Expérimentation Animale, Institut d'Hématologie, Hôpital St-Louis ethical committee, and were performed twice on 7 to 8 mice per group.

For ex-vivo analysis, organs highlighted by bioluminescence in whole mice were removed surgically after sacrifice of the animals and rapidly incubated with D-luciferin before imaging using the IVIS system. For histological analyses, sections (3 µm) of metastatic organs were cut from formalin-fixed, paraffin-embedded tissue blocks, counterstained with hematoxylin-eosin and examined under an inverted microscope.

Tumor cell adhesion to endothelial cells and trans-endothelial migration

For endothelial cell adhesion assay, tumor cells were pre-treated with AngII (100 nM) or vehicle in serum-free medium for 24 hrs prior to labeling using green fluorescent cell tracker CMFDA (Molecular Probes) as recommended by the manufacturer. Fluorescent tumor cells (100.000/well of 96-well plates) were added for 30 min at 37°C to a monolayer of human endothelial cells (HCMEC/D3) either left untreated or pre-treated for 24 hrs with pro-inflammatory cytokines IFNγ (200 U/ml) and TNFα (100 U/ml). After extensive washing, adherent cells were lysed in water and tumor cells were quantified in a fluorescent microplate reader at wavelength 485/530 nm. Experiments were performed in quadruplicate.

For trans-endothelial migration assay, endothelial HCMEC/D3 cells (20.000/well) were plated on collagen type I-coated Transwell filters (8 µm pore filter) and grown to confluence. Serum starved MDA-MB-231 cells (100.000/well) were pre-treated for 24 hrs with AngII (100 nM) or vehicle prior to labeling with CMFDA cell tracker as described before. Fluorescent tumor cells were added to the endothelial monolayer in the presence of chemokine CXCL12 (100 ng/ml) in the lower compartment. After 24 hrs, cells remaining in the upper chamber were removed with a cotton swab and tumor cells having migrated through the endothelial monolayer to the lower face of the filter were lysed with water and quantified in a fluorescent microplate reader at wavelength 485/530 nm. Experiments were performed in triplicate.

Cell migration

For Boyden chamber assays of cell migration, MDA-MB-231 cells (200.000/well) were pre-treated for 24 hrs with AngII (100 nM) or vehicle and were then seeded on the upper chamber of 8 µm-Transwell filters (Corning, NY, USA) either coated or not with 10 µg/ml matrigel (BD Biosciences), and allowed to migrate for 18 hrs in the presence of 10% FCS in the lower compartment. Cells migrating to the lower face of the filters were fixed in methanol, stained with crystal violet and counted under an inverted microscope. Experiments were performed in triplicate.

For wound healing assays, D3H2LN cells were pre-treated for 24 hrs with AngII (100 nM) or vehicle and were then grown to confluence in 24-well plates before cross-shape wounds were performed in the monolayer using a sterile 10 µl pipette tip. Wounds were registered by phase contrast microscopy immediately after scratching (T0) and after 16 hrs in serum-free medium (T16), and quantified using ImageJ software (http://rsb.info.nhi.gov/ij/). For each condition the ratio of wound closure at T16 relative to T0 was calculated.

Gene array studies

Total RNA from MDA-MB-231 cells treated for 24 hrs with AngII (100 nM) or vehicle, was extracted using Trizol (Invitrogen) and analyzed with the Affymetrix Human Genome U133 Plus 2.0 Gene Chips (a genome wide array with 54674 probe sets targeting 19418 transcripts) as described [38]. Gene expression levels were normalized using the GC-RMA algorithm and flags were

computed using MAS5. Quality assessment of the chips was performed with affyQCReport R package (R project for Statistical Computing [http://www.r-project.org/]). Each data set was derived from triplicates of biologically independent samples and compared using Student's *t* test. To estimate the false discovery rate the resulting p values were filtered at 5%. Microarray experiments were performed according to the MIAME consortium guidelines. Data have been submitted to MIAMEarray express under accession number E-MEXP-3470 and the release date is 2012-12-05. Data were submitted to Ingenuity Pathway Analysis (IPA) to model relationships among genes and proteins and to construct putative pathways and relevant biological processes (http://www.ingenuity.com).

RT-PCR analysis

Total RNA was extracted from MDA-MB-231 cells treated as indicated, and cDNA was reverse-transcribed using oligo-dT and superscript RT (Invitrogen) as recommended by the manufacturer. PCR amplification (35 cycles, annealing temperature 55°C) was performed on 25 ng cDNA using oligonucleotide primers as follows: **MMP9-F** 5′AAG TAC TGG CGA TTC TCT GAG GG; **MMP9-R** 5′GGC TTT CTC TCG GTA CTG GAA GAC; **MMP2-F** 5′TTT TCT CGA ATC CAT GAT GG; MMP2-R 5′CTG GTG CAG CTC TCA TAT TT; **MMP3-F** 5′CCT GCT TTG TCC TTT GAT GC; **MMP3-R** 5′TGA GTC AAT CCC TGG AAA GTC; **GAPDH-F** 5′GGA GAA GGC TGG GGC; **GAPDH-R** 5′GAT GGC ATG GAC TGT GG.

FACS analysis

MDA-MB-231 cells were treated for 24 hrs with AngII (100 nM) or vehicle and harvested in 1mM EDTA. Expression levels of ICAM-1 at the cell membrane were evaluated by FACS analysis using Cytomics TM FC500 (Beckman Coulter) after labeling with anti-ICAM-1 antibodies (R&D system).

Gelatin zymography

For analysis of metalloprotease enzymatic activity, conditioned medium of MDA-MB-231 cells treated for 24 hrs with increasing concentrations of AngII, or lipopolysaccharide (LPS, 100 ng/ml) as positive control, were collected and loaded on gelatin (1 mg/ml)-containing SDS-PAGE run at 4°C (zymography gels) as described [23]. MMP9 activity was visualised as a clear band at 90 kDa after coomassie blue coloration, and quantified using ImageJ software.

Statistical analysis

Statistical analyses were conducted using JMP-7 software. Data in bar graphs (mean +/− SEM) were analyzed using Student's t-test. $p<0.05$ was considered statistically significant.

Supporting Information

Figure S1 (**A**). Quantification of the number of metastases per mouse at day 9. Shown are pooled results from 2 independent experiments, black squares and black triangles representing control (n = 15) and AngII-treated (n = 14) mice, respectively. (**B**). Quantification of the number of photons/s per mouse at day 9. Results are expressed as in (A). * $p<0.05$, *** $p<0.001$.
(TIF)

Figure S2 MTT assay of D3H2LN cells proliferation following 24 hrs- pre-treatment with AngII (100 nM) or vehicle. Shown is one representative experiment out of 3 performed in quadruplicate.
(TIF)

Table S1 Shown are the 63 genes up-regulated by AngII (100 nM, 24 hrs) by 1.4-fold or more ($p<0.05$). The genes are listed in alphabetical order, together with their main characteristics and known functions (description/ Gene pathway/ function column), differential regulation by AngII (fold column) and p value. (a): Genes connected to Angiotensinogen pathway AGT (as illustrated in Figure 3A) are indicated by an asterisk *.
(DOC)

Table S2 Shown are the 39 genes down-regulated by AngII (100 nM, 24 hrs) by 1.4-fold or more ($p<0.05$). The genes are listed in alphabetical order as indicated in Table S1. (a): Genes connected to Angiotensinogen pathway AGT (as illustrated in Figure 3A) are indicated by an asterisk *.
(DOC)

Table S3 Genes regulated by AngII are classified according to their major functions namely Inflammation, Cell Proliferation and Apoptosis, Adhesion and Migration, Metabolism. Genes with others functions appear in the "others" section. Number of genes is indicated under parenthesis. Up-regulated genes are indicated in bold whereas down-regulated genes are indicated in standard font.
(DOC)

Table S4 Genes regulated by AngII are organized in four major pathways related to protein kinase signaling, small GTPases, Ubiquitin/proteasome and intracellular traffic. Number of genes is indicated under parenthesis. Up-regulated genes are indicated in bold whereas down-regulated genes are indicated in standard font.
(DOC)

Acknowledgments

This article is dedicated to Pr. A. Donny Strosberg. We acknowledge the Hospital St Louis Animal Facility, as well as Laurence Stouvenel and the Cochin Immunobiology facility, and the Genomic's facility of the Institut Cochin. This work was supported by the University Paris Descartes, the Inserm, the CNRS, the Ligue Contre le Cancer-Comité Ile de France, the Association pour la Recherche Contre le Cancer (ARC), the Association Le Cancer du Sein, Parlons-en!, the Fondation RAJA and the Association Prolific. S.R-F was supported by a fellowship from ARC.

Author Contributions

Conceived and designed the experiments: SR-F MdB CN. Performed the experiments: SR-F MA PD-P A-CL AdT FD CLSP AM MM RIR CMC-N MdB. Analyzed the data: SR-F MA PD-P A-CL AdT FD CLSP AM NC FL MM RIR DEC BT P-OC CMC-N MdB CN. Contributed reagents/materials/analysis tools: NC FL BT P-OC. Wrote the paper: SR-F CMC-N CN.

References

1. Chambers AF, Groom AC, MacDonald IC (2002) Dissemination and growth of cancer cells in metastatic sites. Nat Rev Cancer 2: 563–572.
2. Steeg PS (2006) Tumor metastasis: mechanistic insights and clinical challenges. Nat Med 12: 895–904.
3. Bidard FC, Pierga JY, Vincent-Salomon A, Poupon MF (2008) A "class action" against the microenvironment: do cancer cells cooperate in metastasis? Cancer Metastasis Rev 27: 5–10.
4. Bockhorn M, Jain RK, Munn LL (2007) Active versus passive mechanisms in metastasis: do cancer cells crawl into vessels, or are they pushed? Lancet Oncol 8: 444–448.

5. Eccles SA, Welch DR (2007) Metastasis: recent discoveries and novel treatment strategies. Lancet 369: 1742–1757.
6. Nguyen DX, Bos PD, Massagué J (2009) Metastasis: from dissemination to organ-specific colonization. Nat Rev Cancer 9: 274–284.
7. Joyce JA, Pollard JW (2009) Microenvironmental regulation of metastasis. Nat Rev Cancer 9: 239–352.
8. Witz IP (2008) Tumor-microenvironment interactions: dangerous liaisons. Adv Cancer Res 100: 203–229.
9. Fidler IJ (2003) The pathogenesis of cancer metastasis: the 'seed and soil' hypothesis revisited. Nat Rev Cancer 3: 453–458.
10. Muller A, Homey B, Soto H, Ge N, Catron D, et al. (2001) Involvement of chemokine receptors in breast cancer metastasis. Nature 410: 50–56.
11. Qian BZ, Li J, Zhang H, Kitamura T, Zhang J, et al. (2011) CCL2 recruits inflammatory monocytes to facilitate breast-tumour metastasis. Nature 475: 222–225.
12. Deshayes F, Nahmias C (2005) Angiotensin II receptors: a new role in cancer? Trends Endocrinol Metabol 16: 293–299.
13. George AJ, Thomas WG, Hannan RD (2010) The renin-angiotensin system and cancer: old dog, new tricks. Nat Rev Cancer 10: 745–759.
14. Tahmasebi M, Barker S, Puddefoot JR, Vinson GP (2006) Localisation of renin-angiotensin system (RAS) components in breast. Br J Cancer 95: 67–74.
15. Rhodes DR, Ateeq B, Cao Q, Tomlins SA, Mehra R, et al. (2009) AGTR1 overexpression defines a subset of breast cancer and confers sensitivity to losartan, an AGTR1 antagonist. Proc Natl Acad Sci U S A 106: 10284–10289.
16. Carl-McGrath S, Ebert MP, Lendeckel U, Röcken C (2007) Expression of the Local Angiotensin II System in Gastric Cancer May Facilitate Lymphatic Invasion and Nodal Spread. Cancer Biol Ther 6: 1218–26.
17. Kinoshita J, Fushida S, Harada S, Yagi Y, Fujita H, et al. (2009) Local angiotensin II-generation in human gastric cancer: correlation with tumor progression through the activation of ERK1/2, NF-kappaB and survivin. Int J Oncol 34: 1573–1582.
18. Miyajima A, Kosaka T, Asano T, Seta K, Kawai T, et al. (2002) Angiotensin II type I antagonist prevents pulmonary metastasis of murine renal cancer by inhibiting tumor angiogenesis. Cancer Res 62: 4176–4179.
19. Fujita M, Hayashi I, Yamashina S, Itoman M, Majima M (2002) Blockade of angiotensin AT1a receptor signaling reduces tumor growth, angiogenesis, and metastasis. Biochem Biophys Res Commun 294: 441–447.
20. Egami K, Murohara T, Shimada T, Sasaki K, Shintani S, et al. (2003) Role of host angiotensin II type 1 receptor in tumor angiogenesis and growth. J Clin Invest. 112: 67–75.
21. Imai N, Hashimoto T, Kihara M, Yoshida S, Kawana I, et al. (2007) Roles for host and tumor angiotensin II type 1 receptor in tumor growth and tumor-associated angiogenesis. Lab Invest 87: 189–198.
22. Jenkins DE, Hornig YS, Oei Y, Dusich J, Purchio T (2005) Bioluminescent human breast cancer cell lines that permit rapid and sensitive in vivo detection of mammary tumors and multiple metastases in immune deficient mice. Breast Cancer Res 7: R444–R454.
23. Abdelkarim M, Vintonenko N, Starzec A, Robles A, Aubert J, et al. (2011) Invading basement membrane matrix is sufficient for MDA-MB-231 breast cancer cells to develop a stable in vivo metastatic phenotype. PLoS One 6: e23334.
24. Shibue T, Weinberg RA (2011) Metastatic colonization: settlement, adaptation and propagation of tumor cells in a foreign tissue environment. Semin Cancer Biol 21: 99–106.
25. Bissell MJ, Hines WC (2011) Why don't we get more cancer? A proposed role of the microenvironment in restraining cancer progression. Nat Med 17: 320–329.
26. Naumov GN, MacDonald IC, Weinmeister PM, Kerkvliet N, Nadkarni KV, et al. (2002) Persistence of solitary mammary carcinoma cells in a secondary site: a possible contributor to dormancy. Cancer Res 62: 2162–2168.
27. Hunyady L, Catt KJ (2006) Pleiotropic AT1 receptor signaling pathways mediating physiological and pathogenic actions of angiotensin II. Mol. Endocrinol 20: 953–970.
28. Huang W, Yu LF, Zhong J, Qiao MM, Jiang FX, et al. (2008) Angiotensin II type 1 receptor expression in human gastric cancer and induces MMP2 and MMP9 expression in MKN-28 cells. Dig Dis Sci 53: 163–168.
29. Alvarez A, Cerda-Nicolas M, Naim Abu Nabah Y, Mata M, Issekutz AC, et al. (2004) Direct evidence of leukocyte adhesion in arterioles by angiotensin II. Blood 104: 402–428.
30. Schröder C, Witzel I, Müller V, Krenkel S, Wirtz RM, et al. (2011) Prognostic value of intercellular adhesion molecule (ICAM)-1 expression in breast cancer. J Cancer Res Clin Oncol 137: 1193–1201.
31. Chen Q, Zhang XH, Massagué J (2011) Macrophage Binding to Receptor VCAM-1 Transmits Survival Signals in Breast Cancer Cells that Invade the Lungs. Cancer Cell 20: 538–549.
32. Sipahi I, Debanne SM, Rowland DY, Simon DI, Fang JC (2010) Angiotensin-receptor blockade and risk of cancer: meta-analysis of randomised controlled trials. Lancet Oncol 11: 627–636.
33. ARB Trialists Collaboration (2011) Effects of telmisartan, irbesartan, valsartan, candesartan, and losartan on cancers in 15 trials enrolling 138,769 individuals. J Hypertens 29: 623–635.
34. Yoon C, Yang HS, Jeon I, Chang Y, Park SM (2011) Use of angiotensin-converting-enzyme inhibitors or angiotensin-receptor blockers and cancer risk: a meta-analysis of observational studies. CMAJ 183: E1073–E1084.
35. Chae YK, Valsecchi ME, Kim J, Bianchi AL, Khemasuwan D, et al. (2011) Reduced risk of breast cancer recurrence in patients using ACE inhibitors, ARBs, and/or statins. Cancer Invest 29: 585–593.
36. Rodrigues-Ferreira S, Di Tommaso A, Dimitrov A, Cazaubon S, Gruel N, et al. (2009) 8p22 MTUS1 gene product ATIP3 is a novel anti-mitotic protein underexpressed in invasive breast carcinoma of poor prognosis. PLoS One 4: e7239.
37. Weksler BB, Subileau EA, Perriere N, Charneau P, Holloway K, et al. (2005) Blood-brain barrier-specific properties of a human adult brain endothelial cell line. FASEB J 19: 1872–1874.
38. Nectoux J, Fichou Y, Cagnard N, Bahi-Buisson N, Nusbaum P, et al. (2011) Cell cloning-based transcriptome analysis in cyclin-dependent kinase-like 5 mutation patients with severe epileptic encephalopathy. J Mol Med 89: 193–202.

Supplemental Table S1. List of genes up-regulated by AngII in MDA-MB-231 cells.

Gene Symbol(a)	Gene Name	Description / Gene pathway / Function	fold	p value
ABCC10	ATP-binding cassette, sub-family C (CFTR/MRP) member 10	Transporter, Drug resistance, Metabolism	1.55	0.035
AKT1S1	AKT1 substrate 1 (proline-rich)	Protein kinase signaling, Apoptosis	2.15	0.025
ALDH3B1	Aldehyde dehydrogenase 3 family, member B1	Enzyme, Metabolism, Inflammation	1.57	0.021
ALS2CL	ALS2 C-terminal like	Exchange factor, Small GTPase signaling, Proliferation, Intracellular traffic	2.02	0.044
ARFGAP1*	ADP-ribosylation factor GTPase activating protein 1	Exchange factor, Small GTPase signaling, Intracellular traffic, Cell Adhesion/Migration	1.60	0.022
ARHGEF12*	Rho guanine nucleotide exchange factor (GEF) 12	Exchange factor, Small GTPase signaling, Metabolism, Cell Adhesion/Migration	3.03	0.034
ARPC4	Actin related protein 2/3 complex, subunit 4	Actin binding protein, Small GTPase signaling, Intracellular traffic Cell Adhesion/Migration	1.51	0.027
ARRDC1	Arrestin domain containing 1	Arrestin-related trafficking, Cell Adhesion/Migration	1.82	0.041
ATAD3A	ATPase family, AAA domain containing 3A	ATP binding protein, Apoptosis	4.55	0.032
ATXN7L3	Ataxin 7-like 3	Zn finger, Trancriptional regulator, Histone ubiquitination	1.48	0.045
BSG*	Basigin (EMMPRIN)	Receptor, Protein kinase signaling, Cell Adhesion/Migration, Inflammation, Metabolism	1.81	0.042
CARD10	Caspase recruitment domain family, member 10	Guanylate kinase family member, Protein kinase signaling, Cell Growth and Apoptosis, Cell Adhesion/Migration	1.55	0.035
CDKN1C*	Cyclin-dependent kinase inhibitor 1C (p57, Kip2)	Kinase, Proliferation, Actin dynamics, Neuronal differentiation, Tumor invasion and metastasis	1.50	0.017
CYB5R2	Cytochrome b5 reductase 2	Enzyme, NADH redox activity, Metabolism	1.81	0.015
DDA1	DET1 and DDB1 associated 1	Autophagy, Ubiquitination, Tumor invasion and Metastasis	1.61	0.048
DLGAP4	Discs, large (Drosophila) homolog-associated protein 4	Guanylate kinase, Receptor interacting protein	1.44	0.040
DOK1*	Docking protein (downstream of tyrosine kinase 1)	Scaffold protein, Receptor tyrosine kinase signaling, Proliferation, Cell Adhesion/Migration	2.06	0.004
DOLK	Dolichol kinase	Kinase, Glycosylation, Metabolism	1.55	0.040
EFNB3	Ephrin-B3	Receptor tyrosine kinase, Small GTPase and Protein kinase signaling, Cell Growth and Apoptosis, Cell Adhesion/Migration	1.43	0.047
EIF5A	Eukaryotic translation initiation factor 5A	Translation factor, Cell Growth and Apoptosis, Metabolism, Cell Adhesion/Migration	1.73	0.048
FBXL19	F-box and leucine-rich repeat protein 19	Enzyme, F-Box protein family, Ubiquitin/Proteasome pathway	2.04	0.037
FMNL3	Formin-like 3	Actin binding protein, Small GTPase signaling, Cell Adhesion/Migration	1.48	0.049
FRMD4A	FERM domain containing 4A	Actin interacting domain, Small GTPase signaling, Actin dynamics, Epithelial polarity, Cell Adhesion/Migration	1.43	0.027
FUT4	Fucosyltransferase 4 (alpha (1,3), myeloid-specific)	Enzyme, Protein kinase signaling, Selectin-related interactions, Cell Adhesion/Migration, Inflammation, Metabolism	1.82	0.043
GNG7	Guanine nucleotide binding protein (G protein), gamma 7	Protein G gamma subunit, GPCR signalling, Cell Growth	1.62	0.011
HMG20B	High-mobility group 20B	Transcription regulator, DNA binding, BRCA2 interaction	1.87	0.018
ICAM1*	Intercellular adhesion molecule 1	Transmembrane cell adhesion molecule, Inflammation, Cell Adhesion/Migration	1.43	0.050
IGF1R*	Insulin-like growth factor 1 receptor	Receptor, Protein kinase signaling, Cell Growth and Apoptosis, Inflammation	1.71	0.050

IL17RA	Interleukin 17 receptor A	Receptor, Protein kinase signaling, Inflammation	1.60	0.047
ITGB2*	Integrin, beta 2 (complement component 3 receptor 3 and 4 subunit)	Receptor, Small GTPase signaling, Inflammation, Cell Adhesion/Migration	1.50	0.032
KDELR1*	KDEL (Lys-Asp-Glu-Leu) endoplasmic reticulum protein retention receptor 1	Receptor/Transporter, Protein kinase signaling, Small GTPase signaling, Intracellular traffic, ER stress response	1.85	0.030
MAN1B1	Mannosidase, alpha, class 1B, member 1	Enzyme, Metabolism, Intracellular traffic, Proteasome pathway	1.89	0.046
MAP2K7*	Mitogen-activated protein kinase kinase 7	Kinase, Protein kinase signaling, Cell Growth and Apoptosis, Inflammation		
MAP4K2	Mitogen-activated protein kinase kinase kinase kinase 2	Kinase, Protein kinase signaling, Inflammation	2.20	0.046
MKNK2*	MAP kinase interacting serine/threonine kinase 2	Calcium/calmodulin dependent Protein kinase signaling,Translation, Metabolism, Cell Proliferation, Inflammation, Proteasome pathway	1.89	0.022
MRPS18A	Mitochondrial ribosomal protein S18A	Mitochondrial, ribosomal, Protein synthesis	1.77	0.040
MYH11	Myosin, heavy chain 11, smooth muscle	Actin binding protein, TGFbeta pathway, Motor activity, Cell Proliferation, Cell Adhesion/Migration	1.66	0.024
MYO1C*	Myosin IC	Actin based molecular motor, Cell Proliferation, Intracellular traffic, Cell Adhesion/Migration	1.49	0.036
NAT8L	N-acetyltransferase 8-like (GCN5-related, putative)	Enzyme, Nacetyl methyltransferase superfamily, Membrane-bound protein, neuron-specific, Metabolism	1.74	0.045
NEK8	NIMA (never in mitosis gene a)- related kinase 8	Kinase, Cell Cycle progression, Cell proliferation, Ciliogenesis	1.60	0.042
OTUD5	OTU domain containing 5	Cysteine protease, Deubiquitinase, Innate immune response, Inflammation, Proteasome pathway	1.55	0.046
PCGF1	Polycomb group ring finger 1	Transcriptional regulator, Development, Ubiquitin/Proteasome pathway	1.51	0.036
PCTK1	PCTAIRE protein kinase 1	Cyclin dependent kinase Cdk16, Protein kinase signaling, Intracellular traffic, Exocytosis	1.56	0.029
PRIC285	Peroxisomal proliferator-activated receptor A interacting complex 285	Zinc finger, Transcription regulator, DNA helicase, Metabolism, Inflammation	1.56	0.004
PYCR2	Pyrroline-5-carboxylate reductase family, member 2	Enzyme, Metabolism	1.44	0.023
RAB4B	RAB4B, member RAS oncogene family	Enzyme, Small GTPase signaling, Intracellular traffic, Glut4 transport, Metabolism, Motility	1.56	0.036
RASGRF1*	Ras protein-specific guanine nucleotide-releasing factor 1	Exchange factor, Small GTPase signaling, Protein kinase signaling, Cell Proliferation, Cell Adhesion/Migration	2.90	0.001
SEMA6B	Sema domain, transmembrane domain (TM), and cytoplasmic domain, (semaphorin) 6B	Transmembrane receptor, Axon guidance, Cell Adhesion/Migration	2.64	0.005
SHB	Src homology 2 domain containing adaptor protein B	Adaptator protein, Protein kinase and Small GTPase signaling, Cell Growth and Apoptosis, Cell Adhesion/Migration, Inflammation	1.50	0.026
SIX2	SIX homeobox 2	Transcription factor, Cortisol Secretion, Metabolism	1.48	0.043
SLC2A4RG	SLC2A4 regulator	Transcription factor, Glut4 enhancer, Metabolism	1.51	0.039
SRGAP1	SLIT-ROBO Rho GTPase activating protein 1	Small GTPase signaling, Neuronal Migration	2.03	0.047
STX10	Syntaxin 10	SNAP receptor activity, Vesicular transport, Intracellular traffic	1.47	0.023
TBC1D10A	TBC1 domain family, member 10A	Exchange factor, Small GTPase signaling, Intracellular traffic	1.83	0.020
THRA	Thyroid hormone receptor, alpha	Nuclear hormone receptor, Metabolism	1.51	0.022
TNFRSF12A*	Tumor necrosis factor receptor superfamily, member 12A	Membrane receptor, Protein kinase signaling, Apoptosis, Inflammation	1.86	0.045
TRAF3IP2	TRAF3 interacting protein 2	TNF receptor pathway, Protein kinase signaling, Apoptosis, Inflammation, Proteasome pathway	1.85	0.034
TSPAN4	Tetraspanin 4	Transmembrane protein, Cell Growth and Apoptosis, Cell Adhesion/Migration	1.98	0.034

UBE2M	Ubiquitin-conjugating enzyme E2M (UBC12 homolog)	Enzyme, Ubiquitin/Proteasome pathway, Cell Proliferation and Apoptosis	1.78	0.032
UBE2R2	Ubiquitin-conjugating enzyme E2R 2	Enzyme, Ubiquitin/Proteasome pathway, Cell Growth	1.50	0.024
UBXN11	UBX domain protein 11	Small GTPase signaling, Cell Adhesion/Migration Ubiquitin/Proteasome pathway	1.48	0.015
VPS37D	Vacuolar protein sorting 37 homolog D	Intracellular traffic	2.05	0.047
WIZ	Widely interspaced zinc finger motifs	Zinc finger, Nuclear co-repressor, Histone methylation	2.06	0.025

Supplemental Table S2. List of genes down-regulated by AngII in MDA-MB-231 cells.

Gene	Gene Name	Description / Gene pathway / Function	fold	p value
ANAPC10*	Anaphase promoting complex subunit 10	Enzyme, Cell Proliferation and Apoptosis, Ubiquitination	-2.21	0.041
ARL17	ADP-ribosylation factor-like 17	Metabolism	-1.72	0.040
B4GALT4	UDP-Gal:betaGlcNAc beta 1,4-galactosyltransferase, polypeptide 4	Enzyme, Membrane-bound protein, Metabolism	-1.42	0.038
BTBD3	BTB (POZ) domain containing 3	Interacts with PlexinB3	-1.42	0.035
COG5	Component of oligomeric golgi complex 5	Transporter, Intracellular traffic	-2.14	0.026
DOCK5	Dedicator of cytokinesis 5	Exchange factor, Small GTPase signaling, Cell Adhesion/Migration	-1.57	0.043
DYRK2	Dual-specificity tyrosine-(Y)-phosphorylation regulated kinase 2	Kinase, Protein kinase signaling, Cell Proliferation,	-1.69	0.048
EIF2S3	Eukaryotic translation initiation factor 2, subunit 3 gamma, 52kDa	Translation regulator, Protein synthesis, Cell Proliferation	-2.08	0.024
EXOC8	Exocyst complex component 8	Cell Adhesion/Migration, Intracellular traffic	-1.52	0.032
FBXO45	F-box protein 45	Ubiquitination	-1.69	0.005
FGFR1OP2	FGFR1 oncogene partner 2	Cell Proliferation, Cell Differentiation	-1.75	0.045
HCFC2	Host cell factor C2	Transcription regulator, Cell Proliferation	-1.86	0.049
IDH3A	Isocitrate dehydrogenase 3 (NAD+) alpha	Enzyme, Metabolism	-2.02	0.003
IRAK3	Interleukin-1 receptor-associated kinase 3	Transmembrane receptor, Protein kinase signaling, Inflammation	-1.81	0.037
KIF1B	Kinesin family member 1B	Transporter, Intracellular traffic, Cell Adhesion/Migration	-2.16	0.040
KPNA1	Karyopherin alpha 1 (importin alpha 5)	Transporter, Intracellular traffic, Inflammation	-1.47	0.026
MAP7D3	MAP7 domain containing 3	Microtubule associated protein 7, Cell Adhesion/Migration	-2.51	0.029
MAPK1*	Mitogen-activated protein kinase 1	Kinase, Protein kinase signaling, Transcription regulation, Cell Proliferation	-1.50	0.038
MITF	Microphthalmia-associated transcription factor	Transcription factor, Cell differentiation, Cell Proliferation and Apoptosis	-1.47	0.039
MSRB2	Methionine sulfoxide reductase B2	Transcription regulator, Metabolism	-1.76	0.021
NDUFS1*	NADH dehydrogenase (ubiquinone) Fe-S protein 1, 75kDa (NADH-coenzyme Q reductase)	Enzyme, Metabolism	-1.39	0.013
OSGEPL1	O-sialoglycoprotein endopeptidase-like 1	Enzyme, Metabolism	-1.50	0.032
PAG1	phosphoprotein associated with glycosphingolipid microdomains 1	Transmembrane protein, Protein kinase signaling, Inflammation	-1.66	0.038
PAWR*	PRKC, apoptosis, WT1, regulator	Transcription regulator, Cell Proliferation and Apoptosis	-1.99	0.011
PTPN21	Protein tyrosine phosphatase, non-receptor type 21	Protein tyrosine phosphatase, Cell Proliferation and Apoptosis, Cell Differentiation	-1.52	0.004
RALB	V-ral simian leukemia viral oncogene homolog B (ras related; GTP binding protein)	Enzyme, Small GTPase signaling, Cell Proliferation and Apoptosis, Cell Adhesion/Migration	-1.50	0.026
RGS2*	Regulator of G-protein signaling 2, 24kDa	GTPase activating protein, Small GTPase signaling, Cell Proliferation and Apoptosis	-1.49	0.023
RNF144B	Ring finger protein 144B	Enzyme, Ubiquitination, Metabolism	-1.46	0.009

RTTN	Rotatin	Development	-1.90	0.015
SFRS3	Splicing factor, arginine/serine-rich 3	Splicing factor, Gene expression	-1.81	0.032
SGMS2	Sphingomyelin synthase 2	Enzyme, Metabolism, Cell Growth and Apoptosis	-1.50	0.045
SLC40A1	Solute carrier family 40 (iron-regulated transporter), member 1	Transporter, Metabolism	-1.91	0.023
SMAD2*	SMAD family member 2	Transcription regulator, Cell Proliferation and Apoptosis	-2.48	0.006
SYNE1	Spectrin repeat containing, nuclear envelope 1	Nuclear membrane protein, Cytoskeletal anchoring, Differentiation, Cell Adhesion/Migration	-2.70	0.013
UBE2H	Ubiquitin-conjugating enzyme E2H (UBC8 homolog, yeast)	Enzyme, Ubiquitination	-1.77	0.025
ZFP82	Zinc finger protein 82 homolog (mouse)	Zinc finger protein,Transcription regulator	-1.93	0.001
ZNF354B	Zinc finger protein 354B	Zinc finger protein, Transcription regulator	-2.36	0.041
ZNF57	Zinc finger protein 57	Zinc finger protein, Transcription regulator	-2.24	0.022
ZRANB1	Zinc finger, RAN-binding domain containing 1	Peptidase, Metabolism, Inflammation	-1.40	0.034

Supplemental Table S3: Genes regulated by AngII classified according to their functions

Inflammation (18)	**ALDH3B1, BSG, FUT4, ICAM1, IGF1R**, **IL17RA,** IRAK3, **ITGB2**, KPNA1, **MAP2K7**, **MAP4K2**, **OTUD5,** PAG1, **PRIC285**, **SHB, TNFRSF12A**, **TRAF3IP2**, ZRANB1
Cell Proliferation and Apoptosis (32)	**AKT1S1**, **ALS2CL,** ANAPC10, **ATAD3A**, **CDKN1C, DOK1**, DYRK2, **EFNB3**, EIF2S3, FGFR10P2, **GNG7,** HCFC2, **IGF1R**, MAPK1, **MAP2K7,** MITF, **MYH11, MYOC1, NEK8,** PAWR, PTPN21, RALB, **RASGRF1,** RGS2, SGMS2, **SHB,** SMAD2, **TNFRSF12A**, **TRAF3IP2**, **TSPAN4**, **UBE2M, UBE2R2**
Adhesion and Migration (27)	**ARFGAP1, ARHGEF12**, **ARPC4, ARRDC1, BSG**, **DOK1,** DOCK5, EXOC8, **EFNB3, FMNL3, FRMD4A, FUT4, ICAM1, ITGB2,** KIF1B, MAP7D3, **MYH11, MYOC1, RAB4B,** RALB, **RASGRF1**, **SEMA6B, SHB**, **SRGAP1**, SYNE1, **TSPAN4**, **UBXN11**
Metabolism (25)	**ABCC10, ALDH3B1, ARHGEF12,** ARL17, B4GALT4, **BSG, CYBR5, DOLK, EIF5A, FUT4,** IDH3A, MSRB2, **NATL8,** NDUFS1, OSGEPL1, **PRIC285**, **PYCR2**, **RAB4B**, RNF144B, SGMS2, **SIX2**, **SLC2A4RG,** SLC40A1, **THRA**, ZRANB1
Others (23)	**ATXN7L3**, BTBD3, COG5, **DDA1**, **DLGAP4, FBXL19**, FBX045, **HMG20B, KDELR1**, **MAN1B1, MRPS18A, PCGF1, PCTK1**, RTTN, SFRS3, **STX10, TBC1D10A**, **UBE2H, VPS37D**, **WIZ,** ZFP82, ZNFF354B, ZNF57

Supplemental Table S4: Genes regulated by AngII classified according to their signaling pathways

Protein Kinase Signaling (21)	**AKTS1, BSG, CARD10, DOK1,** DYRK2, **EFNB3, FUT4, IGF1R, IL17RA,** IRAK3, **KDELR1,** MAPK1, **MAP2K7, MAP4K2, MKNK2,** PAG1, **PCTK1, RASGRF1, SHB, TNFRSF12A, TRAF3IP2**
Small GTPase Signaling (18)	**ALS2CL, ARFGAP1, ARHGEF12, ARPC4,** DOCK5, **EFNB3, FMNL3, FRMD4A, ITGB2, KDELR1, RAB4B,** RALB, **RASGRF1,** RGS2, **SHB, SRGAP1, TBC1D10A, UBXN11**
Ubiquitin/Proteasome (13)	ANAPC10, **DDA1, FBXL19,** FBXO45, **MAN1B1, MKNK2, OTUD5, PCGF1,** RNF144B, UBE2H, **UBE2M, UBE2R2, UBXN11**
Intracellular Traffic (10)	COG5, EXOC8, **KDELR1,** KIF1B, KPNA1, **MAN1B1, PCTK1, RAB4B, STX10, VPS37D**

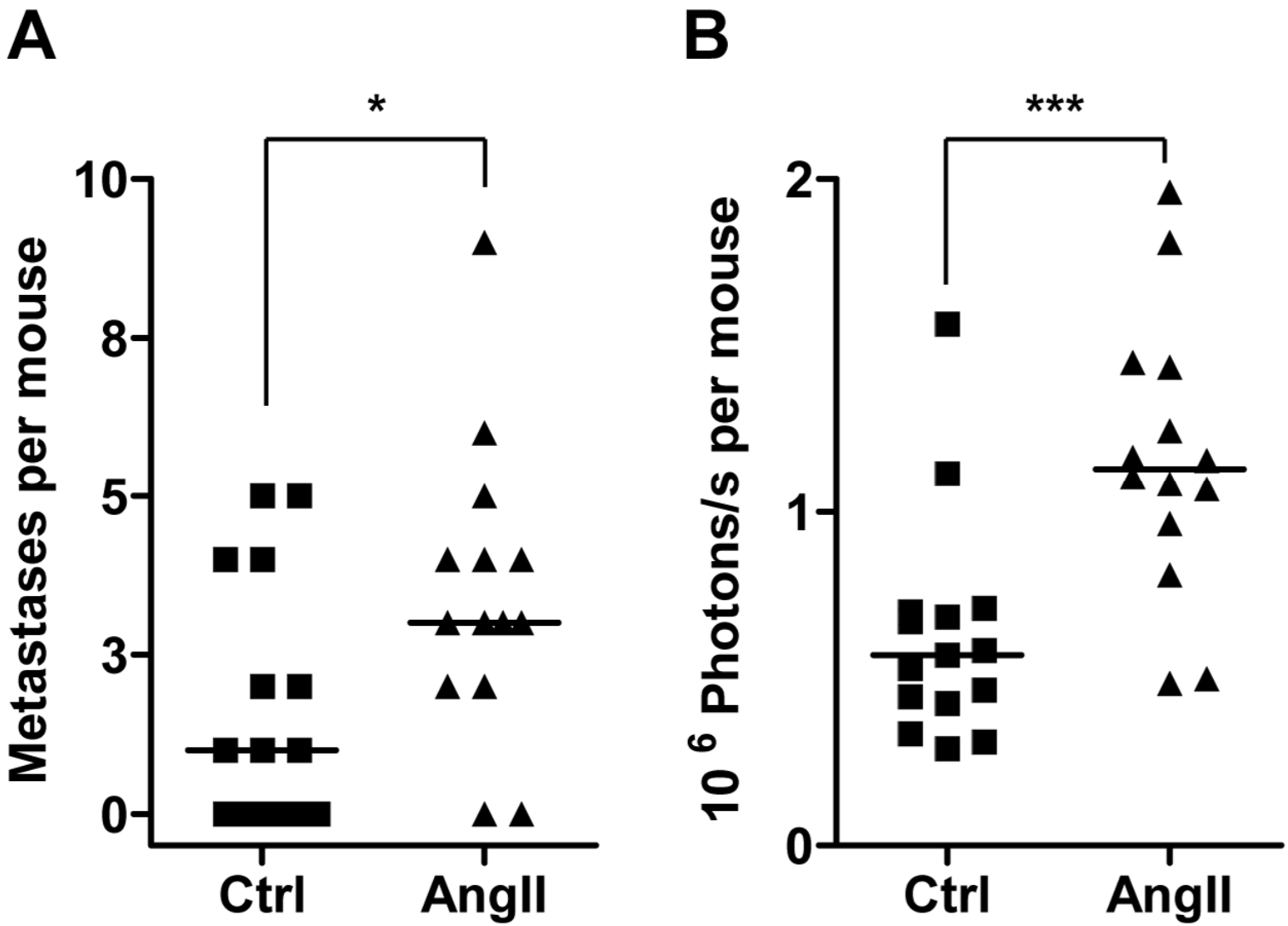

Supplemental Figure S1